

**TRIBOLOGICAL BEHAVIOUR OF RICE HUSK
REINFORCED POLYMER
MATRIX COMPOSITE**

**A THESIS SUBMITTED IN PARTIAL FULFILMENT OF
THE REQUIREMENT FOR THE DEGREE OF**

Doctor of Philosophy

in

Mechanical Engineering

By

Sakti Prasad Samantarai



**Department of Mechanical Engineering
National Institute of Technology
Rourkela -769 008, (India)
July-2014**

**TRIBOLOGICAL BEHAVIOUR OF RICE HUSK
REINFORCED POLYMER
MATRIX COMPOSITE**

**A THESIS SUBMITTED IN PARTIAL FULFILMENT OF
THE REQUIREMENT FOR THE DEGREE OF**

**Doctor of Philosophy
in**

**Mechanical Engineering
By**

Sakti Prasad Samantarai

Under the supervision of

Dr. Samir Kumar Acharya



**Department of Mechanical Engineering
National Institute of Technology
Rourkela -769 008, (India)
July-2014**

Dedicated to

ALL MY WELL-WISHERS



**National Institute of Technology
Rourkela-769008 (Odisha), INDIA**

CERTIFICATE

This is to certify that the thesis entitled “Tribological Behaviour of Rice Husk Reinforced Polymer Matrix Composite” submitted to the National Institute of Technology, Rourkela (Deemed University) by **Sakti Prasad Samantarai**, Roll No. 509-ME-908 for the award of the Degree of Doctor of Philosophy in Mechanical Engineering is a record of bonafide research work carried out by him under my supervision and guidance. The results presented in this thesis has not been, to the best of my knowledge, submitted to any other University or Institute for the award of any degree or diploma.

The thesis, in my opinion, has reached the standards fulfilling the requirement for the award of the degree of **Doctor of Philosophy** in accordance with regulations of the Institute.

Date: - -July-2014

(Dr. S. K. Acharya)

Professor

Mechanical Engineering Department

ACKNOWLEDGEMENT

It is my proud privilege to express my heart felt thanks to my guide professor Dr. S.K.Acharya, Professor, Department of Mechanical Engineering, NIT, Rourkela who has inspired me to pursue the PhD programme . Professor Acharya has extended his whole hearted support and guided me at every stage to make the journey successful. I am greatly indebted to him for his constructive suggestions and guidance from time to time during the course of my work.

I express my sincere thanks to Prof. S.S.Mohapatra, Head of the Department of Mechanical Engineering, NIT, Rourkela for providing me the necessary facilities in the department. I also express my thanks to Dr.R.K Patel of Chemistry department and Dr. S. C. Mishra of Metallurgical and Materials Engineering Department for their help during course of my work..

I am also thankful to all the staff members of the Department of Mechanical Engineering, Metallurgical Engineering, Ceramics and Mining Engineering for their timely help in completing my thesis work.I am thankful Mrs.Niharika, Raghavendra, Ms Sakuntala research scholar of Tribology Lab for giving me support whenever I need realizing that they are traveling in the same boat.

I express my deep gratitude to my organisation Steel Authority of India Limited for permitting me to persue this PhD programme. My special thanks go to my coffee house friends who are source of inspiration from the beginning of the journey to the end..

Finally, I express my thanks and obligation to my wife Snigdha Samantaray, daughter Saswati and Soumya for their sacrifice made in all respect during my PhD work.

Date: - -July-2014

(Sakti Prasad Samantarai)

ABSTRACT

The composite materials constitute a significant portion of engineering materials ranging from every day product like door windows to sophisticated product like aircraft and space application. The biggest advantages of use of composite materials are due to their high strength, low weight apart from other properties like good corrosion resistance, low densities, low thermal conductivities & electrical conductivities, absorption of energy in shock and vibration and finally aesthetic color effect. The material design can be tailor made to specific application and properties requirements. Thus, the composite material offers wide business opportunity in all sectors of industries

Environmental awareness today motivating the researchers, worldwide on the studies of natural fiber reinforced polymer composite and cost effective option to synthetic fiber reinforced composites. The availability of natural fibers and ease of manufacturing have tempted researchers to try locally available inexpensive fibers and to study their feasibility of reinforcement purposes and to what extent they satisfy the required specifications of good reinforced polymer composite for different applications. With low cost and high specific mechanical properties, natural fiber represents a good renewable and biodegradable alternative to the most common synthetic reinforcement, i.e. glass fiber.

Despite the interest and environmental appeal of natural fibers, their use is limited to non bearing applications, due to their lower strength compared with synthetic fiber reinforced polymer composite. The stiffness and strength shortcomings of bio composites can be overcome by structural configurations and better arrangement in a sense of placing the fibers in specific locations for highest strength performance. Accordingly extensive studies on preparation and properties of polymer matrix composite (PMC) replacing the synthetic fiber with natural fiber like Jute, Sisal, Pineapple, Bamboo, Kenaf and Bagasse etc were carried out. These plant fibers have many advantages over glass fiber or carbon fiber like renewable, environmental friendly, low cost, lightweight and high specific mechanical performance.

There are many potential natural resources, which India has in abundance. Most of it comes from the forest and agriculture. Rice husk (RH) is an agricultural waste material abundantly available in rice-producing countries. They are the natural sheaths that forms on rice grains during their growth. Removed during the refining of rice, these husks have no commercial interest. A large quantity of husk, which is known to have a fibrous material with high silica content, is available as waste from rice milling industries. In general, rice husk ash (RHA) might well be considered slightly impure silica. The content of silica and all impurities in RHA vary, depending on the variety; climate and geographic location. RHs contain mainly 15-20 wt% silica and a number of organic constituents that will yield carbon when thermally decomposed. Both the low density and the space in the raw materials facilitate the production of silicon carbide. Therefore RHs are the most economical and promising raw material for the production of silicon carbide.

Against this back ground the present research work has been under taken with an objective to explore the use of rice husk, as a reinforcement material in epoxy base and to study the effect of environment on its mechanical performance and also the tribological behavior, under abrasive and erosive conditions. With these multi-fold objectives the work reported in this dissertation has been carried out in following stages:-

1. A detailed study was undertaken to pull-up the existing literature on natural fiber composites and efforts were put to understand the basic needs of the composite industry. This includes various aspects such as characterization, fabrication, modification of fiber surface, testing, analysis and co-relation between micro-structure and properties obtained.
2. Experimental investigation into tribological behavior has been carried out. Studies such as dry sliding wear behavior, erosive wear characteristics has been studied by using Pin-on-disc machine, Solid particle impact tester. All these experiments have been performed as per ASTM standards.

To study the mechanical properties of the composite, different volume fraction of rice husk have been taken. These fibers were randomly distributed in the matrix. Usual hand-lay-up technique has been adopted for manufacturing the composite. To have a

good compatibility between the fiber and matrix, chemical modification of fibers such as Acetone, Alkali and Benzoyl-Chloride treatments has been carried out. It was found that benzoyl-chloride treated fiber composite exhibits favorable strength and stiffness in comparison to other treatments. Moisture absorption behavior of both treated and untreated fiber composite was also carried out. The moisture sorption kinetics of the composite has also been studied. The study confirms that the Fickian's diffusion can be used to adequately describe the moisture absorption in the composite.

For studying the tribo-potential of rice husk , different wear tests like abrasive wear test (multi-pass condition) on Pin-on-Disc wear testing machine and Solid particle erosion behavior by air jet erosion test rig, have been carried out. All these tests have been carried out as per ASTM standard. The abrasive wear tests were conducted using composites of different volume fractions (5%, 10%, 15% and 20%), at different loads (5N, 7.5N, 10N and 15N) and with different sliding velocities. From the initial study it was found that 10 vol% reinforced fiber composite gives maximum strength. For the second phase of the experimentation only 10% fiber volume fraction has been taken. These fibers were treated with Acetone, Alkali and Benzoyl-chloride and their composites were subsequently tested. It was found that Benzoyl-chloride treated fiber composite exhibits better strength and stiffness than the other treated fiber composites.

It is desirable to remove cellulosic materials from rice husk to fully utilise the potential of silica for tribological use. Charring of rice husk at high temperature helps formation of amorphous silica and carbon. Therefore, char has been prepared from rice husk at temperature 850⁰C, 900⁰C and 950⁰C in absence of air. It was found from the experimental investigation that wear resistance of the rice husk reinforced epoxy composite increases with the incorporation of carbonized rice husk.

For studying the solid particle erosion behaviour of rice husk epoxy composite both for treated and untreated rice husk, the erosion test has been accomplished on an erosion test apparatus designed as per ASTM-G76 standard. Due to incorporation of the rice husk fiber the brittle behavior of the neat epoxy changes to semi-ductile behavior when expose to solid particle erosion.

There are other fabrication techniques available like injection moulding, compression moulding and extrusion, where the volume fraction of reinforcement can be increased. In addition there are other chemical methods by which the fiber surface modification can be done. This work can be further extended to those techniques. However the results reported here can act as a starting point for both industrial designer and researchers to design and develop PMC components using rice husk as reinforcement.

The whole dissertation has been divided in to six chapters to put the analysis independent of each other as far as possible. Major works on moisture absorption characteristics, dry sliding wear behavior, erosive wear characteristics are given in chapter 3, 4, 5, and 6 respectively.

TABLE OF CONTENTS

Certificate	i
Acknowledgements	ii
Abstract	iii
Table of Contents	vi
List of Tables	xii
List of Figures	xvi
List of Symbols	xxii
Chapter-1 Introduction	
1.1 Background	1
1.2 Polymeric Matrix	1
1.3 Types of Composite Materials	5
1.3.1 Fiber-Reinforced Composites	5
1.3.1.1 Continuous or long fiber composite	5
1.3.1.2 Discontinuous or short fiber composite	6
1.3.2 Laminate Composites	6
1.3.3 Particulate composite	6
1.3.4 Flake Composite	7
1.4 Natural Fiber Composites: (Initiative in Product Development)	8
1.5 Rice Husk as a natural fiber.	10
1.6 Present work of the thesis	12
1.7 Structure of the thesis.	12
Chapter 2 Literature Survey	
2.1 Natural Fibers: Source and Classification	13

2.2	Natural Fibers : Initiative in product development	13
2.3	Structure of Plant Fiber	18
2.4	Chemical Composition of Natural Fibers	19
2.4.1	Cellulose	19
2.4.2	Hemicelluloses	20
2.4.3	Lignin	21
2.4.4	Pectin	22
2.5	Fabrication Method of PMC	23
2.5.1	Open Moulding Methods	23
2.5.2	Close Moulding Methods	25
2.6	Natural Fiber Reinforced Polymer Composites	30
Chapter-3	Mechanical Characterization of Rice Husk - epoxy composite	
3.1	Introduction	36
3.2	Chemical Modification of Fiber	38
3.2.1	Methods of Chemical Modifications	
3.2.1.1	Alkaline treatment	39
3.2.1.2	Acetone treatment	40
3.2.1.3	Benzoylation treatment	41
3.2.2	EDX and SEM Micrographs of Treated Fibers	41
3.2.3	FTIR Spectroscopy	43
3.2.4	X-ray Diffraction	44
3.3	Thermo-Gravimetic Analysis	45
3.4	Composite Fabrication	46
3.4.1	Preparation of Rice Husk	46

3.4.2	Epoxy resin	47
3.4.3	Composite preparation	47
3.5	Study of Mechanical Properties of Composite	48
3.6	Study of Environmental Effect	49
3.6.1	Moisture absorption test	49
3.6.2	Results and discussion	50
3.6.2.1	Moisture absorption behaviour	50
3.6.2.2	Measurement of diffusivity	51
3.6.2.3	Thickness swelling behaviour	53
3.6.3	Effect of moisture absorption on Mechanical properties	55
3.7	Conclusions	55

Chapter-4 Abrasive Wear of Rice Husk Epoxy Composites

4.1	Introduction	88
4.2	Recent Trends in Wear Research	90
4.3	Theory of Wear	92
4.4	Types Of Wear	94
4.4.1	Abrasive wear	94
4.4.2	Adhesive wear	95
4.4.3	Erosive wear	95
4.4.4	Surface fatigue wear	96
4.4.5	Corrosive wear	96
4.5	Symptoms of Wear	97

4.6	Experiment	98
4.6.1	Preparation for the test specimens	98
4.6.2	Dry sliding wear test	99
4.6.3	Calculation for Wear	100
4.7	Results and Discussion	101
4.8	Worn Surface Morphology	103
4.9	Conclusions	104
Chapter-5	Study of Wear characteristic of Rice Husk char-Epoxy Composites	
5.1	Introduction	171
5.2	Preparation of Rice Husk Char	172
5.3	Preparation of Test specimen.	172
5.4	Dry sliding wear test	173
5.5	Calculation of wear	174
5.6	Result and Discussion.	174
5.7	Wear surface morphology.	176
5.8	Conclusion	177
Chapter-6	Solid Particle Erosion Studies of Rice Husk Epoxy Composites	
6.1	Introduction	213
6.2	Definition	213
6.3	Solid Particle Erosion of Polymer Composites	214
6.4	Experiment	215
6.4.1	Preparation for the test specimens	215
6.4.2	Test apparatus & experiment	216

6.5	Result and Discussion	217
6.6	Surface Morphology	220
6.7	Conclusions	220
Chapter-7 Conclusions and Future Work		
7.1	Conclusions	261
7.2	Recommendation for Further Research	263
Miscellaneous		
	References	264
	Publication	284
	Bibliography	286

LIST OF TABLES

Table No.	Title	Page No.
1.1	Advantages and limitations of polymer matrix materials	3
1.2	Application temperatures of some matrix material	4
1.3	Trends for temperature application of heat resistant composites	4
2.1	Properties of glass and natural fibers	15
3.1	Silicon content of untreated and treated Rice Husk as obtained from EDX analysis.	57
3.2	Crystalline index of the Rice Husk epoxy composites with chemical treatments.	57
3.3	Thermal Degradation parameter of Rice Husk epoxy composites during Thermo Gravimetric Analysis (TGA)	58
3.4	Mechanical properties of Rice Husk epoxy composites	58
3.5	Percentage of weight gain and thickness swelling of Plane Rice Husk epoxy composite expose at steam, Saline and Subzero environment.	59
3.6	Percentage of weight gain and thickness swelling of Acetone treated_ RH-epoxy composite expose at steam, Saline and Subzero environment.	60
3.7	Percentage of weight gain and thickness swelling of Alkali RH- epoxy at steam, Saline and Subzero environment.	61
3.8	Percentage of weight gain and thickness swelling of Benzoyl Chloride treated RH-Epoxy	62
3.9	Diffusion parameters for 15% Rice Husk Epoxy Composite (Both treated and untreated)	63
3.10	Diffusivity of untreated and treated fiber Rice Husk epoxy composites (15%) at different environments.	63
3.11	Swelling rate parameter of treated and untreated Rice Husk epoxy composite in different environments.	64

Table No.	Title	Page No.
3.12	Mechanical properties of both untreated and treated Rice Husk epoxy composite with 15% volume fraction after exposure to different environmental conditions	65
4.1	Priority in wears research.	91
4.2	Type of wear in industries	91
4.3	Symptom and appearance of different type of wear .	97
4.4	Test parameters for dry sliding wear test.	106
4.5 to 4.16	Wear test of pure epoxy at 5N,7.5N,10N,15N at 200rpm,300rpm and 400 rpm	106
4.17 to 4.28	Wear test of 5% Plain RH-epoxy at 5N,7.5N,10N,15N at 200rpm,300rpm and 400 rpm	112
4.29 to 4.40	Wear test of 10 % Plain RH-epoxy at 5N,7.5N,10N,15N at 200rpm,300rpm and 400 rpm	118
4.41 to 4.52	Wear test of 15 % Plain RH-epoxy at 5N,7.5N,10N,15N at 200rpm,300rpm and 400 rpm	124
4.53 to 4.64	Wear test of 20 % Plain RH-epoxy at 5N,7.5N,10N,15N at 200rpm,300rpm and 400 rpm	130
4.65 to 4.76	Wear test of 10 % Acetone treated RH-epoxy at 5N,7.5N,10N,15N at 200rpm,300rpm and 400 rpm	136
4.77 to 4.88	Wear test of 10 % Alkai treated RH-epoxy at 5N,7.5N,10N,15N at 200rpm,300rpm and 400 rpm	142
4.89 to 4.100	Wear test of 10 % Benzoyl Chloride treated RH-epoxy at 5N,7.5N,10N,15N at 200rpm,300rpm and 400 rpm	148
5.1	Density of RH Char reinforced epoxy composite samples	178
5.2	Test parameter for Dry sliding wear	178
5.3 to 5.6	Wear table RH char-epoxy Char temp: 850 ⁰ C Load 5 N VF 10%,20%,30%,40%	179
5.7 to 5.10	Wear table RH char-epoxy Char temp: 850 ⁰ C Load 10 N VF 10%,20%,30%,40%	181
5.11 to 5.14	Wear table RH char-epoxy Char temp: 850 ⁰ C Load 15 N VF 10%,20%,30%,40%	183

Table No.	Title	Page No.
5.15 to 5.18	Wear table RH char-epoxy Char temp: 850 ⁰ C Load 20 N VF 10%,20%,30%,40%	185
5.19 to 5.22	Wear table RH char-epoxy Char temp: 900 ⁰ C Load 5 N VF 10%,20%,30%,40%	187
5.23 to 5.26	Wear table RH char-epoxy Char temp: 900 ⁰ C Load 10 N VF 10%,20%,30%,40%	189
5.27 to 5.30	Wear table RH char-epoxy Char temp: 900 ⁰ C Load 15N VF 10%,20%,30%,40%	191
5.31 to 5.34	Wear table RH char-epoxy Char temp: 900 ⁰ C Load 20N VF 10%,20%,30%,40%	193
5.35 to 5.38	Wear table RH char-epoxy Char temp: 950 ⁰ C Load 5N VF 10%,20%,30%,40%	195
5.39 to 5.42	Wear table RH char-epoxy Char temp: 950 ⁰ C Load 10N VF 10%,20%,30%,40%	197
5.43 to 5.46	Wear table RH char-epoxy Char temp: 950 ⁰ C Load 15N VF 10%,20%,30%,40%	199
5.47 to 5.50	Wear table RH char-epoxy Char temp: 950 ⁰ C Load 20N VF 10%,20%,30%,40%	201
6.1	Particle velocity under different air pressure	222
6.2	Experimental condition for the erosion test	222
6.3	Cumulative weight loss of 5% PRH epoxy composites.	223
6.4	Cumulative weight loss of 10% PRH epoxy composites at different impact angle and velocity	224
6.5	Cumulative weight loss of 15% PRH epoxy composites at different impact angle and velocity	225
6.6	Cumulative weight loss of 20% PRH epoxy composites at different impact angle and velocity	226
6.7	Cumulative weight loss of 5% Acetone RH epoxy composites at different impact angle and velocity	227
6.8	Cumulative weight loss of 10% Acetone RH epoxy composites at different impact angle and velocity	228
6.9	Cumulative weight loss of 15% Acetone RH epoxy	229

Table No.	Title	Page No.
6.10	Cumulative weight loss of 20% Acetone RH epoxy composites at different impact angle and velocity	230
6.11	Cumulative weight loss of 5% Alkali RH epoxy composites at different impact angle and velocity	231
6.12	Cumulative weight loss of 10% Alkali RH epoxy composites at different impact angle and velocity	232
6.13	Cumulative weight loss of 15% Alkali RH epoxy composites at different impact angle and velocity	233
6.14	Cumulative weight loss of 20% Alkali RH epoxy composites at different impact angle and velocity	234
6.15	Cumulative weight loss of 5% Benzoyl Chloride RH epoxy composites at different impact angle and velocity	235
6.16	Cumulative weight loss of 10% Benzoyl Chloride RH epoxy composites at different impact angle and velocity	236
6.17	Cumulative weight loss of 15% Benzoyl Chloride RH epoxy composites at different impact angle and velocity	237
6.18	Cumulative weight loss of 20% Benzoyl Chloride RH epoxy composites at different impact angle and velocity	238
6.19	Parameters characterizing the velocity dependence of erosion rate of PRH and treated RH composites.	239
6.20	Parameters characterizing the velocity dependence of erosion rate of Acetone treated RH composites.	240
6.21	Parameters characterizing the velocity dependence of erosion rate of Alkali treated RH composites.	241
6.22	Parameters characterizing the velocity dependence of erosion rate of Benzoyl Chloride treated RH composites.	242
6.23	Erosion efficiency of PRH-epoxy composites.	243
6.24	Erosion efficiency of Acetone treated RH-epoxy composites.	244
6.25	Erosion efficiency of Alkali treated RH-epoxy composites.	245
6.26	Erosion efficiency of Benzoyl Chloride treated RH-epoxy composites.	246

LIST OF FIGURES

Figure No.	Title	Page No.
1.1	Schematic diagram of different types of Composite	7
1.2	Cost-Performance comparison of reinforcement materials in Polymer Matrix Composites.	9
2.1	Overview of natural fibers	16
2.2	Classification of Plant fiber that can be used as reinforcements in polymers	17
2.3	Structure of an elementary plant fiber (cell)	18
2.4	Structure of Cellulose	20
2.5	Structure of Hemi-Cellulose	21
2.6	Typical Structure of Lignin and structure of Lignin Monomer	22
2.7	Typical structure of Pectin	23
2.8	Hand Lay-Up Techniques	33
2.9	Spray up Technique	33
2.10	Filament Winding Process	33
2.11	Compression Molding Technique	34
2.12	Pultrusion Process	34
2.13	Vacuum Bag Molding	34
2.14	Vacuum Infusion Process	35
2.15	Resin Transfer Molding	35
3.1	Soxhlet Extractor	65
3.2	SEM micrograph of Rice Husk (a)Untreated; (b) Acetone treated; (c) Alkali treated; (d) Benzoyl-Chloride	66
3.3	EDX Spectra showing presence of Silica in treated and untreated Rice Husk Untreated (b) Acetone (c) Alkali (d) Benzoyl Chloride	68
3.4	FTIR spectra of Rice Husk before and after chemical modification	69
3.5	XRD pattern of PRH and Chemically treated Rice Husk.	70

Figure No.	Title	Page No.
3.6	Graph showing weight loss during thermo Gravimetric Analysis (TGA) both for Plain and treated RH-epoxy.	70
3.7	Mold used for composite preparation	71
3.8	Specimen for Tensile test and Flexural Test	71
3.9	Instron H10KS testing machine with tensile and bending attachment.	72
3.10	Variation of Tensile Strength of RH-Epoxy composite with change in Volume Fraction.	73
3.11	Variation of Young's Modulus of RH-Epoxy composite with change in Volume Fraction.	73
3.12	Variation of Flexure Strength of RH-Epoxy composite with change in Volume Fraction.	74
3.13	Variation of Flexural Modulus of RH-Epoxy composite with change in Volume Fraction.	74
3.14	Variation of Mechanical Properties of Plain RH-Epoxy composite with change in Volume Fraction.	75
3.15	Variation of Mechanical Properties of Acetone Treated RH-Epoxy composite with change in Volume Fraction.	75
3.16	Variation of Mechanical Properties of Alkali Treated RH-Epoxy composite with change in Volume Fraction.	76
3.17	Variation of Mechanical Properties of Benzoyl Chloride Treated RH-Epoxy composite with change in Volume Fraction.	76
3.18	Variation of weight gain of the Rice Husk epoxy composites with immersion time at steam environment.	77
3.19	Variation of weight gain of the Rice Husk epoxy with immersion time at saline water environment	77
3.20	Variation of weight gain of the Rice Husk epoxy with immersion time at sub-zero temperature environment	78
3.21	Comparison of Maximum moisture absorption of Plain and chemically treated Rice Husk epoxy composites	78

Figure No.	Title	Page No.
3.22	Variation of thickness of Plain and Chemically treated Rice Husk epoxy composites with immersion time at steam environment	79
3.23	Variation of thickness of the treated Rice Husk epoxy composites with immersion time at saline water environment	79
3.24	Variation of thickness of the treated Rice Husk epoxy composites with immersion time at sub-zero temperature environment	80
3.25	Comparison of maximum thickness swelling of treated and untreated Rice Husk epoxy composites in all the three environments	80
3.26	Variation of $\log (M_t/M_m)$ with $\log (t)$ for RH epoxy composites at steam water environment	81
3.27	Variation of $\log (M_t/M_m)$ with $\log (t)$ for RH epoxy composites at saline water environment	81
3.28	Variation of $\log (M_t/M_m)$ with $\log (t)$ for RH epoxy composites at sub-zero temperature environment	82
3.29	Example Plot of percentage of moisture absorption versus square root of time for calculation of Difusivity	82
3.30	Moisture absorption of RH epoxy at steam nvironment	83
3.31	Moisture absorption of RH epoxy composite at saline water environment	83
3.32	Moisture absorption of RH epoxy composites at sub-zero temperature.	84
3.33	Variation of moisture absorption of Plain RH epoxy composites with square root of immersion time at different environment	84
3.34	Variation of moisture absorption of Acetone treated Rice Husk epoxy composites with square root of immersion time at different environment	85

Figure No.	Title	Page No.
3.35	Variation of moisture absorption of Alkali treated RH epoxy composites with sq root of immersion time at different environment	85
3.36	Variation of moisture absorption of Benzoyl Chloride treated RH epoxy composites with sq root of time.	86
4.1	Abrasive wear mechanism.	95
4.2	Adhesive wear mechanism	95
4.3	Erosive wear mechanism.	96
4.4	Surface fatigue wear mechanism	96
4.5	Corrosive Wear mechanism	97
4.6	Mould for fabrication of pin	155
4.7	Pin-on-Disc machine and experimental setup	156
4.8 to 4.10	Volumetric Wear rate (Wv) with Load for Plain RH composite at different Sliding Velocity	157
4.11	Variation of wear rate as function of sliding velocity for 10 Vol% of rice husk under different loads (5N to15N)	158
4.12 to 4.14	Specific Wear rate (Ws) with Load for Plain RH composite at different Sliding Velocity	159
4.15 to 4.17	Specific Wear rate with Sliding Distance for Plain RH epoxy composite at different velocity	160
4.18 to 4.21	Volumetric Wear rate with Volume Fraction for Plain RH composite at different load	162
4.22 to 4.25	Specific Wear rate (Ws) with Volume fraction for Plain RH-epoxy composite at different load.	164
4.26	Volumetric Wear rate with Sliding Distance for Plain and Chemically treated RH - epoxy composite at 15N	166
4.27	Specific Wear rate with Sliding Distance for Chemically treated RH -epoxy composite at 15 N	166
4.28 to 4.30	Coefficient of friction Vrs. Load for RH -epoxy composite of different VF at sliding velocity	167
4.31	SEM micrographs of worn surface of composite	168

Figure No.	Title	Page No.
5.1	Preparation of RH-Char	172
5.2 to 5.4	Wear with Slide distance Char Temp 850 ⁰ C, 900 ⁰ C, 950 ⁰ C	203
5.5 to 5.7	Vol.Wear with Load Char Temp 850 ⁰ C, 900 ⁰ C, 950 ⁰ C	204
5.8 to 5.10	Sp.Wear with Slide distance Char Temp 850 ⁰ C, 900 ⁰ C, 950 ⁰ C	206
5.11 to 5.13	Wear with Volume Fraction Char Temp 850 ⁰ C, 900 ⁰ C, 950 ⁰ C	207
5.14 to 5.16	Friction Coefficient with Time Char Temp 850 ⁰ C, 900 ⁰ C, 950 ⁰ C	209
5.17	SEM of worn out surface	211
6.1	Details of erosion test rig.	247
6.2 to 6.5	Erosion rate with angle of impingement Velocity 48 m/Sec, VF 5,10,15,20%	248
6.6 to 6.9	Erosion rate with angle of impingement Velocity 70 m/Sec, VF 5,10,15,20%	250
6.10 to 6.13	Erosion rate with angle of impingement Velocity 82 m/Sec, VF 5,10,15,20%	252
6.14 to 6.17	Erosion rate with angle of impingement Velocity 109 m/Sec, VF 5,10,15,20%	254
6.18 to 6.21	Histogram on Erosion rate of Plane, AcetoneAlkali and Benzoyl Chloride treated Rice Husk epoxy composite at impingement angle 40 ⁰	256
6.22 to 6.25	Erosion rate with Velocity Epoxy and Plane, Acetone,Alkali and Benzoyl Chloride treated Rice Husk epoxy composite at impingement angle 60 ⁰	258
6.26	SEM of eroded surface	260

LIST OF SYMBOLS

D_x	Diffusion coefficient
E_r	Erosion rate
FTIR	Fourier Transform Infrared
GS	Abrasive grit size
$H(t)$	Sample thickness at any time 't'
I_c	Crystallinity index
K_{SR}	Thickness swelling parameter
L	Applied Normal Load
M_m	Maximum percentage of moisture content
M_t	Moisture absorption
Δm	Wear loss/ Mass loss
S_d	Sliding Distance
RH	Rice Husk
PRH	Plain Rice Husk
AC	Acetone treated
AL	Alkali Treated
BC	Benzoyl Chloride
SEM	Scanning electron microscope
t	Time
T(s)	Thickness swelling
V	Velocity
VF	Volume Fraction
W	Wear rate
W_v	Volumetric Wear rate

W_s	Specific Wear rate
XRD	X-ray Diffraction
\hat{w}	Cumulative weight loss
α	Impingement / Impact angle
η	Erosion efficiency
μ	Coefficient of friction
ρ	Density

Chapter 1

INTRODUCTION

1.1 BACK GROUND

“Growth in quality of human life, protecting the environment” has been a buzz word of human civilisation. The development of science and technology has created a need to develop engineering materials having light weight, high strength with specific properties as per service requirement at low cost and minimum energy consumption. Thus, the concept of composite materials has come into existence partially replacing existing metals, non-metals and alloys in various engineering applications. Many composites used today are at the leading edge of materials technology, enabling their use in advanced applications such as aircraft and aerospace structures. The idea of composite materials however is not a new or recent one but has been around thousands of years.

Since the early 1960s, there has been an increase in the demand for stronger, stiffer and more lightweight materials for use in the aerospace, transportation and construction industries. Demands on high performance engineering materials have led to the extensive research and development in the field of composite material. Just as mankind has moved from stone age to the composite age, so have composites evolved from the chopped straw bricks of primitive times to today’s sophisticated ceramic matrix composite and metal matrix composite. There has been an extraordinary explosion in composite usage, research and application. Now composites find unusual and exotic applications such as stealth aircraft and superconductive composite. Composites are one of the fastest growing industries and continue demonstrate a significant impact on the material world. [1]

1.2 Polymeric Matrix

Generally, a composite material is composed of reinforcement (fibers, particles, flakes, and/or fillers) embedded in a matrix (polymers, metals, or ceramics). The reinforcement materials provides strength to the composites where as the matrix holds the fibre in desired shape and transfer the load from one fibre to other. A very large number of polymeric materials, both thermosetting and thermoplastic, are used as matrix materials for the composites. Some of the major advantages and limitations of resin matrices are shown in Table-1.1. Some common thermoplastics polymer includes polypropylene, polyvinyl chloride (PVC), nylon, polyurethane, poly-ether-ether ketone (PEEK), polyphenylene sulfide (PPS), polysulpone e.t.c. They have higher toughness, high volume, low processing cost and used within Temperature range $\geq 225^\circ$. Thermoplastics are increasingly used over

thermosets. Their processing is faster than thermoset composites since no curing reaction is required. Thermoplastic composites require only heating, shaping and cooling. They have high toughness, low moisture absorption chemical resistance and low toxicity e.t.c.

Thermosets resin includes polyesters, epoxies and polyamides. Polyesters have Low cost, good mechanical strength, low viscosity and versatility, good electrical properties and good heat resistance. They can be used in cold and hot moulding with curing temperature is 120°C. Epoxy resins are widely used for most advanced composites. They have low shrinkage during curing, high strength and flexibility, adjustable curing range, better adhesion between fibre and matrix, better electrical properties and resistance to chemicals and solvents. However epoxies are somewhat toxic in nature. They have limited temperature application range up to 175°C and moisture absorption affecting dimensional properties. They have also high thermal coefficient of expansion and slow curing. Polyamides have excellent mechanical strength, excellent strength retention for long term temperature range of 260-315°C (500-600°F) and short term in 370°C (700°F) range. They have also excellent electrical properties, good fire resistance and low smoke emission. The composite can be hot mould under pressure and the curing temperature is 175°C and 315°C

Usually the resinous binders (polymer matrices) are selected on the basis of adhesive strength, fatigue resistance, heat resistance, chemical and moisture resistance etc. The resin must have mechanical strength commensurate with that of the reinforcement. It must be easy to use in the fabrication process selected and also stand up to the service conditions. The resin matrix must also be capable of wetting and penetrating into the bundles of fibres which provide the reinforcement, replacing the dead air spaces therein and offering those physical characteristics capable of enhancing the performance of fibres.

Shear, chemical and electrical properties of a composite depend primarily on the resin. Again, it is the nature of the resin that will determine the usefulness of the laminates in the presence of a corroding environment and service temperature. Rule of mixture is a tool to predict the properties like density, tensile strength and modulus etc. of the composite when the properties of matrix and fiber and their volume fraction are known.

Table-1.2 and 1.3 indicate the approximate service temperature ranges for the resins and composites [2, 3]. It should be remembered that there is no place for compromise as to the nature of the matrix material, particularly when it comes to the application temperature of the composite. If the application temperature exceeds 300-350°C metal matrix appears to be the only alternative, at least for the present.

Table- 1.1 Advantages and limitations of polymer matrix materials

Advantages	Limitation
<ul style="list-style-type: none"> ● High strength and Low densities material. ● Good stiffness and toughness, ● Good corrosion resistance ● Low thermal conductivities ● Low electrical conductivities ● Good fatigue life ● Acoustic insulation ● Energy dissipation ● Tailorable properties ● Aesthetic Colour effects 	<ul style="list-style-type: none"> ● Low transverse strength ● Low operational temperature limits ● Susceptibility to environmental degradation due to moisture, radiation, atomic oxygen (in space) ● High residual stress due to large mismatch in coefficients of thermal expansion both fiber and matrix ● Polymer matrix can not be used near or above the glass transition temperature ● High cost of raw materials and fabrication. ● Composites are brittle and thus are more easily damagable. ● Reuse and disposal may be difficult. ● Health hazards during manufacturing , during and after use. ● Joining to parts is difficult ● Hot curing is necessary in many cases requiring special tooling and curing takes time ● Analysis is difficult.

Table- 1.2 Application temperatures of some matrix material

Matrix material	Limit of	
	Long term exposure, °C	Short term exposure, °C
Unsaturated polyesters	70	100
Epoxies	125	200
Phenolics	250	1600
Polyimides	315	400
Aluminium	300	350

Table - 1.3 Trends for temperature application of heat resistant composites[3]

Fiber reinforced Composite	Maximum service temperature, °C	Specific weight g/cm ³
Carbon / Epoxy	180	1.4
Boron/Epoxy	180	2.1
Borsic / Aluminium	310	2.8
Carbon/Polyimide	310	1.4
Boron/Polyimide	310	2.1
Carbon/Polyaminoxaline	350	1.4
Carbon/Polybenzthiazole	400	14
Borsic/Titanium	540	3.6
Carbon/Nickel	930	5.3
Whisker/Metals	1800	2.8-5.6

1.3 TYPES OF COMPOSITE MATERIALS

The composite materials are broadly classified into the following categories as shown in Figure-1.1 (a - e).

1.3.1 Fiber-reinforced composites

Reinforced-composites are popularly being used in many industrial applications because of their inherent high specific strength and stiffness. Due to their excellent structural performance, the composites are gaining potential also in tribological applications. Fiber reinforced composites materials consists of fiber of high strength and modulus bonded in to a matrix with distinct interfaces (boundary) between them [4,5]. In this form both fibers and matrix retain their physical and chemical identities. Yet they produce a combination of properties that cannot be achieved with either of the constituents acting alone. In general, fibers are the principal load carrying candidates, while the surrounding matrix keeps them in the desired location and orientation [6, 7]. A Fibrous composite can be classified into two broad groups: continuous (long) fiber composite and discontinuous (short) fiber composite.

1.3.1.1 Continuous or long fiber composite

Continuous or long fibre composite consists of a matrix reinforced by a dispersed phase in the form of continuous fibers. A continuous fiber is geometrically characterized as having a very high length-to- diameter ratio. They are generally stronger and stiffer than bulk material. Based on the manner in which fibers are packed within the matrix, it is again subdivided in to two categories: (a) unidirectional reinforcement and (b) bidirectional reinforcement. In unidirectional reinforcement, the fibres are oriented in one direction only where as in bidirectional reinforcement the fibres are oriented in two directions either at right angle to one another (cross-ply), or at some desired angle (angle-ply). When fibres are large and continuous, they impart certain degree of anisotropy to the properties of the composites particularly when they are oriented. Multi-axially oriented continuous fiber composites are also display near isotropic properties.

1.3.1.2 Discontinuous or short fiber composite

Short-fiber reinforced composites consist of a matrix reinforced by a dispersed phase in form of discontinuous fibers (length $< 100^*$ diameter). The low cost, ease of fabricating complex parts, and isotropic nature are enough to make the short fiber composites the material of choice for large-scale production. Consequently, the short-fiber reinforced composites have successfully established its place in lightly loaded component manufacturing. Further the discontinuous fiber reinforced composite divided into: (a) biased or preferred oriented fiber composite and (b) random oriented fiber composite. In the former, the fibers are oriented in predetermined directions, whereas in the latter type, fibers remain randomly. The orientation of short fibers can be done by sprinkling of fiber on to given plane or addition of matrix in liquid or solid state before or after the fiber deposition. The discontinuities can produce a material response that is anisotropic, but the random reinforcement produces nearly isotropic properties.

1.3.2 Laminate Composites

Laminate Composites are composed of layers of materials held together by matrix. Generally, these layers are arranged alternatively for the better bonding between reinforcement and the matrix. These laminates can have uni- directional or bi-directional orientation of the fiber reinforcement according to the end use of the composite. The different types of composite laminates are: unidirectional, angle-ply, cross-ply and symmetric laminates. A hybrid laminate can also be fabricated by the use of different constituent materials or of the same material with different reinforcing pattern. In most of the applications of laminate composites, man-made fibers are used due to their good combination of physico-mechanical and thermal behaviour.

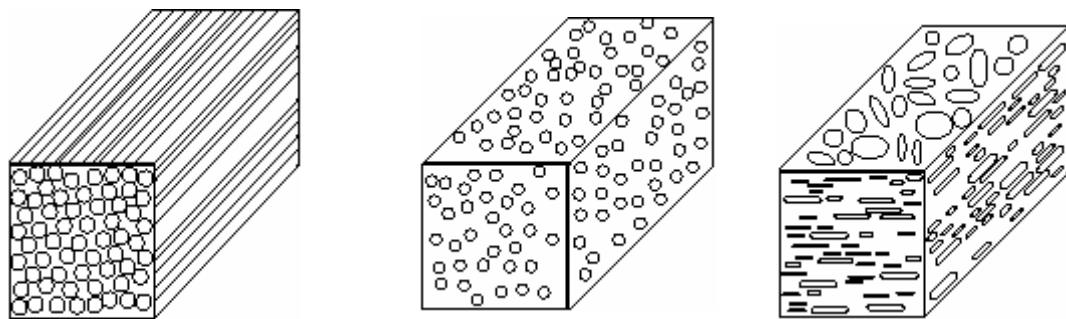
1.3.3 Particulate Composite

Particulate composite consists of the composite material in which the filler materials are roughly round. An example of this type of composite would be the unreinforced concrete where the cement is the matrix and the sand serves as the filler. Lead particles in

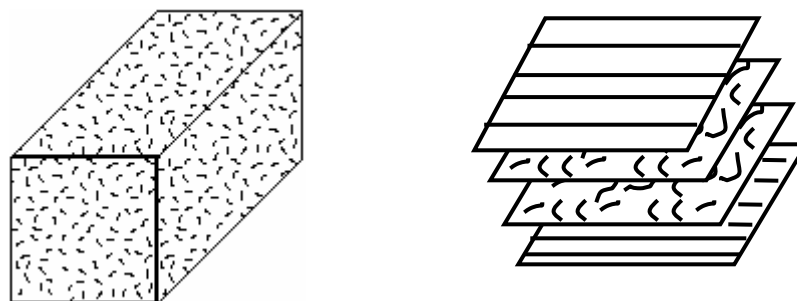
copper matrix is another example where both the matrix and the filler are metals. Cermet is a metal matrix with ceramic filler. Particulate composites offer isotropic properties of composite along with increase in toughness. Particulate composites are used with all three types of matrix materials – metals, polymers and ceramics.

1.3.4 Flake composites

Flakes are often used in place of fibers as can be densely packed. Metal flakes that are in close contact with each other in polymer matrices can conduct electricity or heat, while mica flakes and glass can resist both. Flakes are not expensive to produce and usually cost less than fibers. But they fall short of expectations in aspects like control of size, shape and show defects in the end product. Glass flakes tend to have notches or cracks around the edges, which weaken the final product. They are also resistant to be lined up parallel to each other in a matrix, causing uneven strength.



(a) Continuous fiber composite (b) Particulate composite (c) Flake composite



(d) Random fiber (short fiber) Composite (e) Laminate Composite

Figure-1.1 (a-e) Schematic diagram of different types of Composite

1.4 NATURAL FIBER COMPOSITES:

The charm of using synthetic fibers in polymer composites is fading because they are expensive and non-biodegradable. Environmental awareness on the other hand today motivates the researchers worldwide on the studies of natural fiber reinforced polymer composite as a cost effective option to synthetic fiber reinforced composites. The availability of natural fibers and ease of manufacturing have tempted researchers to try locally available inexpensive fibers and to study their feasibility of reinforcement purposes and to what extent they satisfy the required specifications of a good reinforcement in polymer composite for different applications. With low cost and high specific mechanical properties, natural fiber represents a good renewable and biodegradable alternative to the most common synthetic reinforcement, i.e. glass fiber. Natural fibers require very little energy to produce, and because they possess high calorific values, can be incinerated at the end of their lifetime for energy recovery. All plant-derived fibers utilize carbon dioxide when they are grown and can be considered CO₂ natural, meaning that they can be burned at the end of their lifetime without additional CO₂ being released into the atmosphere [8]. On the other hand, glass fibers are not CO₂ natural and require the burning of fossil fuels to provide the energy needed for production. The burning of fossil fuel-based products releases enormous amounts of CO₂ into the atmosphere and this phenomenon is believed to be the main cause of the greenhouse effect and the climatic changes that are being observed in the world today [9]. The geometry and properties of natural fibers depend, for example, on the species, growing conditions, cambium age, harvesting, defibration and processing conditions. Since cellulose fibers have the possibility to show a wide range with both poor and strong bonding to polymer matrix materials, depending on fiber-matrix modification and compatibility, the optimal interface is typically somewhere between the two extreme cases. For instance, if the interface is too strong, the composite material can become too brittle, resulting in a notch-sensitive material with low strength, since stress concentrating defects are inevitable [10].

The term “natural fiber” covers a broad range of vegetable, animal and mineral fibers. However in the composite industry, it is usually refers to wood fiber and agro based bast, leaf, seed, and stem fibers. These fibers often contribute greatly to the structural

performance of plant and, when used in plastic composites, can provide significant reinforcement.

Despite the interest and environmental appeal of natural fibers, their use is limited to non-bearing applications due to their lower strength compared with synthetic fiber reinforced polymer composite. The stiffness and strength shortcomings of bio composites can be overcome by structural configurations and better arrangement in a sense of placing the fibers in specific locations for highest strength performance. Accordingly extensive studies on preparation and properties of polymer matrix composite (PMC) replacing the synthetic fiber with natural fiber like Jute, Sisal, Pineapple, Bamboo, Kenaf and Bagasse were carried out [11-16]. These plant fibers have many advantages over glass fiber or carbon fiber like renewable, environmental friendly, low cost, lightweight, high specific mechanical performance.

Increased technical innovation, identification of new applications, continuing political and environmental pressure and government investments in new methods for fiber harvesting and processing are leading to projections of continued growth in the use of natural fibers in composites. The easy availability of natural fibers and manufacturing have motivated researchers world wide recently to try locally available inexpensive fibers and to study their feasibility of reinforcement purposes and to what extent they satisfy the required specifications of good reinforced polymer composite for tribological applications [17]. In terms of cost and performance, the lignocellulose composites are placed between filler and the synthetic fibers composites (fig.1.2) [18]

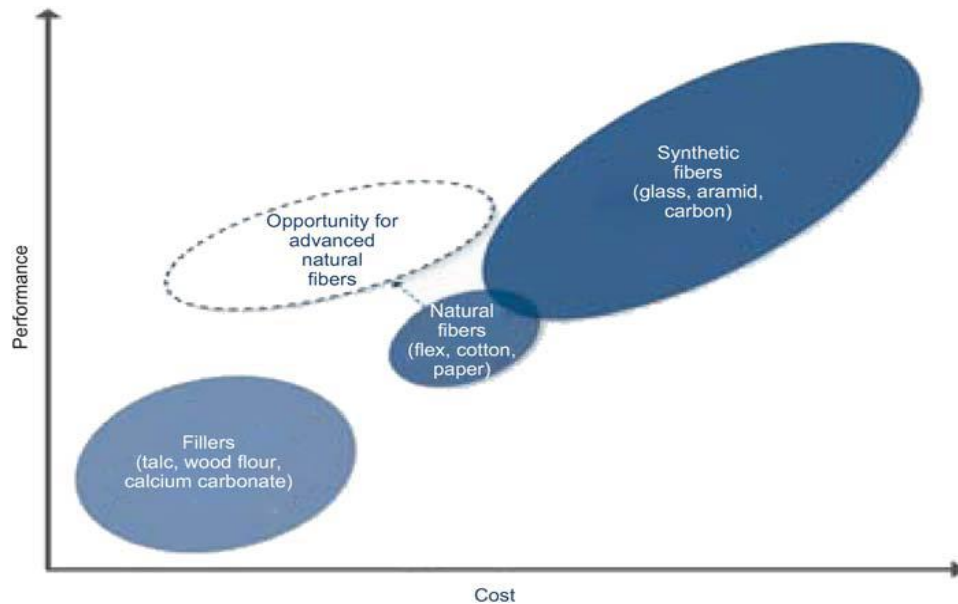


Figure-1.2 Cost-Performance comparison of reinforcement materials in Polymer Matrix Composites.[18]

1.5 RICE HUSK AS NATURAL FIBER :

There are many potential natural resources, which India has in abundance. Most of it comes from agriculture or forest. Rice husk (RH), a cellulose based fiber is an agricultural waste material abundantly available in rice-producing countries. They are the natural sheaths that form on rice grains during their growth and removed during the refining of rice. These husks have no commercial interest. Globally, approximately 600 million tons of rice paddy is produced each year [19]. On an average 20% of the rice paddy is husk, giving an annual total production of 120 million tones. A large quantity of husk, which is known to have a fibrous material with high silica content, is available as waste from rice milling industries. The moisture content of RH ranges from 8.68 to 10.44% and the bulk density ranges from 86 to 114 kg/m³[18]. The calorific value of RH is 13-15 MJ/Kg. [20]. The RH generally contains 20% ash, 20% lignin, 35% cellulose, 25% hemicellulose. The chemical composition of the RH varies from sample to sample which may be due to the different geographical conditions, type of paddy, climatic conditions and type of fertilizer used.

RH is unusually high in ash compared to other biomass fuels – close to 20% of husk. The ash is with 92 to 95% silica, highly porous and lightweight, with a very high external surface area. Its absorbent and insulating properties are useful to many research studies.

Silicon [21] enters the rice plant through its root in a soluble form, probably as a silicate or monosilicic acids, and then moves to the outer surface of the plant, where it is become concentrated by evaporation and polymerization to form a cellulose silica membrane. There is quite general agreement that the silica is predominantly in inorganic linkages, but some of the silica is also bonded covalently to the organic compounds. This portion of the silica cannot be dissolved in alkali and can withstand very high temperatures. The outer surface of RH is relatively rougher than the inner surface that houses the rice grain. It contains significant amounts of silica (20% w/w). Silica exists on the outer surface [22] of RH in the form of silicon cellulose membrane that forms a natural protective layer against termites and other micro-organisms attack on the paddy.

RH is available in abundance in nature with several important applications. It can be used as pet food fiber, pillow stuffing, fertilizer, etc. Rice hulls can be utilized for brewing beer to increase the lautering ability of a mash. They are used as a press aid to improve extraction efficiency of apple pressing. It can be used to produce mesoporous molecular sieves, which are usually used as a catalysts support for various chemical reactions for drug delivery systems, and as adsorbent in waste water treatment, etc. Silicon carbide “whiskers” can be synthesized from RH and subsequently used to reinforce ceramic cutting tools to increase their strength manifold. It is also used to produce energy by combustion. India is a major rice-producing country and the husk generated during milling is mostly used as a fuel to produce energy through direct combustion and/or by gasification. After combustion, a substantial amount of rice husk ash (RHA) is generated. The specific use of RHA is usually as an aggregate and filler for concrete and board production, an economical substitute for micro silica/silica fumes, an absorbent for oils and chemicals, soil ameliorants, as a source of silicon, as insulation powder in steel mills, as repellents in the form of vinegar-tar, as a release agent in the ceramics industry, and as an insulation material for homes and refrigerants. RHA has also been used in the manufacture of refractory bricks [19].

Going through the available information on the utilisation of RH, it is seen that RH is a fibrous material and has a varied range of aspect ratio. Thus, it can be used as filler for making light weight polymer composites which provides an effective means for proper and optimum utilization of a large quantity of rice husk produced every year. Research efforts

are in progress to incorporate RH in polymers so that they can enhance the physical, mechanical and tribological properties of the latter [23-27].

1.6 PRESENT WORK OF THE THESIS

The present work deals with the preparation of Polymer Matrix Composite (PMC) using epoxy resin as the matrix material and RH as reinforcement material. Simple hand lay-up technique is used to fabricate the composite. Volume fractions of fiber were varied from 5-20%. The lignocellulosic fibers are hydrophilic and absorb moisture. Removal of moisture from the fiber is an essential step before the preparation of composite. Chemical fiber treatments have been carried out on the fibers to improve the strength, separation, crystallinity and removal of hydrophilic and thermally unstable Rice Husk constituents. Moisture absorption behavior of the developed composites was studied after modifying the fiber surface. To assess the suitability of the composite in tribological needs different tribological tests have been carried out under simulated laboratory conditions. The surface of fractured and worn out samples were studied using Scanning Electron Microscope (SEM) to have an idea about the fractured behavior of the composite.

1.7 STRUCTURE OF THE THESIS

The present thesis contains six chapters. The first chapter introduces the polymer matrix composite and also discusses the use of natural fiber as a reinforcement material in polymer composite. In the second chapter detail discussion of structure and chemical composition of natural fibers, over view of fabrication process of polymer matrix composite and work related to present investigation available in literature are presented. The effect of environment on mechanical properties of both untreated and treated rice husk reinforced composite along with moisture absorption characteristics have been presented. In the fourth chapter abrasive wear behavior of different doses of rice husk reinforced composite has been studied. Fifth chapter discusses the wear behavior of rice husk char (prepared by different carbonization temperature) reinforced epoxy composite. In the sixth chapter solid particle erosion wear behavior of the composite is presented. Finally, conclusions from the present study and future scopes are included in chapter seven.

Chapter 2

LITERATURE SURVEY

2.1 NATURAL FIBERS: Source and Classification

The wonder materials Composites, with light weight, high strength to weight ratio and stiffness properties has replaced most of the metal and alloys in recent times. Properties of composites are strongly dependent on the properties of their constituent materials, their distribution and the interaction among them. Generally, fibers are the principal load carrying members, while the matrix keeps them at the desired location and orientation, acts as a load transfer medium between the fibers, and protects them from environmental damages. The composite properties may be the volume fraction sum of the properties of the constituents or the constituents may interact in a synergistic way resulting in improved or better properties. Apart from the nature of the constituent materials, the geometry of the reinforcement (shape, size and size distribution) influences the properties of the composite to a great extent. The concentration distribution and orientation of the reinforcement also affect the properties. Industries today are under tremendous pressure to design ecologically friendly materials for their products. This is because of growing environmental awareness and new rules and regulations that are binding on industries. As a result researcher's choices are shifting from synthetic fiber reinforced composite and plastics to natural fiber composites. Polymeric materials reinforced with synthetic fibers such as glass, carbon and aramid provide advantages of high stiffness and strength to weight ratio compared to conventional construction material like wood, concrete and steel. Despite its several advantages, the use of natural fiber application in polymeric composites is increasing day by day. A substantial increase in the agricultural by products and wastes of different types has attracted many researchers to develop and characterize new and low cost materials from renewable local resources.

2.2 Natural fiber : Initiative in product development

Natural fibers can be obtained from natural resources such as plants, animals or minerals. With the increase of global crisis and ecological risk, the unique advantages of plant fibers such as abundant, nontoxic, non-irritation of skin, eyes or respiratory system, non-corrosive property, plant-based fibre reinforced polymer composites has lately received increasing attention both from academia and by industries. It can be brought to notice that compared to most synthetic fibers, natural fibers have emerged to be more environment friendly and appeared realistic alternative for the following reasons:

(1) Natural fiber production has consumed of non-renewable energy lesser than synthetic fiber and thus lesser pollution emissions.

(2) The higher volume fraction of natural fiber than synthetic fiber for equivalent performance has decreased the volume and weight of base synthetic polymer matrix, which decreases the energy use and emissions in production of polymer.

(3) The lower weight (20-30 wt. %) and higher volume of natural fiber compared to synthetic fiber has improved the fuel efficiency and reduced emission in the use phase (auto applications)

(4) The incinerated of natural fiber composite direct to positive carbon credit and enhanced the net effects on air emissions and energy recovery due to the lower mass

(5) Natural fiber composites are claim to offer environmental advantages such as reduced dependence on non-renewable energy/material sources, lower pollutant emissions, lower greenhouse gas emissions, enhanced energy recovery and end of life biodegradability of components.

(6) Natural fibers have lower cost (US\$ 200-1000/ton) and energy to produce (4GJ/ton) whereas glass cost US\$ 1200-1800/ton and energy to produce is 30GJ and carbon cost US\$ 12500/ton and energy to produce it is 130GJ. Such superior advantages are important driver of increased future use of natural fiber composite in various applications and under different loading

Natural organic fibers can be derived from either animal or plant sources. The majority of useful natural fibers are plant derived, with the exceptions of wool and silk. All plant fibers are composed of cellulose, whereas fibers of animal origin consist of proteins. Natural fibers in general can be classified based on their origin, and the plant-based fibers can be further categorized based on part of the plant they are recovered from. An overview of natural fibers is presented in Figure-2.1.

Generally, plant or vegetable fibers are used to reinforce polymer matrices and a classification of vegetable fibers is given in Figure-2.2. Plant fibers are a renewable resource and have the ability to be recycled. The plant fibers leave little residue if they are burned for disposal, returning less carbon dioxide (CO₂) to the atmosphere than is removed during the plant's growth. The leading driver for substituting natural fibers for glass is that they can be grown with lower cost than glass. As can be seen from Table-2.1, the tensile strength of natural fibers is substantially lower than that of glass fibers though the modulus

is of the same order of magnitude. However, when the specific modulus of natural fibers (modulus per unit specific gravity) is considered, the natural fibers show values that are comparable to or even better than glass fibers. Material cost savings, due to the use of natural fibers and high fiber filling levels, coupled with the advantage of being non-abrasive to the mixing and moulding equipment make natural fibers an exciting prospect. These benefits show different avenues of the natural fibers for their applications in Polymer Matrix Composite for use in automotive, household appliances, and other applications.

Table-2.1 Properties of glass and natural fibers [28]

Properties	Fiber						
	E-glass	Hemp	Flax	Jute	Sisal	Coir	Ramie
Density (gm/cc)	2.25	1.48	1.4	1.46	1.33	1.25	1.5
Tensile strength (MPa)	2400	550-900	800-1500	400-800	600-700	220	500
Young's Modulus (GPa)	73	70	60-80	10-30	38	6	44
Specific Modulus (GPa)	29	-	26-46	7-21	29	5	2
Failure Strain (%)	3	1.6	1.2-1.6	1.8	2-3	15-25	2
Moisture absorption(%)	-	8	7	12	11	10	12-17

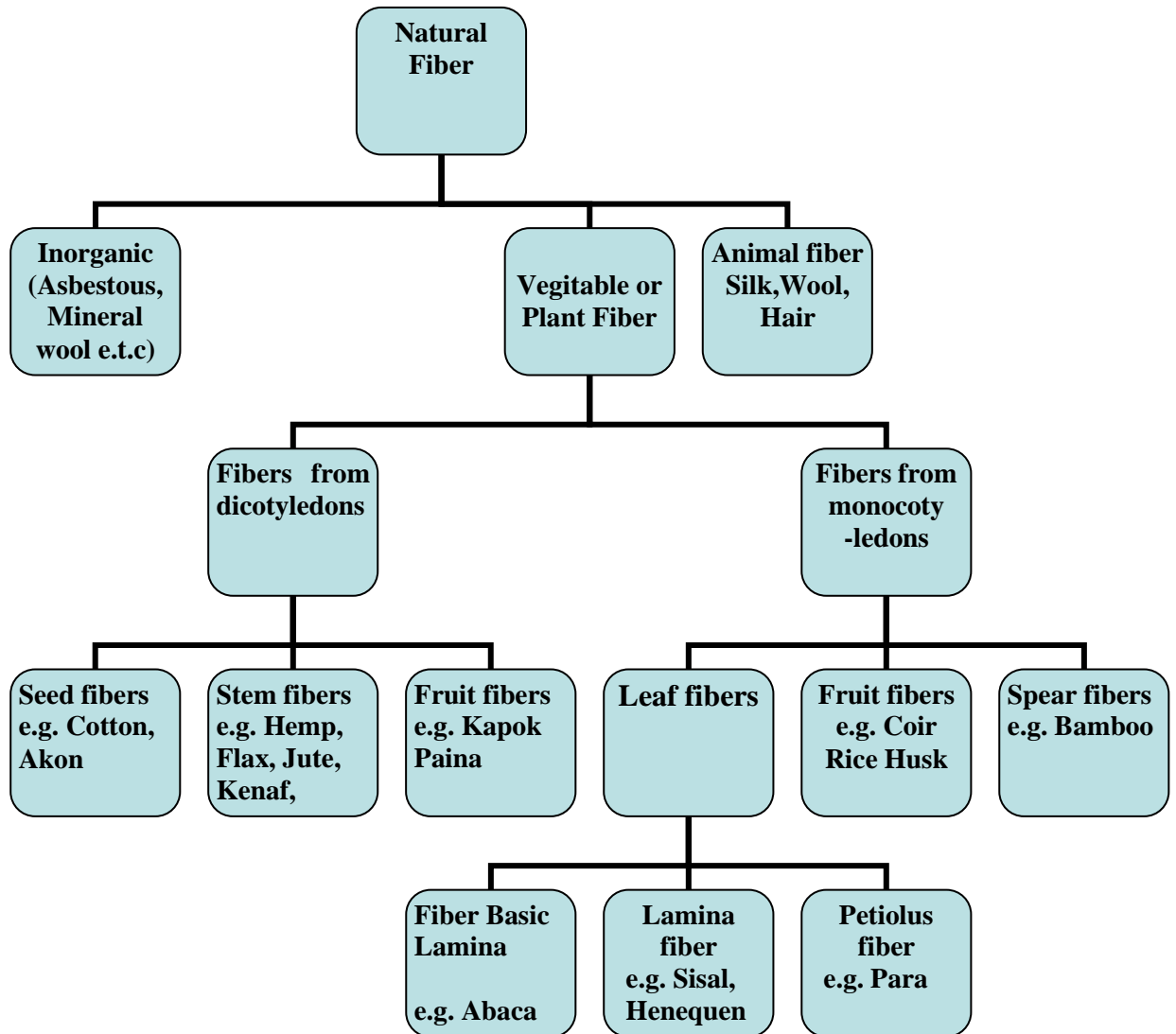


Figure-2.1 Overview of natural fibers [28]

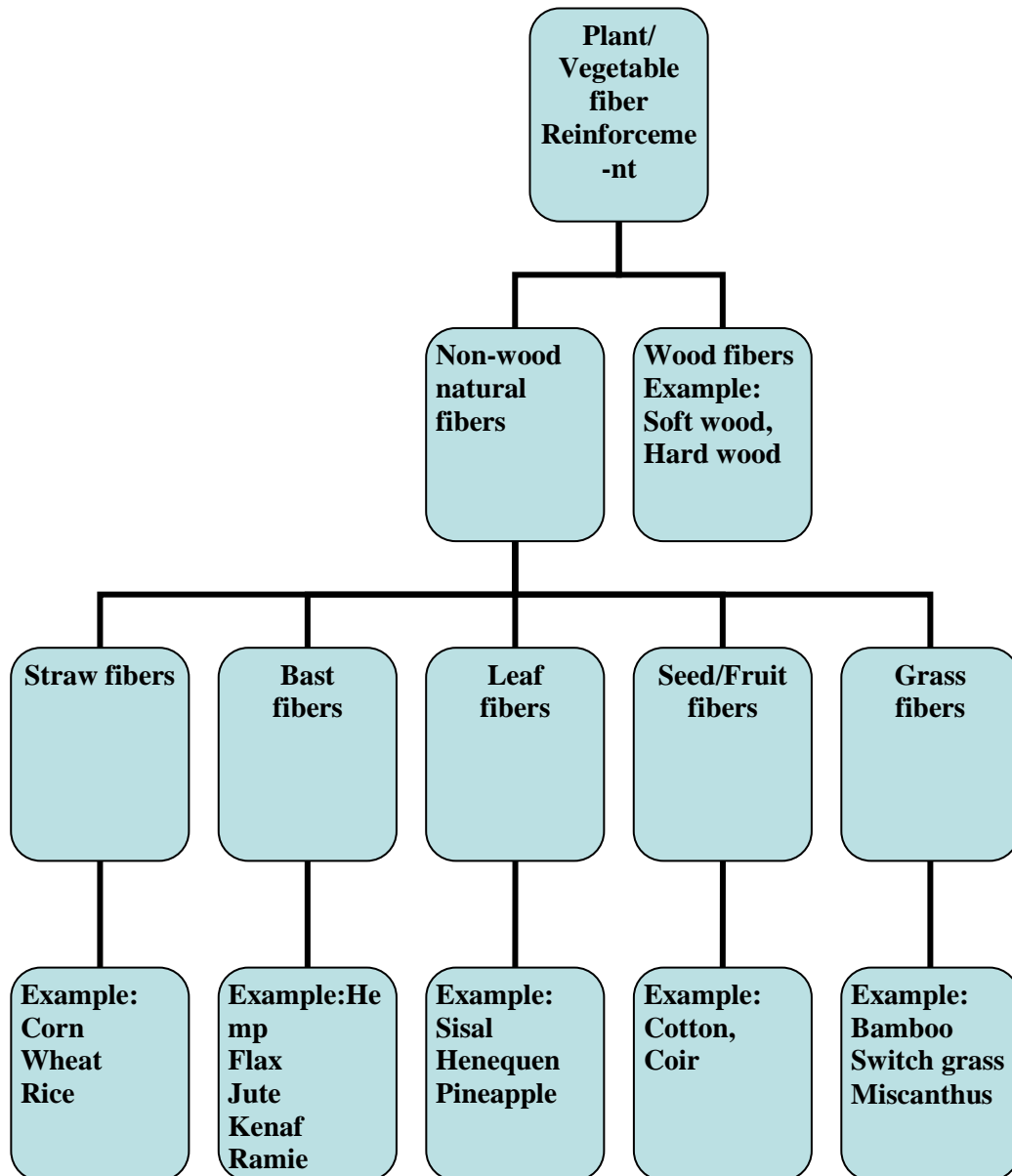


Figure-2.2 Classification of Plant fiber that can be used as reinforcements in polymers [29]

2.3 STRUCTURE OF PLANT FIBER

Natural fibers can be considered as composites of hollow cellulose fibrils held together by a lignin and hemicellulose matrix. The cell wall in a fiber is not a homogenous membrane [30]. Each fiber has a complex, layered structure consisting of a thin primary wall which the first layer deposited during cell growth is encircling a secondary wall shown in fig.2.3. The secondary wall is made up of three layers and the thick middle layer determines the mechanical properties of the fiber. The middle layer consists of a series of helically wound cellular micro fibrils formed from long chain cellulose molecules. The angle between the fiber axis and the micro fibrils is called the micro fibrillar angle. The characteristic value of micro fibrillar angle varies from one fiber to another. Such microfibrils have typically a diameter of about 10– 30 nm and are made up of 30–100 cellulose molecules in extended chain conformation and provide mechanical strength to the fiber. The amorphous matrix phase in a cell wall is very complex and consists of hemicellulose, lignin, and in some cases pectin. The hemicellulose molecules are hydrogen bonded to cellulose and act as cementing matrix between the cellulose microfibrils, forming the cellulose–hemicellulose network, which is thought to be the main structural component of the fiber cell. The hydrophobic lignin acts as matrix material which binds and provides stiffness to cellulose/hemicellulose in cell wall composite.

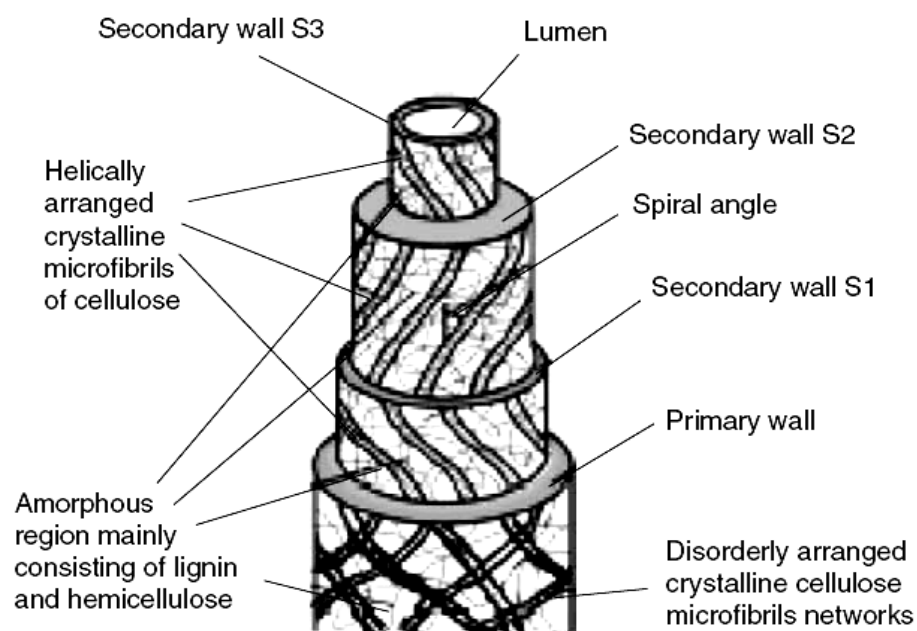


Figure-2.3 Structure of an elementary plant fiber (cell)

2.4 CHEMICAL COMPOSITION OF NATURAL FIBERS

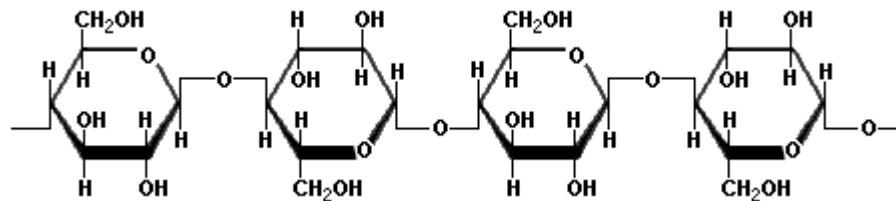
The constituent of any natural fiber vary with origin, area of production, variety and maturation of plant. The major constituent of a fully developed natural fiber cell walls are cellulose, hemicellulose, lignin and pectin. These hydroxyl-containing polymers are distributed throughout the fiber wall [31].

2.4.1 Cellulose

Cellulose is a polymer of β -D-Glucose oriented in which -CH₂OH group is alternating above and below the plane of the cellulose molecule thus producing long, unbranched chains (Fig.2.4) . The absence of side chains allows cellulose molecules to lie close together and form rigid structures. Cellulose is the major structural material of plants. The long thin crystalline micro-fibrils in the secondary cell wall are made of cellulose. It is the reinforcing material and is responsible for the high mechanical strength of fibers. It consists of a linear polymer of D-anhydroglucose units where two adjacent glucose units are linked together by β -1, 4-glycosidic linkages with elimination of one water molecule between their -OH groups at carbon atoms 1 and 4. Chemically, cellulose is defined as a highly crystalline segment alternating with regions of non-crystalline or amorphous cellulose [32, 33].

The of β -D-Glucose monomers (C₆H₁₀O₅) in cellulose form hydrogen bonds both within its own chain (intra-molecular) forming fibrils and with neighboring chains (intermolecular), forming micro-fibrils. These hydrogen bonds lead to formation of a linear crystalline structure with high rigidity and strength. The amorphous cellulose regions have a lower frequency of intermolecular hydrogen bonding, thus exposing reactive intermolecular -OH groups to be bonded with water molecules. Amorphous cellulose can therefore be considered as hydrophilic in nature due to their tendency to bond with water. On the other hand, very few accessible intermolecular -OH are available in crystalline cellulose and it is far less hydrophilic than amorphous cellulose. Crystalline micro-fibrils have tightly packed cellulose chains within the fibrils, with accessible -OH groups present on the surface of the structure. Only very strong acids and alkalis can penetrate and modify the crystalline lattice of cellulose. Wood is largely cellulose, and cotton is almost pure cellulose. Cellulose can be

hydrolyzed to its constituent glucose units by microorganisms that inhabit the digestive tract of termites and ruminants



Cellulose

Figure-2.4 Structure of Cellulose

2.4.2 Hemicellulose

They comprise a group of polysaccharides composed of a combination of 5- and 6-carbon ring sugars. Hemicelluloses comprise almost one-third of the carbohydrates in woody plant tissue. The chemical structure of hemicelluloses consists of long chains of a variety of pentoses, hexoses, and their corresponding uronic acids (Fig.2.5). Hemicelluloses may be found in fruit, plant stems, and grain hulls. Although hemicelluloses are not digestible, they can be fermented by yeasts and bacteria. The polysaccharides yielding pentoses on hydrolysis are called pentosans. Xylan is an example of a pentosan consisting of D-xylose units with 1 β →4 linkages. Hemicellulose is very hydrophilic, soluble in alkali, and easily hydrolyzed in acids.

Hemicelluloses differ from cellulose in three different ways. Firstly, unlike cellulose (containing only 1,4- β -D-glucopyranose units) they contain several different sugar units. Secondly, they exhibit a considerable degree of chain branching, whereas cellulose is a linear polymer. Thirdly, the degree of polymerization of native cellulose is ten to hundred times higher than that of hemicelluloses. Unlike cellulose, the constituents of hemicelluloses differ from plant to plant. Hemicelluloses contain substituents like acetyl (-COCH₃) groups and glucuronic acid. By attaching ferulic acid and p-coumaric residues, hemicelluloses can

form covalent bonds to lignin [34]. Due to this linking ability of hemicelluloses, degradation of it leads to disintegration of the fibers into cellulose micro-fibrils resulting in lower fiber bundle strength [35].

Mainly the acid residues attached to hemicelluloses make it highly hydrophilic and increase the fiber water uptake, which increases the risk of microbiological fiber degradation. It has been found that hemicelluloses thermally degrade more at lower temperatures (150-180°C) than cellulose (200-230°C) [36].

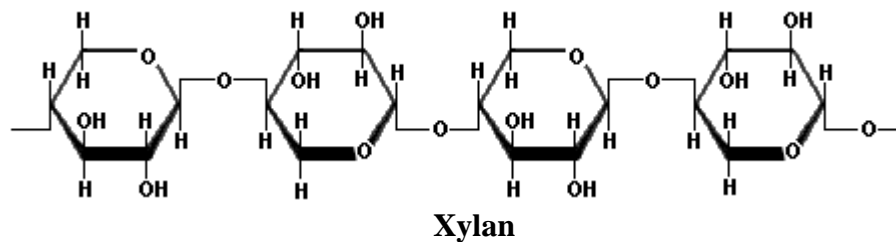


Figure-2.5 Structure of Hemi-Cellulose

2.4.3 Lignin

Lignin is a complex hydrocarbon polymer with both aliphatic and aromatic constituents. They are totally insoluble in most solvents and cannot be broken down to monomeric units. Lignin is totally amorphous and hydrophobic in nature. It is the compound that gives rigidity to the plants.

Lignin glues the cellulose fibers together to form a stiff structure, making it possible for trees of 100 meters to remain upright. Lignin is essentially a disordered, polyaromatic, and cross-linked polymer arising from the free radical polymerizations of mainly three monomers (monolignols) structurally related to phenyl-propane [37]. These three monomers make almost all lignin found in nature [Fig2.6(a),(b)]. The *p*-Coumaryl alcohol is a minor component of grass and forage type lignins. Coniferyl alcohol is the predominant lignin monomer found in softwoods (hence the name). Both coniferyl and sinapyl alcohols are the building blocks of hardwood lignin. Hydroxyl, methoxyl, and carbonyl groups have been identified in lignin. Free radical coupling of the lignin monomers gives rise to a very condensed, reticulated, and cross-linked structure. The lignin matrix is therefore analogous to a thermoset polymer in conventional polymer terminology. The dissolution of lignin

using chemicals aids fiber separation. When exposed to ultraviolet light, lignin undergoes photochemical degradation [38]. The lignin seems to act like a matrix material within the fibers, making stress transfer on a micro-fibril scale and single fiber scale possible.

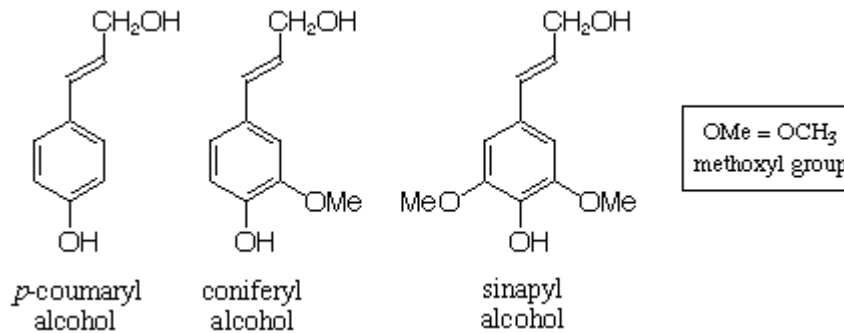


Figure-2.6(a). Structure of Lignin Monomer

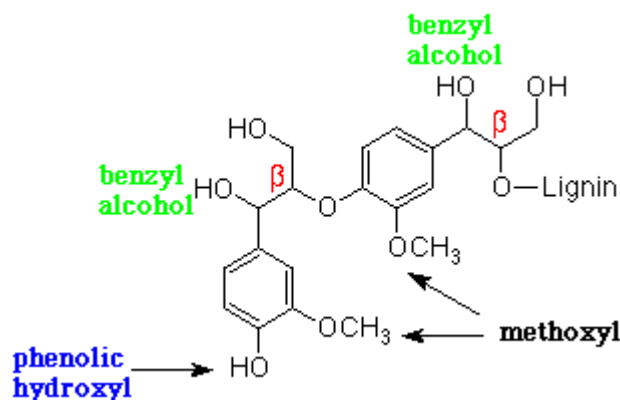


Figure-2.6(b). Typical Structure of Lignin

2.4.4 Pectin

Pectin is a complex branched structure of acidic structural polysaccharides, found in fruits and bast fibers. The majority of the structure consists of homopolymeric partially methylated poly- α -(1-4)-D-galacturonic acid residues, but there are substantial 'hairy' non-gelling areas of alternating α -(1-2)-L-rhamnosyl- α -(1-4)-Dgalacturonosyl sections containing branch-points with mostly neutral side chains (1-20 residues) of mainly L-arabinose and D-galactose (rhamnogalacturonan-I). Pectin is the most hydrophilic compound in plant fibres due to the carboxylic acid groups and is easily degraded by de-

fibrated with fungi [32]. Pectin along with lignin and hemicelluloses present in natural fibers can be hydrolysed at elevated temperatures.

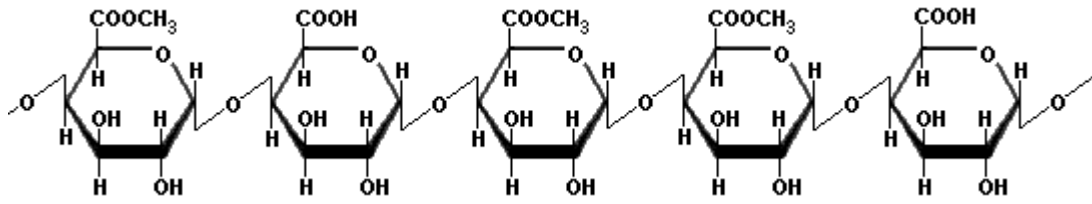


Figure-2.7 Typical Structure of pectin

2.5 FABRICATION METHODS OF PMCs:

There are two general divisions of composites manufacturing processes: open molding and closed molding. With open molding, the gel coat and laminate are exposed to the atmosphere during the fabrication process. In closed molding, the composite is processed in a two-part mold set, or within a vacuum bag. There are a variety of processing methods within the open and closed molding categories:

- a) **Open Molding Method:** Hand Lay-Up, Spray-Up, Filament Winding
- b) **Closed Molding Method:** Compression molding, Pultrusion, Vacuum Bag Molding, Vacuum Infusion Processing, Resin Transfer Molding (RTM)

2.5.1 Open Molding:

Open molding process is saturating fiber reinforcement with resin, using manual rollout techniques to consolidate the laminate and removing the entrapped air. A major factor in this operation is the transfer of resin from a drum or storage tanks to the mold. The means used to transport the resin, in many cases, characterizes the specific process method.

a) Hand Lay –Up:

Hand lay-up is an open molding method suitable for making a wide variety of composites products including: boats, tanks bathware, housings, truck/auto components, architectural products and many other products ranging from very small to very large.

Production volume per mold is low; however, it is feasible to produce substantial production quantities using multiple molds. Simple, single-cavity molds of fiberglass composites construction are generally used.

Moulds can range from very small to very large and are low cost in the spectrum of soft composites moulds.

Gel coat is first applied to the mold using a spray gun for a high-quality surface. When the gel coat has cured sufficiently, roll stock fiberglass reinforcement is manually placed on the mold. The lamination resin is applied by pouring, brushing, spraying, or using a paint roller. FRP rollers, paint rollers, or squeegees are used to consolidate the laminate, thoroughly wetting the reinforcement, and removing entrapped air. Subsequent layers of fiberglass reinforcement are added to build laminate thickness (Fig 2.7).

Simplest method offering low-cost tooling, simple processing and wide range of part sizes are the major advantages of this process. Design changes are readily made. There is a minimum investment in equipment. With skilled operators, good production rates consistent quality is obtainable.

b) Spray Lay-Up:

Spray-up or chopping is similar to hand lay-up in its suitability for making boats, tanks, transportation components and tub/shower units in a large variety of shapes and sizes. A chopped laminate has good conformability and is sometimes faster than hand lay-up in molding complex shapes. In the spray-up process the operator controls thickness and consistency, therefore the process is more operator dependent than hand lay-up. Although production volume per mold is low, it is feasible to produce substantial production quantities using multiple molds. As with hand lay-up, gel coat is first applied to the mold prior to spray-up of the substrate laminate.

Continuous strand glass roving and catalyzed resin are fed through a chopper gun, which deposits the resin-saturated “chop” on the mold as shown in fig 2.8. The laminate is then rolled to thoroughly saturate the glass strands and compact the chop. Additional layers of chop laminate are added as required for thickness.

c) Filament Winding:

Filament winding is an automated open molding process that uses a rotating mandrel as the mold. The male mold configuration produces a finished inner surface and a laminated rough surface on the outside diameter of the product. Filament winding results in a high degree of fiber loading, which provides high tensile strengths in the manufacture of hollow, generally cylindrical products such as chemical and fuel storage tanks, pipes, stacks, pressure vessels, and rocket motor cases. Mandrels of suitable size and shape, made of steel or aluminium form the inner surface of the hollow part. Some mandrels are collapsible to facilitate part removal.

Figure 2.9 shows the schematic picture of a typical filament winding process. Continuous strand roving is fed through a resin bath and wound onto a rotating mandrel. The roving feed runs on a trolley that traverses the length of the mandrel. The filament is laid down in a predetermined geometric pattern to provide maximum strength in the directions required. When sufficient layers have been applied, the laminate is cured on the mandrel. The molded part is then stripped from the mandrel. Equipment is available for filament winding on a continuous basis with two axes winding for pressure cylinders. This process makes high strength-to-weight ratio laminates and provides a high degree of control over uniformity and fiber orientation. The filament winding process can be used to make structures, which are highly engineered and meet strict tolerances. Because filament winding is automated, the labor factor for filament winding is lower than other open molding processes.

2.5.2 Closed Molding Method:

This is a process where the amount of molding material is measured and inserted before the molding takes place. The molding material is preheated and loaded into a chamber known as the *pot*. Then the material flows through runner system into the mold cavities. The mold remains closed as the material is inserted and is opened to release the part after curing. The moulding can be through both compression and transfer molding process. Closed Molding technology is used to manufacturing of polymer composite parts in less time, high dimensional accuracy, repetitive in nature at low cost . A wide range of industries use closed mold technologies to make precision parts like aerospace, transportation, and recreation industries etc.

a) Compression Molding:

Compression molding is a high-volume, high-pressure method suitable for molding complex, fiberglass-reinforced plastic parts on a rapid cycle time. There are several types of compression molding including: sheet molding compound (SMC) which are, bulk molding compound (BMC), thick molding compound (TMC), and wet lay-up compression molding.

Compression molding tooling consists of heated metal molds mounted in large presses. Tooling is usually machined steel or cast alloy molds that can be in either single or multiple-cavity configurations. Steel molds are hardened and sometimes chrome plated for enhanced durability. The molds are heated using steam, hot oil, or electricity. Side cores, provisions for inserts, and other refinements are often employed. Mold materials include cast of forged steel, cast iron, and cast aluminum.

The mold set is mounted in a hydraulic or mechanical molding press. The molds are heated to 2500 to 4000 F. A weight charge of molding compound is placed in the open mold as shown in fig 2.10. The two halves of the mold are closed and pressure is applied. Depending on thickness, size, and shape of the part, curing cycles range from less than a minute to about five minutes. The mold is opened and the finished part is removed. Typical parts include: automobile components, appliance housings and structural components, furniture, electrical components, and business machine housings and parts.

Compression molding produces fast molding cycles and high part uniformity. The process can be automated. Good part design flexibility and features such as inserts, ribs, bosses, and attachments can be molded in .Good surface finishes are obtainable, contributing to lower part finishing cost. Subsequent trimming and machining operations are minimized in compression molding.

b) Pultrusion:

Pultrusion is a continuous process for the manufacture of products having a constant cross section, such as rod stock, structural shapes, beams channels, pipe, tubing, fishing rods, and golf club shafts. Pultrusion produces profiles with extremely high fiber loading,

thus pultruded products have high structural properties. Hardened steel dies are machined and include a perform area to do the initial shaping of the resin- saturated roving. The dies include heating which can be electric or hot oil. The latest pultrusion technology uses direct injection dies, in which the resin is introduced inside the die, rather than through an external resin bath, which may be called as partial RTM.

Continuous strand fiberglass roving, mat, cloth, or surfacing veil is impregnated in a resin bath, then pulled (pul-trusion) through a steel die, by a powerful tractor mechanism (Refer fig 2.11). The steel die consolidates the saturated reinforcement, sets the shape of the stock, and controls the fiber/resin ratio. The die is heated to rapidly cure the resin. Many creels (balls) of roving are positioned on a rack, and a complex series of tensioning devices and roving guides direct the roving into the die.

The process is a continuous operation that can be readily automated. It is adaptable to both simple and complex cross-sectional shapes. Very high strengths are possible due to the fiber loading and labor costs are low.

c) Vacuum Bag Molding:

The mechanical properties of open-mold laminates can be improved with vacuum bagging. By reducing the pressure inside the vacuum bag, external atmospheric pressure exerts force on the bag. The pressure on the laminate removes entrapped air, excess resin, and compacts the laminate. Vacuum bagging can be used with wet-lay laminates and prepreg advanced composites. In wet lay-up bagging the reinforcement is saturated using hand lay-up, then the vacuum bag is mounted on the mold and used to compact the laminate and remove air voids. In the case of pre-impreg advanced composites molding, the prepreg material is laid-up on the mold, the vacuum bag is mounted and the mold is heated or the mold is placed in an autoclave that applies both heat and external pressure, adding to the force of atmospheric pressure. The prepreg-vacuum bag-autoclave method is most often used to create advanced composites used in aircraft and military products. Molds are similar to those used for conventional open-mold processes.

In the simplest form of vacuum bagging, a flexible film (PVA, nylon, mylar, or polyethylene) is placed over the wet lay-up, the edges sealed, and a vacuum drawn. A more

advanced form of vacuum bagging places a release film over the laminate, followed by a bleeder ply of fiberglass cloth, non-woven nylon, polyester cloth, or other material that absorbs excess resin from the laminate. Fig 2.12 shows the schematic picture of vacuum bag molding process. A breather ply of a non-woven fabric is placed over the bleeder ply, and the vacuum bag is mounted over the entire assembly. Pulling a vacuum from within the bag uses atmospheric pressure to eliminate voids and force excess resin from the laminate. The addition of pressure further results in high fiber concentration and provides better adhesion between layers of sandwich construction. When laying non-contoured sheets of PVC foam or balsa into a female mold, vacuum bagging is the technique of choice to ensure proper secondary bonding of the core to the outer laminate.

Vacuum bag processing can produce laminates with a uniform degree of consolidation, while at the same time removing entrapped air, thus reducing the finished void content. Structures fabricated with traditional hand lay-up techniques can become resin rich and vacuum bagging can eliminate the problem. Additionally, complete fiber wet-out can be accomplished if the process is done correctly. Improved core-bonding is also possible with vacuum bag processing.

d) Vacuum Infusion Processing:

Vacuum infusion is a variation of vacuum bagging where the resin is introduced into the mold after the vacuum has pulled the bag down and compacted the laminate. The method is defined as having lower than atmospheric pressure in the mold cavity. The reinforcement and core material are laid-up dry in the mold. This is done by hand and provides the opportunity to precisely position the reinforcement. When the resin is pulled into the mold the laminate is already compacted; therefore, there is no room for excess resin. Very high resin to glass ratio are possible with vacuum infusion and the mechanical properties of the laminate are superior. Vacuum infusion is suitable to mold very large structures and is considered a low volume molding process. Molds are similar to those used for conventional open-mold processes.

The mold may be gel coated in the tradition fashion. After the gel coat cures, the dry reinforcement is positioned in the mold. This includes all the plies of the laminate and core material if required. A perforated release film is placed over the dry reinforcement. Next a

flow media consisting of a coarse mesh or a “crinkle” ply is positioned, and perforated tubing is positioned as a manifold to distribute resin across the laminate. The vacuum bag is then positioned and sealed at the mold perimeter. A tube is connected between the vacuum, bag and the resin container. A vacuum is applied to consolidate the laminate and the resin is pulled into the mold (fig 2.13).

Vacuum infusion can produce laminates with a uniform degree of consolidation, producing high strength, lightweight structures. This process uses the same low cost tooling as open molding and requires minimal equipment. Very large structures can be fabricated using this method. Vacuum infusion offers a substantial emissions reduction compared to either open molding or wet lay-up vacuum bagging.

e) Resin Transfer Molding:

Resin transfer molding is an intermediate volume molding process for producing composites. The RTM process is to inject resin under pressure into a mold cavity. Vacuum assist can be used to enhance resin flow in the mold cavity. RTM can use a wide variety of tooling, ranging from low cost composite molds to temperature controlled metal tooling. RTM can utilize either “hard” or “soft” tooling, depending upon the expected duration of the run. Soft tooling would be either polyester or epoxy molds, while hard tooling may consist of cast machined aluminum, electroformed nickel shell, or machined steel molds. RTM can take advantage of the broadest range of tooling.

Figure 2.14 shows the picture of resin transfer molding process of polyester resin with peroxide catalyst. The mold set is gel coated conventionally, if required. The reinforcement (and core material) is positioned in the mold and the mold is closed and clamped. The resin is injected under pressure, using mix/meter injection equipment, and the part is cured in the mold. The reinforcement can be either preforms or pattern cut roll stock material. Preforms are reinforcement that is pre-formed in a separate process and can be quickly positioned in the mold. RTM can be done at room temperature; however, heated molds are required to achieve fast cycle times and product consistency.

This closed molding process produces parts with two finished surfaces. By laying up reinforcement material dry inside the mold, any combination of materials and orientation can be used, including 3-D reinforcements. Part thickness is determined by the tool cavity.

2.6 NATURAL FIBER REINFORCED POLYMER COMPOSITES

Natural fiber reinforced polymer composites are hybrid with their properties, with characteristics of both natural fibres and polymers. In the beginning of the 20th century wood- or cotton fiber reinforced phenol- or melamine formaldehyde resins were fabricated and used in electrical applications for their non-conductive and heat-resistant properties. Incorporation of natural fibers in to polymer is now a standard technology to improve the mechanical properties of polymer. Mechanical properties like tensile strength and young's modulus are enhanced in the end products (composites) as the fibres in the composites determine the tensile strength and young's modulus of the materials [39].

One of the largest areas of recent growth in natural fiber plastic composites in world-wide is the automotive industry, where natural fibers are advantageously used as a result of their low density and increasing environmental pressures. Natural fibers composites found application where load bearing capacity and dimensional stability under moist and high thermal conditions are of second order importance. For example, flax fiber reinforced polyolefins are extensively used today in the automotive industry, but the fiber acts mainly as filler material in non-structural interior panels [40]. Natural fiber composites used for structural purposes do exist, but then usually with synthetic thermo-set matrices which of course limit the environmental benefits [41, 42].

Plant fibers, such as hemp, flax and wood, have large potential as reinforcement in structural materials due to the high aspect ratio and high specific strength- and stiffness of the fibers [43-46]. Apart from good specific mechanical properties and positive environmental impact, other benefits from using natural fibers worth mentioning are low cost, friendly processing, low tool wear, no skin irritation and good thermal and acoustic insulating properties [46].

A complete biodegradable system may be obtained if the matrix material also comes from a renewable resource. Examples of such materials are lignophenolics, starch and polylactic acid (PLA). Some of these systems show encouraging results. For example Oksman et al. [47] have reported that flax fiber composites with PLA matrix can compete with and even outperform flax/polypropylene composites in terms of mechanical properties. In a recent study [48] it was found that composites of poly-L-lactide acid (PLLA) reinforced by flax fibers can show specific tensile modulus equivalent to that of glass/polyester short fiber composites. The specific strength of flax/PLLA composites was lower than that of glass/polyester, but higher than that of flax/polyester.

There are many application of natural fiber composite in every day life. For example, jute is a common reinforcement for composites in India. Jute fibers with polyester resins are used in buildings, elevators, pipes, and panels [49]. Natural fiber composites can also be very cost effective material for application in building and construction areas (e.g. walls, ceiling, partition, window and door frames), storage devices (e.g. bio-gas container, post boxes, etc.), furniture (e.g. chair, table, tools, etc.), electronic devices (outer casing of mobile phones), automobile and railway coach interior parts (inner fenders and bumpers), toys and other miscellaneous applications (helmets, suitcases).

During the last few years, a series of works have been done to replace the conventional synthetic fiber with natural fiber composites [50-57]. For instant, hemp, sisal, jute, cotton, flax and broom are the most commonly fibers used to reinforce polymers like polyolefins [57, 58], polystyrene [59], and epoxy resins [60]. In addition, fibers like sisal, jute, coir, oil palm, bamboo, bagasse, wheat and flax straw, waste silk and banana [52, 53, 59,60,58-69] have proved to be good and effective reinforcement in the thermoset and thermoplastic matrices.

The limited use of natural fiber composites is due to their bio-degradation character when exposed to environment [69]. Natural fibers are hydrophilic in nature as they are derived from lignocellulose, which contain strongly polarized hydroxyl groups in hemicellulose and amorphous cellulose. These fibers, therefore, are inherently incompatible with hydrophobic thermoplastics, such as polyolefins. The major limitations of using these fibers as reinforcements in such matrices include poor interfacial adhesion between polar-hydrophilic fiber and non-polar hydrophobic matrix, and difficulties in mixing due to poor wetting of the fiber with the matrix. This

in turn would lead to composites with weak interface. Natural fiber composites tend to swell considerably with water uptake and affect mechanical properties, such as stiffness and strength. The fiber-matrix adhesion may be improved and the fiber swelling reduced by means of chemical, enzymatic or mechanical modifications [44].

Certain aspects of natural fiber reinforced composite behaviour still poorly understood such as their visco-elastic, visco-plastic or time-dependent behaviour due to creep and fatigue loadings [70], interfacial adhesion [71, 72], and tribological properties. Little information concerning the tribological performance of natural fiber reinforced composite material [64-66, 73] has been available in the literatures. In this context, long plant fibers, like hemp, flax [71, 72], bagasse and bamboo [65, 66] have considerable potential in the manufacture of composite materials for tribo applications. Few works have been attempted to investigate the tribological behaviour of polymeric composites based on other natural fibres such as Kenaf [74], Oil palm [75], Sisal [76], cotton [77], Jute [78], Betelnut [79]. Likewise rice husk the abundance of availability, low cost and high silica content in the fiber has made it a potential candidate for reinforcement in polymer composite for various applications and provides advantages when substitute for synthetic fibers.

After reviewing the existing literature available on natural fiber composites, efforts are put to understand the basic needs of the growing composite industry. The conclusions drawn from this is that, the success of combining natural fiber with polymer matrices results in the improvement of mechanical properties of the composites compared with the matrix materials. These fillers are cheap and nontoxic, can be obtained from renewable sources, and are easily recyclable. Moreover, despite their low strength, they can lead to composites with high specific strengths because of their low density.

Thus the priority of this work is to prepare polymer Matrix Composites (PMCs) using rice husk (waste from rice mill industry) as reinforcement material. In the present work it is proposed to prepare two series of composites using randomly oriented unmodified and modified rice husk reinforced epoxy composite. To improve the interfacial strength between the rice husk and the matrix, it is planned to modify the surface of the fiber by various chemical methods. The composite will then be subjected to different weathering condition like steam, saline and subzero condition. The fiber characterization will be done by Fourier Transform Infrared (FTIR) spectroscopy and X-Ray Diffraction (XRD) before and after the treatment of the fibers. The mechanical properties of the

composite will be evaluated along with moisture absorption characteristics for both treated and untreated fiber reinforced composites.

The potential of rice husk and rice husk char to be prepared with different carbonization temperature (850,900 and 950 °C) for tribological application will be investigated by performing different tribological tests like abrasive wear test and solid particle erosion test as per ASTM standards.

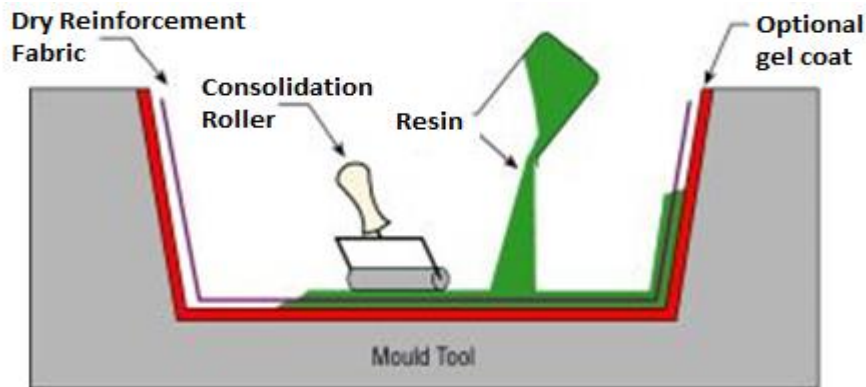


Figure 2.8 Hand Lay-Up Techniques

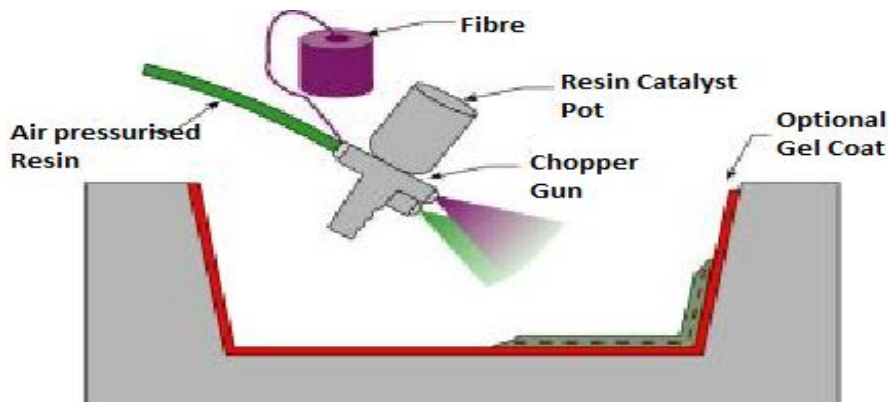


Figure 2.9 Spray up Technique

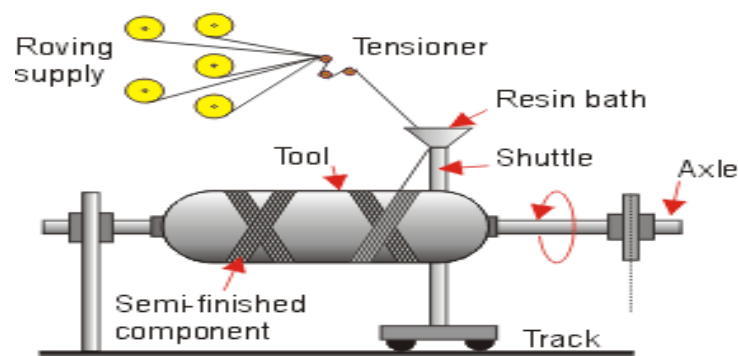


Figure 2.10 Filament Winding Process

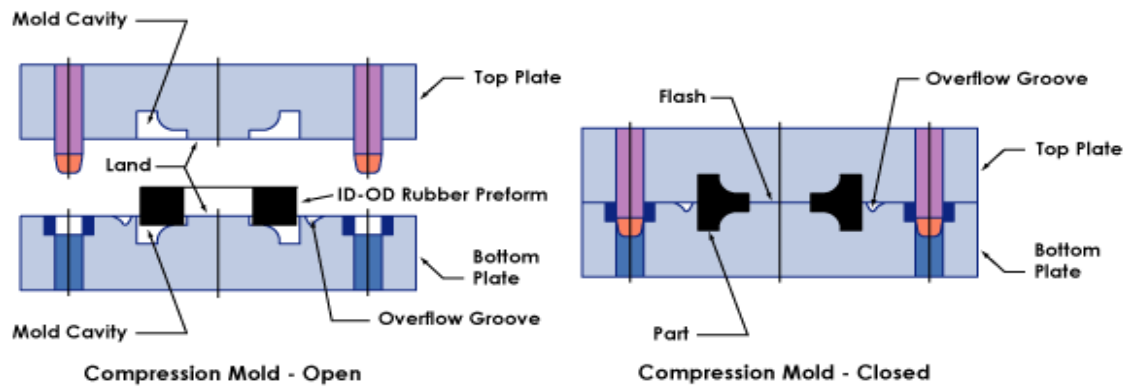


Figure 2.11 Compression Molding Technique

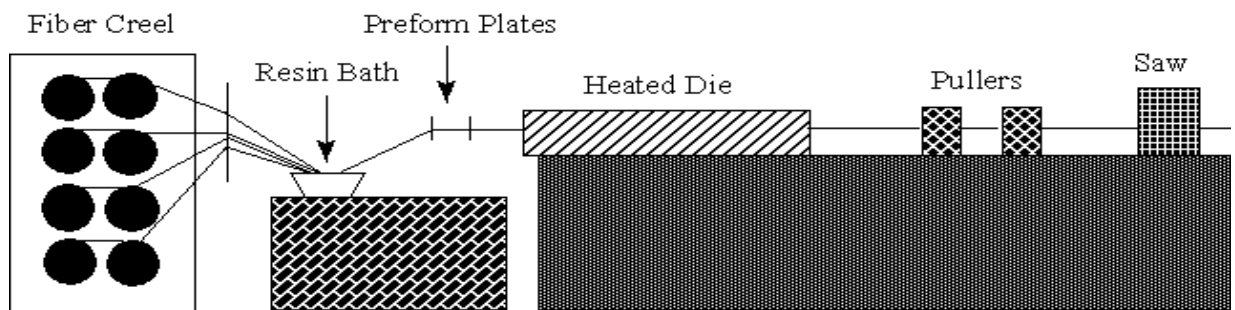


Figure 2.12 Pultrusion Process

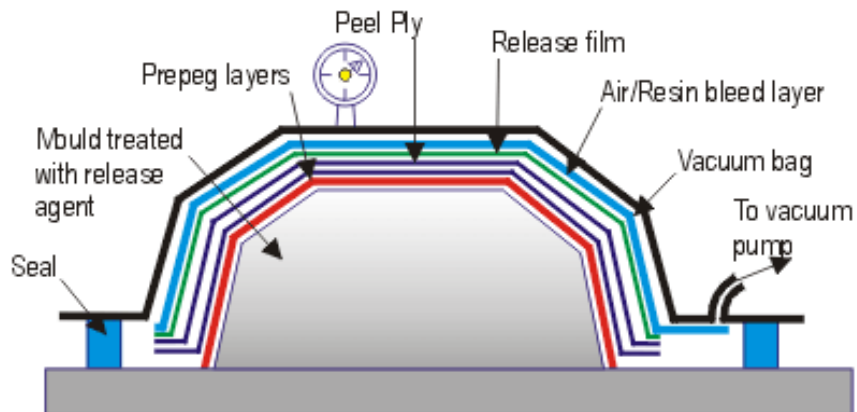


Figure 2.13 Vacuum Bag Molding

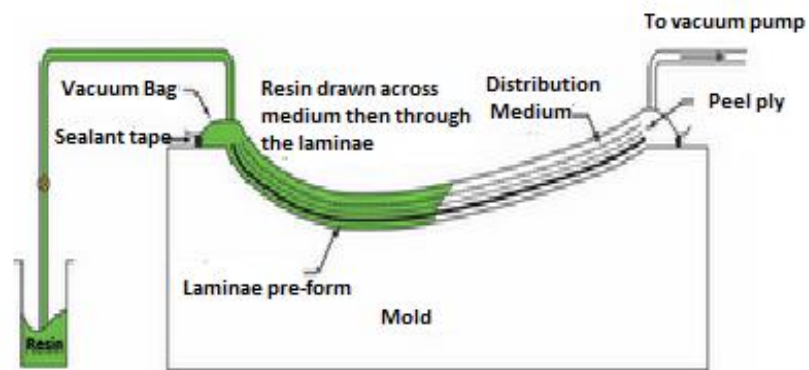


Figure 2.14 Vacuum Infusion Process

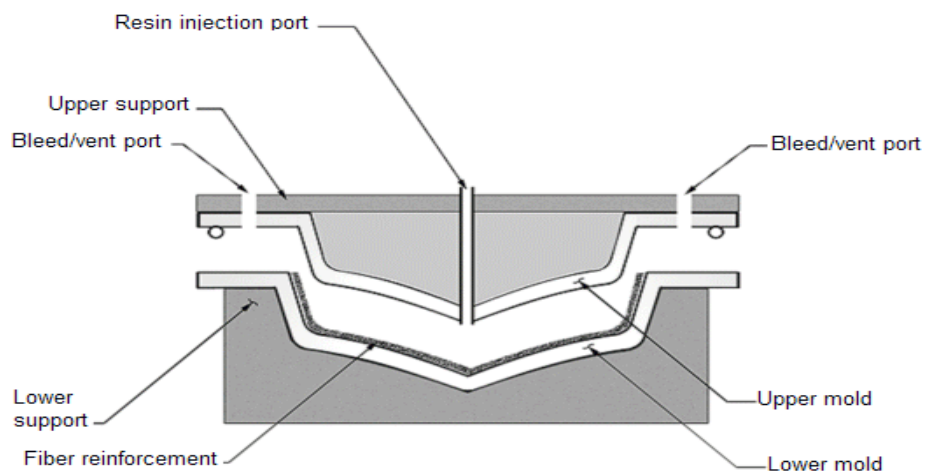


Figure 2.15 Resin Transfer Molding

Chapter 3

MECHANICAL CHARACTERIZATION OF RICE HUSK EPOXY COMPOSITES

3.1 INTRODUCTION

Natural fibres are widely used for reinforcing polymer. There are many applications of natural fiber composites in everyday life. However the main disadvantage of natural fiber is their hydrophilic nature. They also have a poor environmental and dimensional stability that prevent wider use of natural fiber composites. The possibility of using these materials in outdoor applications makes it necessary to analyse their mechanical behaviour under the influence of different weathering conditions such as humidity, saline water, sunlight or micro-organisms. The moisture absorption by composites containing natural fibers has several adverse effects on their properties and thus affects their long-term performance. For example, increased moisture absorption decreases their mechanical properties, provides the necessary condition for biodegradation, and changes their dimensions [80]. Numerous efforts have been made to address this issue. Coupling agents, compatibilizers or other chemical modifications methods are used to improve the moisture resistance of composites. The composite absorb or release moisture depending on environmental conditions [81]. The Hydroxyl group ($-OH$) in amorphous cellulose, hemicellulose and lignin that are present in the natural fiber are mostly responsible for the high moisture absorption due to formation of hydrogen bond by hydroxyl groups with water molecules within the fiber cell wall. This leads to a moisture build-up in the fiber-matrix interface and causes swelling of the composite, reduction in interfacial strength, debonding of fibre and matrix, reduction in glass transition temperature and change in visco-elastic properties [82]. The other reasons of moisture absorption by Polymer composites may be due to capillary transport into the gaps and flaws at the interfaces between fibers and polymer, because of incomplete wettability and impregnation and transport by micro cracks in the matrix, formed during the compounding process [83].

The moisture absorption by composite reinforced with natural fibers have several adverse effects on their performance. In view of the severity of moisture absorption and its effect on composite properties, a number of studies have already been made by several researchers to address this issue. The chemical treatment has been considered as a good technique to reduce the hydroxyl group in the natural fibers, improve cellulose exposure of the fiber, improve surface roughness of fiber for better fibre matrix adhesion and mechanical strength, improve thermal stability and improves crystallinity of fiber by delignification etc. Different chemical treatments such as mercerization or alkali (NaOH) Peroxide, isocyanate, acrylation and acrylonitrile grafting, benzoylation, permanganate treatment, acetone treatment, acetylation, silane treatment etc. are reported by different researchers [84-88].

George et al. [89] investigated the relationship between the moisture absorption of pineapple-leaf fiber reinforced low density polyethylene (LDPE) composites with different fiber

loadings. They found that the moisture absorption increased almost linearly with the fiber loading. Similar, results have been reported by K. Hardinnawirda et al on Rice Husk –unsaturated polyester composites [90].

Joseph et al. [91] studied the environmental effects on sisal fiber reinforced PP composites. The chemically modified fiber composites showed a reduction in water uptake because of better interfacial bonding. Water uptake of the composite was found to increase with temperature since temperature activates the diffusion process. Reduction in tensile properties was observed due to the plasticization effect of water. The fiber/matrix bonding becomes weak with increasing moisture content, resulting in interfacial failure.

Stark [92] found that wood flour-polypropylene (PP) composites with 20 wt% wood flour reached equilibrium after 1500 h in a water bath and absorbed only 1.4% moisture while composites with 40 wt% loading reached equilibrium after 1200 h water submersion and absorbed approximately 9.0% moisture. After the analysis, she concluded that the wood flour is inhibited from absorbing moisture due to encapsulation of the wood flour by the PP matrix and that the degree of encapsulation is greater for the 20% wood flour composite than that for the 40% wood flour composite.

Yuan et al. [93] studied the plasma treatment of sisal fibers and its effects on tensile strength and interfacial bonding. They suggested that the interfacial adhesion between the fiber and matrix could be enhanced by cleaned and chemically modified fiber surface. The strong intermolecular fiber-matrix bonding decreases the rate of moisture absorption in bio-composite.

Stamboulis et al. [94] reported that the moisture absorption and swelling of the treated flax fiber polypropylene composites is approximately 30% lower than that of composites based on untreated flax fibers.

Thomas et al. [95], while studying water absorption characteristics of sisal fiber polyester composites found that diffusion coefficient decreases with chemical treatment of fiber. In addition to this the chemical treatment also decreases water absorption capacity of the composite. They also showed that the composite with benzoyl-chloride treated sisal fiber composite exhibited lower water absorption capacity.

A.Athijayamani et.al [96] reported variation of mechanical properties for roselle and sisal hybrid polyester composite at dry and wet condition. They have the opinion that the moisture absorption characteristic of the natural fiber is very important to produce the natural fiber hybrid composite material with positive hybrid effect.

Z Leman et.al[97] studied the moisture absorption behaviour of Sugar Palm fiber reinforced epoxy composite and have reported that composite that contain higher fiber composition the moisture absorption rate is higher for them.

Deo, Acharya[98] and Mishra, Acharya [99] studied the effect of moisture absorption and weathering behaviour of chopped Lantana Camara and short bagasse fiber reinforced epoxy composites for both treated and untreated fibers. Their results indicate significant improvement on the mechanical properties of the composites due to chemical modification of fiber surface. Both the investigators modified the surface with same chemical methods. But Benzoyl chloride treated fiber gives the better result for Lantana-Camara fiber where as Alkali treated fiber gives better result for bagasse fiber.

For potential application of natural fiber polymer composites a comprehensive study on the moisture absorption characteristic and its effect on mechanical properties are required. In this chapter, the characteristics of moisture sorption kinetics, thickness swelling and effect of moisture absorption on mechanical properties of both untreated and chemically treated Rice Husk epoxy composite under different environments (Steam, Saline water and Sub-zero temperature) are investigated.

3.2 CHEMICAL MODIFICATION OF FIBER

Processing of plastic composites using natural fibers as reinforcement has increased dramatically in recent years [47, 57, 100, 101]. A better understanding of the chemical composition and surface adhesive bonding of natural fiber is necessary for developing natural fiber reinforced composites. The interfacial bonding between the reinforcing fibers and the resin matrix is an important element for improving the mechanical properties of the composites. Realizing this, several authors [102-105] have focused their studies on the treatment of fibers to improve the bonding with resin matrix. The mechanical properties of the composites are controlled by the properties and quantities of the individual component and by the character of the interfacial region between matrix and reinforcement.

Lack of good interfacial adhesion makes the use of cellular fiber composites less attractive. Often the interfacial properties between the fiber and polymer matrix is low, because of hydrophilic nature of natural fiber which reduces its potential of being used as reinforcing agents. Hence chemical modifications are considered to optimize the interface of fibers. Chemicals may activate hydroxyl groups or introduce new moieties that can effectively interlock with the matrix. There are various chemical treatments available for the fiber surface modification. Chemical treatment including alkali, silane, acetylation, benzylation, acrylation, isocyanates, maleated coupling agents, permanganate treatment are discussed in details in [106].

The chemical treatment of fiber aimed at improving the adhesion between the fiber surface and the polymer matrix by modifying the fiber surface and the fiber strength. It also reduces the water absorption capacity of the fiber and helps in improving the mechanical properties. Out of the available treatments, for the present case to have a good bonding between the fiber and the resin matrix Rice Husk have been treated with alkali, acetone & benzoyl chloride. The subsequent section will elaborate separately the treatment of the fiber surface by these chemical, results of fiber modification through XRD, FTIR, SEM and TGA, study of mechanical properties of both untreated and treated fiber reinforced polymer composite and environmental effects on mechanical performance of the composite along with moisture absorption characteristics.

3.2.1 Methods of Chemical Modifications

3.2.1.1 Alkaline Treatment

Alkaline treatment or mercerization is one of the most used chemical treatments of natural fibers when used to reinforce thermoplastics and thermosets. The important modification done by alkaline treatment is the disruption of hydrogen bonding in the network structure, thereby increasing surface roughness. This treatment removes a certain amount of lignin, wax and oils covering the external surface of the fiber cell wall, depolymerizes cellulose and exposes the short length crystallites [107]. Addition of aqueous sodium hydroxide (NaOH) to natural fiber promotes the ionization of the hydroxyl group to the alkoxide [108].

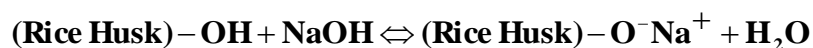


Thus, alkaline processing directly influences the cellulosic fibril, the degree of polymerization and the extraction of lignin and hemicellulosic compounds [109]. It is reported that alkaline treatment has two effects on the fiber:

- 1) It increases surface roughness resulting in better mechanical interlocking, and
- 2) It increases the amount of cellulose exposed on the fiber surface, thus increasing the number of possible reaction sites [57].

Consequently, alkaline treatment has a lasting effect on the mechanical behaviour of flax fiber, especially on fiber strength and stiffness.

For alkali treatment, the Rice Husk were soaked in a 5% NaOH solution at room temperature maintaining a liquor ratio of 15:1. Before putting the Rice Husk in alkali, the raw rice husks were washed with plain water to remove the foreign matter/particle that adhere the rice husk surface. The Rice Husks were dried in sun light. After complete drying the fibers were kept immersed in the alkali solution for 4hrs. The fibers were then washed several times with fresh water to remove any NaOH sticking to the fiber surface, neutralized with dilute acetic acid and finally washed again with distilled water. A final pH of 7 was maintained. The fibers were then dried at room temperature for 48 hrs followed by oven drying at 100°C for 6hrs. The alkali reaction between Rice Husk fiber and NaOH is as follows:



3.2.1.2 Acetone Treatment

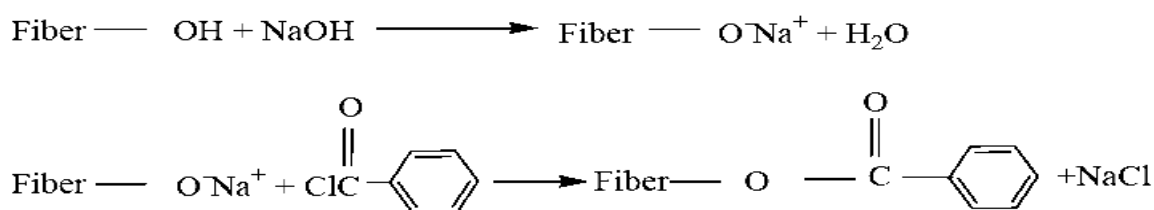
When the fiber is treated with acetone, the lignin, cellulolignin and other such material get dissolved in acetone. As acetone is a non-polar organic solvent it usually dissolves the non-polar organic component.

The Rice Husk were washed in soxhlet extractor (Figure-3.1) with acetone for approximately 1-1.5 hrs. The acetone was evaporated (boiled at 63⁰C) and condensed back into the volume with the fibers. This process was repeated four times for each batch. The

used acetone was discarded before the new batch was cleaned in the same manner. The acetone changed from transparent to light green after treatment due to the presence of waxes and organic materials after the extraction. All the fibers were washed with pressurized water at room temperature for 10 minutes before acetone treatment. The fibers were then dried at room temperature for 24 hrs.

3.2.1.3 Benzoylation Treatment

Benzoylation is an important transformation in organic synthesis [110]. Benzoyl chloride is most often used in fiber treatment. Benzoyl chloride includes benzoyl ($C_6H_5C=O$) which is attributed to the decreased hydrophilic nature of the treated fiber and improved interaction with the hydrophobic polymer matrix. The reaction between the cellulosic hydroxyl group of the fiber and benzoyl chloride is given as follows:



Benzoylation of fiber improves fiber matrix adhesion, thereby considerably increasing the strength of composite, decreasing its water absorption and improving its thermal stability [59, 111, 112].

The pre-treated Rice Husk were suspended in 10% NaOH solution and agitated with benzoyl chloride. The mixture was kept for 15 min, filtered, washed thoroughly with water and dried between filter papers. The isolated fibers were then soaked in ethanol for 1 h to remove the benzoyl chloride and finally was washed with water and dried in the oven at 80⁰ C for 24 h.

3.2.2 EDX and SEM Micrographs of Treated Fibers

The morphology of the untreated and treated fiber surfaces has been studied using scanning electron microscope (SEM) JEOL JSM-6480LV. The sample surfaces were platinum coated to make them conductive prior to SEM observation. EDX and SEM micrographs of the untreated and treated Rice Husk are shown in Figures-3.2 and Figure-3.3

Silica exists on the outer surface of rice husk seems to be relatively rougher than the inner surface that houses the rice grain. Silica exists on the outer surface of rice husks in the form of silicon–cellulose membrane [22] that forms a natural protective layer against termites and other micro-organisms attack on the paddy. EDX analysis of peak of outer surface of untreated Rice Husk (Figure-3.2(a) and Fig 3.3 (a)) reveals deposit pure Silica in form of thorn. This Silica is responsible for insufficient adhesion between accessible functional groups on rice husks' surfaces and various matrix binders. Removal of silica and other surface impurities by chemical treatments (Figure-3.2 (b),(c),(d)) can be expected to improve the adhesion properties of rice husks with the binders to improve the properties of the composite. The inner surface of rice husk is smooth and may contain wax and natural fats that provide good shelter for the grain. However, presence of these impurities on the inner surfaces of rice husks also affects the adhesion properties of rice husks chemically and physically. The total removal of silica by different chemical method is not possible. However, it limits their presence on the top by chemical treatment like Acetone, Alkali and Benzoyl Chloride. The table 3.1 indicates silicon content of treated and untreated of Rice Husk obtained through spectra as shown in figure 3.3.

It is well established that the cellulose chains of natural fiber are strongly bound by chemical constituents, lignin, and hemicellulose, resulting in the formation of multi-cellular fiber [113]. The surface of untreated fiber appeared smooth due to the presence of lignin, wax, oil, and surface impurities [Figure-3.2(a)], which are partially removed with acetone [Figure-3.2(b)] and further removed with alkali and benzoyl-chloride treatments [Figure-3.2(c) & (d)]. These clean surfaces are expected to provide direct bonding between the fiber cellulose and a matrix such as epoxy resin. By comparing treated fibers with the untreated fibers, it can be seen that the alkali and benzoyl-chloride treatments resulted in separation of the microfibrillar structure (fibrillation) and reduction in thickness of fiber because of the removal of cemented materials (i.e. lignin and hemicellulose) [114, 115]. Moreover these two treatments increase the effective surface area by fibrillation which promotes the mechanical interlocking between the fiber and the matrix. Where as the acetone treatment does not affects the fiber surface very much.

3.2.3 FTIR Spectroscopy

The effect of chemical modifications on the fiber surface was observed by using FTIR spectroscopy. FTIR measurement was performed using an IR-Prestige-21 spectrometer with scan rate 40 and range 400-4000 cm^{-1} wave number. KBr powder was used for making pellets for use in spectroscopic analysis. The comparison of the representative FTIR spectra of Rice Husk before and after chemical treatment (acetone, alkali and benzoyl-chloride treatment) is shown in Figure-3.4. In comparison to the unmodified Rice Husk, the alkali treated, acetone treated and benzoylated rice husk showed a reduction in absorption spectra due to dissolution of non-polar covalent compound like wax, fat etc in the treated chemicals. The effect is more significant in case of Benzoyl Chloride treatment as this is a strong non-polar solvent. As shown in Fig-3.3 the broad absorption peak of plain rice husk around 3404.31 cm^{-1} indicates the existence of free hydroxyl groups. The C-H stretching vibration around 2925.81 cm^{-1} indicates the presence of alkane functional group. The peaks around 1641.31 to 1737.74 cm^{-1} correspond to the C=O stretching that may be attributed to the hemicelluloses and lignin carbonyl groups. The C=C stretching vibrations between 1546.80-1652.88 cm^{-1} indicative of alkenes and aromatic functional groups. The peaks around 1461.94 cm^{-1} indicate the presence of CH₂ and CH₃ groups while those at 1380 cm^{-1} are indicative of CH₃. A peak at 1379.01 cm^{-1} band may be attributed to the aromatic CH and carboxyl-carbonate structures. The peaks in the 1153.35-1300 cm^{-1} corresponds to vibration of CO group in lactones. The peaks around 1076, 813 and 470 cm^{-1} indicates presence of Silica in form of Si-O-Si and Si-H.

The major functional groups in Rice Husk, by and large remain same even after chemical treatments. However, they show reduction of peak intensity and shifting in many cases. The chemically treated fiber show the reduction in O-H stretching intensity and shifting of the peak from 3425.34 cm^{-1} to 3382.91, indicating participation of some free hydroxyl groups in these chemical reactions. The point of reaction was probably at the lignin -OH and C₂-OH of the glucopyranose unit in the cellulose component. A strong and sharp band at 1730.14 cm^{-1} is observed due to C=O stretching of carbonyl groups (>C=O) in hemicellulose components for untreated fiber, which disappeared in alkali treated fiber. Alkali treatment of Rice Husk destroys the C=O unit of the uronic acid residue in hemicellulose, perhaps arising from the intermolecular addition of the alcoholate (-CH₂-O⁻ Na⁺) from cellulose and lignin components to the C=O group. The benzoylation of Rice

Husk fiber introduces the new absorption peaks at about 1726.29 cm^{-1} owing to the presence of phenyl nucleus [116]. This band in benzoylated fiber is more intense, indicating a combined effect of $-\text{O}-\text{CO}-\text{Ph}$ and $-\text{O}-\text{CO}-\text{CH}_3$ groups arising from benzoylation. The acetone extracted Rice Husk spectrum is similar to that of the untreated RH. The band of medium intensity at 935.41 cm^{-1} due to b-glycosidic linkage in the unmodified Rice Husk underwent shifting to a lower wave number.. This relates to the rotation of glucose residue around the glycosidic bond [117] and indicates a slow transition from unmodified to chemically modified Rice Husk

3.2.4 X-ray Diffraction

X-ray diffraction was carried out to evaluate the crystallographic structure of semi-crystalline materials such Rice Husk and to ascertain the change in crystalline character of material after chemical treatments. A Philips X-ray diffractometer, employing $\text{CuK}\alpha$ ($\lambda = 1.54$) radiation and a graphite monochromator with a current of 40 mA and a voltage of 40 mV was used with a diffraction intensity in the range of 5 to 45° (2θ -angle range). The X-ray diffractograms of untreated, alkali treated, acetone treated and benzoyl-chloride treated Rice Husk can be seen in Figure-3.5. It is observe that the major crystalline peak of each profile occurred at around 2θ value ranging from 22° to 22.5° , which represents the cellulose crystallographic plane (002) where as the amorphous peak occurred at 2θ value ranging from 15.5° to 16.5° . The X-ray diffractograms show that the intensity of the (002) crystallographic plane and amorphous plane (am) ware increased significantly with Benzoyl Chloride treatments of RH.

The fiber crystallinity index (I_c) of the treated and untreated samples were calculated by using equation:

$$I_c = \left(\frac{I_{002} - I_{am}}{I_{002}} \right) \quad (3.1)$$

where ' I_{002} ' is the maximum intensity of diffraction of the (002) lattice peak at a 2θ angle of between 22° and 22.5° , and ' I_{am} ' is the intensity of diffraction of the amorphous material, which is taken at a 2θ angle between 15.5° and 16.5° where the intensity is at a minimum [118]. The results are summarized in Table-3.2 It is seen that, the crystallinity index of RH

decreased upon chemical treatments possibly due to fibrillation of cellulose fiber. Kelly C.C Karvalo et.al [119] have reported similar result during alkali treatment of coconut fiber composite. The surface area of the fiber increases with fibrillation resulting better fiber-matrix adhesion. However, the mechanical strength of the fiber reduces due to loss in crystalline character of the fiber.

3.3 THERMO GRAVIMETRIC ANALYSIS (TGA)

Thermo Gravimetric analysis were carried out on RH composites (both treated and untreated) using DTG-60 H SHIMADZU apparatus, applying heating rate of 10⁰C/min upto 500⁰C as shown in Figure-3.6, . The objective was to ascertain the thermal stability of Rice Husk epoxy composite and the specific the role of silica in RH. As such, the lignocellulosic materials have poor thermal stability. The natural fiber consists of three main components, i.e., cellulose, hemicellulose and lignin. The thermal degradation of Lignin, hemicellulose, and cellulose take place over a range of temperature i.e 160–900°C, 220–315°C and 315–400 °C, respectively. The process is irreversible. Lignin decomposed at a slower rate compared to the other components in lignocellulose[120]. The broader degradation temperature range of lignin can be explained by the presence of various oxygen-containing functional groups in its structure. These complex structures of lignin show varying thermal degradation behaviors, since the scissions occurring at different temperatures. The temperature range of lignin degradation overlaps with those of hemicellulose and cellulose. The degradation of composite occurs in stages. The moisture and other volatile impurities of the composite are removed at lower temperature (100°C-200°C) followed by hemicellulose and cellulose degradation of the fiber. The degradation process is accelerated once epoxy starts degrading. The TGA curve shows that the weight loss in the composites is more than pure epoxy in the initial range upto 340°C. Thereafter, pure epoxy has very faster degradation whereas the composites have slower rate of degradation. As shown in the figure the major degradation takes place between temperature range 340-450°C. However, the lignin component continues to degrade forming char up to 650⁰C [20].

The initial degradation temperatures were ascertained considering a moderate weight loss of 5% original sample (Table.3.3). The result indicates that the Epoxy possess a degradation at 328⁰C where as Plain Rice husk composite shows lower degradation temperature at 258⁰C.

The treated samples show higher degradation temperature than plain rice husk and offers better service temperature as shown in the table. Similar result have been obtained on TGA analysis of Alkali treated jute fiber [121]. The decomposition of the cellulosic substances shift slightly to higher temperatures for the treated fibres. The increase in thermal stability in the cellulose material may be due to ordering of cellulose chains leading to higher thermal stability[122]. However, a study on Sisal fiber has revealed reduction of thermal stability with Alkali treatment (possibly due to high fibrillation) but increase with Benzoyl Peroxide treatment[123].

The silica in Rice Husk has distinct role in slowing down the process of degradation as revealed in the figure .The thermal stability of composite also improve due to addition of Rice Husk [124]. As the samples were heated beyond to 270⁰C, the RH component starts decomposing forming byproducts including silica. The silica ash gradually accumulated on the polymer matrix which delays the degradation process and makes the polymer more thermally stable

3.4 COMPOSITE FABRICATION

For preparation of composite the following materials have been used;

1. Rice Husk
2. Epoxy
3. Hardener

3.4.1 Preparation of Rice Husk

The Rice husks were collected locally. They were washed several times with plain water to remove the dust and other foreign particles adherence to the fibers and were dried in sun light for 3 days to remove all superficial moisture. The Rice Husk sample contains the fiber of different length. The segregation of sizes was made through sieving in a sieve shaker machine having sieves of 4, 3.35,2.8, 2.36 and 2 mm size. The majority content RH was of size range +2 to -2.36. This size of rice husk fiber is chosen for the experiment. The length and diameter of fiber has bearing on the performance of composite. The RH is a short

fiber and standardization of fiber length was considered to eliminate the effect of property variation of composite due to fiber length.

3.4.2 Epoxy Resin

The type of epoxy resin used in the present investigation is Araldite LY-556 which chemically belongs to epoxide family. Its common name is Bisphenol-A-Diglycidyl-Ether. The hardener with IUPAC name NNO-bis (2-aminoethylethane-1,2-diamin) has been used with the epoxy designated as HY 951. Both the epoxy and hardener were supplied by Ciba-Geigy of India Ltd.

3.4.3 Composite preparation

The hand lay-up technique was used for preparation of the samples. A wooden mold of dimension (150x60x6) mm was used for casting the composite sheet (figure 3.7). A mold release spray was applied at the inner surface of the mold for quick and easy release of the composite sheet. For different weight fraction of fibers, a calculated amount of epoxy resin and hardener (ratio of 10:1 by weight) was thoroughly mixed in a glass jar and placed in a vacuum chamber to remove air bubbles that got introduced. Then calculated amount of rice husk is added to the mixture of epoxy resin and hardener and mixed properly. Then the composite mixture is poured in to the mold.

Care has been taken to avoid formation of air bubbles. Pressure was then applied from the top and the mold was allowed to cure at room temperature for 72 hrs. During application of pressure some amount of epoxy and hardener squeezes out. Adequate care has been taken to consider this loss during manufacturing so that a constant thickness of sample can be maintained. This procedure was adopted for preparation of 5, 10, 15 and 20 weight percentage of fiber reinforced epoxy composite slabs. After 72 hrs the samples were taken out from the mold and then cut in to required sizes as per ASTM standards for Mechanical test.

3.5 STUDY OF MECHANICAL PROPERTIES OF COMPOSITE

The study of mechanical properties such as tensile and flexural strength and modulus of both untreated and treated Rice Husk composites were carried out as per ASTM standards using samples as shown in figure 3.8. The machine Instron h10ks testing machine with tensile and bending attachment is used (figure 3.9). The results are tabulated in Table-3.4. The tensile strength, flexural strength, Young's Modulus and flexural modulus of the RH composite increases with increase in fiber content in comparison to neat epoxy. The increase in Young's modulus with fiber content is in line with other works [125-127].

From the above investigation, it can be concluded that the composite containing 15 percent by volume fiber provided the best combination of strength and modulus (Figure 3.10 to figure 3.17). Decrease in the mechanical properties is observed at higher fiber loading i.e. beyond 15 vol%. This may be due to poor fiber matrix adhesion which might have promoted micro-crack formation at the interface as well as non-uniform stress transfer due to fiber agglomeration within the matrix [128, 129]. Similar results have been reported by Mohanty et al. [107] and Rana et al. [101] while they worked with jute fiber.

The effect of different chemical modifications of fibers on mechanical properties of the composite has been studied. It is clearly seen from Table-3.4 that, the mechanical properties of the composite enhanced significantly due to chemical modification of fiber surface. This improvement in properties occurs due to rough fiber surface produce by removal of natural and artificial impurities, fibrillation of fiber which facilitate the mechanical anchoring between fiber and matrix which is explained in section 3.2.2. Higher increase in properties was observed in the case of benzoyl-chloride treated fiber composite. Similar observations were reported by Manikandan et al. [59], Sreenivasan et al. [130] and Britton et al. [131] while working with benzoylated sisal fibers, alkali treated coir fibers and acetone treated bagasse fibers respectively. The chemical treatment also reduces fiber diameter. Both fiber diameter and length have also bearing on mechanical properties [132,133]

3.6 STUDY OF ENVIRONMENTAL EFFECT

The performances of Rice Husk epoxy composite under different environmental conditions are essential to study. Therefore effect of environment on performance of RH reinforced epoxy composite samples for both treated and untreated fibers were subjected to following environments.

- (a) Steam exposures.
- (b) Saline water exposures
- (c) Subzero condition

3.6.1 Moisture absorption test

The moisture absorption and thickness swelling tests were conducted in accordance with ASTM D570-98. Three specimens for each composite system were cut with dimensions of 64 x 12.7mm (length x width) and the experiment was performed using test samples. The steady state dry weights of specimens were found out prior to conducting the above tests. Before taking the dry weights, the specimens were dried in an oven at 80⁰ C and then were allowed to cool to room temperature and kept in desiccators. The procedures were repeated for each sample of steam, saline water and sub-zero temperature environments. The increase in weight due to moisture absorption was recorded for each sample after exposure of every 10 hr. The specimens were taken out from the moist environment and all surface moisture was removed with a clean dry cloth or tissue paper. The specimens were weighed to the nearest 0.001 mg within 1 min. of removing them from the environment chamber. The experiments were conducted continuously for 110 hours. The moisture absorption was calculated by the weight difference. The percentage weight gain of the samples was measured at different time intervals by using the following equation:

$$\%M_t = \frac{(W_t - W_0) \times 100}{W_0} \quad (3.2)$$

where ' W_0 ' and ' W_t ' denote the dry weight and weight after time ' t ', respectively. The Equilibrium Moisture Content (EMC) in the sample was considered when the increase in moisture content was less than 0.1% by weight. The thickness swelling (TS) was determined by using the following equation:

$$TS(t) = \frac{H_t - H_0}{H_0} \times 100 \quad (3.3)$$

where ' H_t ' and ' H_0 ' are the composite thickness after and before the water immersion respectively.

3.6.2 Results and discussion

3.6.2.1 Moisture absorption behavior

The results of both untreated and treated fiber composite samples exposed to different environments are shown in Table-3.5 to 3.8. The percentage of moisture absorption characteristics of composite samples with untreated fiber exposed to Steam, Saline water and Sub-Zero temperature environment with time are shown in Figure-3.18 to 3.20. It is known both the moisture absorption quantity and rate for any lignocellulosic composite increases with increase in fiber loading [134]. K. Hardinnawirda and I. SitiRabiatull Aisha during their experiment on Rice Husk- Unsaturated Polyester Resin composite have also established same effect [96]. The initial rate and quantity of moisture absorption in the composite is higher and follows a linear trend. Thereafter, the moisture absorption rate decreases and continue for a longer time till the composite achieve equilibrium moisture after saturation time [135]. When the composite is exposed to moisture, the hydrophilic lignocellulosic fibers absorb moisture and swell. The result of fiber swelling causes micro cracks in the brittle thermosetting resin. As the composite cracks and gets damaged, capillarity and transport via micro cracks become active. The capillarity mechanism involves the flow of water molecules along fibre-matrix interfaces and a process of diffusion through the bulk matrix starts. The water molecules actively attack the interface, resulting in debonding of the fibre and the matrix. The water transport in this material follows a typical dual sorption-diffusion process and the diffusion process (molecular movement) obeys the Fick's law.

For the present case moisture absorption characteristic is studied for RH composites made with 15% fiber content which has the highest Tensile and flexural strength. The maximum moisture absorption of plain Rice Husk composites was found to be 6.62% in steam, 2.56% in saline water and 0.62% in sub-zero temperature environments.

It is observed that, the moisture absorption increases with immersion time, and got saturated after certain time period. Time to reach the saturation point is not same for all the environments. The saturation time is approximately 70 hrs for steam, and 80hrs for saline water and sub-zero temperature treatment. Environmental conditions also play a significant role in moisture absorption process. Figure-3.21 shows the moisture absorption behavior of composite in all three environments. In steam environment moisture absorption is higher as compare to saline water and sub-zero temperature environments irrespective of treatment of fiber surface . The moisture absorption behaviour of composite in steam environment is found to be higher irrespective of treatment of fiber surface followed by saline and subzero treatment. It can be concluded that the higher temperature in case of steam environment seem to accelerate the moisture uptake behaviour [134,136]. The absorption rate in case of saline water is less than that of steam. This happens because of the accumulation of NaCl ions in the fiber's surface immersed in saline water, which increases with time and hinders subsequent moisture diffusion [137]. Again the absorption rate of water in sub-zero temperature might be due to lower molecular movement of water particle at sub-zero temperature which is responsible for this type of behaviour.

In addition, the changes in surface chemistry of the fiber have reduced the affinity of fibers to moisture. Due to surface modification by chemical treatment, the fibers get masked with the epoxy resin with a stronger adhesion, resulting in greater hydrophobicity and less moisture absorption. For Benzoyl chloride treated surface, it is found to decrease about 25.38% for steam,30.46% saline and 22.4% for sub-zero treatment for rice husk composite.

3.6.2.2 Measurement of Diffusivity

Moisture penetration into lignocellulosic polymer matrix composite materials is conducted, by three different mechanisms [136] . The main process consists of diffusion of water molecules inside the microgaps between polymer chains. The other common mechanisms are capillary transport into the gaps and flaws at the interfaces between fibres and polymer,

because of incomplete wettability and impregnation; and transport by microcracks in the matrix, formed during the compounding process. In spite of the fact that all three mechanisms are active jointly in case of moisture exposure of the composite materials, the overall effect can be modeled conveniently considering only the diffusional mechanism. The theoretical equation of moisture absorption through diffusion has been developed by Ficks is given at Eq. 3.4. [137, 138]:

$$\frac{M_t}{M_m} = kt^n \quad (3.4)$$

where ' M_t ' is the moisture content at specific time ' t ', ' M_m ' the equilibrium moisture content (EMC), and ' k ' and ' n ' are constants. The above equation can be rewritten in logarithmic form as ;

$$\log (M_t / M_m) = \log (k) + n \log (t) \quad (3.5)$$

The value of k and n were determined from the slope and the intercept of M_t / M_m versus ' t ' in the log plot which was drawn from experimental data of moisture absorption with time. The Figure-3.26 to 3.28 showed the typical curve of $\log (M_t / M_m)$ as a function of $\log (t)$ for both untreated and treated RH reinforced epoxy composite respectively, used to determine these constants. The water sorption kinetics of the composite are studied through the diffusion constants k and n . The value of n varies: for Fickian diffusion, $n=0.5$; for pseudo-Fickian, $n<0.5$ while for relaxation controlled or non-Fickian $0.5 < n < 1$ [149]. The value of $n > 0.5$ indicates the predominant mechanism of moisture absorption is due to transport through capillary or crack. The dominant mechanism depends on several factors such as chemical structure of the polymer, dimensions and morphology of the filler, and the polymer–filler interfacial adhesion and void content in the composite.

The values of k and n resulting from the fitting of all formulations are shown in Table-3.9.

It was observed that the value of n is close to 0.5 in most of the composites. This confirms that the Fickian diffusion in lignocellulosic composites, can be adequately describe the moisture absorption in the composite, which is consistent with previous studies [140, 141]. A higher value of n and k indicates that the composite needs shorter time to attain equilibrium water absorption. The value of k was found to higher in some samples possibly due to void and micro-cracks developed during manufacturing [139]. A higher value of n and k indicates that the composite needs shorter time to attend equilibrium in

water absorption capacity. The value of K for untreated fiber composite was higher treated fiber composites.

The diffusion coefficient or diffusivity (D_x) of moisture absorption is the measurement of speed of diffusion. The diffusion coefficient characterises the ability of solvent molecules to move among the polymer segments [142]. The diffusion coefficient increases with fibre loading and with temperature [133, 141]. . The D_x is calculated using the following equation [143].

$$D_x = \pi \left[\frac{h}{4M_m} \right]^2 \left(\frac{M_2 - M_1}{\sqrt{t_2} - \sqrt{t_1}} \right)^2 \quad (3.6)$$

where ' M_m ' is the maximum percentage of moisture content, ' h ' is the sample thickness, ' t_1 ' and ' t_2 ' are the selected points in the initial linear portion of the plot of moisture absorption (M_t) versus \sqrt{t} (Figure-3.29) and ' M_1 ' and ' M_2 ' are the respective moisture content. From the plot of M_t verses square root of time (t) (Figure-3.30 to 3.36) the value of D_x has been evaluated and summarized in Table-3.10. The value of diffusion coefficient was found in the range of 1.8 to 5.7 x 10⁻⁵ mm²/sec which is in conformity with the work of W. Wang, M. Sain et.al with HDPE-Rice Husk composite. [80].

The rate diffusion should be less with treated fiber with better fiber-matrix adhesion due to decrease in velocity of diffusion in interfacial gap and blocking of Hydroxyl group[136]. Thus the treated material should show lower value of D_x . The steam environment should show higher value of diffusion coefficient considering the effect of temperature in diffusion. Nevertheless, these behaviour is not reproduced in the experimental values of diffusion coefficient given at table. This could be possible due to high porosity or existence of voids formed during processing that could accelerate the diffusion in these cases.

3.6.2.3 Thickness swelling behaviour

The thickness swelling processes for RH reinforced epoxy composites at different ambient environments has been studied by considering the thickness swelling (TS) and swelling rate parameter (K_{SR}). The value of K_{SR} was evaluated through a non-linear regression curve fitting method to fit the experimental data (Table-3.11) in equation-3.7 [144], using computer software with curve fitting routines.

$$TS(t) = \left(\frac{H_{\infty}}{H_0 + (H_{\infty} - H_0)e^{-K_{SR}t}} - 1 \right) \times 100 \quad (3.7)$$

where 'TS (t)' is the thickness swelling at specific time (t), 'H₀' and 'H_∞' are the initial and equilibrium thickness respectively.

Figure-3.22 to 3.24 shows the thickness swelling behaviour of untreated RH reinforced epoxy composites at various environments. The thickness swelling (TS) increases with an increase in fiber content and immersion time. The Rice-Husk composites of 15% volume fraction were studied for thickness swelling behaviour under steam, saline and subzero environment both for treated and untreated fibers. The thickness increase of plane Rice Husk was found to be 2.62% in steam, 1.463% in saline water and 1.212% at sub-zero temperature environments, which corresponds to the highest water absorption. The swelling tendency is always more in steam environment followed by saline water and then subzero environment both for treated and untreated Rice Husk Composite.

However, the chemical treatments reduces the swelling character of RH reinforced epoxy composites as shown in Figure-3.25. The thickness swelling behavior in 15% RH composites was reduced by 12.59% in Acetone treatment, 20.89 in Alkali treatment and 32.44% in case of Benzoyl-chloride treated Rice Husk.

The experimental data was used to obtain the swelling rate parameter (K_{SR}) by using equation-3.7. Table-3.11 summarizes the respective value of K_{SR} obtained through non-linear curve fitting. The swelling parameter, K_{SR}, quantifies the rate of the composites approaching the equilibrium value for thickness swelling after sufficient time of water immersion. The higher value of K_{SR} indicates, the higher rate of swelling along with reaching of equilibrium thickness swelling in a shorter period of time. As per the literature the swelling rate parameter of the composites increases with increase in fiber content but it reduces significantly with chemical treatment of fiber surface which was due to the improved compatibility between polymer and fiber. The experimental result has not established the fact. Though moisture absorption and the swelling in case of steam environment is highest where as the value of K_{SR} is lower in Subzero and lowest in saline

water in most of the experiments. This might have happened because of the increased number of micro voids caused by the larger amount of poorly bonded area between the hydrophilic filler and the hydrophobic matrix polymer

3.6.3 Effect of moisture absorption on Mechanical properties

The moisture absorption has a significant influence on the mechanical properties of the natural fiber polymer composite. As explained earlier, the hydrophilic properties of natural fibers are due to presence of hydroxyl group (-OH) in cellulose and Hemicellulose. These hydroxyl groups form Hydrogen bond when come in contact with water molecule. Thus the natural fibers in the polymer matrix composite absorb moisture and swells. This in turn develops shear stress at fiber matrix interface of the composite and break interfacial bond resulting reduction in mechanical strength [91,134]. Table-3.12 shows the result of mechanical properties of the composite with both treated and untreated fiber reinforced composite after expose to different moist environment for a period of 110hrs. The increase in volume fraction increases the moisture absorption. As seen in Figure 3.21, the moisture absorption is the highest in steam environment. The experimental data has shown maximum reduction in tensile strength and flexural strength in steam environment. The reduction in the strength is to the extent of 41% of the original strength. The Chemical treatment of fibers helps preventing reduction of properties due to environmental effect. The benzoyl-chloride treated fiber composite exhibits the best result in all environments in comparison to other two treated fiber composite. Because the benzoyl-chloride treatment reduces the hydrophilic nature of the fiber to great extend which leads to less moisture absorption.

3.7 CONCLUSIONS

Based on experimental results, this study has led to the following conclusions:

- The Rice Husk can successfully be used as reinforcing agent to fabricate composite by suitably bonding with epoxy resin.
- On increasing the fiber content the strength, modulus increases and the best combination is found with 15 vol% of fiber.

- The silicon content is unevenly distributed on the Rice Husk. The Outer surface crest portion contains high Silicon in the untreated RH. The chemical treatments remove Silicon content.
- The fiber surface modification by chemical treatments significantly improves the fiber matrix adhesion, which in turn improves the mechanical properties of composite. Benzoyl-chloride treatment shows the highest improvement in comparison to alkali and acetone treatment. These results are confirmed through SEM and FTIR analysis.
- RH also contain Crystalline Cellulose which can offer better strength as a lignocellulosic fiber. Chemical treatment reduces crystalline index due to fibrillation.
- Silica content in RH slowdown degradation process of RH composite and make them thermally stable.
- The moisture uptake and thickness swelling values of RH composites are higher in case of untreated RH in Steam, Saline water and Sub-Zero environments. The chemical treatments in Acetone, Alkali and Benzoyl Chloride reduce moisture absorption and swelling. But the Benzoyl chloride treatment is very effective of all. The moisture absorption and swelling are found to be higher in steam environment than in saline water and sub-zero temperature environments.
- The tensile and flexural strength of the RH composites reduces when exposed to steam, saline water or sub-zero environment.

Table 3.1 Silicon content of untreated and treated Rice Husk as obtained from EDX analysis.

Type of treatment	Element	Percent of element at Crest	Percent of element at Trough
Untreated	Si	100	42.05
	O	0	57.95
Acetone	Si	50.94	49.73
	O	49.06	50.27
Alkali	Si	60.65	42.45
	O	39.35	57.55
Benzoyl Chloride	Si	59.41	43.12
	O	40.59	56.88

Table-3.2 Variation of crystalline index of the Rice Husk epoxy composites with chemical treatments.

Fiber Treatment	Max Intensity of I_{am}	Angle 2Q at I_{am}	Max Intensity of I_{002}	Angle 2Q at I_{002}	Crystalline Index
Plain	144	15.63	269	22.25	0.465
Actone	117	15.89	213	22.13	0.451
Alkali	130	15.73	219	22.23	0.406
Benzoyl Chloride	222	16.15	400	22.47	0.445

Table-3.3 Thermal Degradation parameter of Rice Husk epoxy composites during Thermo Gravimetric Analysis (TGA) .

Material	Temperature required for 5% weight loss in °C	Weight loss % of the sample at 100°C
EPOXY	328.00	0.30
PLAIN RH	253.13	1.70
ACETONE RH	296.41	0.90
ALKALI RH	303.80	0.60
BENZOYL RH	269.23	0.80

Table-3.4 Mechanical properties of Rice Husk epoxy composites

	Treatment Type	Tensile strength (Mpa)	Young's Modulus (Mpa)	Flexural strength (MPa)	Flexural Modulus (MPa)
5%	PRH	15.41	917.51	20.65	2427.88
	Acetone	15.37	1270.21	21.01	2531.36
	Alkali	16.18	1011.33	16.75	2611.44
	Benzoyl- Chloride	17.21	994.98	22.91	2987.96
10%	PRH	17.81	1047.91	22.60	2549.43
	Acetone	18.74	1388.21	29.32	3440.56
	Alkali	18.96	1053.61	22.88	3330.41
	Benzoyl- Chloride	20.02	1143.79	30.34	3486.29
15%	PRH	18.52	1187.09	25.87	2854.47
	Acetone	19.61	1390.90	33.07	3888.41
	Alkali	19.51	1219.07	20.29	2981.36
	Benzoyl- Chloride	23.24	1320.52	37.51	4409.54
20%	PRH	16.70	988.21	21.27	2412.79
	Acetone	17.10	877.16	29.11	3435.92
	Alkali	13.67	854.18	18.75	2503.25
	Benzoyl- Chloride	18.67	818.79	29.62	3411.21

Table-3.5 Percentage of weight gain and thickness swelling of Plane Rice Husk epoxy composite expose at steam, Saline and Subzero environment.

Condition of testing.	Immersion time 't' (hrs)	Weight of the sample (W_t)	Percentage of weight gain (%M)	Thickness at time 't' H(t)	Thickness swelling TS(t) (%)
Steam	0	15.972	0.000	5.920	0.000
	10	16.413	2.759	5.967	0.800
	20	16.583	3.824	6.013	1.578
	30	16.675	4.400	6.032	1.890
	40	16.736	4.780	6.047	2.150
	50	16.806	5.219	6.054	2.260
	60	16.883	5.702	6.059	2.350
	70	16.938	6.050	6.062	2.400
	80	16.989	6.370	6.067	2.490
	90	17.017	6.540	6.071	2.550
	100	17.026	6.600	6.075	2.620
110	17.029	6.620	6.075	2.620	
Saline	0	16.244	0.000	6.080	0.000
	10	16.366	0.750	6.132	0.861
	20	16.436	1.180	6.147	1.103
	30	16.488	1.500	6.152	1.180
	40	16.530	1.760	6.156	1.248
	50	16.569	2.000	6.161	1.331
	60	16.608	2.240	6.165	1.395
	70	16.624	2.340	6.167	1.429
	80	16.637	2.420	6.167	1.429
	90	16.645	2.470	6.168	1.454
	100	16.658	2.550	6.169	1.462
110	16.660	2.560	6.169	1.463	
Sub-zero	0	18.201	0.000	6.293	0.000
	10	18.224	0.124	6.328	0.560
	20	18.242	0.226	6.341	0.760
	30	18.257	0.309	6.347	0.859
	40	18.271	0.382	6.352	0.941
	50	18.280	0.432	6.357	1.018
	60	18.288	0.480	6.361	1.088
	70	18.298	0.532	6.364	1.129
	80	18.305	0.574	6.367	1.176
	90	18.310	0.597	6.369	1.204
	100	18.313	0.615	6.369	1.212
110	18.313	0.615	6.369	1.212	

Table-3.6 Percentage of weight gain and thickness swelling of Acetone treated RH- epoxy composite expose at steam, Saline and Subzero environment.

Condition of testing.	Immersion time 't' (hrs)	Weight of the sample (W_t)	Percentage of weight gain (%M)	Thickness at time 't' H(t)	Thickness swelling TS(t) (%)
Steam	0	15.513	0.000	5.640	0.000
	10	15.907	2.542	5.675	0.620
	20	16.045	3.430	5.710	1.240
	30	16.146	4.082	5.730	1.596
	40	16.183	4.320	5.743	1.826
	50	16.251	4.760	5.747	1.897
	60	16.310	5.140	5.753	2.010
	70	16.369	5.520	5.757	2.074
	80	16.410	5.780	5.763	2.180
	90	16.444	6.000	5.764	2.200
	100	16.464	6.130	5.769	2.280
110	16.469	6.160	5.769	2.290	
Saline	0	20.277	0.000	7.060	0.000
	10	20.398	0.597	7.105	0.644
	20	20.488	1.040	7.126	0.937
	30	20.549	1.340	7.134	1.055
	40	20.581	1.500	7.140	1.136
	50	20.630	1.740	7.146	1.224
	60	20.658	1.880	7.150	1.273
	70	20.679	1.982	7.153	1.317
	80	20.709	2.130	7.154	1.338
	90	20.723	2.198	7.155	1.351
	100	20.746	2.315	7.156	1.358
110	20.750	2.333	7.156	1.360	
Sub-zero	0	14.150	0.000	6.607	0.000
	10	14.162	0.082	6.632	0.382
	20	14.173	0.160	6.645	0.576
	30	14.180	0.212	6.653	0.694
	40	14.188	0.268	6.657	0.753
	50	14.195	0.320	6.662	0.835
	60	14.203	0.374	6.665	0.880
	70	14.211	0.429	6.669	0.935
	80	14.214	0.453	6.671	0.965
	90	14.217	0.476	6.672	0.982
	100	14.219	0.488	6.673	0.994
110	14.219	0.488	6.673	0.994	

Table-3.7 Percentage of weight gain and thickness swelling of Alkali treated RH- epoxy composite expose at steam, Saline and Subzero environment.

Condition of testing.	Immersion time 't' (hrs)	Weight of the sample (W_t)	Percentage of weight gain (%M)	Thickness at time 't' H(t)	Thickness swelling TS(t) (%)
Steam	0	17.646	0.000	5.450	0.000
	10	18.026	2.153	5.471	0.377
	20	18.191	3.090	5.494	0.800
	30	18.269	3.530	5.513	1.160
	40	18.357	4.030	5.528	1.440
	50	18.417	4.370	5.537	1.594
	60	18.477	4.710	5.545	1.739
	70	18.537	5.050	5.553	1.884
	80	18.579	5.290	5.555	1.928
	90	18.620	5.520	5.558	1.986
	100	18.634	5.600	5.561	2.029
	110	18.634	5.600	5.563	2.072
Saline	0	18.058	0.000	5.663	0.000
	10	18.114	0.308	5.693	0.530
	20	18.183	0.690	5.710	0.830
	30	18.239	1.000	5.716	0.941
	40	18.278	1.220	5.720	1.015
	50	18.309	1.390	5.723	1.060
	60	18.336	1.540	5.726	1.120
	70	18.363	1.690	5.729	1.160
	80	18.390	1.840	5.730	1.190
	90	18.410	1.950	5.732	1.217
	100	18.425	2.030	5.733	1.230
	110	18.432	2.070	5.733	1.230
Sub-zero	0	16.950	0.000	5.573	0.000
	10	16.958	0.047	5.586	0.242
	20	16.968	0.106	5.597	0.429
	30	16.976	0.156	5.602	0.529
	40	16.985	0.206	5.607	0.618
	50	16.993	0.256	5.611	0.680
	60	17.000	0.297	5.614	0.741
	70	17.007	0.338	5.616	0.776
	80	17.014	0.376	5.618	0.812
	90	17.017	0.397	5.619	0.829
	100	17.019	0.406	5.620	0.840
	110	17.019	0.406	5.620	0.840

Table-3.8 Percentage of weight gain and thickness swelling of Benzoyl Chloride

Condition of testing.	Immersion time 't' (hrs)	Weight of the sample (W_t)	Percentage of weight gain (%M)	Thickness at time 't' H(t)	Thickness swelling TS(t) (%)
Steam	0	20.082	0.000	6.900	0.000
	10	20.398	1.573	6.915	0.220
	20	20.574	2.450	6.935	0.510
	30	20.662	2.890	6.958	0.840
	40	20.751	3.330	6.977	1.120
	50	20.845	3.800	6.997	1.400
	60	20.905	4.100	7.004	1.510
	70	20.968	4.410	7.010	1.590
	80	21.022	4.680	7.016	1.680
	90	21.056	4.850	7.019	1.730
	100	21.068	4.910	7.021	1.760
Saline	0	19.774	0.000	6.833	0.000
	10	19.833	0.301	6.861	0.410
	20	19.879	0.530	6.882	0.713
	30	19.920	0.740	6.890	0.840
	40	19.962	0.950	6.895	0.914
	50	20.003	1.160	6.900	0.975
	60	20.039	1.340	6.904	1.040
	70	20.065	1.470	6.907	1.089
	80	20.096	1.630	6.908	1.103
	90	20.116	1.730	6.910	1.129
	100	20.124	1.770	6.911	1.136
Sub-zero	0	21.201	0.000	6.917	0.000
	10	21.207	0.029	6.928	0.153
	20	21.215	0.068	6.939	0.320
	30	21.224	0.109	6.947	0.435
	40	21.236	0.165	6.953	0.524
	50	21.244	0.203	6.958	0.594
	60	21.253	0.247	6.962	0.653
	70	21.262	0.288	6.966	0.706
	80	21.270	0.326	6.968	0.735
	90	21.275	0.350	6.969	0.747
	100	21.276	0.354	6.969	0.750
110	21.276	0.356	6.969	0.753	

Table-3.9 Diffusion parameters for 15% Rice Husk Epoxy Composite (Both treated and untreated)

Environment	Type of fiber	N	K	K(h) ²
Steam	PRH	0.3708	0.185	6.480
	Acetone	0.3745	0.179	5.695
	Alkali	0.4029	0.160	4.739
	Benzoyl	0.4811	0.113	5.360
Saline water	PRH	0.5176	0.097	3.589
	Acetone	0.5519	0.081	4.041
	Alkali	0.7630	0.031	1.010
	Benzoyl	0.7710	0.030	1.404
Sub-zero Temperature	PRH	0.6708	0.048	1.910
	Acetone	0.7590	0.032	1.411
	Alkali	0.9113	0.016	0.509
	Benzoyl	1.0808	0.008	0.364

Table-3.10 Diffusivity of untreated and treated fiber Rice Husk epoxy composites (15%) at different environments

Environment	Type of fiber treatment	EMC (percentage)	Diffusivity (D _x) x 10 ⁻⁵ (mm ² /sec)
Steam	PRH	6.620	2.887E-05
	Acetone	6.160	2.102E-05
	Alkali	5.600	2.641E-05
	Benzoyl Chloride	4.940	4.771E-05
Saline water	PRH	2.560	3.315E-05
	Acetone	2.330	5.718E-05
	Alkali	2.070	3.463E-05
	Benzoyl Chloride	1.780	2.460E-05
Sub-zero Temperature	PRH	0.620	3.463E-05
	Acetone	0.490	3.545E-05
	Alkali	0.410	2.085E-05
	Benzoyl Chloride	0.360	1.825E-05

Table-3.11 Swelling rate parameter of treated and untreated Rice Husk epoxy composite in different environments.

Environment	Type of Fiber	T₀ (mm)	T_∞ (mm)	TS (%)	Swelling Rate Parameter (K_{SR}) x10⁻³ (h⁻¹)
Steam	PRH	5.920	6.075	2.620	37.9
	Acetone	5.640	5.769	2.290	36.0
	Alkali	5.450	5.563	2.072	35.7
	Benzoyl Cl	6.900	7.022	1.770	41.5
Saline water	PRH	6.080	6.169	1.463	50.1
	Acetone	7.060	7.156	1.360	51.8
	Alkali	5.663	5.733	1.230	44.2
	Benzoyl Cl	6.833	6.911	1.136	49.9
Sub-zero temperature	PRH	6.293	6.369	1.212	47.0
	Acetone	6.607	6.673	0.994	45.1
	Alkali	5.573	5.620	0.840	44.6
	Benzoyl Cl	6.917	6.969	0.753	50.4

Table-3.12 Mechanical properties of both untreated and treated Rice Husk epoxy composite with 15% volume fraction under different environments

Environment Exposure	Type of Fiber	Tensile Strength MPa	Young's Modulus MPa	Flexural Strength MPa	Flexural Modulus MPa
Natural	PRH	18.52	1187.08	25.87	2854.47
	Acetone	19.61	1390.90	33.07	3888.41
	Alkali	19.51	1219.07	20.29	2981.36
	Benzoyl Cl	23.24	1320.52	37.51	4409.54
Steam	PRH	10.87	811.48	14.71	1640.76
	Acetone	13.92	959.78	18.18	1911.17
	Alkali	12.23	873.88	16.35	1745.16
	Benzoyl Cl	16.03	1014.62	20.98	2148.65
Saline water	PRH	13.05	900.04	16.38	1778.54
	Acetone	16.02	1061.15	20.84	2198.91
	Alkali	14.94	996.21	17.84	1869.61
	Benzoyl Cl	17.59	1135.11	23.02	2312.98
Sub-zero temperature	PRH	14.65	1024.17	18.42	1937.07
	Acetone	17.14	1158.32	22.57	2353.29
	Alkali	15.97	1101.46	19.47	2104.46
	Benzoyl Cl	19.04	1228.33	24.88	2574.36



Figure-3.1 Soxhlet Extractor

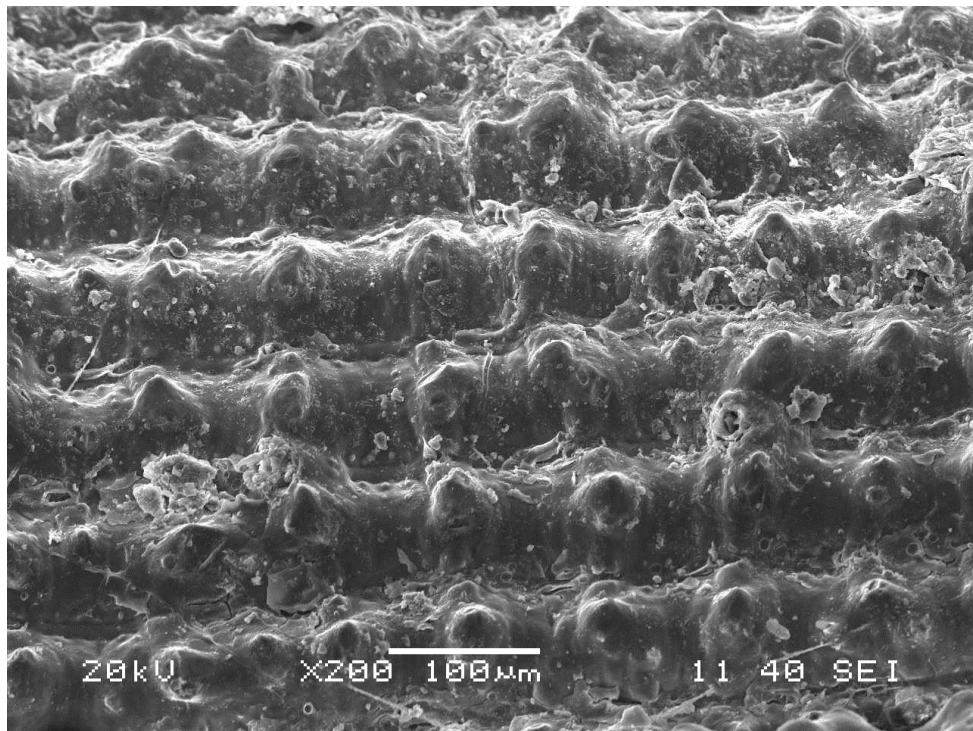


Figure-3.2 (a)

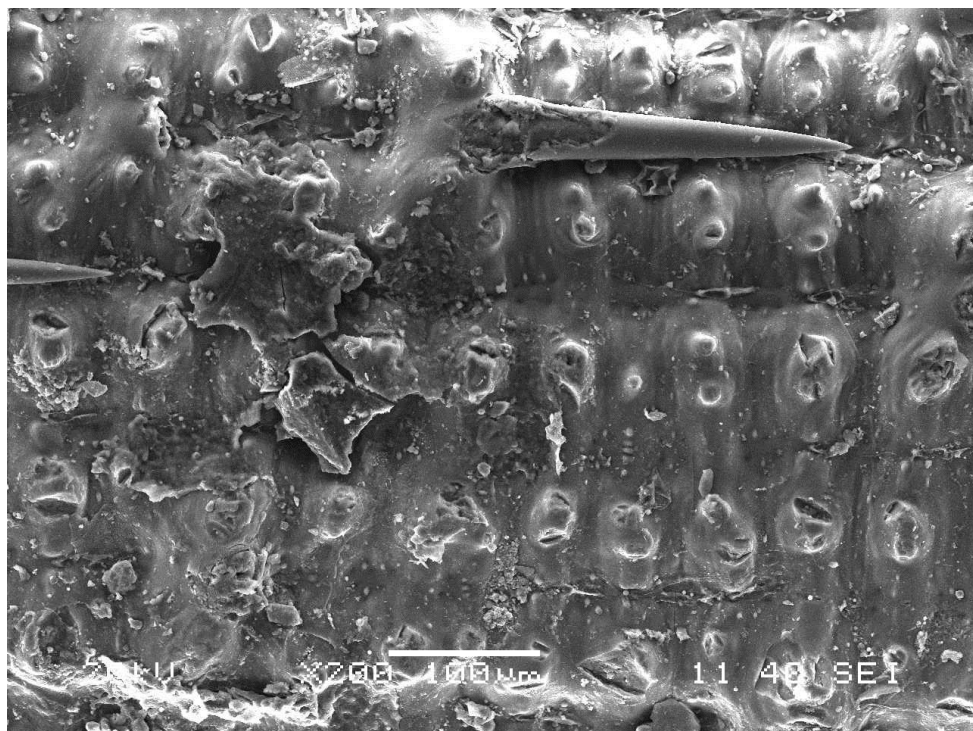


Figure-3.2 (b)

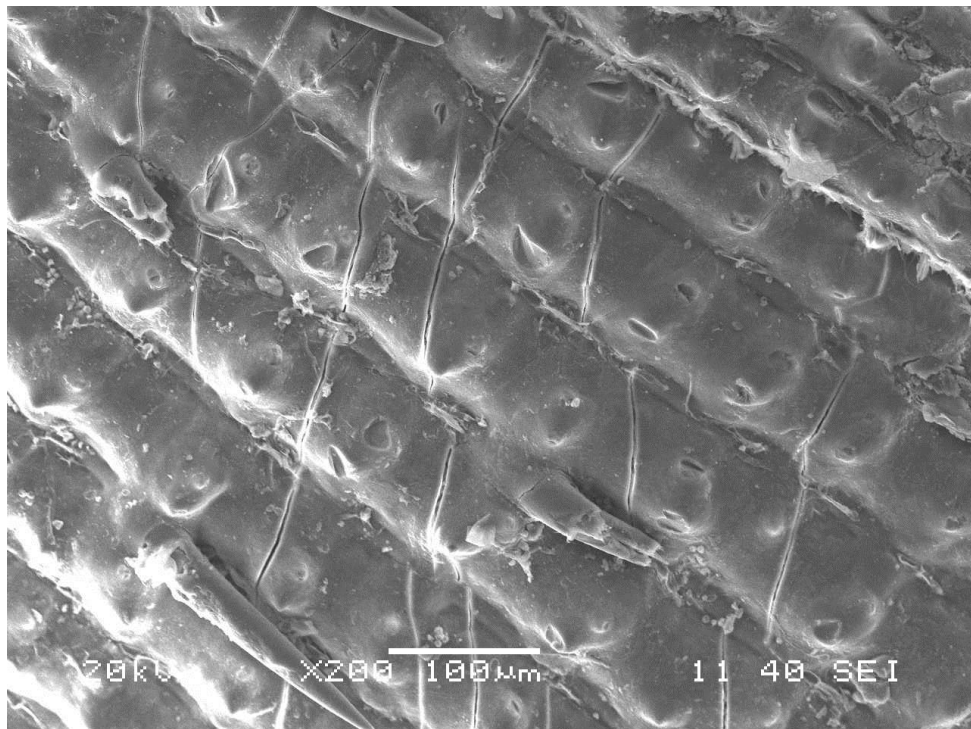


Figure-3.2 (c)

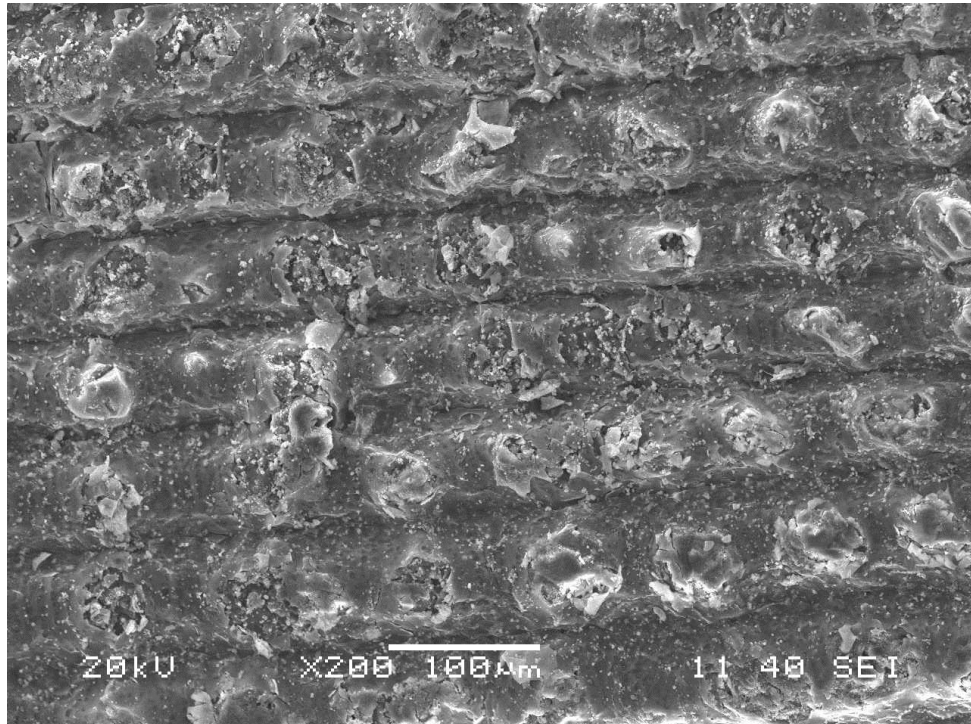


Figure-3.2 (d)

Figure-3.2 SEM micrograph of Rice Husk (a) Untreated; (b) Acetone treated; (c) Alkali treated; (d) Benzoyl-Chloride treated

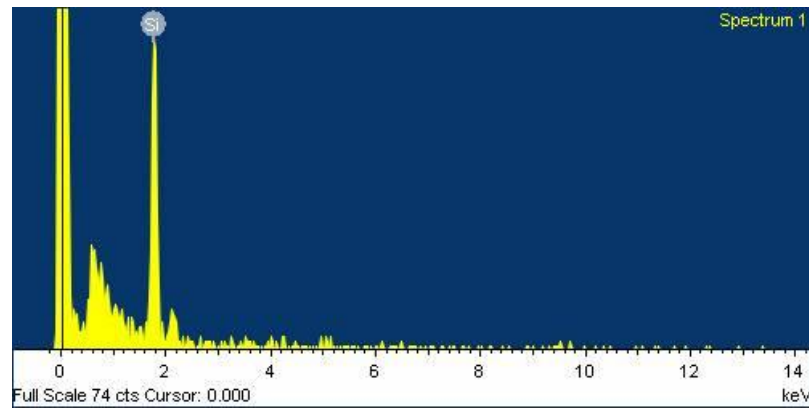


Fig 3.3 (a)

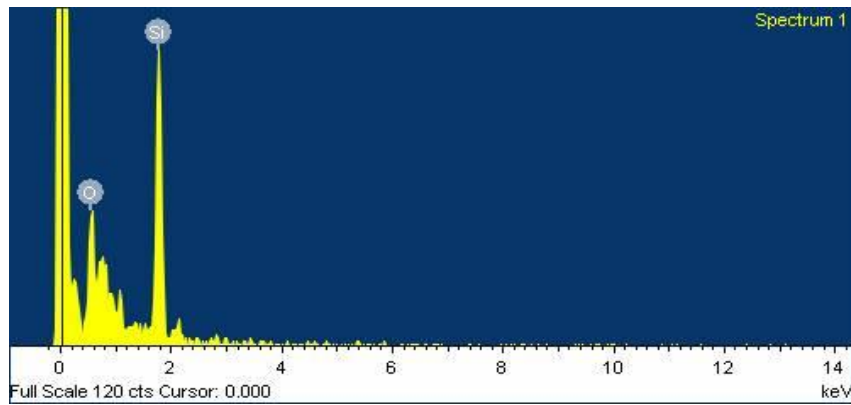


Fig 3.3 (b)

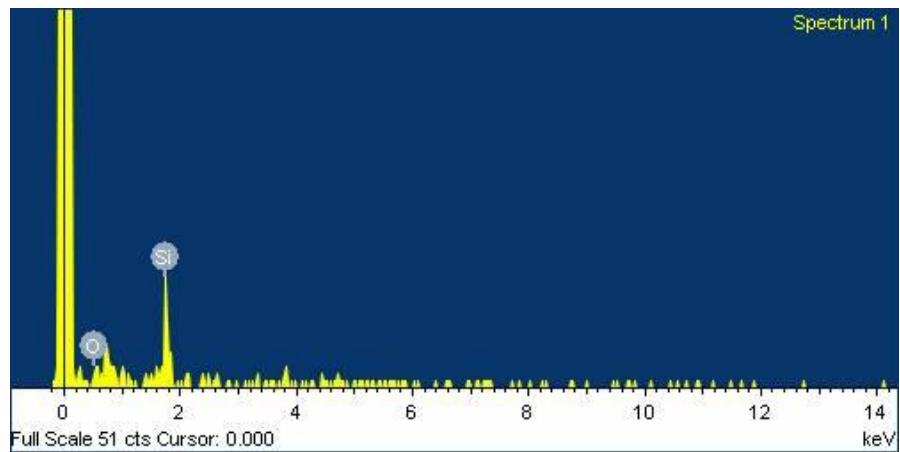


Fig 3.3 (c)

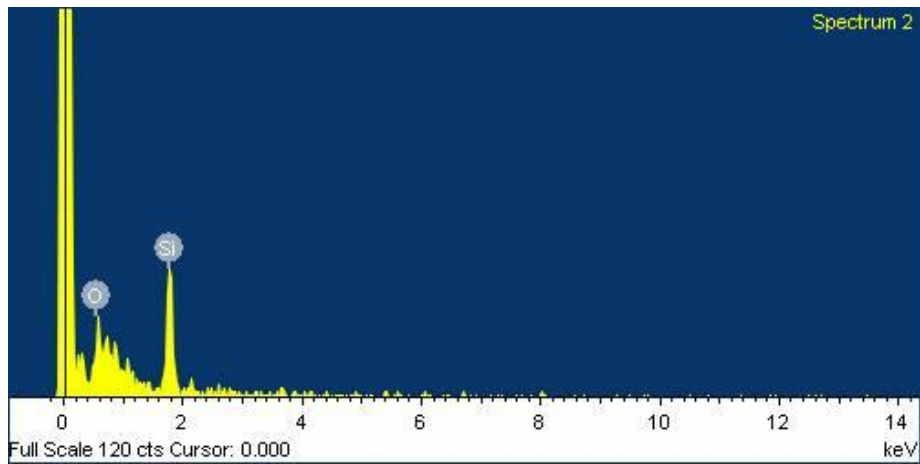


Fig. 3.3 (d)

Fig. 3.3 EDX Spectra showing presence of Silica in treated and untreated Rice Husk
(a) Untreated (b) Acetone (c) Alkali (d) Benzoyl Chloride

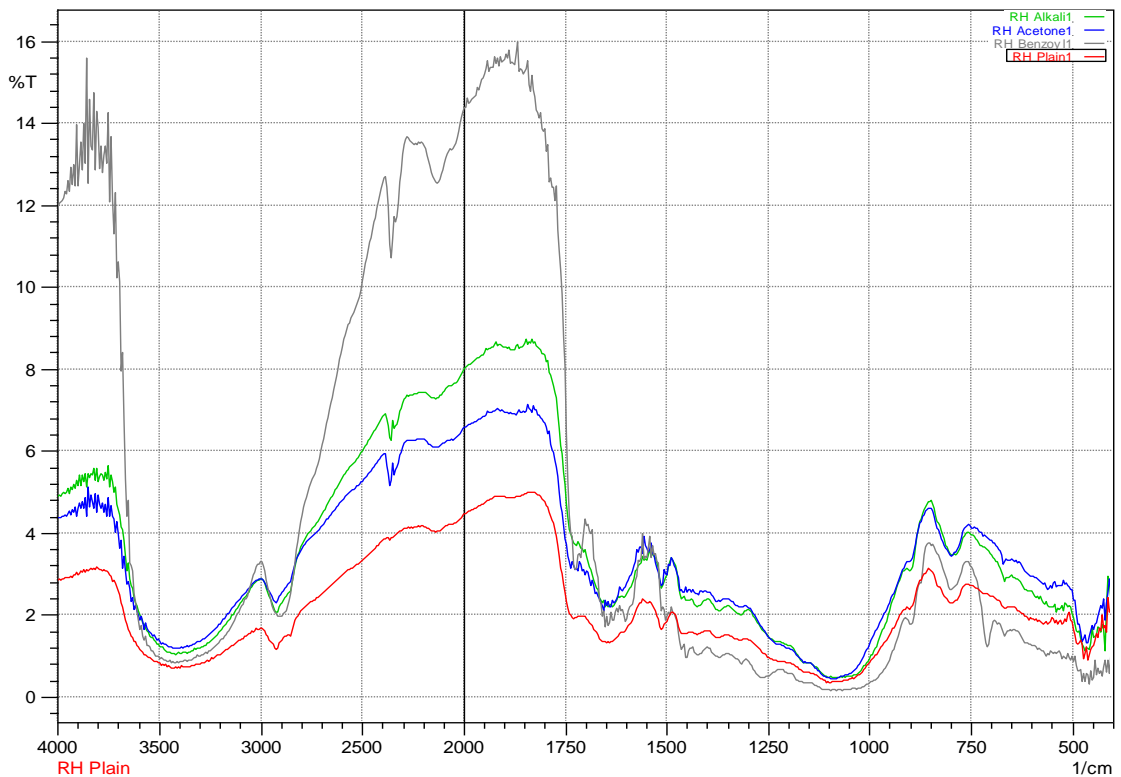


Figure-3.4 FTIR spectra of Rice Husk before and after chemical modification

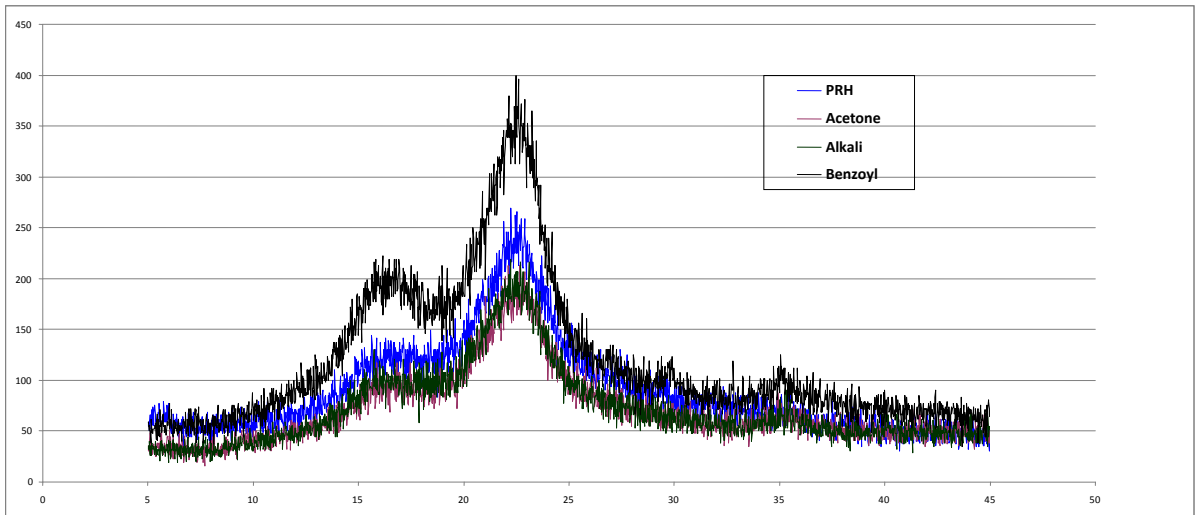


Figure-3.5 XRD pattern of Plain Rice Husk and Chemically treated Rice Husk.

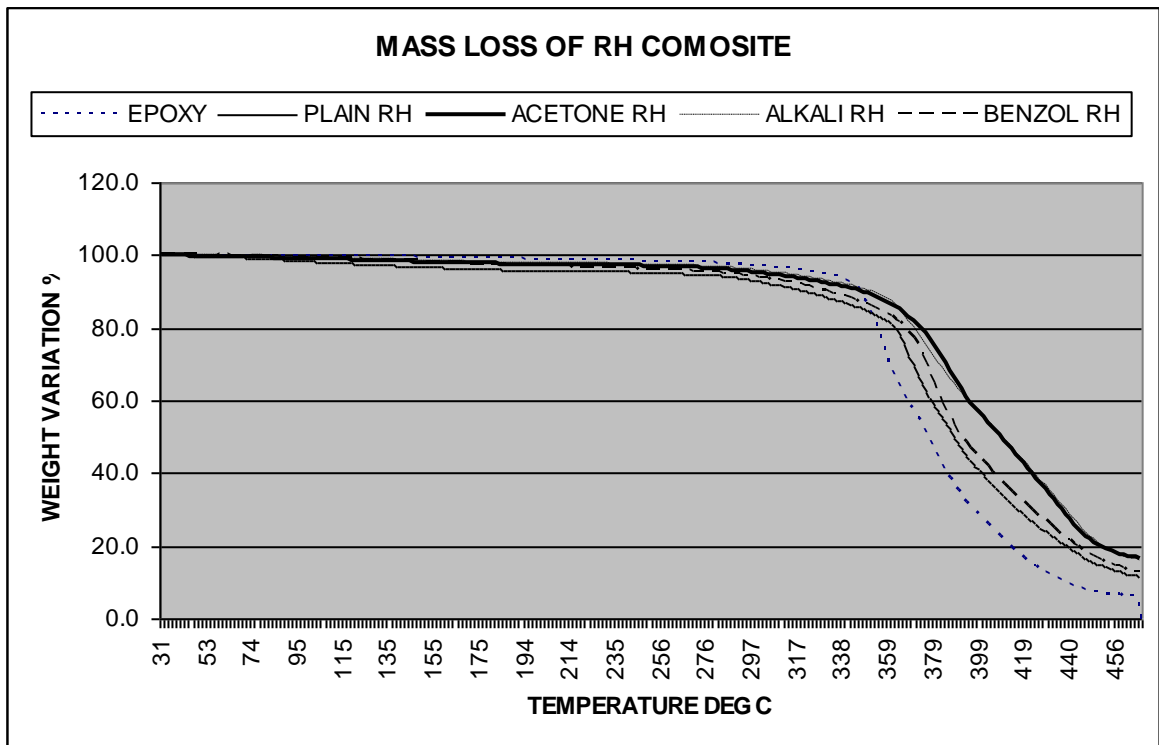


Figure-3.6 Graph showing weight loss the Rice Husk epoxy composites during Thermo Gravimetric Analysis (TGA) both for Plain and chemically treated RH.



Figure-3.7 Mold used for composite preparation



(a)



(b)



(c)

Figure-3.8 (a) Rice Husk epoxy composite sample (b) Specimen for Tensile test and (c) Flexural Test

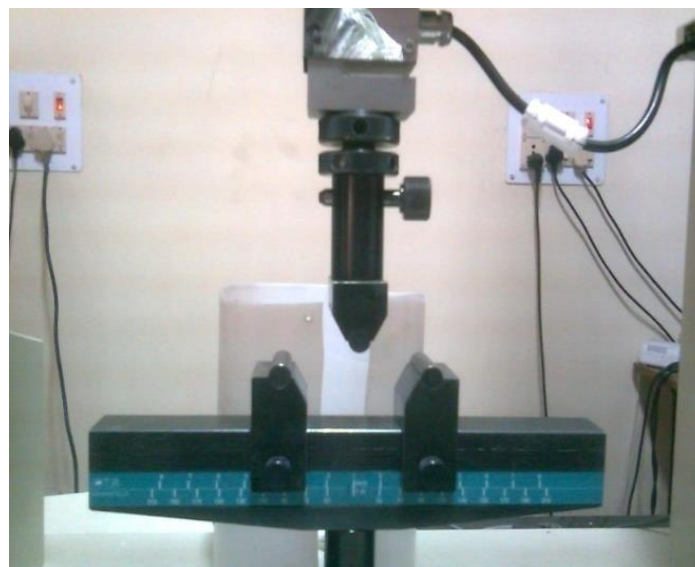
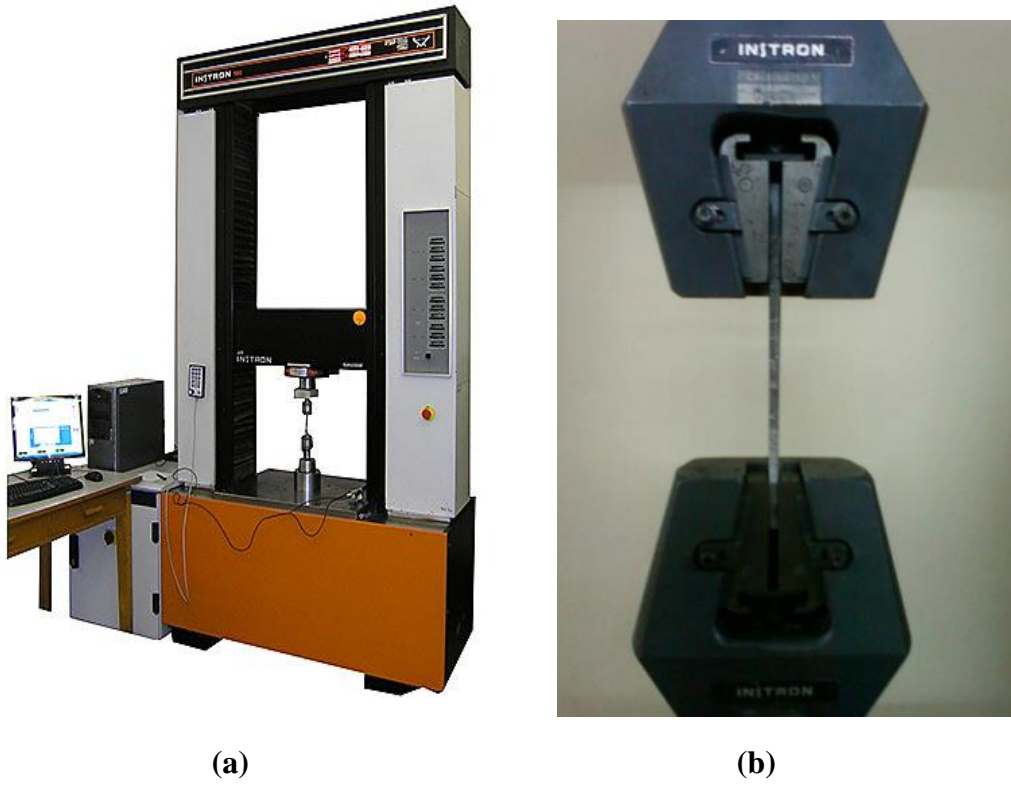


Figure-3.9 (a) Instron H10KS testing machine (b)Specimen under tensile loading (c)bending attachment.

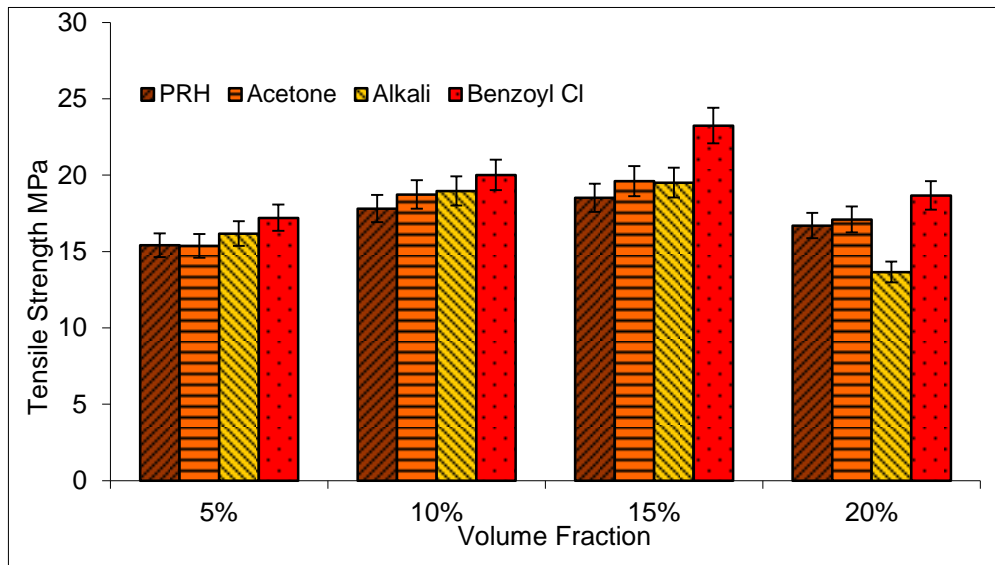


Figure-3.10 Variation of Tensile Strength of RH-Epoxy composite with change in Volume Fraction.

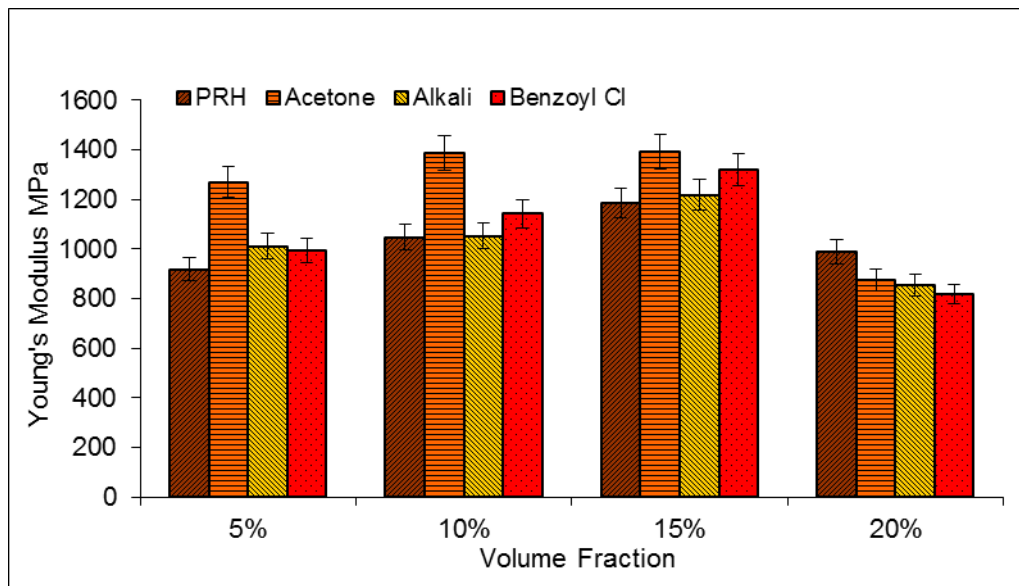


Figure-3.11 Variation of Young's Modulus of RH-Epoxy composite with change in Volume Fraction.

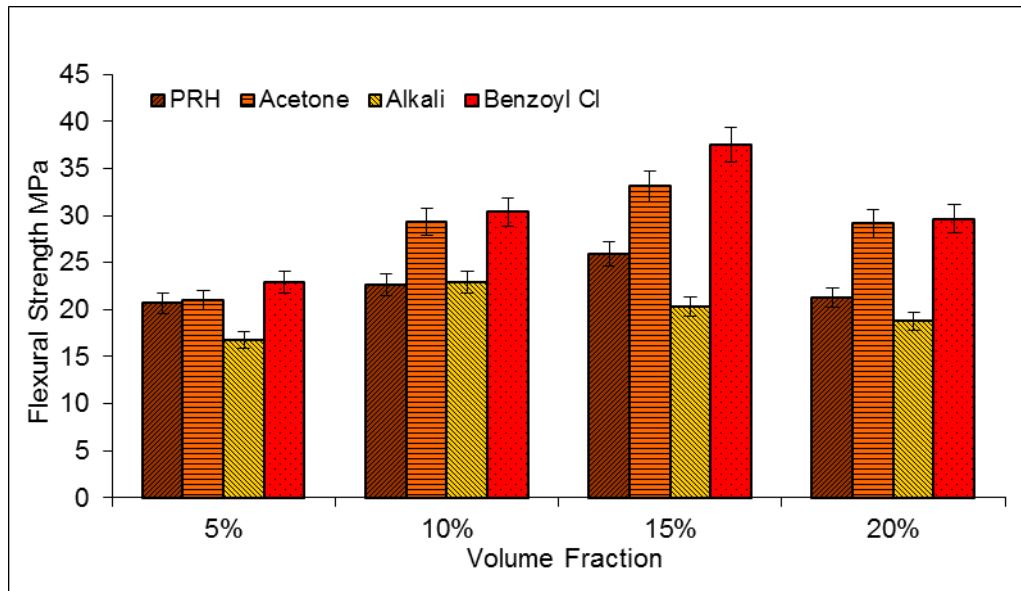


Figure-3.12 Variation of Flexural Strength of RH-Epoxy composite with change in Volume Fraction.

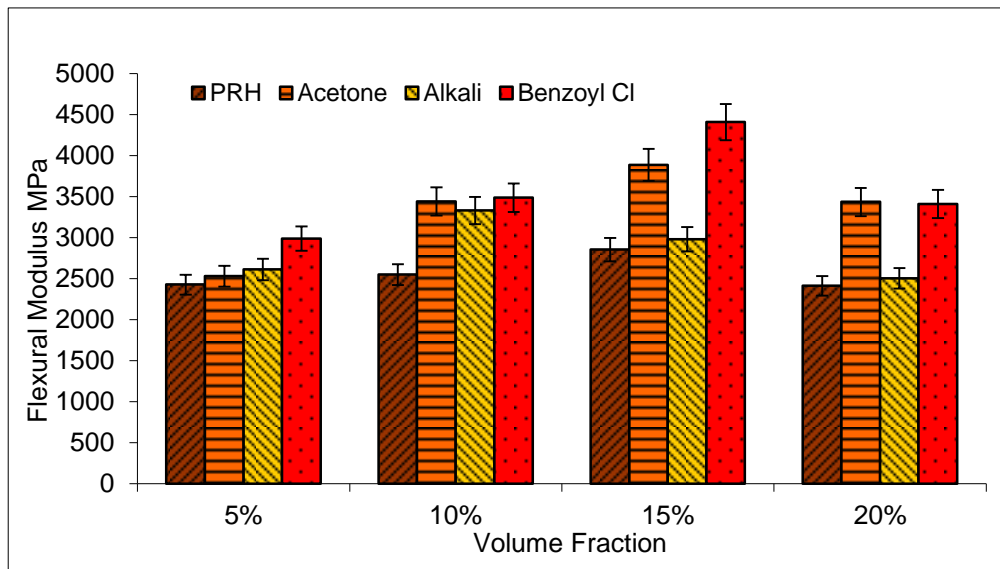


Figure-3.13 Variation of Flexural Modulus of RH-Epoxy composite with change in Volume Fraction.

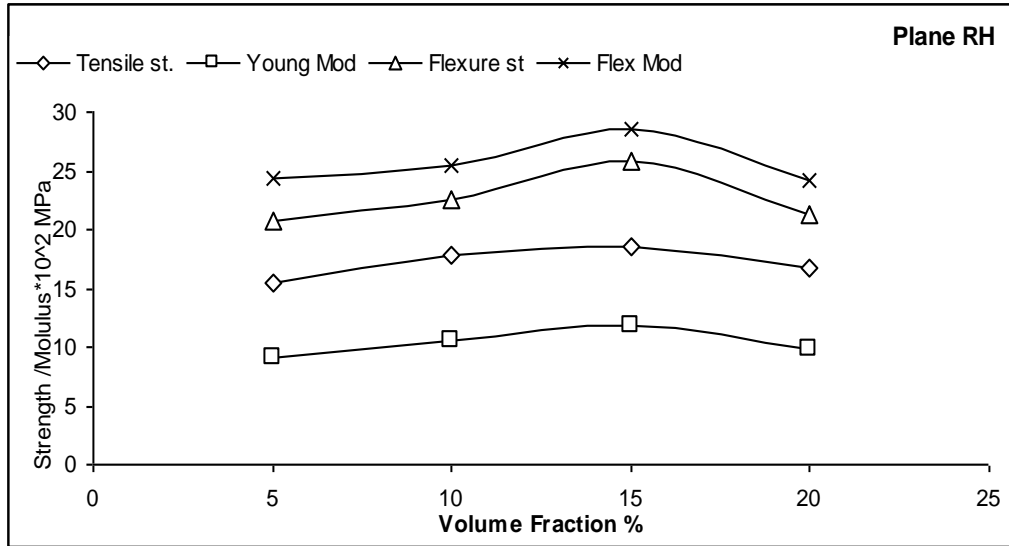


Figure-3.14 Variation of Mechanical Properties of Plain RH-Epoxy composite with change in Volume Fraction.

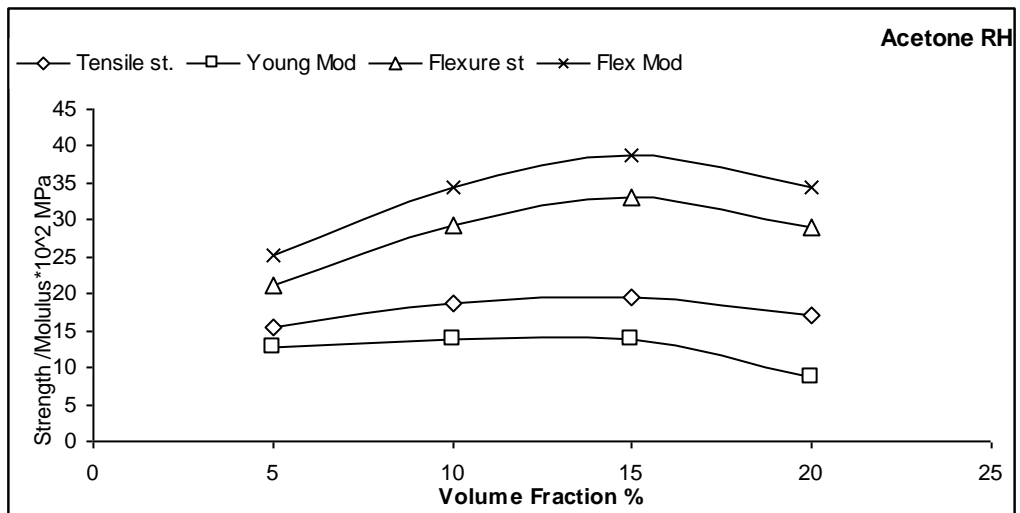


Figure-3.15 Variation of Mechanical Properties of Acetone Treated RH-Epoxy composite with change in Volume Fraction.

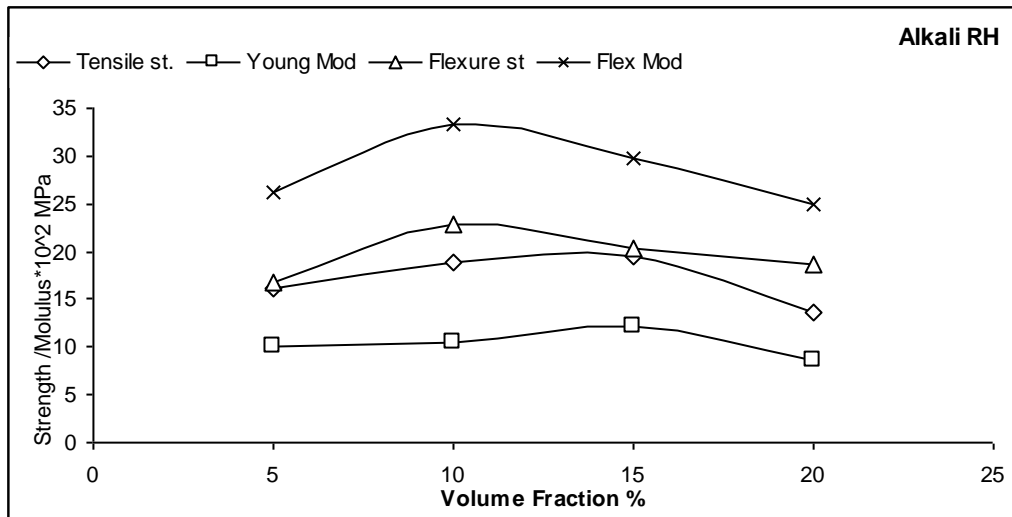


Figure-3.16 Variation of Mechanical Properties of Alkali Treated RH-Epoxy composite with change in Volume Fraction.

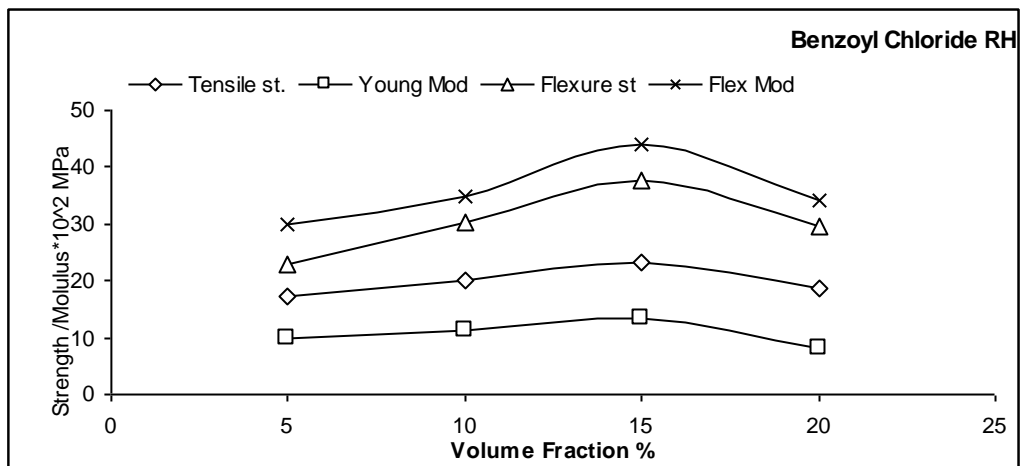


Figure-3.17 Variation of Mechanical Properties of Benzoyl Chloride Treated RH-Epoxy composite with change in Volume Fraction.

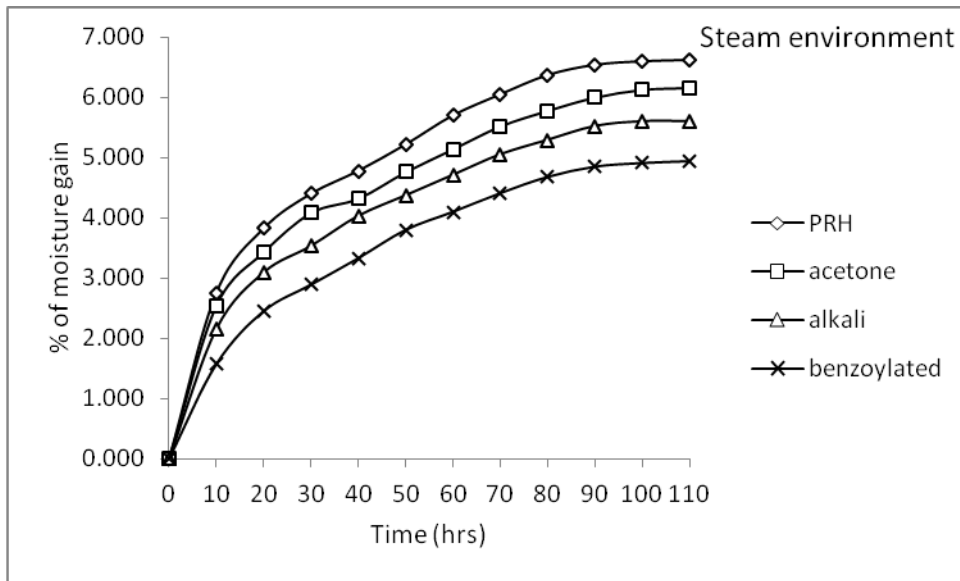


Figure-3.18 Variation of weight gain of the Rice Husk epoxy composites with immersion time at steam environment

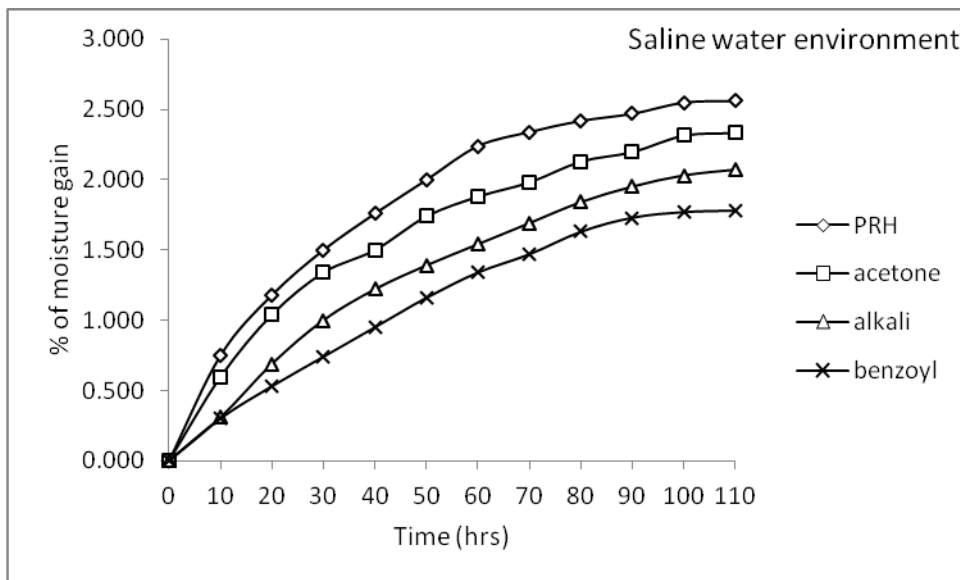


Figure-3.19 Variation of weight gain of the Rice Husk epoxy composites with immersion time at saline water environment

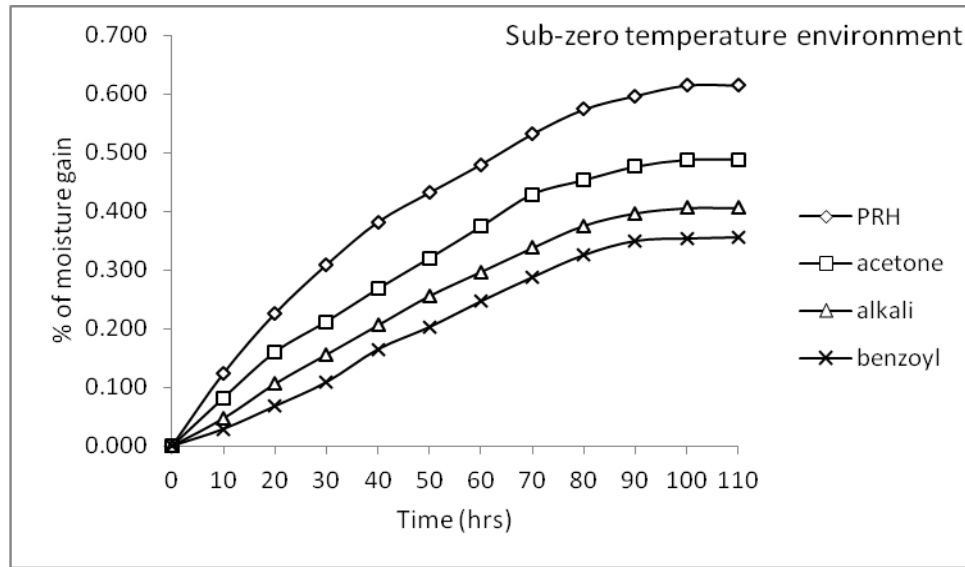


Figure-3.20 Variation of weight gain of the Rice Husk epoxy composites with immersion time at sub-zero temperature environment

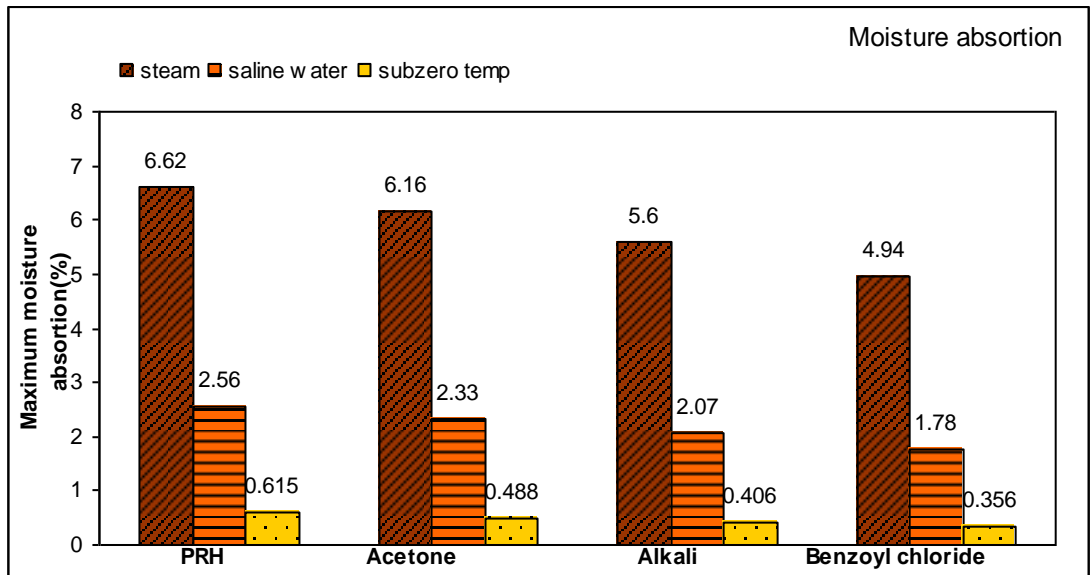


Figure-3.21 Comparison of Maximum moisture absorption of Plain and chemically treated Rice Husk epoxy composites in all the three environments

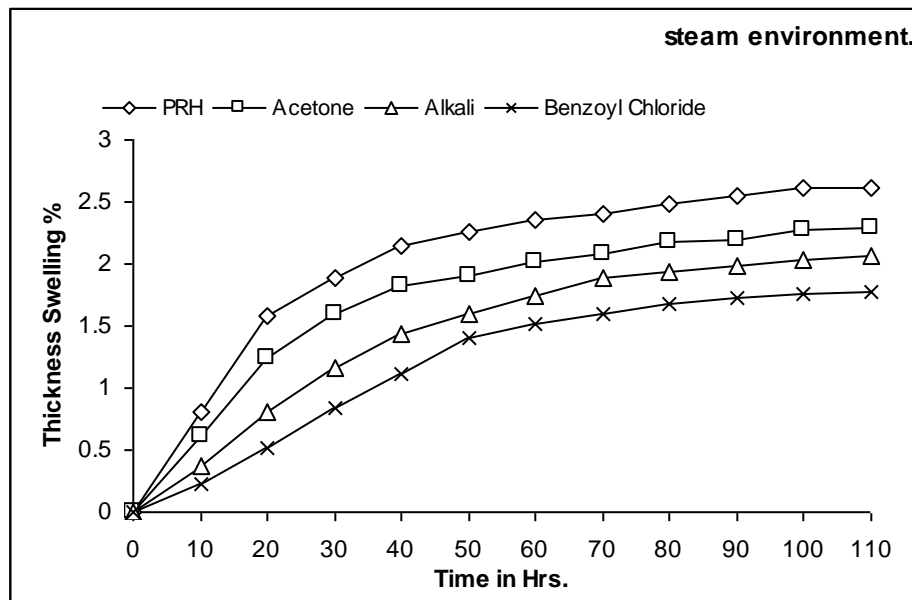


Figure-3.22 Variation of thickness of Plain and Chemically treated Rice Husk epoxy composites with immersion time at steam environment

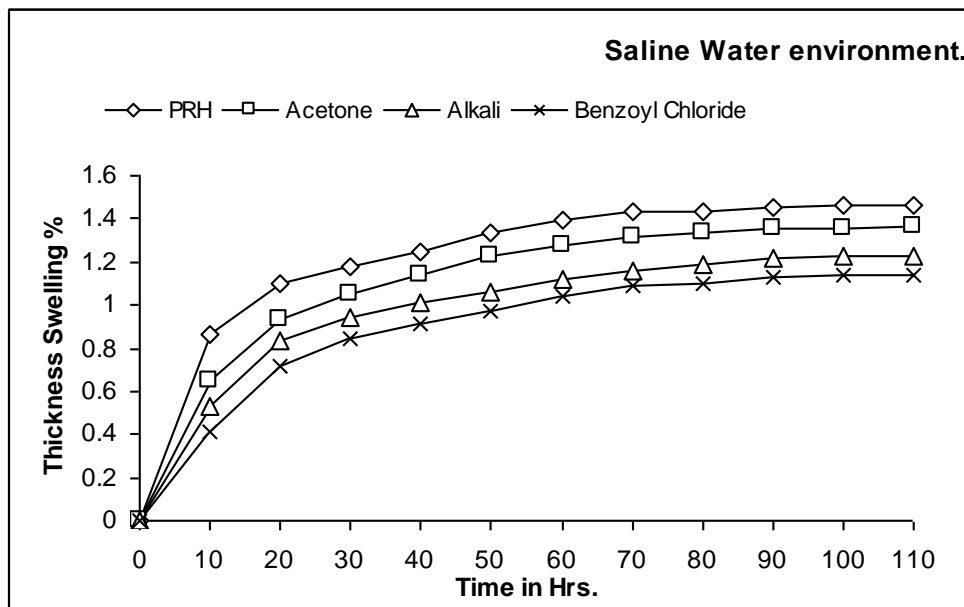


Figure-3.23 Variation of thickness of the treated Rice Husk epoxy composites with immersion time at saline water environment

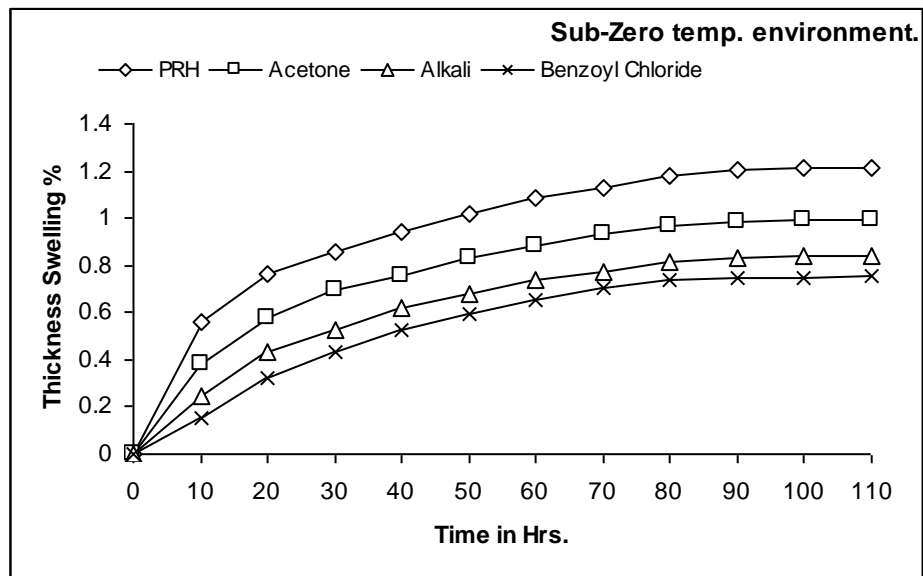


Figure-3.24 Variation of thickness of the treated Rice Husk epoxy composites with immersion time at sub-zero temperature environment

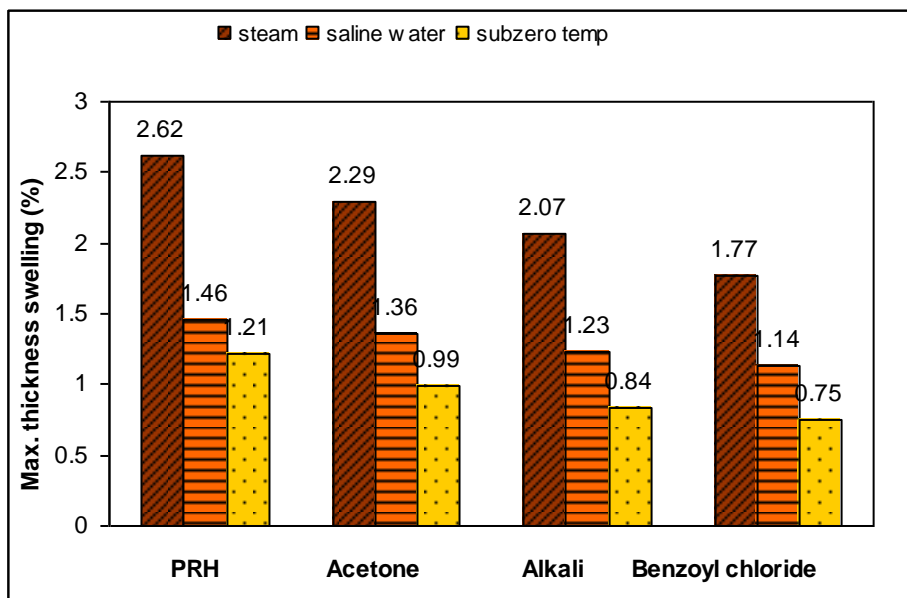


Figure-3.25 Comparison of maximum thickness swelling of treated and untreated Rice Husk epoxy composites in all the three environments

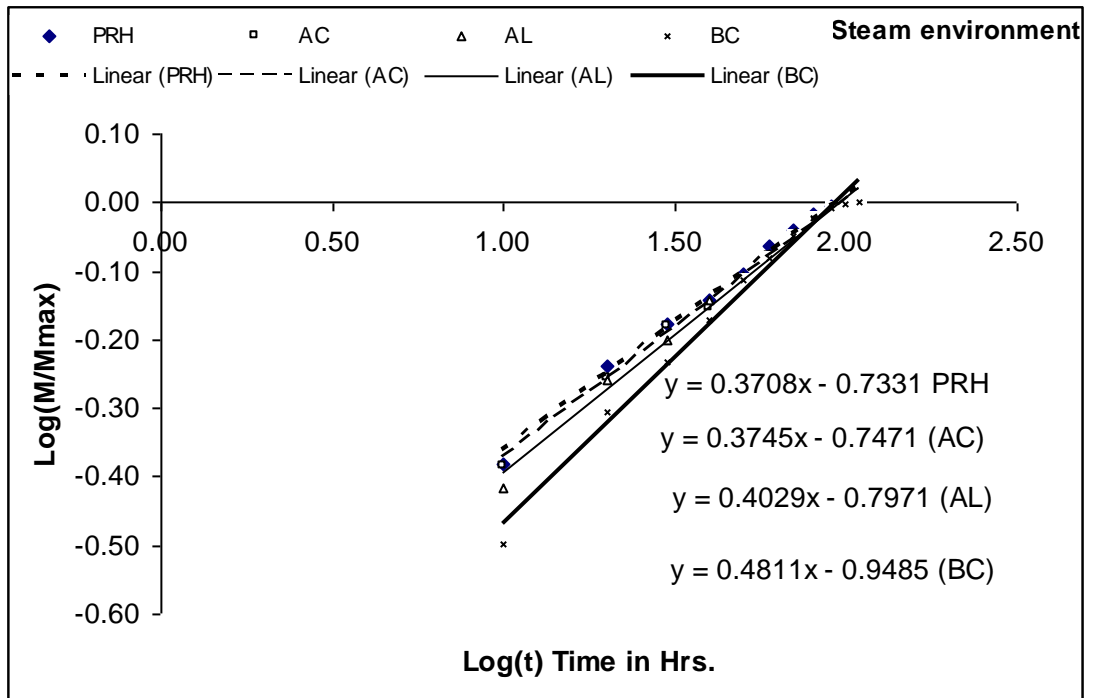


Figure-3.26 Variation of $\log (M_t/M_m)$ with $\log (t)$ for Rice Husk epoxy composites at steam environment

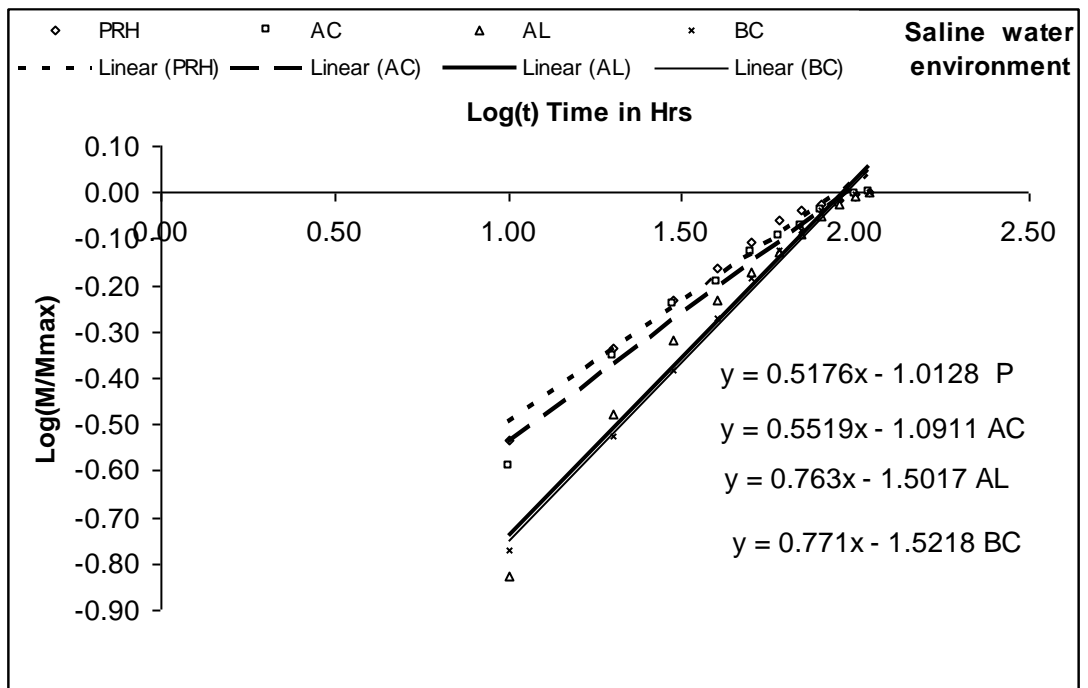


Figure-3.27 Variation of $\log (M_t/M_m)$ with $\log (t)$ for Rice Husk epoxy composites at saline water environment

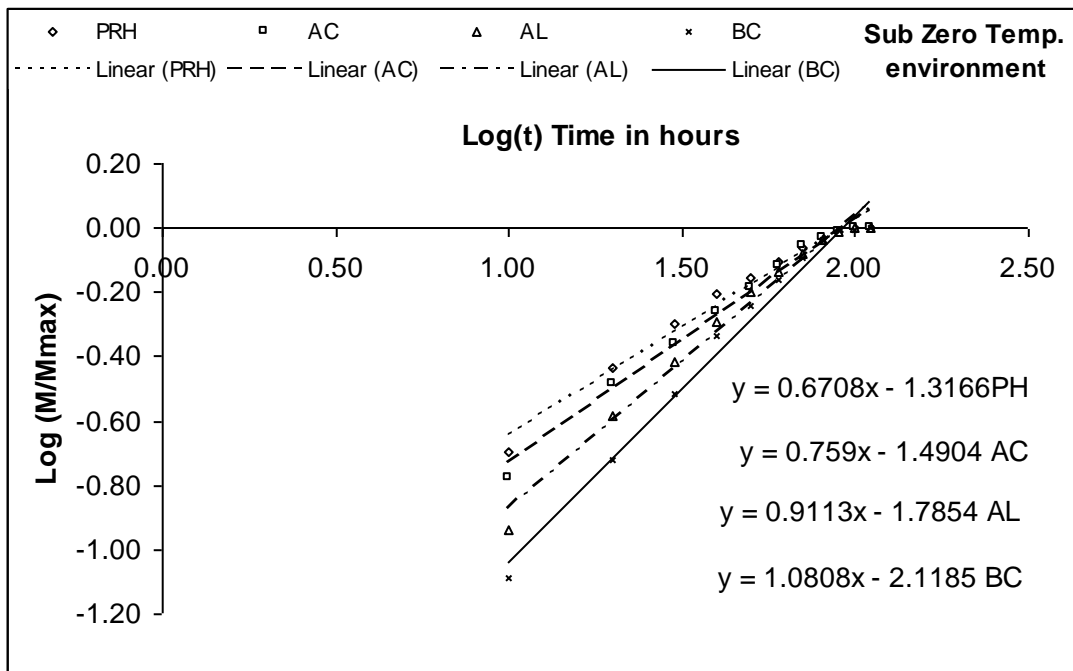


Figure-3.28 Variation of $\log (M_t/M_m)$ with $\log (t)$ for Rice Husk epoxy composites at sub-zero temperature environment

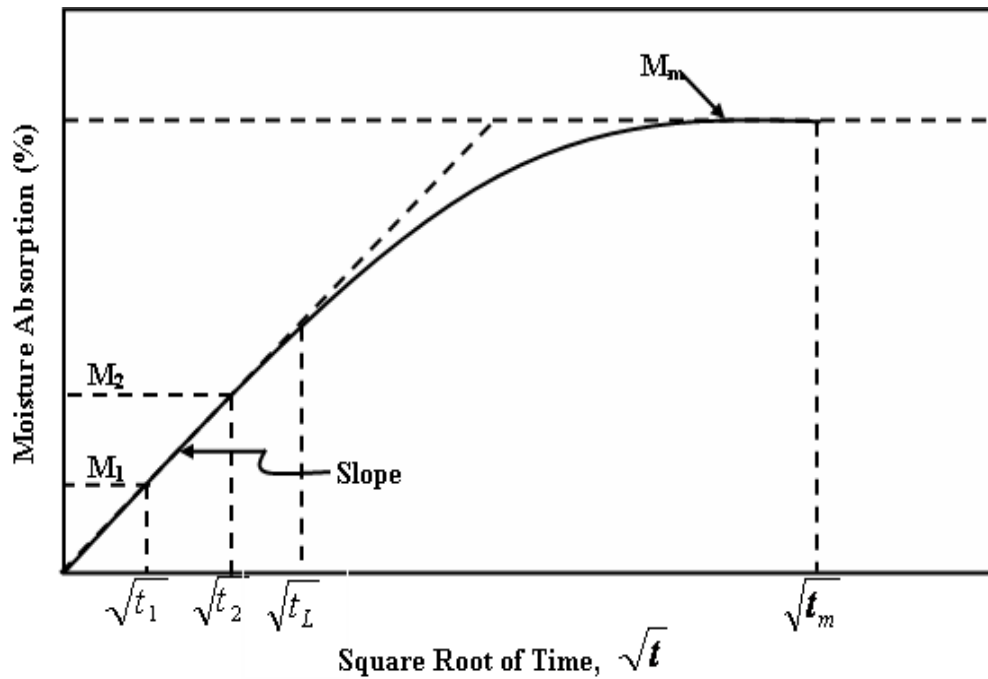


Figure-3.29 Example Plot of percentage of moisture absorption versus square root of time for calculation of Diffusivity

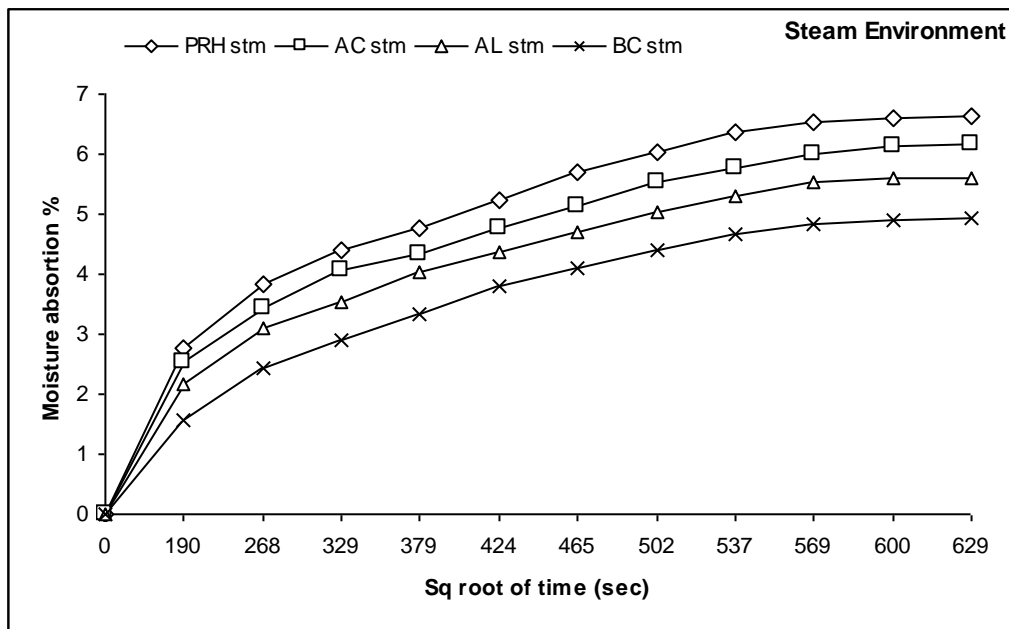


Figure-3.30 Variation of moisture absorption of Rice Husk epoxy composites with square root of immersion time at steam environment

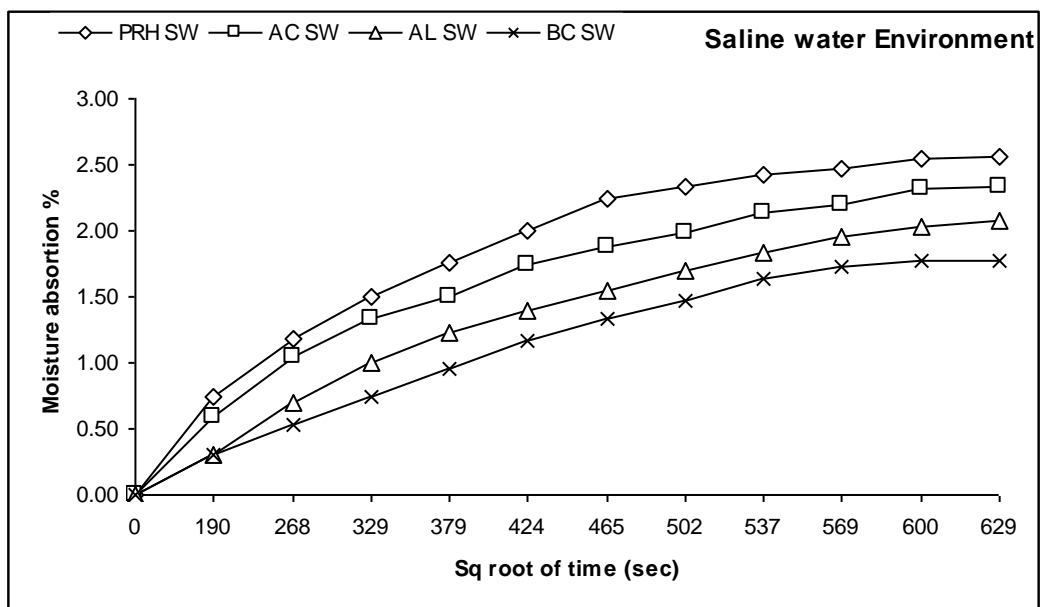


Figure-3.31 Variation of moisture absorption of Rice Husk epoxy composites with square root of immersion time at saline water environment

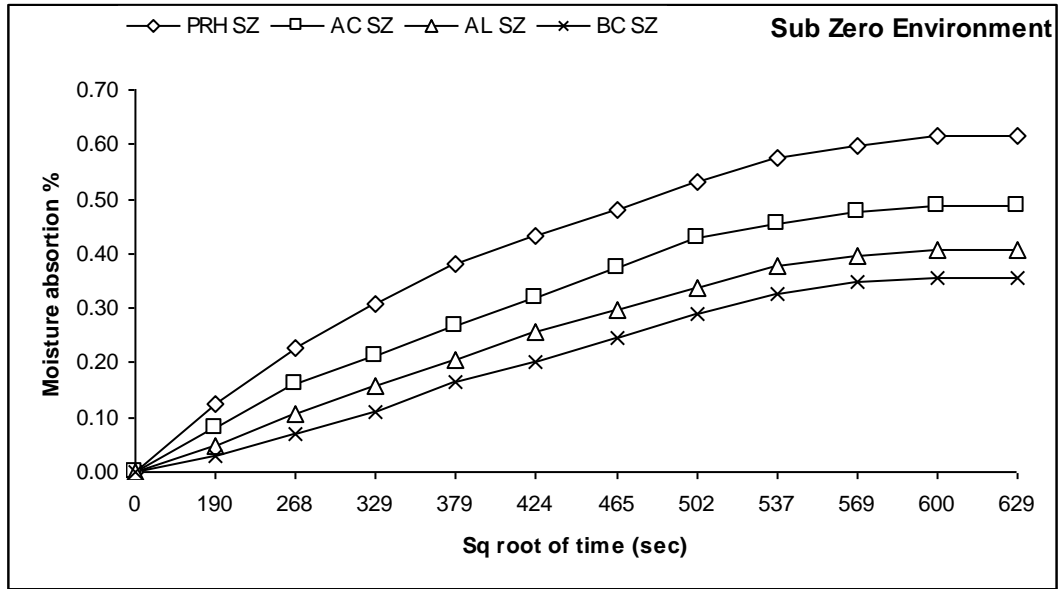


Figure-3.32 Variation of moisture absorption of Rice Husk epoxy composites with square root of immersion time at sub-zero temperature environment

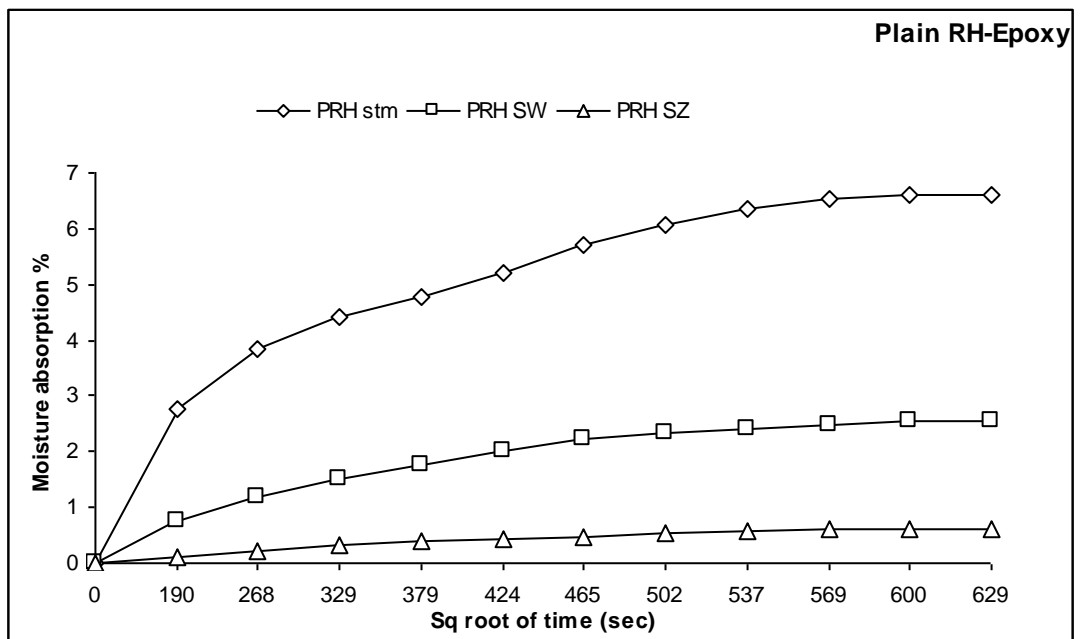


Figure-3.33 Variation of moisture absorption of Plain Rice Husk epoxy composites with square root of immersion time at different environment

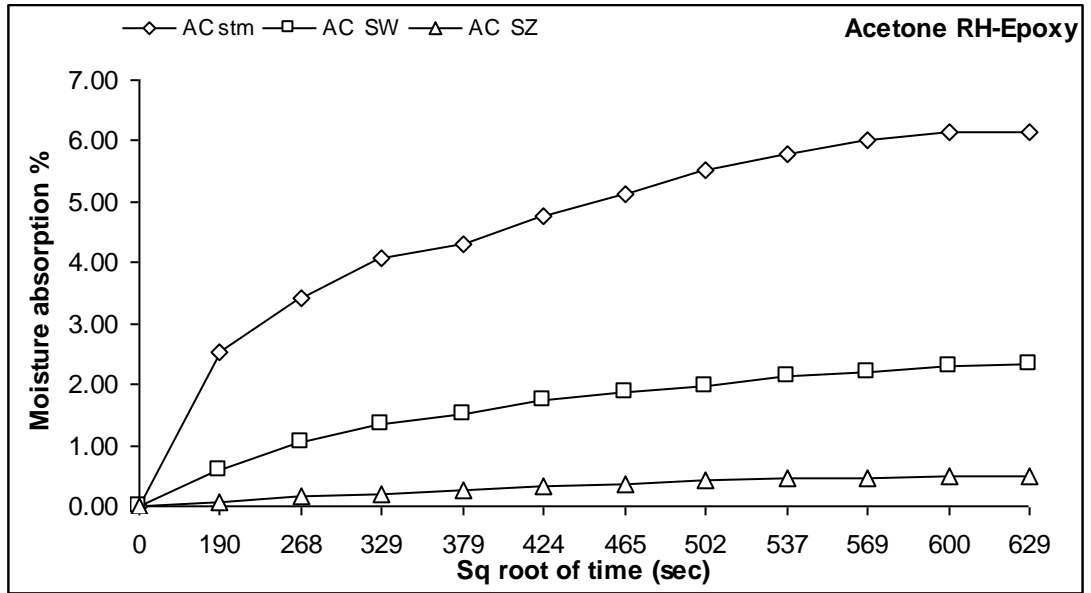


Figure-3.34 Variation of moisture absorption of Acetone treated Rice Husk epoxy composites with square root of immersion time at different environment

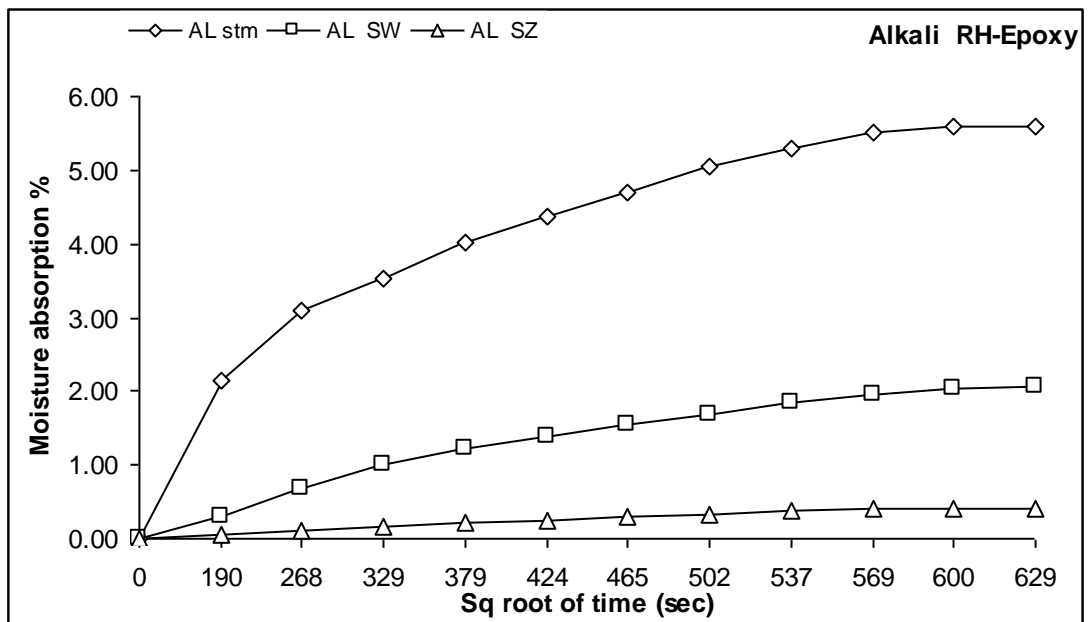


Figure-3.35 Variation of moisture absorption of Alkali treated Rice Husk epoxy composites with square root of immersion time at different environment

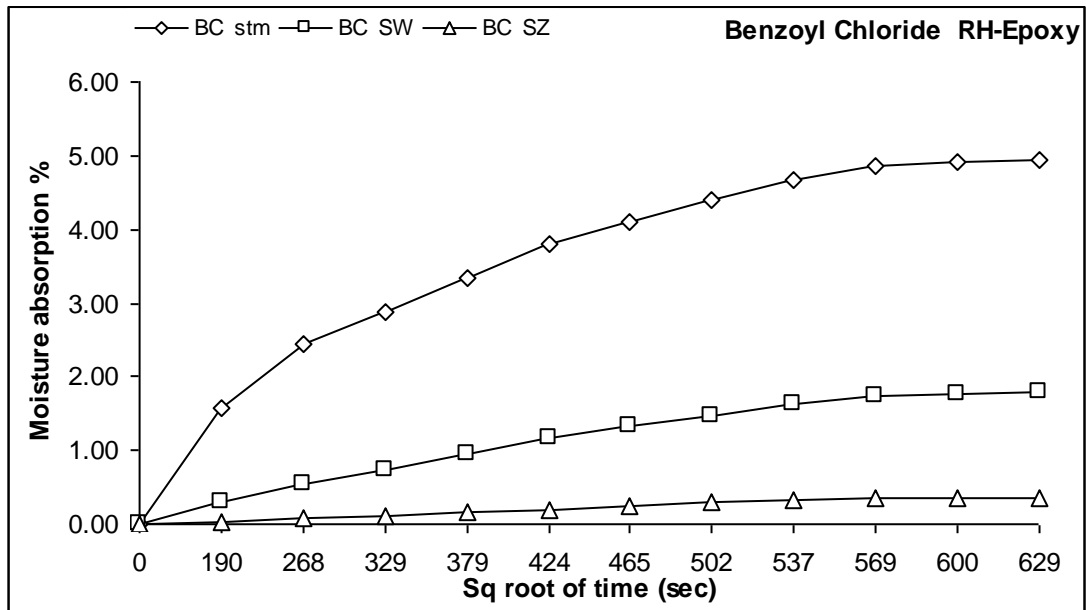


Figure-3.36 Variation of moisture absorption of Benzoyl Chloride treated Rice Husk epoxy composites with square root of immersion time at different environment

Chapter 4

ABRASIVE WEAR

BEHAVIOUR OF RICE

HUSK EPOXY

COMPOSITES

4.1 INTRODUCTION

Tribology is a recent development in study of material science in three aspects e.g friction, wear and lubrication. When two surfaces are in contact and are in relative motion, there are loss of energy, wearing of surface resulting change in dimension, and occasional formation of cracks. The worn out component of an engineering system needs to be replaced for proper functioning. The economy and efficiency of an engineering system can be achieved through a proper tribological study, implementation and monitoring. Wear by definition, is mechanical damage to a surface of a body as a result of relative motion with respect to another surface. The surface damage may be in form of removal of material from the surface, plastic deformation, formation of crack or change in geometry of the surface e.t.c. Wear can also be caused by a fluid entrained with solid particle as in the case of slurry. The friction is the cause of the wear. The friction is the opposing force to the motion acting parallel to the surface and proportional to the normal force. The friction force is a measure of coefficient of friction (μ) between two mating surface. The distinction has been made to identify initial friction force with static coefficient of friction (μ_s) and sliding or rolling friction with dynamic/kinetic coefficient of friction(μ_k) The lubrication is an effort to reduce friction or wear or both. The findings of Guillaume Amontons in 1699 [145] establishing scientific studies of friction are of 300 years old, while Petrov [146], Tower [147] and Reynolds [148] have further studied the subject of lubrication in 1880s. The study of wear and classification has been made since 1950, after R. Holm [149] investigated the fundamental aspects of surface inter-actions in electrical contacts. Attempt has been made by engineers to classify wear based on the appearance (like scar, pitted scuffing, scratches e.t.c) or physical mechanism of wear (like adhesion, abrasion, fatigue, oxidation type of wear e.t.c) or condition of wear (like lubricated, dry, sliding, rolling e.t.c) . The purpose of classification is to develop wear model and predict wear life by controlling significance design parameter. Interrelationship exists between these classifications. For example, scuffing is an appearance on worn out parts caused by adhesive wear mechanism in a sliding condition. However, the classifications are not equivalent nor the interrelationship is simple, direct, unique or complete. There are some minor category or special type of wear like delamination, scuffing, fretting, slurry erosion in pipeline and cavitations etc. which combination of different wear mechanism.

Considerable energy is wasted in form of heat due to friction. Approximately, one third of global energy consumption in industries is wasted in friction. Apart from energy loss, additional cost is also incurred in manufacturing and replacement of worn out parts. Therefore, effective decrease and control of friction and wear of metals are always desired [150]. The abrasive wear is most prominent mechanism of wear in industries. Particularly in agriculture industries, as many as 40% of the components replaced on equipment fail by abrasive wear. The wear phenomena is the major cause of expenditure due to losses of production consequent upon lower efficiency and plant shutdown, the need to invest more frequently in capital equipment and increased energy consumption as equipment wears. Estimates of direct cost of abrasive wear to industrial nations vary from 1 to 4 % of gross national product and Rigney [151] has estimated that about 10% of all energy generated by man is dissipated in various friction processes.

Wear is the characteristics of the engineering system. The wear manifest in the form of loss of volume, reduction in mass, change in dimension, reduction in life of component, increase in vibration level, change in roughness of the surface, change in appearance, increase in friction level, increase in noise level and increase in surface crack. The mechanism of wear and condition of wear has significant effect on wear. The wear volume depends on load, speed, temperature, hardness, presence of foreign material and the environmental condition [152] etc . In most cases wear occurs through surface interactions at asperities. During relative motion, material on contacting surface may be removed from a surface, may result in the transfer to the mating surface, or may break loose as a wear particle. The wear resistance of materials is related to its microstructure may take place during the wear process and hence, it seems that in wear research emphasis is placed on microstructure [153]. Wear of material depends on many variables. With the present state knowledge within tribology, complete co-relationship between operating condition, wear mechanism and appearance is generally not possible in practical engineering situation. So a wear research program must be planned systematically. Therefore researchers have normalized some of the data to make them more useful. The wear map proposed by Lim [154] is very useful in this regard to understand the wear mechanism in different sliding conditions as well as the anticipated rates of wear.

4.2 RECENT TRENDS IN WEAR RESEARCH

Numerous wear researches have been carried out in the 1940's and 1950's by mechanical engineers and metallurgists to generate data for the construction of motor drive, trains, brakes, bearings, bushings and other types of moving mechanical assemblies [155].

It became apparent during the survey that wear of materials was a prominent topic in a large number of the responses regarding some future priorities for research in tribology. Some 22 experienced technologists in this field, who attended the 1983 'Wear of Materials Conference' in Reston, prepared a ranking list [156]. Their proposals with top priority were further investigations of the mechanism of wear and this no doubt reflects the judgments that particular effects of wear should be studied against a background of the basic physical and chemical processes involved in surface interactions. The list proposed is shown in Table- 4.1.

Peterson [150] reviewed the development and use of tribo-materials and concluded that metals and their alloys are the most common engineering materials used in wear applications. Grey cast iron for example has been used as early as 1388. Much of the wear research conducted over the past 50 years is in ceramics, polymers, composite materials and coatings [157].

Table-4.1 Priority in wears research [156]

Ranking	Topics
1.	Mechanism of Wear
2.	Surface Coatings and treatments
3.	Abrasive Wear
4.	Materials
5.	Ceramic Wear
6.	Metallic Wear
7.	Polymer Wear
8.	Wear with Lubrication
9.	Piston ring-cylinder liner Wear
10.	Corrosive Wear
11.	Wear in other Internal Combustion Machine component

Wear of materials encountered in industrial situations can be grouped into different categories as shown in Table-4.2. Though there are situations where one type changes to another or where two or more mechanism plays together.

Table-4.2 Type of wear in industry [155]

Type of wear in Industry	Approximate percentage involved
Abrasive	50
Adhesive	15
Erosion	8
Fretting	8
Chemical	5

4.3 THEORY OF WEAR

Wear is a material failure mechanism on surface when two surfaces with a relative motion interact with each other. Wear may be defined as the progressive loss of material from contacting surfaces in relative motion. Wear generally occur through formation of particle rather than loss of individual atom. Scientists have developed various wear theories in which the Physico-Mechanical characteristics of the materials and the physical conditions (e.g. the resistance of the rubbing body and the stress state at the contact area) are taken in to consideration. The wear mechanism is build around the concept of brittle fracture, plastic deformation, fatigue, cohesive and abrasive failures in bounded structures. The complexities associated with each of the mechanism are further compounded by the fact that more than one body is involved as well as unique properties and feature of the wear surface. In 1940 Holm [149] starting from the atomic mechanism of wear, calculated the volume of substance worn over unit sliding path.

Barwell and Strang [158] in 1952: Archard [159] in 1953 and Archard and Hirst [160] in 1956 developed the adhesion theory of wear and proposed a theoretical equation identical in structure with Holm's equation. In 1957, Kragelski [161] developed the fatigue theory of wear. This theory of wear has been widely accepted by scientists in different countries. Because of the Asperities in real bodies, their interactions in sliding is discrete, and contact occurs at individual locations, which, taken together, form the real contact area. Under normal force the asperities penetrate into each other or are flattened out and in the region of real contact points corresponding stress and strain rise. In sliding, a fixed volume of material is subjected to the many times repeated action, which weakens the material and leads finally to rupture. In 1973, Fleischer [162] formulated his energy theory of wear. The main concept of this theory is that the separation of wear particles requires that a certain volume of material accumulates a specific critical store of internal energy. It is known that a large part of the work done in sliding is dissipated as heat, and that a small proportion of it accumulates in the material as internal potential energy. When the energy attains a critical value, plastic flow of the material occurs in this volume or a crack is formed. Further theories of wear are found in [161]. Though all the theories are based on different mechanisms of wear, the basic consideration is the frictional work.

In past few decades, numerous research works have been carried out on abrasive wear performance of polymer and polymer based composite in view of their extensive application in the field industry and agricultural sectors where abrasive wear is a predominant mode of failure. Conveyor aids, vanes, gears, bushes, seals, bearings, chute liners etc. are some examples of their applications [163-167]. Since abrasive wear is the most severe form of wear accounting for 50% of total wear, several researches have been devoted to exploring abrasive wear of polymer composites. Evans et al. [168] studied the abrasion wear behavior for 18 polymers and they noticed that low density polyethylene (LDPE) showed the lowest wear rate in abrasion against rough mild steel, but a higher wear rate in abrasion with coarse corundum paper. Unal et al. [169] studied abrasive wear behaviour of polymeric materials. They concluded that the specific wear rate decreases with the decrease in abrasive surface roughness. They also concluded that, the abrasive wear include micro-cracking, micro-cutting, and micro-ploughing mechanisms. Whereas in another investigation [170] they concluded that the sliding speed has a stronger effect on the specific wear rate. Shipway and Ngao [171] investigated the abrasive behaviour of polymeric materials in micro-scale level. They concluded that the wear behaviour and wear rates of polymers depended critically on the polymer type. Harsha and Tewari [172] investigated the abrasive wear behaviour of polyaryletherketone (PAEK) and its composites against SiC abrasive paper. They concluded that the sliding distance, load, abrasive grit size have a significant influence on abrasive wear performance. Further there are many references that illustrate the influence of fillers and fiber reinforcement on the abrasive wear resistance of polymeric composites. Cirino et al. [173, 174] investigated the sliding and abrasive wear behavior of polyetheretherketone (PEEK) with different continuous fiber types and reported that the wear rate decreases with increase in the fiber content. Chand et al. [175] studied low stress abrasive wear behavior of short E-glass fiber reinforced polymer composites with and without fillers by using rubber wheel abrasion test apparatus. They reported that higher weight fraction of glass fibers (45%) in the composites improves the wear resistance as compared to the composite containing less glass fibers (40%). Bijwe et al. [176] tested polyamide 6, polytetrafluoroethylene (PTFE) and their various composites in abrasive wear under dry and multi-pass conditions against silicon carbide (SiC) paper on pin-on-disc arrangement. They concluded that the polymers without fillers had better abrasive wear resistance than their composites. Liu et al. [177] investigated the abrasive wear behaviour of ultrahigh molecular weight polyethylene (UHMWPE) polymer. They concluded that the applied load is the main parameter and the wear resistance improvement

of filler reinforced UHMWPE was attributed to the combination of hard particles which prevent the formation of deep, wide and continuous furrows.

With regards to the usage of natural fiber as reinforcement for tribological application in polymeric composite, few works have been attempted. However, in recent years, some work has been done on natural fiber like jute [178], cotton [179, 180], oil palm [181], coir [182], kenaf [183], betel-nut [184], betel palm [185], wood flour [186], bagasse fiber [187], Lantana camara fiber [188], Ipomea Carnia [189] and bamboo powder [190] as reinforcement. In these works, the wear resistance of polymeric composites has been improved when natural fibers are introduced as reinforcement.

4.4 TYPES OF WEAR

In most basic wear studies where the problems of wear have been a primary concern, the dry friction has been investigated to avoid the influences of fluid lubricants.

Dry friction is defined as friction under not intentionally lubricated conditions but it is well known that it is friction under lubrication by atmospheric gases, especially by oxygen [191].

A fundamental scheme to classify wear was first outlined by Burwell and Strang [192]. Later Burwell [193] modified the classification to include five distinct types of wear, namely (1) Abrasive (2) Adhesive (3) Erosive (4) Surface fatigue (5) Corrosive.

4.4.1 Abrasive wear

Abrasive wear (Figure 4.1) can be defined as the wear that occurs when a hard surface slides against and cuts groove from a softer surface. It can account for most failures in practice. Hard particles or asperities that cut or groove one of the rubbing surfaces produce abrasive wear. This hard material may be originated from one of the two rubbing surfaces. In sliding mechanisms, abrasion can arise from the existing asperities on one surface (if it is harder than the other), from the generation of wear fragments which are repeatedly deformed and hence get work hardened for oxidized until they became harder

than either or both of the sliding surfaces, or from the adventitious entry of hard particles, such as dirt from outside the system. Two body abrasive wear occurs when one surface (usually harder than the second) cuts material away from the second, although this mechanism very often changes to three body abrasion as the wear debris then acts as an abrasive between the two surfaces. Abrasives can act as in grinding where the abrasive is fixed relative to one surface or as in lapping where the abrasive tumbles producing a series of indentations as opposed to a scratch. According to the recent tribological survey, abrasive wear is responsible for the largest amount of material loss in industrial practice [194].

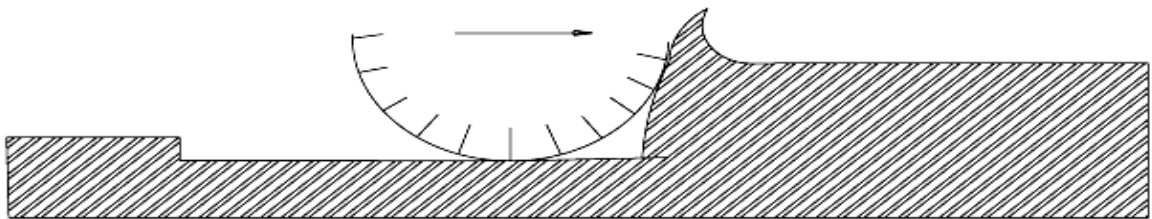


Figure-4.1 Schematic representations of the abrasion wear mechanism

4.4.2 Adhesive wear

Adhesive wear (Figure 4.2) can be defined as the wear due to localized bonding between contacting solid surfaces leading to material transfer between the two surfaces or the loss from either surface. For adhesive wear to occur it is necessary for the surfaces to be in intimate contact with each other. Surfaces, which are held apart by lubricating films, oxide films etc. reduce the tendency for adhesion to occur.

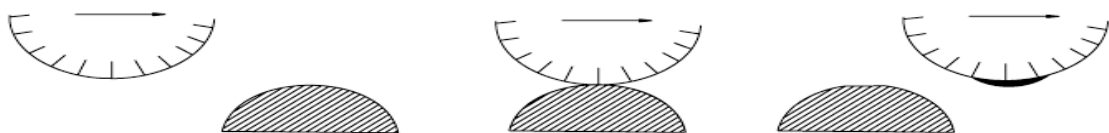


Figure-4.2 Schematic representations of the adhesive wear mechanism

4.4.3 Erosive wear

Erosive wear (figure 4.3) can be defined as the process of metal removal due to impingement of solid particles on a surface. Erosion is caused by a gas or a liquid, which

may or may not carry, entrained solid particles, impinging on a surface. When the angle of impingement is small, the wear produced is closely analogous to abrasion. When the angle of impingement is normal to the surface, material is displaced by plastic flow or is dislodged by brittle failure.

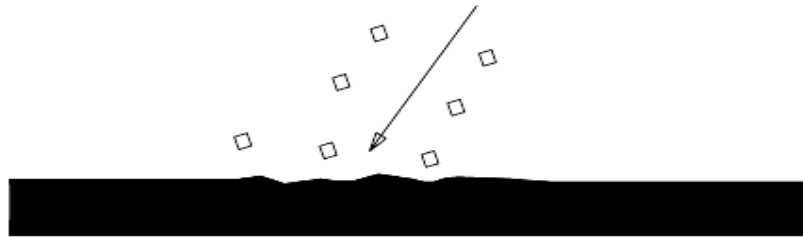


Figure-4.3 Schematic representations of the erosive wear mechanism

4.4.4 Surface fatigue wear

Wear of a solid surface is caused by fracture arising from material fatigue (Figure 4.4). The term ‘fatigue’ is broadly applied to the failure phenomenon where a solid is subjected to cyclic loading involving tension and compression above a certain critical stress. Repeated loading causes the generation of micro cracks, usually below the surface, at the site of a pre-existing point of weakness. On subsequent loading and unloading, the micro crack propagates. Once the crack reaches the critical size, it changes its direction to emerge at the surface, and thus flat sheet like particles is detached during wearing. The number of stress cycles required to cause such failure decreases as the corresponding magnitude of stress increases. Vibration is a common cause of fatigue wear.

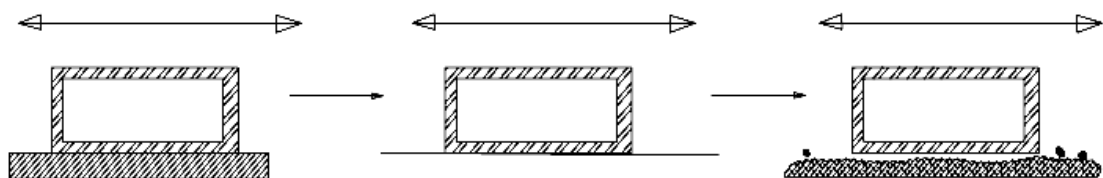


Figure-4.4 Schematic representations of the surface fatigue wear mechanism

4.4.5 Corrosive wear

Most metals are thermodynamically unstable in air and react with oxygen to form an oxide, which usually develop layer or scales on the surface of metal or alloys when their interfacial bonds are poor. Corrosion wear (figure 4.5) is the gradual eating away or deterioration of unprotected metal surfaces by the effects of the atmosphere, acids, gases,

alkalis, etc. This type of wear creates pits and perforations and may eventually dissolve metal parts.

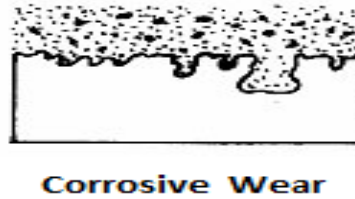


Figure-4.5 Schematic representations of the corrosive wear mechanism

4.5 SYMPTOMS OF WEAR

A summary of the appearance and symptoms of different wear mechanism is indicated in Table-4.3 and the same is a systematic approach to diagnose the wear mechanisms.

Table-4.3 Symptoms and appearance of different types of wear [195]

Types of wear	Symptoms	Appearance of the worn-out surface
Abrasive	Presence of clean furrows cut out by abrasive particles.	Grooves
Adhesive	Metal transfer is the prime symptoms.	Seizure, catering rough and torn-out surfaces.
Erosion	Presence of abrasives in the fast moving fluid and short abrasion furrows.	Waves and troughs.
Corrosion	Presence of metal corrosion products.	Rough pits or depressions.
Fatigue	Presence of surface or subsurface cracks accompanied by pits and spalls.	Sharp and angular edges around pits.
Impacts	Surface fatigue, small sub-micron particles or formation of spalls.	Fragmentation, peeling and pitting.
Delamination	Presence of subsurface cracks parallel to the surface with semi-dislodged or loose flakes.	Loose, long and thin sheet like particles
Fretting	Production of voluminous amount of loose debris.	Roughening, seizure and development of oxide ridges
Electric attack	Presence of micro craters or a track with evidence of smooth molten metal.	Smooth holes

Literature available on the rate of controlling abrasive wear mechanism demonstrate that it may change abruptly from one another at certain sliding velocities and contact loads, resulting in abrupt increases in wear rates. The conflicting results in the abrasive wear literature arise partly because of the differences in testing conditions, but they also make clear that a deeper understanding of the abrasive wear mechanism is required if an improvement in the wear resistances of the polymer matrix composites is to be achieved. This in turn requires a systematic study of the wear under different loads and velocities. It is generally recognized that abrasive wear is a characteristic of a system and is influenced by many parameters. Laboratory scale investigation if designed properly allows careful control of the tribo system where by the effects of different variables on wear behaviour of PMCs can be isolated and determined. The data generated through such investigation under controlled conditions may help in correct interpretation of the results.

As new developments are still under way to explore innovative fields for tribo-application of natural fiber base materials, in this chapter an attempt has been made to study the potential of Rice Husk (RH) as reinforcement material in polymer base for tribological applications. In the current study the effect of fiber loading, sliding velocity and normal load on abrasive wear behaviour of RH reinforced epoxy composite has been evaluated and possible wear mechanism has been discussed with SEM observation.

4.6 EXPERIMENT

4.6.1 Preparation for the test specimens

The weighted quantity of rice husk fibers (5, 10, 15, and 20 vol %) were added to resin with required quantity of hardener. The procedure of mixing the resin, same and as per the procedure explained in chapter-3, Art-3.4.3. A steel mould has been designed and fabricated in the department work-shop and used for preparation of cylindrical (pin) type specimen of length 35mm & diameter of 10 mm which is shown in Figure-4.6. The mixture of Rice Husk and resin has been poured into the cylindrical cavity present in the mould and then the two halves of the mould are fixed properly. During fixing some of the resin mix may squeezed out. Adequate care has been taken for squeezing out of resin-mix during preparation of composites. After closing of the mould the specimens were allowed to

solidify in the mould at the room temperature for 24 hrs. For the purpose of comparison the matrix material was also cast under similar condition. After curing the samples were taken out from the mould, finished ground to required shape, sizes for wear testing. The samples were prepared using both plain and chemically treated RH. The chemical treatments include treatment with Acetone, Alkali and Benzoyl Chloride. The detail procedures of chemical treatment have been explained in chapter 3.

4.6.2 Dry sliding wear test

Dry sliding wear test has been carried out under multi-pass condition on a pin-on-disc type wear testing machine (As per ASTM G-99 standard) supplied by Magnum Engineers, Bangalore (Figure-4.7). Abrasive paper of 400 grade (grit-23 μm) has been pasted on a rotating disc (EN 31 Steel disc) of 120mm diameter using double-sided adhesive tape. The specimens under tests were fixed to the sample holder. The holder along with the specimen (Pin) was positioned at a particular track diameter. A track radius of 50 mm was selected for this experiment and was kept constant for the entire investigation. For each test new abrasive paper was used and the sample was abraded for a total sliding distance. During experiment the specimen remains fixed and disc rotates. Load is applied through a dead weight loading system to press the pin against the disc. The speed of the disc or motor rpm can be varied through the controller and interval of time can be set by the help of timer provided at the control panel. The mass loss in the specimen after each test was estimated by measuring the weight of the specimen before and after each test using an electronic balance with an accuracy of ± 0.001 mg. care has been taken that the specimen under test are continuously cleaned woolen cloth to avoid entrapment of wear debris and achieve uniformity in the experimental procedure. Test pieces are cleaned with acetone prior and after each test. The machine is fixed with data acquisition system with 'MAGVIEW-2010' software from which the frictional force that arises at the contact can be read out/recorded directly. The test under which the experiment has been carried out is given in Table-4.4.

4.6.3 Calculation for Wear

Wear rate was estimated by measuring the weight loss of the specimen after each test. The weight loss was calculated by taking the weight difference of the sample before and after each test. The weight loss:

$$\Delta m = (m_1 - m_2) \text{ g} \quad (4.1)$$

where Δm is the weight loss in g and m_1 and m_2 are the weight of the sample after and before the abrasion test in grams. The abrasive wear rate (W) which relates to the mass loss to sliding distance (SD) can be calculated by using the following formula:

$$W = \Delta m / SD \quad (4.2)$$

The volumetric wear rate (W_v) can be calculated by using the equation:

$$W_v = \frac{\Delta m}{(\rho \times SD)} \quad (4.3)$$

where ' W_v ' is the volumetric wear rate in m^3/m , ' ρ ' is the density (g/cc) of the composite, Δm is the weight loss in g and ' SD ' is the sliding distance in m. The average value of weight loss and wear rate for each batch is listed in Table-4.5 to 4.100. For characterization of the abrasive wear behavior of composite, the specific wear rate is employed. This is defined as the volume loss of the composite per unit sliding distance and per unit applied load. Often the inverse of the specific wear rate can be expressed in terms of volumetric wear rate. The specific wear rate (W_s) can also be calculated by using equation:

$$W_s = \frac{\Delta m}{(\rho \times SD \times L)} \quad (4.4)$$

where ' W_s ' is the specific wear rate in m^3/Nm , ' Δm ' is the weight loss in grams, ' SD ' is the sliding distance in meter, and ' L ' is the applied load in N.

4.7 RESULTS AND DISCUSSION

Based on the experiment and tabulated results, various graphs are plotted and presented in Figure-4.8 to 4.30 for different percentage of reinforcement under different test conditions.

The influence of normal loads on the abrasive wear rate of the un-reinforced and reinforced composites for different sliding velocities are shown in Figures-4.8 to 4.10. It has been observed that irrespective of sliding velocity the volumetric wear rate of all composite samples increases with normal load. This is because at higher load, the frictional force increases, which results in increased debonding and fracture. A similar effect of normal load on volumetric wear rate has been observed by Cirino et.al. [173] in the case of carbon epoxy composite and Verma et. al. [196] for GRP composite. Deo, Acharya[188] and Mishra,Acharya[189] also found the same type of results while they studied the abrasive wear behavior of Lantana Camara and Bagasse fiber reinforced epoxy composite. It has also been observed that the abrasive wear rate decreases with addition of rice husk up to 10vol% under all testing conditions. Thus it can be conclude here that addition of the Rice Husk in epoxy is very effective in improving its wear resistance. Further increase in fiber content (beyond 10 vol %), wear rate again increases. This increase in wear rate for higher volume fraction of fiber (>10 vol %) might have happened due to insufficient wetting of fiber or agglomeration of fiber within the matrix which leads to poor interfacial adhesion between the fiber and the matrix. Similar type of behavior was reported by Wu and Cheng [197], while they studied the tribological properties of Kevlar pulp reinforced epoxy composites.

Figure- 4.11 illustrate the effect of sliding velocity on the abrasive wear behavior of 10 volume % RH reinforced epoxy composite under different loads (5N to 15N).It is clear from the plot that the abrasive wear rate of the composite increase with increase in sliding velocity at all normal load. It is also seen that when load increase from 5N to 15N, the percentage increase in wear rate is about 111%, but when the velocity increase from 1.047m/s to 2.094m/s the percentage increase in wear rate is limited to about 50%.Hence it can be conclude that, the abrasive wear of Rice Husk reinforced composite is very sensitive to normal load than the sliding velocity. Since similar trend has been observed for all other reinforcement they have not been shown here.

Figures 4.12 to 4.14 have been plotted to explain the variation of specific wear rate of the composite with different sliding velocities. It is clear from the plots that irrespective of the sliding velocities the specific wear rate of the composite decreases with increasing in load. It also indicates that the specific wear rate is much less in comparison to pure epoxy for different volume fraction of rice husk and is minimum for 10vol% of fiber for all sliding velocities. Thus it can be conclude here that the optimum fiber volume fraction for the composite is 10 vol% which gives maximum wear resistance to the composite.

Fig 4.15 to 4.17 shows the variation of wear rate with sliding distance for different applied loads (5N to 15N) and with different sliding velocities for 10 vol% of Rice Husk only. It is seen that for all loads and for different sliding velocities the wear rate is maximum at the initial period and gradually decrease as the sliding distance increases and then remains almost same for the rest of the test period.

Fig 4.18 to 4.21 shows the volumetric wear rate of the composite with different volume fraction of the fiber for different loads (5N-20N). It can be seen from the plot that wear rate of composite is maximum for pure epoxy. As the fiber volume fraction increase the wear rate decreases up to 10 vol % and again increases for 15 and 20 vol % of fiber for all loads. Thus it can be conclude here that 10 vol % of fiber is the optimum fiber combination which gives maximum wear resistance to the composite. These results supplements to the observations presented in fig 4.12 to 4.14.

Fig 4.22 to 4.25 shows a comparative analysis of the specific wear rate of the composite with different volume fraction of fiber with loads 5N to 20N for different sliding velocities. These figures clearly indicate that for all combination of different parameters i.e. sliding velocity, load and volume fraction of fiber 10 vol % of fiber gives the better wear resistance to the composite.

Fig 4.26 and 4.27 shows the volumetric and specific wear rate of the modified Rice Husk reinforced epoxy composite. Both the figures shown here are with a load of 15N and velocity of 2.094 m/s. It is seen that both volumetric and specific wear rate decrease as the sliding distance increases and almost remains same at about 3000 meters sliding distance. The nature of the graph for treated composite is same as per the plain Rice Husk. However the value of both volumetric and specific wear rate decrease for different type of treatment and is found minimum for the fiber treated with Benzol Chloride. The decrease in specific wear rate ranges from 8 to 40% depending Normal load and sliding velocity. This has happened due to increase in the effective surface area by fibrillation due to chemical

modification of fiber surface which promotes the mechanical interlocking between the fiber and matrix as explained in chapter 3 art 3.22 which is also confirmed through EDX and SEM analysis. For other loads and velocity for treated rice husk are not reproduced here because they indicate the same type of trend.

The variation of friction coefficient for Rice Husk reinforced epoxy composite with varying load for different sliding velocity are shown in figure 4.28 and 4.30. From the figures it has been found that the friction coefficient decreases with increase in load. Again reduction in friction coefficient is also noticed with addition of Rice Husk. The 10 vol % reinforced Rice Husk composite shows the best friction performance (minimum coefficient of friction), whereas the neat epoxy shows the worst. This attribute to the fact that the incorporation of Rice Husk into epoxy matrix effectively improves the tribo performance. A similar trend was reported by Hasmi et.al. [180] while studying the tribological properties graphite modified cotton fiber reinforced polyester composite.

4.8 WORN SURFACE MORPHOLOGY

The worn surface morphologies of neat epoxy and its composites have been examined by scanning electron microscopy (SEM). The worn surfaces of neat epoxy samples are shown in Figure-4.31(A) (a) and (b). The removal of debris of brittle fragmented matrix forms the wear tracks has been observed in Figure-4.31(a). In addition to this plastic deformation and adherence are also noticed at higher load of 15N on the worn surface of neat epoxy [Figure-4.31 (b)]. This might have happened due to thermal softening effect because of generation of high frictional heat at sliding surface under higher normal load. The filling of space between the abrasives by the wear debris formed during abrasion with consecutive runs can be seen in Figure-4.31(c). This makes abrasive grits smooth and reduces the penetration of abrasive to composite. The fiber surface deterioration under 15N load of 10 vol% reinforcement for plain rice husk is illustrated in Figure-4.31 (d). It has been observed from this figure that matrix cracking and surface damage are more pronounced. Both longitudinal and transverse cracks are found on the fiber surface. Figure 4.31(e) shows the micrographs of the modified fiber surface with benzoyl chloride after wear test for 15N load. It is seen that though the fiber topography is not smooth, surface damage appears to be minimal and only longitudinal cracks are visible on the fiber surface in the direction of rolling. The chemical treatment probably restricted the cracks to

propagate in the transverse direction which in turns improves the wear resistant of the composite.

4.9 CONCLUSIONS

Based on experimental results of abrasive wear of Rice Husk epoxy composite tested under different normal loads, sliding velocity and sliding distances, the following conclusions have been drawn:

- The incorporation of Rice Husk in to epoxy can significantly reduce abrasive wear loss. The optimum wear resistance property was obtained at the fiber content of 10% weight fraction. But excessive addition of fiber beyond 10% weight fraction results matrix cracking and surface damage of fibers are found. Drawing out of fibers from the matrix is also found during the test due to poor interfacial adhesion.
- Dispersion of fibers in the matrix improves the hardness of matrix material and also the wear behavior of composite. The effect is increases in interfacial area between the matrix and the fiber leading to increase in strength.
- The abrasive wear rate is found to be more sensitive to normal load in comparison to sliding velocity and it also increase marginally with increase in sliding velocity.
- The specific wear rate of composite decreases with addition of fiber up to an optimum value. In this present study, the optimum volume fraction which gives maximum wear resistance to the composite is found to be 10 volume percent.
- Different chemical modification of fiber surface improves the wear and specific wear resistance properties of RH epoxy composites. Out of all the process carried out for the present investigation Benzoyl chloride treated fibers gives the best result.
- Coefficient of friction is lowest at a particular fiber volume fraction (10%). Though the static coefficient of friction is same, sliding coefficient of friction varies with load and sliding velocity.

- Fragmentation, adherence and plastic deformation are primary wear mechanisms for the neat epoxy. However the addition of Rice Husk reduces this adherence and plastic deformation to a great extent. Both longitudinal and transverse cracks are found on the untreated fiber surface whereas only longitudinal cracks are visible on the fiber surface in the direction of rolling. The chemical modification of fiber surface restricted the cracks to propagate in the transverse direction which in turns improves the wear resistant of the composite.

Table-4.4 Test parameter for Dry Sliding wear test

Test Parameters	Units	Values
Load (L)	N	5, 7.5,10, 15
Volume Fraction	%	5,10,15,20
Sliding Velocity (v)	m/s	1.0472, 1.5708, 2.0944 for 5 minutes duration each time. The test is repeated for 6 times.
Track radius (r)	mm	50
Temperature	^o C	20
Abrasive		Abrasive paper of 400 grade (grit-23 μm)

Table-4.5

Pure Epoxy (ρ=1.1) Load 5N RPM 200 (V=1.047 m/sec)

M1 (gm)	m2 (gm)	Δm (gm)	T(Sec)	μ	SD x 10 ³ (m)	W _v X10 ⁻⁵ (N/m)	W _v X10 ⁻¹¹ (m ³ /m)	W _s X10 ⁻¹¹ (m ³ /N.m)
3.390	3.280	0.110	300	0.980	0.314	0.350	31.831	6.366
3.390	3.230	0.160	600	0.970	0.628	0.255	23.150	4.630
3.390	3.190	0.200	900	0.950	0.942	0.212	19.291	3.858
3.390	3.160	0.230	1200	0.960	1.257	0.183	16.639	3.328
3.390	3.140	0.250	1500	0.950	1.571	0.159	14.469	2.894
3.390	3.130	0.260	1800	0.960	1.885	0.138	12.539	2.508

Table-4.6

Pure Epoxy ($\rho=1.1$) Load 5N RPM 300 ($V=1.5708$ m/sec)

m1 (gm)	m2 (gm)	Δm (gm)	T(Sec)	μ	$SD \times 10^3$ (m)	$WX10^{-5}$ (N/m)	$W_v X10^{-11}$ (m³/m)	$W_s X10^{-11}$ (m³/N.m)
2.620	2.400	0.220	300	0.990	0.471	0.467	42.441	8.488
2.620	2.340	0.280	600	0.980	0.942	0.297	27.008	5.402
2.620	2.290	0.330	900	0.960	1.414	0.233	21.221	4.244
2.620	2.240	0.380	1200	0.970	1.885	0.202	18.327	3.665
2.620	2.210	0.410	1500	0.960	2.356	0.174	15.819	3.164
2.620	2.180	0.440	1800	0.950	2.827	0.156	14.147	2.829

Table-4.7

Pure Epoxy ($\rho=1.1$) Load 5N RPM 400 ($V=2.0944$ m/sec)

m1 (gm)	m2 (gm)	Δm (gm)	T(Sec)	μ	$SD \times 10^3$ (m)	$WX10^{-5}$ (N/m)	$W_v X10^{-11}$ (m³/m)	$W_s X10^{-11}$ (m³/N.m)
3.190	2.840	0.350	300	0.990	0.628	0.557	50.640	10.128
3.190	2.740	0.450	600	0.980	1.257	0.358	32.554	6.511
3.190	2.660	0.530	900	0.970	1.885	0.281	25.561	5.112
3.190	2.610	0.580	1200	0.970	2.513	0.231	20.979	4.196
3.190	2.570	0.620	1500	0.960	3.142	0.197	17.941	3.588
3.190	2.540	0.650	1800	0.960	3.770	0.172	15.674	3.135

Table-4.8

Pure Epoxy ($\rho=1.1$) Load 7.5N RPM 200 ($V=1.0472$ m/sec)

m1 (gm)	m2 (gm)	Δm (gm)	T(Sec)	M	$SD \times 10^3$ (m)	$WX10^{-5}$ (N/m)	$W_y X10^{-11}$ (m³/m)	$W_s X10^{-11}$ (m³/N.m)
2.860	2.740	0.120	300	0.970	0.314	0.382	34.725	4.630
2.860	2.680	0.180	600	0.960	0.628	0.286	26.043	3.472
2.860	2.640	0.220	900	0.950	0.942	0.233	21.221	2.829
2.860	2.600	0.260	1200	0.960	1.257	0.207	18.809	2.508
2.860	2.570	0.290	1500	0.950	1.571	0.185	16.784	2.238
2.860	2.550	0.310	1800	0.950	1.885	0.164	14.951	1.993

Table-4.9

Pure Epoxy ($\rho=1.1$) Load 7.5N RPM 300 ($V=1.5708$ m/sec)

m1 (gm)	m2 (gm)	Δm (gm)	T(Sec)	M	$SD \times 10^3$ (m)	$WX10^{-5}$ (N/m)	$W_y X10^{-11}$ (m³/m)	$W_s X10^{-11}$ (m³/N.m)
2.350	2.070	0.280	300	0.980	0.471	0.594	54.016	7.202
2.350	1.980	0.370	600	0.970	0.942	0.393	35.689	4.759
2.350	1.900	0.450	900	0.960	1.414	0.318	28.937	3.858
2.350	1.860	0.490	1200	0.960	1.885	0.260	23.632	3.151
2.350	1.830	0.520	1500	0.950	2.356	0.221	20.063	2.675
2.350	1.800	0.550	1800	0.940	2.827	0.195	17.684	2.358

Table-4.10

Pure Epoxy ($\rho=1.1$) Load 7.5N RPM 400 ($V=2.0944$ m/sec)

m1 (gm)	m2 (gm)	Δm (gm)	T(Sec)	M	$SD \times 10^3$ (m)	$WX10^{-5}$ (N/m)	$W_v X10^{-11}$ (m³/m)	$W_s X10^{-11}$ (m³/N.m)
2.980	2.510	0.470	300	0.980	0.471	0.997	90.670	12.089
2.980	2.390	0.590	600	0.980	1.257	0.470	42.682	5.691
2.980	2.310	0.670	900	0.970	1.885	0.355	32.313	4.308
2.980	2.260	0.720	1200	0.960	2.513	0.286	26.043	3.472
2.980	2.220	0.760	1500	0.960	3.142	0.242	21.992	2.932
2.980	2.180	0.800	1800	0.950	3.770	0.212	19.291	2.572

Table-4.11

Pure Epoxy ($\rho=1.1$) Load 10N RPM 200 ($V=1.0472$ m/sec)

m1 (gm)	m2 (gm)	Δm (gm)	T(Sec)	μ	$SD \times 10^3$ (m)	$WX10^{-5}$ (N/m)	$W_v X10^{-11}$ (m³/m)	$W_s X10^{-11}$ (m³/N.m)
3.180	3.000	0.180	300	0.970	0.314	0.573	52.087	5.209
3.180	2.920	0.260	600	0.960	0.628	0.414	37.618	3.762
3.180	2.870	0.310	900	0.960	0.942	0.329	29.902	2.990
3.180	2.830	0.350	1200	0.950	1.257	0.279	25.320	2.532
3.180	2.800	0.380	1500	0.940	1.571	0.242	21.992	2.199
3.180	2.780	0.400	1800	0.930	1.885	0.212	19.291	1.929

Table-4.12

Pure Epoxy ($\rho=1.1$) Load 10N RPM 300 ($V=1.5708$ m/sec)

m1 (gm)	m2 (gm)	Δm (gm)	T(Sec)	M	$SD \times 10^3$ (m)	$WX10^{-5}$ (N/m)	W_vX10^{-11} (m³/m)	W_sX10^{-11} (m³/N.m)
3.620	3.140	0.480	300	0.970	0.471	1.019	92.599	9.260
3.620	2.980	0.640	600	0.960	0.942	0.679	61.733	6.173
3.620	2.890	0.730	900	0.960	1.414	0.516	46.943	4.694
3.620	2.830	0.790	1200	0.950	1.885	0.419	38.101	3.810
3.620	2.790	0.830	1500	0.940	2.356	0.352	32.024	3.202
3.620	2.750	0.870	1800	0.930	2.827	0.308	27.973	2.797

Table-4.13

Pure Epoxy ($\rho=1.1$) Load 10N RPM 400 ($V=2.0944$ m/sec)

m1 (gm)	m2 (gm)	Δm (gm)	T(Sec)	M	$SD \times 10^3$ (m)	$WX10^{-5}$ (N/m)	W_vX10^{-11} (m³/m)	W_sX10^{-11} (m³/N.m)
2.480	1.940	0.540	300	0.970	0.628	0.859	78.130	7.813
2.480	1.780	0.700	600	0.960	1.257	0.557	50.640	5.064
2.480	1.680	0.800	900	0.960	1.885	0.424	38.583	3.858
2.480	1.610	0.870	1200	0.950	2.513	0.346	31.469	3.147
2.480	1.560	0.920	1500	0.960	3.142	0.293	26.622	2.662
2.480	1.520	0.960	1800	0.950	3.770	0.255	23.150	2.315

Table-4.14

Pure Epoxy ($\rho=1.1$) Load 15N RPM 200 ($V=1.0472$ m/sec)

m1 (gm)	m2 (gm)	Δm (gm)	T(Sec)	μ	$SD \times 10^3$ (m)	$WX10^{-5}$ (N/m)	$W_y X10^{-11}$ (m³/m)	$W_s X10^{-11}$ (m³/N.m)
2.450	2.230	0.220	300	0.960	0.314	0.700	63.662	4.244
2.450	2.100	0.350	600	0.950	0.628	0.557	50.640	3.376
2.450	2.020	0.430	900	0.940	0.942	0.456	41.477	2.765
2.450	1.970	0.480	1200	0.930	1.257	0.382	34.725	2.315
2.450	1.930	0.520	1500	0.940	1.571	0.331	30.095	2.006
2.450	1.900	0.550	1800	0.930	1.885	0.292	26.526	1.768

Table-4.15

Pure Epoxy ($\rho=1.1$) Load 15N RPM 300 ($V=1.5708$ m/sec)

m1 (gm)	m2 (gm)	Δm (gm)	T(Sec)	μ	$SD \times 10^3$ (m)	$WX10^{-5}$ (N/m)	$W_y X10^{-11}$ (m³/m)	$W_s X10^{-11}$ (m³/N.m)
3.390	2.870	0.520	300	0.960	0.471	1.103	100.316	6.688
3.390	2.690	0.700	600	0.960	0.942	0.743	67.520	4.501
3.390	2.600	0.790	900	0.950	1.414	0.559	50.801	3.387
3.390	2.550	0.840	1200	0.940	1.885	0.446	40.512	2.701
3.390	2.510	0.880	1500	0.930	2.356	0.373	33.953	2.264
3.390	2.470	0.920	1800	0.920	2.827	0.325	29.580	1.972

Table-4.16

Pure Epoxy ($\rho=1.1$) Load 15N RPM 400 ($V=2.0944$ m/sec)

m1 (gm)	m2 (gm)	Δm (gm)	T(Sec)	M	$SD \times 10^3$ (m)	$WX10^{-5}$ (N/m)	$W_v X10^{-11}$ (m³/m)	$W_s X10^{-11}$ (m³/N.m)
3.310	2.690	0.620	300	0.960	0.628	0.987	89.705	5.980
3.310	2.520	0.790	600	0.950	1.257	0.629	57.151	3.810
3.310	2.440	0.870	900	0.950	1.885	0.462	41.959	2.797
3.310	2.380	0.930	1200	0.940	2.513	0.370	33.639	2.243
3.310	2.330	0.980	1500	0.940	3.142	0.312	28.358	1.891
3.310	2.290	1.020	1800	0.930	3.770	0.271	24.597	1.640

Table-4.17

Volume Fraction= 5% ($\rho=1.077$) Load 5N RPM 200 ($V=1.0472$ m/sec)

m1 (gm)	m2 (gm)	Δm (gm)	T(Sec)	M	$SD \times 10^3$ (m)	$WX10^{-5}$ (N/m)	$W_v X10^{-11}$ (m³/m)	$W_s X10^{-11}$ (m³/N.m)
3.660	3.590	0.070	300	0.980	0.314	0.223	20.689	4.138
3.660	3.560	0.100	600	0.980	0.628	0.159	14.778	2.956
3.660	3.540	0.120	900	0.960	0.942	0.127	11.822	2.364
3.660	3.520	0.140	1200	0.950	1.257	0.111	10.344	2.069
3.660	3.510	0.150	1500	0.950	1.571	0.095	8.867	1.773
3.660	3.500	0.160	1800	0.940	1.885	0.085	7.881	1.576

Table-4.18

Volume Fraction= 5% ($\rho=1.077$) Load 5N RPM 300 ($V=1.5708$ m/sec)

m1 (gm)	m2 (gm)	Δm (gm)	T(Sec)	M	$SD \times 10^3$ (m)	$WX10^{-5}$ (N/m)	$W_V X10^{-11}$ (m³/m)	$W_S X10^{-11}$ (m³/N.m)
3.510	3.400	0.110	300	0.980	0.471	0.233	21.674	4.335
3.510	3.350	0.160	600	0.980	0.942	0.170	15.763	3.153
3.510	3.310	0.200	900	0.970	1.414	0.141	13.136	2.627
3.510	3.280	0.230	1200	0.960	1.885	0.122	11.329	2.266
3.510	3.250	0.260	1500	0.950	2.356	0.110	10.246	2.049
3.510	3.230	0.280	1800	0.950	2.827	0.099	9.195	1.839

Table-4.19

Volume Fraction= 5% ($\rho=1.077$) Load 5N RPM 400 ($V=2.0944$ m/sec)

m1 (gm)	m2 (gm)	Δm (gm)	T(Sec)	M	$SD \times 10^3$ (m)	$WX10^{-5}$ (N/m)	$W_V X10^{-11}$ (m³/m)	$W_S X10^{-11}$ (m³/N.m)
2.570	2.410	0.160	300	0.990	0.628	0.255	23.644	4.729
2.570	2.340	0.230	600	0.980	1.257	0.183	16.994	3.399
2.570	2.280	0.290	900	0.960	1.885	0.154	14.285	2.857
2.570	2.240	0.330	1200	0.970	2.513	0.131	12.192	2.438
2.570	2.210	0.360	1500	0.950	3.142	0.115	10.640	2.128
2.570	2.190	0.380	1800	0.950	3.770	0.101	9.359	1.872

Table-4.20

Volume fraction= 5% ($\rho=1.077$) Load 7.5N RPM 200 (V=1.0472 m/sec)

m1 (gm)	m2 (gm)	Δm (gm)	T(Sec)	M	SD x 10³ (m)	WX10⁻⁵ (N/m)	W_vX10⁻¹¹ (m³/m)	W_sX10⁻¹¹ (m³/N.m)
2.790	2.720	0.070	300	0.980	0.314	0.223	20.689	2.758
2.790	2.680	0.110	600	0.970	0.628	0.175	16.255	2.167
2.790	2.650	0.140	900	0.950	0.942	0.149	13.792	1.839
2.790	2.630	0.160	1200	0.950	1.257	0.127	11.822	1.576
2.790	2.610	0.180	1500	0.940	1.571	0.115	10.640	1.419
2.790	2.600	0.190	1800	0.940	1.885	0.101	9.359	1.248

Table-4.21

Volume fraction= 5% ($\rho=1.077$) Load 7.5N RPM 300 (V=1.5708 m/sec)

m1 (gm)	m2 (gm)	Δm (gm)	T(Sec)	M	SD x 10³ (m)	WX10⁻⁵ (N/m)	W_vX10⁻¹¹ (m³/m)	W_sX10⁻¹¹ (m³/N.m)
3.190	3.080	0.110	300	0.970	0.471	0.233	21.674	2.890
3.190	3.020	0.170	600	0.980	0.942	0.180	16.748	2.233
3.190	2.970	0.220	900	0.970	1.414	0.156	14.449	1.927
3.190	2.930	0.260	1200	0.960	1.885	0.138	12.807	1.708
3.190	2.900	0.290	1500	0.950	2.356	0.123	11.428	1.524
3.190	2.870	0.320	1800	0.940	2.827	0.113	10.509	1.401

Table-4.22

Volume fraction= 5% ($\rho=1.077$) Load 7.5N RPM 400 (V=2.0944 m/sec)

m1 (gm)	m2 (gm)	Δm (gm)	T(Sec)	M	SD x 10³ (m)	WX10⁻⁵ (N/m)	W_VX10⁻¹¹ (m³/m)	W_SX10⁻¹¹ (m³/N.m)
2.090	1.920	0.170	300	0.980	0.628	0.271	25.122	3.350
2.090	1.850	0.240	600	0.980	1.257	0.191	17.733	2.364
2.090	1.790	0.300	900	0.960	1.885	0.159	14.778	1.970
2.090	1.740	0.350	1200	0.960	2.513	0.139	12.930	1.724
2.090	1.690	0.400	1500	0.950	3.142	0.127	11.822	1.576
2.090	1.650	0.440	1800	0.950	3.770	0.117	10.837	1.445

Table-4.23

Volume fraction= 5% ($\rho=1.077$) Load 10N RPM 200 (V=1.0472 m/sec)

m1 (gm)	m2 (gm)	Δm (gm)	T(Sec)	M	SD x 10³ (m)	WX10⁻⁵ (N/m)	W_VX10⁻¹¹ (m³/m)	W_SX10⁻¹¹ (m³/N.m)
3.290	3.200	0.090	300	0.970	0.314	0.286	26.600	2.660
3.290	3.150	0.140	600	0.960	0.628	0.223	20.689	2.069
3.290	3.120	0.170	900	0.950	0.942	0.180	16.748	1.675
3.290	3.100	0.190	1200	0.950	1.257	0.151	14.039	1.404
3.290	3.090	0.200	1500	0.940	1.571	0.127	11.822	1.182
3.290	3.080	0.210	1800	0.930	1.885	0.111	10.344	1.034

Table-4.24

Volume fraction= 5% ($\rho=1.077$) Load 10N RPM 300 ($V=1.5708$ m/sec)

m1 (gm)	m2 (gm)	Δm (gm)	T(Sec)	M	$SD \times 10^3$ (m)	$WX10^{-5}$ (N/m)	$W_v X10^{-11}$ (m³/m)	$W_s X10^{-11}$ (m³/N.m)
3.240	3.080	0.160	300	0.970	0.471	0.340	31.526	3.153
3.240	3.000	0.240	600	0.960	0.942	0.255	23.644	2.364
3.240	2.940	0.300	900	0.950	1.414	0.212	19.703	1.970
3.240	2.890	0.350	1200	0.960	1.885	0.186	17.241	1.724
3.240	2.860	0.380	1500	0.940	2.356	0.161	14.975	1.497
3.240	2.820	0.420	1800	0.940	2.827	0.149	13.792	1.379

Table-4.25

Volume fraction= 5% ($\rho=1.077$) Load 10N RPM 400 ($V=2.0944$ m/sec)

m1 (gm)	m2 (gm)	Δm (gm)	T(Sec)	M	$SD \times 10^3$ (m)	$WX10^{-5}$ (N/m)	$W_v X10^{-11}$ (m³/m)	$W_s X10^{-11}$ (m³/N.m)
2.840	2.670	0.170	300	0.970	0.628	0.271	25.122	2.512
2.840	2.600	0.240	600	0.950	1.257	0.191	17.733	1.773
2.840	2.530	0.310	900	0.960	1.885	0.164	15.270	1.527
2.840	2.480	0.360	1200	0.940	2.513	0.143	13.300	1.330
2.840	2.440	0.400	1500	0.950	3.142	0.127	11.822	1.182
2.840	2.410	0.430	1800	0.940	3.770	0.114	10.591	1.059

Table-4.26

Volume fraction= 5% ($\rho=1.077$) Load 15N RPM 200 (V=1.0472 m/sec)

m1 (gm)	m2 (gm)	Δm (gm)	T(Sec)	M	SD x 10³ (m)	WX10⁻⁵ (N/m)	W_vX10⁻¹¹ (m³/m)	W_sX10⁻¹¹ (m³/N.m)
3.030	2.910	0.120	300	0.960	0.314	0.382	35.466	2.364
3.030	2.860	0.170	600	0.950	0.628	0.271	25.122	1.675
3.030	2.820	0.210	900	0.950	0.942	0.223	20.689	1.379
3.030	2.790	0.240	1200	0.950	1.257	0.191	17.733	1.182
3.030	2.760	0.270	1500	0.930	1.571	0.172	15.960	1.064
3.030	2.740	0.290	1800	0.930	1.885	0.154	14.285	0.952

Table-4.27

Volume fraction= 5% ($\rho=1.077$) Load 15N RPM 300 (V=1.5708 m/sec)

m1 (gm)	m2 (gm)	Δm (gm)	T(Sec)	M	SD x 10³ (m)	WX10⁻⁵ (N/m)	W_vX10⁻¹¹ (m³/m)	W_sX10⁻¹¹ (m³/N.m)
2.720	2.550	0.170	300	0.960	0.471	0.361	33.496	2.233
2.720	2.470	0.250	600	0.960	0.942	0.265	24.629	1.642
2.720	2.410	0.310	900	0.950	1.414	0.219	20.360	1.357
2.720	2.360	0.360	1200	0.940	1.885	0.191	17.733	1.182
2.720	2.320	0.400	1500	0.940	2.356	0.170	15.763	1.051
2.720	2.290	0.430	1800	0.930	2.827	0.152	14.121	0.941

Table-4.28

Volume fraction= 5% ($\rho=1.077$) Load 15N RPM 400 (V=2.0944 m/sec)

m1 (gm)	m2 (gm)	Δm (gm)	T(Sec)	M	SD x 10³ (m)	WX10⁻⁵ (N/m)	W_vX10⁻¹¹ (m³/m)	W_sX10⁻¹¹ (m³/N.m)
2.800	2.590	0.210	300	0.950	0.628	0.334	31.033	2.069
2.800	2.500	0.300	600	0.950	1.257	0.239	22.166	1.478
2.800	2.430	0.370	900	0.950	1.885	0.196	18.226	1.215
2.800	2.380	0.420	1200	0.940	2.513	0.167	15.516	1.034
2.800	2.350	0.450	1500	0.930	3.142	0.143	13.300	0.887
2.800	2.310	0.490	1800	0.920	3.770	0.130	12.068	0.805

Table-4.29

Volume fraction= 10% ($\rho=1.08$) Load 5N RPM 200 (V=1.0472 m/sec)

m1 (gm)	m2 (gm)	Δm (gm)	T(Sec)	M	SD x 10³ (m)	WX10⁻⁵ (N/m)	W_vX10⁻¹¹ (m³/m)	W_sX10⁻¹¹ (m³/N.m)
3.340	3.290	0.050	300	0.960	0.314	0.159	14.737	2.947
3.340	3.270	0.070	600	0.950	0.628	0.111	10.316	2.063
3.340	3.250	0.090	900	0.950	0.942	0.095	8.842	1.768
3.340	3.240	0.100	1200	0.940	1.257	0.080	7.368	1.474
3.340	3.230	0.110	1500	0.940	1.571	0.070	6.484	1.297
3.340	3.220	0.120	1800	0.920	1.885	0.064	5.895	1.179

Table-4.30

Volume fraction= 10% ($\rho=1.08$) Load 5N RPM 300 (V=1.5708 m/sec)

m1 (gm)	m2 (gm)	Δm (gm)	T(Sec)	μ	SD x 10^3 (m)	WX10^{-5} (N/m)	W_vX10^{-11} (m³/m)	W_sX10^{-11} (m³/N.m)
2.230	2.150	0.080	300	0.980	0.471	0.170	15.719	3.144
2.230	2.110	0.120	600	0.960	0.942	0.127	11.789	2.358
2.230	2.090	0.140	900	0.950	1.414	0.099	9.169	1.834
2.230	2.070	0.160	1200	0.950	1.885	0.085	7.859	1.572
2.230	2.050	0.180	1500	0.940	2.356	0.076	7.074	1.415
2.230	2.050	0.180	1800	0.930	2.827	0.064	5.895	1.179

Table-4.31

Volume fraction= 10% ($\rho=1.08$) Load 5N RPM 400 (V=2.0944 m/sec)

m1 (gm)	m2 (gm)	Δm (gm)	T(Sec)	M	SD x 10^3 (m)	WX10^{-5} (N/m)	W_vX10^{-11} (m³/m)	W_sX10^{-11} (m³/N.m)
1.730	1.610	0.120	300	0.980	0.628	0.191	17.684	3.537
1.730	1.570	0.160	600	0.970	1.257	0.127	11.789	2.358
1.730	1.540	0.190	900	0.980	1.885	0.101	9.333	1.867
1.730	1.510	0.220	1200	0.960	2.513	0.088	8.105	1.621
1.730	1.480	0.250	1500	0.950	3.142	0.080	7.368	1.474
1.730	1.460	0.270	1800	0.950	3.770	0.072	6.631	1.326

Table-4.32

Volume fraction= 10% ($\rho=1.08$) Load 7.5N RPM 200 (V=1.0472 m/sec)

m1 (gm)	m2 (gm)	Δm (gm)	T(Sec)	μ	SD x 10³ (m)	WX10⁻⁵ (N/m)	W_vX10⁻¹¹ (m³/m)	W_sX10⁻¹¹ (m³/N.m)
3.290	3.230	0.060	300	0.960	0.314	0.191	17.684	2.358
3.290	3.210	0.080	600	0.950	0.628	0.127	11.789	1.572
3.290	3.190	0.100	900	0.940	0.942	0.106	9.824	1.310
3.290	3.180	0.110	1200	0.940	1.257	0.088	8.105	1.081
3.290	3.170	0.120	1500	0.930	1.571	0.076	7.074	0.943
3.290	3.170	0.120	1800	0.920	1.885	0.064	5.895	0.786

Table-4.33

Volume fraction= 10% ($\rho=1.08$) Load 7.5N RPM 300 (V=1.5708 m/sec)

m1 (gm)	m2 (gm)	Δm (gm)	T(Sec)	μ	SD x 10³ (m)	WX10⁻⁵ (N/m)	W_vX10⁻¹¹ (m³/m)	W_sX10⁻¹¹ (m³/N.m)
2.260	2.170	0.090	300	0.960	0.471	0.191	17.684	2.358
2.260	2.120	0.140	600	0.940	0.942	0.149	13.754	1.834
2.260	2.100	0.160	900	0.950	1.414	0.113	10.479	1.397
2.260	2.080	0.180	1200	0.940	1.885	0.095	8.842	1.179
2.260	2.060	0.200	1500	0.940	2.356	0.085	7.859	1.048
2.260	2.050	0.210	1800	0.930	2.827	0.074	6.877	0.917

Table-4.34

Volume fraction= 10% ($\rho=1.08$) Load 7.5N RPM 400 (V=2.0944 m/sec)

m1 (gm)	m2 (gm)	Δm (gm)	T(Sec)	μ	SD x 10³ (m)	WX10⁻⁵ (N/m)	W_yX10⁻¹¹ (m³/m)	W_sX10⁻¹¹ (m³/N.m)
2.750	2.600	0.150	300	0.970	0.628	0.239	22.105	2.947
2.750	2.540	0.210	600	0.970	1.257	0.167	15.473	2.063
2.750	2.500	0.250	900	0.960	1.885	0.133	12.280	1.637
2.750	2.460	0.290	1200	0.960	2.513	0.115	10.684	1.425
2.750	2.420	0.330	1500	0.950	3.142	0.105	9.726	1.297
2.750	2.390	0.360	1800	0.940	3.770	0.095	8.842	1.179

Table-4.35

Volume fraction= 10% ($\rho=1.08$) Load 10N RPM 200 (V=1.0472 m/sec)

m1 (gm)	m2 (gm)	Δm (gm)	T(Sec)	μ	SD x 10³ (m)	WX10⁻⁵ (N/m)	W_yX10⁻¹¹ (m³/m)	W_sX10⁻¹¹ (m³/N.m)
1.840	1.780	0.060	300	0.960	0.314	0.191	17.684	1.768
1.840	1.750	0.090	600	0.950	0.628	0.143	13.263	1.326
1.840	1.730	0.110	900	0.940	0.942	0.117	10.807	1.081
1.840	1.710	0.130	1200	0.930	1.257	0.103	9.579	0.958
1.840	1.700	0.140	1500	0.930	1.571	0.089	8.252	0.825
1.840	1.690	0.150	1800	0.920	1.885	0.080	7.368	0.737

Table-4.36

Volume fraction= 10% ($\rho=1.08$) Load 10N RPM 300 (V=1.5708 m/sec)

m1 (gm)	m2 (gm)	Δm (gm)	T(Sec)	μ	SD x 10³ (m)	WX10⁻⁵ (N/m)	W_vX10⁻¹¹ (m³/m)	W_sX10⁻¹¹ (m³/N.m)
3.280	3.180	0.100	300	0.960	0.471	0.212	19.649	1.965
3.280	3.140	0.140	600	0.960	0.942	0.149	13.754	1.375
3.280	3.120	0.160	900	0.940	1.414	0.113	10.479	1.048
3.280	3.090	0.190	1200	0.940	1.885	0.101	9.333	0.933
3.280	3.070	0.210	1500	0.920	2.356	0.089	8.252	0.825
3.280	3.050	0.230	1800	0.920	2.827	0.081	7.532	0.753

Table-4.37

Volume fraction= 10% ($\rho=1.08$) Load 10N RPM 400 (V=2.0944 m/sec)

m1 (gm)	m2 (gm)	Δm (gm)	T(Sec)	μ	SD x 10³ (m)	WX10⁻⁵ (N/m)	W_vX10⁻¹¹ (m³/m)	W_sX10⁻¹¹ (m³/N.m)
2.610	2.450	0.160	300	0.970	0.628	0.255	23.578	2.358
2.610	2.390	0.220	600	0.950	1.257	0.175	16.210	1.621
2.610	2.340	0.270	900	0.950	1.885	0.143	13.263	1.326
2.610	2.300	0.310	1200	0.950	2.513	0.123	11.421	1.142
2.610	2.270	0.340	1500	0.940	3.142	0.108	10.021	1.002
2.610	2.240	0.370	1800	0.930	3.770	0.098	9.088	0.909

Table-4.38

Volume fraction= 10% ($\rho=1.08$) Load 15N RPM 200 (V=1.0472 m/sec)

m1 (gm)	m2 (gm)	Δm (gm)	T(Sec)	μ	$SD \times 10^3$ (m)	$WX10^{-5}$ (N/m)	$W_v X10^{-11}$ (m³/m)	$W_s X10^{-11}$ (m³/N.m)
2.920	2.840	0.080	300	0.950	0.314	0.255	23.578	1.572
2.920	2.810	0.110	600	0.950	0.628	0.175	16.210	1.081
2.920	2.790	0.130	900	0.930	0.942	0.138	12.772	0.851
2.920	2.780	0.140	1200	0.930	1.257	0.111	10.316	0.688
2.920	2.760	0.160	1500	0.910	1.571	0.102	9.431	0.629
2.920	2.750	0.170	1800	0.900	1.885	0.090	8.351	0.557

Table-4.39

Volume fraction= 10% ($\rho=1.08$) Load 15N RPM 300 (V=1.5708 m/sec)

m1 (gm)	m2 (gm)	Δm (gm)	T(Sec)	μ	$SD \times 10^3$ (m)	$WX10^{-5}$ (N/m)	$W_v X10^{-11}$ (m³/m)	$W_s X10^{-11}$ (m³/N.m)
2.570	2.420	0.150	300	0.950	0.471	0.318	29.473	1.965
2.570	2.330	0.240	600	0.950	0.942	0.255	23.578	1.572
2.570	2.290	0.280	900	0.940	1.414	0.198	18.339	1.223
2.570	2.250	0.320	1200	0.930	1.885	0.170	15.719	1.048
2.570	2.220	0.350	1500	0.930	2.356	0.149	13.754	0.917
2.570	2.190	0.380	1800	0.920	2.827	0.134	12.444	0.830

Table-4.40

Volume fraction= 10% ($\rho=1.08$) Load 15N RPM 400 (V=2.0944 m/sec)

m1 (gm)	m2 (gm)	Δm (gm)	T(Sec)	M	SD x 10³ (m)	WX10⁻⁵ (N/m)	W_vX10⁻¹¹ (m³/m)	W_sX10⁻¹¹ (m³/N.m)
2.700	2.520	0.180	300	0.960	0.628	0.286	26.526	1.768
2.700	2.450	0.250	600	0.950	1.257	0.199	18.421	1.228
2.700	2.400	0.300	900	0.940	1.885	0.159	14.737	0.982
2.700	2.360	0.340	1200	0.920	2.513	0.135	12.526	0.835
2.700	2.320	0.380	1500	0.920	3.142	0.121	11.200	0.747
2.700	2.290	0.410	1800	0.910	3.770	0.109	10.070	0.671

Table-4.41

Volume fraction= 15% ($\rho=1.09$) Load 5N RPM 200 (V=1.0472 m/sec)

m1 (gm)	m2 (gm)	Δm (gm)	T(Sec)	μ	SD x 10³ (m)	WX10⁻⁵ (N/m)	W_vX10⁻¹¹ (m³/m)	W_sX10⁻¹¹ (m³/N.m)
3.190	3.140	0.050	300	0.980	0.314	0.159	14.601	2.920
3.190	3.110	0.080	600	0.980	0.628	0.127	11.681	2.336
3.190	3.090	0.100	900	0.960	0.942	0.106	9.734	1.947
3.190	3.070	0.120	1200	0.950	1.257	0.095	8.761	1.752
3.190	3.060	0.130	1500	0.940	1.571	0.083	7.593	1.519
3.190	3.060	0.130	1800	0.940	1.885	0.069	6.327	1.265

Table-4.42

Volume fraction= 15% (ρ=1.09) Load 5N RPM 300 (V=1.5708 m/sec)

m1 (gm)	m2 (gm)	Δm (gm)	T(Sec)	M	SD x 10³ (m)	WX10⁻⁵ (N/m)	W_vX10⁻¹¹ (m³/m)	W_sX10⁻¹¹ (m³/N.m)
2.850	2.770	0.080	300	0.980	0.471	0.170	15.575	3.115
2.850	2.730	0.120	600	0.970	0.942	0.127	11.681	2.336
2.850	2.700	0.150	900	0.960	1.414	0.106	9.734	1.947
2.850	2.680	0.170	1200	0.960	1.885	0.090	8.274	1.655
2.850	2.660	0.190	1500	0.950	2.356	0.081	7.398	1.480
2.850	2.640	0.210	1800	0.940	2.827	0.074	6.814	1.363

Table-4.43

Volume fraction= 15% (ρ=1.09) Load 5N RPM 400 (V=2.0944 m/sec)

m1 (gm)	m2 (gm)	Δm (gm)	T(Sec)	μ	SD x 10³ (m)	WX10⁻⁵ (N/m)	W_vX10⁻¹¹ (m³/m)	W_sX10⁻¹¹ (m³/N.m)
2.410	2.300	0.110	300	0.980	0.628	0.175	16.061	3.212
2.410	2.230	0.180	600	0.970	1.257	0.143	13.141	2.628
2.410	2.190	0.220	900	0.960	1.885	0.117	10.708	2.142
2.410	2.160	0.250	1200	0.980	2.513	0.099	9.126	1.825
2.410	2.130	0.280	1500	0.950	3.142	0.089	8.177	1.635
2.410	2.110	0.300	1800	0.950	3.770	0.080	7.301	1.460

Table-4.44

Volume fraction= 15% (ρ=1.09) Load 7.5N RPM 200 (V=1.0472 m/sec)

m1 (gm)	m2 (gm)	Δm (gm)	T(Sec)	M	SD x 10³ (m)	WX10⁻⁵ (N/m)	W_vX10⁻¹¹ (m³/m)	W_sX10⁻¹¹ (m³/N.m)
3.140	3.080	0.060	300	0.980	0.314	0.191	17.522	2.336
3.140	3.050	0.090	600	0.970	0.628	0.143	13.141	1.752
3.140	3.030	0.110	900	0.960	0.942	0.117	10.708	1.428
3.140	3.020	0.120	1200	0.940	1.257	0.095	8.761	1.168
3.140	3.010	0.130	1500	0.940	1.571	0.083	7.593	1.012
3.140	3.010	0.130	1800	0.930	1.885	0.069	6.327	0.844

Table-4.45

Volume fraction= 15% (ρ=1.09) Load 7.5N RPM 300 (V=1.5708 m/sec)

m1 (gm)	m2 (gm)	Δm (gm)	T(Sec)	M	SD x 10³ (m)	WX10⁻⁵ (N/m)	W_vX10⁻¹¹ (m³/m)	W_sX10⁻¹¹ (m³/N.m)
2.090	1.960	0.130	300	0.970	0.471	0.276	25.309	3.375
2.090	1.920	0.170	600	0.980	0.942	0.180	16.548	2.206
2.090	1.890	0.200	900	0.960	1.414	0.141	12.979	1.731
2.090	1.870	0.220	1200	0.950	1.885	0.117	10.708	1.428
2.090	1.850	0.240	1500	0.950	2.356	0.102	9.345	1.246
2.090	1.830	0.260	1800	0.940	2.827	0.092	8.436	1.125

Table-4.46

Volume fraction= 15% ($\rho=1.09$) Load 7.5N RPM 400 (V=2.0944 m/sec)

m1 (gm)	m2 (gm)	Δm (gm)	T(Sec)	M	SD x 10³ (m)	WX10⁻⁵ (N/m)	W_vX10⁻¹¹ (m³/m)	W_sX10⁻¹¹ (m³/N.m)
1.860	1.670	0.190	300	0.980	0.628	0.302	27.743	3.699
1.860	1.600	0.260	600	0.970	1.257	0.207	18.982	2.531
1.860	1.530	0.330	900	0.960	1.885	0.175	16.061	2.142
1.860	1.480	0.380	1200	0.960	2.513	0.151	13.871	1.850
1.860	1.440	0.420	1500	0.950	3.142	0.134	12.265	1.635
1.860	1.410	0.450	1800	0.940	3.770	0.119	10.951	1.460

Table-4.47

Volume fraction= 15% ($\rho=1.09$) Load 10N RPM 200 (V=1.0472 m/sec)

m1 (gm)	m2 (gm)	Δm (gm)	T(Sec)	M	SD x 10³ (m)	WX10⁻⁵ (N/m)	W_vX10⁻¹¹ (m³/m)	W_sX10⁻¹¹ (m³/N.m)
2.050	1.970	0.080	300	0.960	0.314	0.255	23.362	2.336
2.050	1.930	0.120	600	0.960	0.628	0.191	17.522	1.752
2.050	1.900	0.150	900	0.950	0.942	0.159	14.601	1.460
2.050	1.880	0.170	1200	0.940	1.257	0.135	12.411	1.241
2.050	1.860	0.190	1500	0.930	1.571	0.121	11.097	1.110
2.050	1.850	0.200	1800	0.930	1.885	0.106	9.734	0.973

Table-4.48

Volume fraction= 15% ($\rho=1.09$) Load 10N RPM 300 (V=1.5708 m/sec)

m1 (gm)	m2 (gm)	Δm (gm)	T(Sec)	M	SD x 10³ (m)	WX10⁻⁵ (N/m)	W_vX10⁻¹¹ (m³/m)	W_sX10⁻¹¹ (m³/N.m)
1.810	1.680	0.130	300	0.960	0.471	0.276	25.309	2.531
1.810	1.620	0.190	600	0.960	0.942	0.202	18.495	1.850
1.810	1.580	0.230	900	0.950	1.414	0.163	14.926	1.493
1.810	1.560	0.250	1200	0.940	1.885	0.133	12.168	1.217
1.810	1.540	0.270	1500	0.940	2.356	0.115	10.513	1.051
1.810	1.520	0.290	1800	0.930	2.827	0.103	9.410	0.941

Table-4.49

Volume fraction= 15% ($\rho=1.09$) Load 10N RPM 400 (V=2.0944 m/sec)

m1 (gm)	m2 (gm)	Δm (gm)	T(Sec)	μ	SD x 10³ (m)	WX10⁻⁵ (N/m)	W_vX10⁻¹¹ (m³/m)	W_sX10⁻¹¹ (m³/N.m)
2.760	2.570	0.190	300	0.970	0.628	0.302	27.743	2.774
2.760	2.490	0.270	600	0.950	1.257	0.215	19.712	1.971
2.760	2.430	0.330	900	0.950	1.885	0.175	16.061	1.606
2.760	2.380	0.380	1200	0.960	2.513	0.151	13.871	1.387
2.760	2.340	0.420	1500	0.960	3.142	0.134	12.265	1.227
2.760	2.310	0.450	1800	0.940	3.770	0.119	10.951	1.095

Table-4.50

Volume fraction= 15% ($\rho=1.09$) Load 15N RPM 200 (V=1.0472 m/sec)

m1 (gm)	m2 (gm)	Δm (gm)	T(Sec)	M	$SD \times 10^3$ (m)	$WX10^{-5}$ (N/m)	$W_v X10^{-11}$ (m³/m)	$W_s X10^{-11}$ (m³/N.m)
2.260	2.170	0.090	300	0.950	0.314	0.286	26.282	1.752
2.260	2.120	0.140	600	0.940	0.628	0.223	20.442	1.363
2.260	2.080	0.180	900	0.940	0.942	0.191	17.522	1.168
2.260	2.060	0.200	1200	0.920	1.257	0.159	14.601	0.973
2.260	2.040	0.220	1500	0.920	1.571	0.140	12.849	0.857
2.260	2.020	0.240	1800	0.910	1.885	0.127	11.681	0.779

Table-4.51

Volume fraction= 15% ($\rho=1.09$) Load 15N RPM 300 (V=1.5708 m/sec)

m1 (gm)	m2 (gm)	Δm (gm)	T(Sec)	M	$SD \times 10^3$ (m)	$WX10^{-5}$ (N/m)	$W_v X10^{-11}$ (m³/m)	$W_s X10^{-11}$ (m³/N.m)
1.740	1.580	0.160	300	0.980	0.471	0.340	31.150	2.077
1.740	1.500	0.240	600	0.960	0.942	0.255	23.362	1.557
1.740	1.450	0.290	900	0.940	1.414	0.205	18.820	1.255
1.740	1.410	0.330	1200	0.940	1.885	0.175	16.061	1.071
1.740	1.370	0.370	1500	0.930	2.356	0.157	14.407	0.960
1.740	1.340	0.400	1800	0.910	2.827	0.141	12.979	0.865

Table-4.52

Volume fraction= 15% ($\rho=1.09$) Load 15N RPM 400 (V=2.0944 m/sec)

m1 (gm)	m2 (gm)	Δm (gm)	T(Sec)	M	SD x 10³ (m)	WX10⁻⁵ (N/m)	W_vX10⁻¹¹ (m³/m)	W_sX10⁻¹¹ (m³/N.m)
3.440	3.190	0.250	300	0.960	0.628	0.398	36.503	2.434
3.440	3.090	0.350	600	0.960	1.257	0.279	25.552	1.703
3.440	3.020	0.420	900	0.950	1.885	0.223	20.442	1.363
3.440	2.970	0.470	1200	0.950	2.513	0.187	17.157	1.144
3.440	2.930	0.510	1500	0.940	3.142	0.162	14.893	0.993
3.440	2.900	0.540	1800	0.930	3.770	0.143	13.141	0.876

Table-4.53

Volume fraction= 20% ($\rho=1.079$) Load 5N RPM 200 (V=1.0473 m/sec)

m1 (gm)	m2 (gm)	Δm (gm)	T(Sec)	M	SD x 10³ (m)	WX10⁻⁵ (N/m)	W_vX10⁻¹¹ (m³/m)	W_sX10⁻¹¹ (m³/N.m)
3.150	3.090	0.060	300	0.980	0.314	0.191	17.700	3.540
3.150	3.060	0.090	600	0.980	0.628	0.143	13.275	2.655
3.150	3.040	0.110	900	0.970	0.942	0.117	10.817	2.163
3.150	3.030	0.120	1200	0.950	1.257	0.095	8.850	1.770
3.150	3.010	0.140	1500	0.940	1.571	0.089	8.260	1.652
3.150	3.000	0.150	1800	0.940	1.885	0.080	7.375	1.475

Table-4.54

Volume fraction= 20% ($\rho=1.079$) Load 5N RPM 300 (V=1.5708 m/sec)

m1 (gm)	m2 (gm)	Δm (gm)	T(Sec)	M	SD x 10³ (m)	WX10⁻⁵ (N/m)	W_vX10⁻¹¹ (m³/m)	W_sX10⁻¹¹ (m³/N.m)
3.210	3.100	0.110	300	0.990	0.471	0.233	21.634	4.327
3.210	3.060	0.150	600	0.980	0.942	0.159	14.750	2.950
3.210	3.040	0.170	900	0.970	1.414	0.120	11.145	2.229
3.210	3.010	0.200	1200	0.950	1.885	0.106	9.833	1.967
3.210	2.980	0.230	1500	0.950	2.356	0.098	9.047	1.809
3.210	2.960	0.250	1800	0.950	2.827	0.088	8.195	1.639

Table-4.55

Volume fraction= 20% ($\rho=1.079$) Load 5N RPM 400 (V=2.0944 m/sec)

m1 (gm)	m2 (gm)	Δm (gm)	T(Sec)	M	SD x 10³ (m)	WX10⁻⁵ (N/m)	W_vX10⁻¹¹ (m³/m)	W_sX10⁻¹¹ (m³/N.m)
2.480	2.360	0.120	300	0.990	0.628	0.191	17.700	3.540
2.480	2.280	0.200	600	0.980	1.257	0.159	14.750	2.950
2.480	2.230	0.250	900	0.970	1.885	0.133	12.292	2.458
2.480	2.190	0.290	1200	0.970	2.513	0.115	10.694	2.139
2.480	2.160	0.320	1500	0.960	3.142	0.102	9.440	1.888
2.480	2.130	0.350	1800	0.950	3.770	0.093	8.604	1.721

Table-4.56

Volume fraction= 20% ($\rho=1.079$) Load 7.5N RPM 200 (V=1.0472 m/sec)

m1 (gm)	m2 (gm)	Δm (gm)	T(Sec)	M	SD x 10³ (m)	WX10⁻⁵ (N/m)	W_vX10⁻¹¹ (m³/m)	W_sX10⁻¹¹ (m³/N.m)
2.850	2.780	0.070	300	0.980	0.314	0.223	20.650	2.753
2.850	2.740	0.110	600	0.960	0.628	0.175	16.225	2.163
2.850	2.720	0.130	900	0.960	0.942	0.138	12.783	1.704
2.850	2.700	0.150	1200	0.950	1.257	0.119	11.063	1.475
2.850	2.690	0.160	1500	0.950	1.571	0.102	9.440	1.259
2.850	2.690	0.160	1800	0.930	1.885	0.085	7.867	1.049

Table-4.57

Volume fraction= 20% ($\rho=1.079$) Load 7.5N RPM 300 (V=1.5708 m/sec)

m1 (gm)	m2 (gm)	Δm (gm)	T(Sec)	M	SD x 10³ (m)	WX10⁻⁵ (N/m)	W_vX10⁻¹¹ (m³/m)	W_sX10⁻¹¹ (m³/N.m)
3.070	2.950	0.120	300	0.970	0.471	0.255	23.600	3.147
3.070	2.880	0.190	600	0.970	0.942	0.202	18.684	2.491
3.070	2.840	0.230	900	0.960	1.414	0.163	15.078	2.010
3.070	2.820	0.250	1200	0.950	1.885	0.133	12.292	1.639
3.070	2.800	0.270	1500	0.920	2.356	0.115	10.620	1.416
3.070	2.780	0.290	1800	0.930	2.827	0.103	9.506	1.267

Table-4.58

Volume fraction= 20% ($\rho=1.079$) Load 7.5N RPM 400 (V=2.0944 m/sec)

m1 (gm)	m2 (gm)	Δm (gm)	T(Sec)	M	SD x 10³ (m)	WX10⁻⁵ (N/m)	W_vX10⁻¹¹ (m³/m)	W_sX10⁻¹¹ (m³/N.m)
2.680	2.480	0.200	300	0.980	0.628	0.318	29.500	3.933
2.680	2.390	0.290	600	0.970	1.257	0.231	21.388	2.852
2.680	2.310	0.370	900	0.970	1.885	0.196	18.192	2.426
2.680	2.270	0.410	1200	0.960	2.513	0.163	15.119	2.016
2.680	2.230	0.450	1500	0.950	3.142	0.143	13.275	1.770
2.680	2.200	0.480	1800	0.950	3.770	0.127	11.800	1.573

Table-4.59

Volume fraction= 20% ($\rho=1.079$) Load 10N RPM 200 (V=1.0472 m/sec)

m1 (gm)	m2 (gm)	Δm (gm)	T(Sec)	M	SD x 10³ (m)	WX10⁻⁵ (N/m)	W_vX10⁻¹¹ (m³/m)	W_sX10⁻¹¹ (m³/N.m)
2.380	2.300	0.080	300	0.980	0.314	0.255	23.600	2.360
2.380	2.250	0.130	600	0.960	0.628	0.207	19.175	1.918
2.380	2.220	0.160	900	0.950	0.942	0.170	15.734	1.573
2.380	2.200	0.180	1200	0.940	1.257	0.143	13.275	1.328
2.380	2.180	0.200	1500	0.920	1.571	0.127	11.800	1.180
2.380	2.170	0.210	1800	0.920	1.885	0.111	10.325	1.033

Table-4.60

Volume fraction= 20% ($\rho=1.079$) Load 10N RPM 300 (V=1.5708 m/sec)

m1 (gm)	m2 (gm)	Δm (gm)	T(Sec)	M	SD x 10³ (m)	WX10⁻⁵ (N/m)	W_vX10⁻¹¹ (m³/m)	W_sX10⁻¹¹ (m³/N.m)
2.670	2.540	0.130	300	0.960	0.471	0.276	25.567	2.557
2.670	2.460	0.210	600	0.960	0.942	0.223	20.650	2.065
2.670	2.420	0.250	900	0.950	1.414	0.177	16.389	1.639
2.670	2.390	0.280	1200	0.950	1.885	0.149	13.767	1.377
2.670	2.360	0.310	1500	0.940	2.356	0.132	12.193	1.219
2.670	2.340	0.330	1800	0.930	2.827	0.117	10.817	1.082

Table-4.61

Volume fraction= 20% ($\rho=1.079$) Load 10N RPM 400 (V=2.0944 m/sec)

m1 (gm)	m2 (gm)	Δm (gm)	T(Sec)	M	SD x 10³ (m)	WX10⁻⁵ (N/m)	W_vX10⁻¹¹ (m³/m)	W_sX10⁻¹¹ (m³/N.m)
2.030	1.820	0.210	300	0.970	0.628	0.334	30.975	3.098
2.030	1.730	0.300	600	0.950	1.257	0.239	22.125	2.213
2.030	1.660	0.370	900	0.960	1.885	0.196	18.192	1.819
2.030	1.600	0.430	1200	0.960	2.513	0.171	15.856	1.586
2.030	1.560	0.470	1500	0.940	3.142	0.150	13.865	1.387
2.030	1.530	0.500	1800	0.940	3.770	0.133	12.292	1.229

Table-4.62

Volume fraction= 20% ($\rho=1.079$) Load 15N RPM 200 (V=1.0472 m/sec)

m1 (gm)	m2 (gm)	Δm (gm)	T(Sec)	M	SD x 10³ (m)	WX10⁻⁵ (N/m)	W_vX10⁻¹¹ (m³/m)	W_sX10⁻¹¹ (m³/N.m)
2.670	2.580	0.090	300	0.960	0.314	0.286	26.550	1.770
2.670	2.520	0.150	600	0.950	0.628	0.239	22.125	1.475
2.670	2.470	0.200	900	0.940	0.942	0.212	19.667	1.311
2.670	2.440	0.230	1200	0.940	1.257	0.183	16.963	1.131
2.670	2.420	0.250	1500	0.930	1.571	0.159	14.750	0.983
2.670	2.400	0.270	1800	0.920	1.885	0.143	13.275	0.885

Table-4.63

Volume fraction= 20% ($\rho=1.079$) Load 15N RPM 300 (V=1.5708 m/sec)

m1 (gm)	m2 (gm)	Δm (gm)	T(Sec)	M	SD x 10³ (m)	WX10⁻⁵ (N/m)	W_vX10⁻¹¹ (m³/m)	W_sX10⁻¹¹ (m³/N.m)
2.160	1.990	0.170	300	0.970	0.471	0.361	33.434	2.229
2.160	1.900	0.260	600	0.960	0.942	0.276	25.567	1.704
2.160	1.850	0.310	900	0.950	1.414	0.219	20.322	1.355
2.160	1.800	0.360	1200	0.950	1.885	0.191	17.700	1.180
2.160	1.760	0.400	1500	0.940	2.356	0.170	15.734	1.049
2.160	1.730	0.430	1800	0.930	2.827	0.152	14.095	0.940

Table-4.64

Volume fraction= 20% ($\rho=1.079$) Load 15N RPM 400 (V=2.0944 m/sec)

m1 (gm)	m2 (gm)	Δm (gm)	T(Sec)	M	SD x 10³ (m)	WX10⁻⁵ (N/m)	W_vX10⁻¹¹ (m³/m)	W_sX10⁻¹¹ (m³/N.m)
1.890	1.600	0.290	300	0.980	0.628	0.462	42.776	2.852
1.890	1.500	0.390	600	0.960	1.257	0.310	28.763	1.918
1.890	1.420	0.470	900	0.950	1.885	0.249	23.109	1.541
1.890	1.370	0.520	1200	0.940	2.513	0.207	19.175	1.278
1.890	1.330	0.560	1500	0.930	3.142	0.178	16.520	1.101
1.890	1.300	0.590	1800	0.930	3.770	0.157	14.504	0.967

Table-4.65

Acetone treated rice husk composite

Volume fraction= 10% ($\rho=1.114$) Load 5N RPM 200 (V=1.0472 m/sec)

m1 (gm)	m2 (gm)	Δm (gm)	T(Sec)	M	SD x 10³ (m)	WX10⁻⁵ (N/m)	W_vX10⁻¹¹ (m³/m)	W_sX10⁻¹¹ (m³/N.m)
2.880	2.830	0.050	300	0.960	0.314	0.159	14.291	2.858
2.880	2.810	0.070	600	0.950	0.628	0.111	10.003	2.001
2.880	2.800	0.080	900	0.950	0.942	0.085	7.622	1.524
2.880	2.790	0.090	1200	0.940	1.257	0.072	6.431	1.286
2.880	2.780	0.100	1500	0.930	1.571	0.064	5.716	1.143
2.880	2.780	0.100	1800	0.920	1.885	0.053	4.764	0.953

Table-4.66

Acetone treated rice husk composite

Volume fraction= 10% ($\rho=1.114$) Load 5N RPM 300 (V=1.5708 m/sec)

m1 (gm)	m2 (gm)	Δm (gm)	T(Sec)	M	SD x 10³ (m)	WX10⁻⁵ (N/m)	W_vX10⁻¹¹ (m³/m)	W_sX10⁻¹¹ (m³/N.m)
3.190	3.120	0.070	300	0.970	0.471	0.149	13.338	2.668
3.190	3.090	0.100	600	0.960	0.942	0.106	9.527	1.905
3.190	3.070	0.120	900	0.960	1.414	0.085	7.622	1.524
3.190	3.050	0.140	1200	0.950	1.885	0.074	6.669	1.334
3.190	3.040	0.150	1500	0.940	2.356	0.064	5.716	1.143
3.190	3.030	0.160	1800	0.940	2.827	0.057	5.081	1.016

Table-4.67

Acetone treated rice husk composite

Volume fraction= 10% ($\rho=1.114$) Load 5N RPM 400 (V=2.0944 m/sec)

m1 (gm)	m2 (gm)	Δm (gm)	T(Sec)	μ	SD x 10³ (m)	WX10⁻⁵ (N/m)	W_vX10⁻¹¹ (m³/m)	W_sX10⁻¹¹ (m³/N.m)
3.100	2.970	0.130	300	0.990	0.628	2.028	18.578	3.716
3.100	2.930	0.170	600	0.970	1.257	1.326	12.147	2.429
3.100	2.900	0.200	900	0.960	1.885	1.040	9.527	1.905
3.100	2.870	0.230	1200	0.960	2.513	0.897	8.217	1.643
3.100	2.850	0.250	1500	0.950	3.142	0.780	7.145	1.429
3.100	2.830	0.270	1800	0.940	3.770	0.702	6.431	1.286

Table-4.68

Acetone treated rice husk composite

Volume fraction= 10% ($\rho=1.114$) Load 7.5N RPM 200 (V=1.0472 m/sec)

m1 (gm)	m2 (gm)	Δm (gm)	T(Sec)	μ	$SD \times 10^3$ (m)	$WX10^{-5}$ (N/m)	W_vX10^{-11} (m³/m)	W_sX10^{-11} (m³/N.m)
3.470	3.420	0.050	300	0.950	0.314	0.160	14.361	1.915
3.470	3.399	0.071	600	0.950	0.628	0.113	10.103	1.347
3.470	3.379	0.091	900	0.940	0.942	0.096	8.644	1.153
3.470	3.369	0.101	1200	0.940	1.257	0.080	7.225	0.963
3.470	3.358	0.112	1500	0.930	1.571	0.071	6.391	0.852
3.470	3.358	0.112	1800	0.930	1.885	0.059	5.312	0.708

Table-4.69

Acetone treated rice husk composite

Volume fraction= 10% ($\rho=1.114$) Load 7.5N RPM 300 (V=1.5708 m/sec)

m1 (gm)	m2 (gm)	Δm (gm)	T(Sec)	μ	$SD \times 10^3$ (m)	$WX10^{-5}$ (N/m)	W_vX10^{-11} (m³/m)	W_sX10^{-11} (m³/N.m)
1.320	1.230	0.090	300	0.960	0.471	0.191	17.149	2.286
1.320	1.190	0.130	600	0.950	0.942	0.138	12.385	1.651
1.320	1.170	0.150	900	0.940	1.414	0.106	9.527	1.270
1.320	1.150	0.170	1200	0.940	1.885	0.090	8.098	1.080
1.320	1.140	0.180	1500	0.930	2.356	0.076	6.859	0.915
1.320	1.130	0.190	1800	0.920	2.827	0.067	6.034	0.805

Table-4.70

Acetone treated rice husk composite

Volume fraction= 10% ($\rho=1.114$) Load 7.5N RPM 400 (V=2.0944 m/sec)

m1 (gm)	m2 (gm)	Δm (gm)	T(Sec)	M	SD x 10³ (m)	WX10⁻⁵ (N/m)	W_vX10⁻¹¹ (m³/m)	W_sX10⁻¹¹ (m³/N.m)
2.860	2.710	0.150	300	0.980	0.628	0.239	21.436	2.858
2.860	2.640	0.220	600	0.980	1.257	0.175	15.720	2.096
2.860	2.600	0.260	900	0.960	1.885	0.138	12.385	1.651
2.860	2.560	0.300	1200	0.950	2.513	0.119	10.718	1.429
2.860	2.530	0.330	1500	0.950	3.142	0.105	9.432	1.258
2.860	2.500	0.360	1800	0.940	3.770	0.095	8.826	1.177

Table-4.71

Acetone treated rice husk composite

Volume fraction= 10% ($\rho=1.114$) Load 10N RPM 200 (V=1.0472 m/sec)

m1 (gm)	m2 (gm)	Δm (gm)	T(Sec)	M	SD x 10³ (m)	WX10⁻⁵ (N/m)	W_vX10⁻¹¹ (m³/m)	W_sX10⁻¹¹ (m³/N.m)
3.170	3.120	0.050	300	0.960	0.314	0.159	14.291	1.429
3.170	3.090	0.080	600	0.950	0.628	0.127	11.432	1.143
3.170	3.070	0.100	900	0.940	0.942	0.106	9.527	0.953
3.170	3.060	0.110	1200	0.920	1.257	0.088	7.860	0.786
3.170	3.050	0.120	1500	0.920	1.571	0.076	6.859	0.686
3.170	3.040	0.130	1800	0.910	1.885	0.069	6.193	0.619

Table-4.72

Acetone treated rice husk composite

Volume fraction= 10% ($\rho=1.114$) Load 10N RPM 300 (V=1.5708 m/sec)

m1 (gm)	m2 (gm)	Δm (gm)	T(Sec)	M	SD x 10³ (m)	WX10⁻⁵ (N/m)	W_vX10⁻¹¹ (m³/m)	W_sX10⁻¹¹ (m³/N.m)
3.470	3.370	0.100	300	0.960	0.471	0.212	19.054	1.905
3.470	3.340	0.130	600	0.950	0.942	0.138	12.385	1.239
3.470	3.320	0.150	900	0.940	1.414	0.106	9.527	0.953
3.470	3.290	0.180	1200	0.940	1.885	0.095	8.574	0.857
3.470	3.270	0.200	1500	0.920	2.356	0.085	7.622	0.762
3.470	3.250	0.220	1800	0.920	2.827	0.078	6.987	0.699

Table-4.73

Acetone treated rice husk composite

Volume fraction= 10% ($\rho=1.114$) Load 10N RPM 400 (V=2.0944 m/sec)

m1 (gm)	m2 (gm)	Δm (gm)	T(Sec)	M	SD x 10³ (m)	WX10⁻⁵ (N/m)	W_vX10⁻¹¹ (m³/m)	W_sX10⁻¹¹ (m³/N.m)
2.490	2.340	0.150	300	0.960	0.628	0.239	21.436	2.144
2.490	2.280	0.210	600	0.950	1.257	0.167	15.005	1.501
2.490	2.240	0.250	900	0.940	1.885	0.133	11.909	1.191
2.490	2.200	0.290	1200	0.940	2.513	0.115	10.361	1.036
2.490	2.170	0.320	1500	0.950	3.142	0.102	9.146	0.915
2.490	2.150	0.340	1800	0.940	3.770	0.090	8.098	0.810

Table-4.74

Acetone treated rice husk composite

Volume fraction= 10% ($\rho=1.114$) Load 15N RPM 200 (V=1.0472 m/sec)

m1 (gm)	m2 (gm)	Δm (gm)	T(Sec)	M	SD x 10³ (m)	WX10⁻⁵ (N/m)	W_vX10⁻¹¹ (m³/m)	W_sX10⁻¹¹ (m³/N.m)
3.330	3.260	0.070	300	0.950	0.314	0.223	20.007	1.334
3.330	3.230	0.100	600	0.940	0.628	0.159	14.291	0.953
3.330	3.210	0.120	900	0.930	0.942	0.127	11.432	0.762
3.330	3.190	0.140	1200	0.930	1.257	0.111	10.003	0.667
3.330	3.180	0.150	1500	0.920	1.571	0.095	8.574	0.572
3.330	3.170	0.160	1800	0.900	1.885	0.085	7.622	0.508

Table-4.75

Acetone treated rice husk composite

Volume fraction= 10% ($\rho=1.114$) Load 15N RPM 300 (V=1.5708 m/sec)

m1 (gm)	m2 (gm)	Δm (gm)	T(Sec)	M	SD x 10³ (m)	WX10⁻⁵ (N/m)	W_vX10⁻¹¹ (m³/m)	W_sX10⁻¹¹ (m³/N.m)
3.060	2.910	0.150	300	0.950	0.471	0.318	28.581	1.905
3.060	2.860	0.200	600	0.940	0.942	0.212	19.054	1.270
3.060	2.820	0.240	900	0.950	1.414	0.170	15.243	1.016
3.060	2.790	0.270	1200	0.930	1.885	0.143	12.862	0.857
3.060	2.760	0.300	1500	0.930	2.356	0.127	11.432	0.762
3.060	2.740	0.320	1800	0.910	2.827	0.113	10.162	0.677

Table-4.76

Acetone treated rice husk composite

Volume fraction= 10% ($\rho=1.114$) Load 15N RPM 400 (V=2.0944 m/sec)

m1 (gm)	m2 (gm)	Δm (gm)	T(Sec)	M	SD x 10³ (m)	WX10⁻⁵ (N/m)	W_vX10⁻¹¹ (m³/m)	W_sX10⁻¹¹ (m³/N.m)
3.210	3.070	0.140	300	0.960	0.628	0.223	20.007	1.334
3.210	3.000	0.210	600	0.950	1.257	0.167	15.005	1.000
3.210	2.950	0.260	900	0.940	1.885	0.138	12.385	0.826
3.210	2.910	0.300	1200	0.930	2.513	0.119	10.718	0.715
3.210	2.870	0.340	1500	0.910	3.142	0.108	9.718	0.648
3.210	2.840	0.370	1800	0.900	3.770	0.098	8.813	0.588

Table-4.77

Alkali treated rice husk composite

Volume fraction= 10% ($\rho=1.114$) Load 5N RPM 200 (V=1.0472 m/sec)

m1 (gm)	m2 (gm)	Δm (gm)	T(Sec)	M	SD x 10³ (m)	WX10⁻⁵ (N/m)	W_vX10⁻¹¹ (m³/m)	W_sX10⁻¹¹ (m³/N.m)
3.210	3.170	0.040	300	0.960	0.314	0.127	11.432	2.286
3.210	3.140	0.070	600	0.950	0.628	0.111	10.003	2.001
3.210	3.120	0.090	900	0.950	0.942	0.095	8.574	1.715
3.210	3.110	0.100	1200	0.940	1.257	0.080	7.145	1.429
3.210	3.110	0.100	1500	0.930	1.571	0.064	5.716	1.143
3.210	3.120	0.090	1800	0.920	1.885	0.048	4.287	0.857

Table-4.78

Alkali treated rice husk composite

Volume fraction= 10% ($\rho=1.114$) Load 5N RPM 300 (V=1.5708 m/sec)

m1 (gm)	m2 (gm)	Δm (gm)	T(Sec)	M	SD x 10³ (m)	WX10⁻⁵ (N/m)	W_vX10⁻¹¹ (m³/m)	W_sX10⁻¹¹ (m³/N.m)
3.050	2.990	0.060	300	0.970	0.471	0.127	11.432	2.286
3.050	2.960	0.090	600	0.960	0.942	0.095	8.574	1.715
3.050	2.940	0.110	900	0.960	1.414	0.078	6.987	1.397
3.050	2.920	0.130	1200	0.950	1.885	0.069	6.193	1.239
3.050	2.910	0.140	1500	0.940	2.356	0.059	5.335	1.067
3.050	2.900	0.150	1800	0.940	2.827	0.053	4.764	0.953

Table-4.79

Alkali treated rice husk composite

Volume fraction= 10% ($\rho=1.114$) Load 5N RPM 400 (V=2.0944 m/sec)

m1 (gm)	m2 (gm)	Δm (gm)	T(Sec)	M	SD x 10³ (m)	WX10⁻⁵ (N/m)	W_vX10⁻¹¹ (m³/m)	W_sX10⁻¹¹ (m³/N.m)
1.970	1.860	0.110	300	0.990	0.628	1.716	15.720	3.144
1.970	1.800	0.170	600	0.970	1.257	1.326	12.147	2.429
1.970	1.760	0.210	900	0.960	1.885	1.092	10.003	2.001
1.970	1.730	0.240	1200	0.960	2.513	0.936	8.574	1.715
1.970	1.710	0.260	1500	0.950	3.142	0.811	7.431	1.486
1.970	1.690	0.280	1800	0.940	3.770	0.728	6.669	1.334

Table-4.80

Alkali treated rice husk composite

Volume fraction= 10% ($\rho=1.114$) Load 7.5N RPM 200 (V=1.0472 m/sec)

m1 (gm)	m2 (gm)	Δm (gm)	T(Sec)	M	SD x 10³ (m)	WX10⁻⁵ (N/m)	W_vX10⁻¹¹ (m³/m)	W_sX10⁻¹¹ (m³/N.m)
2.980	2.930	0.050	300	0.950	0.314	0.159	14.291	1.905
2.980	2.910	0.070	600	0.950	0.628	0.111	10.003	1.334
2.980	2.890	0.090	900	0.940	0.942	0.095	8.574	1.143
2.980	2.880	0.100	1200	0.940	1.257	0.080	7.145	0.953
2.980	2.870	0.110	1500	0.930	1.571	0.070	6.288	0.838
2.980	2.870	0.110	1800	0.930	1.885	0.058	5.24	0.699

Table-4.81

Alkali treated rice husk composite

Volume fraction= 10% ($\rho=1.114$) Load 7.5N RPM 300 (V=1.5708 m/sec)

m1 (gm)	m2 (gm)	Δm (gm)	T(Sec)	M	SD x 10³ (m)	WX10⁻⁵ (N/m)	W_vX10⁻¹¹ (m³/m)	W_sX10⁻¹¹ (m³/N.m)
2.190	2.110	0.080	300	0.960	0.471	0.170	15.243	2.032
2.190	2.060	0.130	600	0.950	0.942	0.138	12.385	1.651
2.190	2.030	0.160	900	0.940	1.414	0.113	10.162	1.355
2.190	2.000	0.190	1200	0.940	1.885	0.101	9.051	1.207
2.190	1.980	0.210	1500	0.930	2.356	0.089	8.003	1.067
2.190	1.970	0.220	1800	0.920	2.827	0.078	6.987	0.932

Table-4.82

Alkali treated rice husk composite

Volume fraction= 10% ($\rho=1.114$) Load 7.5N RPM 400 (V=2.0944 m/sec)

m1 (gm)	m2 (gm)	Δm (gm)	T(Sec)	M	SD x 10³ (m)	WX10⁻⁵ (N/m)	W_vX10⁻¹¹ (m³/m)	W_sX10⁻¹¹ (m³/N.m)
2.780	2.610	0.170	300	0.980	0.628	0.271	24.294	3.239
2.780	2.520	0.260	600	0.980	1.257	0.207	18.578	2.477
2.780	2.470	0.310	900	0.960	1.885	0.164	14.767	1.969
2.780	2.430	0.350	1200	0.950	2.513	0.139	12.504	1.667
2.780	2.410	0.370	1500	0.950	3.142	0.118	10.575	1.410
2.780	2.390	0.390	1800	0.940	3.770	0.103	9.561	1.275

Table-4.83

Alkali treated rice husk composite

Volume fraction= 10% ($\rho=1.114$) Load 10N RPM 200 (V=1.0472 m/sec)

m1 (gm)	m2 (gm)	Δm (gm)	T(Sec)	M	SD x 10³ (m)	WX10⁻⁵ (N/m)	W_vX10⁻¹¹ (m³/m)	W_sX10⁻¹¹ (m³/N.m)
3.330	3.280	0.050	300	0.960	0.314	0.159	14.291	1.429
3.330	3.260	0.070	600	0.950	0.628	0.111	10.003	1.000
3.330	3.230	0.100	900	0.940	0.942	0.106	9.527	0.953
3.330	3.210	0.120	1200	0.920	1.257	0.095	8.574	0.857
3.330	3.200	0.130	1500	0.920	1.571	0.083	7.431	0.743
3.330	3.120	0.210	1800	0.910	1.885	0.111	10.003	1.000

Table-4.84

Alkali treated rice husk composite

Volume fraction= 10% ($\rho=1.114$) Load 10N RPM 300 (V=1.5708 m/sec)

m1 (gm)	m2 (gm)	Δm (gm)	T(Sec)	M	SD x 10³ (m)	WX10⁻⁵ (N/m)	W_vX10⁻¹¹ (m³/m)	W_sX10⁻¹¹ (m³/N.m)
2.170	2.070	0.100	300	0.960	0.471	0.212	19.054	1.905
2.170	2.040	0.130	600	0.950	0.942	0.138	12.385	1.239
2.170	2.010	0.160	900	0.940	1.414	0.113	10.162	1.016
2.170	1.980	0.190	1200	0.940	1.885	0.101	9.051	0.905
2.170	1.960	0.210	1500	0.920	2.356	0.089	8.003	0.800
2.170	1.940	0.230	1800	0.920	2.827	0.081	7.304	0.730

Table-4.85

Alkali treated rice husk composite

Volume fraction= 10% ($\rho=1.114$) Load 10N RPM 400 (V=2.0944 m/sec)

m1 (gm)	m2 (gm)	Δm (gm)	T(Sec)	M	SD x 10³ (m)	WX10⁻⁵ (N/m)	W_vX10⁻¹¹ (m³/m)	W_sX10⁻¹¹ (m³/N.m)
2.170	2.000	0.170	300	0.960	0.628	0.271	24.294	2.429
2.170	1.910	0.260	600	0.950	1.257	0.207	18.578	1.858
2.170	1.840	0.330	900	0.940	1.885	0.175	15.720	1.572
2.170	1.810	0.360	1200	0.940	2.513	0.143	12.862	1.286
2.170	1.780	0.390	1500	0.950	3.142	0.124	11.147	1.115
2.170	1.750	0.420	1800	0.940	3.770	0.111	10.003	1.000

Table-4.86

Alkali treated rice husk composite

Volume fraction= 10% ($\rho=1.114$) Load 15N RPM 200 (V=1.0472 m/sec)

m1 (gm)	m2 (gm)	Δm (gm)	T(Sec)	M	SD x 10³ (m)	WX10⁻⁵ (N/m)	W_vX10⁻¹¹ (m³/m)	W_sX10⁻¹¹ (m³/N.m)
3.660	3.600	0.060	300	0.950	0.314	0.191	17.149	1.143
3.660	3.570	0.090	600	0.940	0.628	0.143	12.862	0.857
3.660	3.550	0.110	900	0.930	0.942	0.117	10.480	0.699
3.660	3.530	0.130	1200	0.930	1.257	0.103	9.289	0.619
3.660	3.520	0.140	1500	0.920	1.571	0.089	8.003	0.534
3.660	3.510	0.150	1800	0.900	1.885	0.080	7.145	0.476

Table-4.87

Alkali treated rice husk composite

Volume fraction= 10% ($\rho=1.114$) Load 15N RPM 300 (V=1.5708 m/sec)

m1 (gm)	m2 (gm)	Δm (gm)	T(Sec)	M	SD x 10³ (m)	WX10⁻⁵ (N/m)	W_vX10⁻¹¹ (m³/m)	W_sX10⁻¹¹ (m³/N.m)
3.010	2.870	0.140	300	0.950	0.471	0.297	26.676	1.778
3.010	2.820	0.190	600	0.940	0.942	0.202	18.101	1.207
3.010	2.780	0.230	900	0.950	1.414	0.163	14.608	0.974
3.010	2.750	0.260	1200	0.930	1.885	0.138	12.385	0.826
3.010	2.730	0.280	1500	0.930	2.356	0.119	10.670	0.711
3.010	2.710	0.300	1800	0.910	2.827	0.106	9.527	0.635

Table-4.88

Alkali treated rice husk composite

Volume fraction= 10% ($\rho=1.114$) Load 15N RPM 400 (V=2.0944 m/sec)

m1 (gm)	m2 (gm)	Δm (gm)	T(Sec)	M	$SD \times 10^3$ (m)	$WX10^{-5}$ (N/m)	$W_v X10^{-11}$ (m³/m)	$W_s X10^{-11}$ (m³/N.m)
3.410	3.270	0.140	300	0.960	0.628	0.223	20.007	1.334
3.410	3.190	0.220	600	0.950	1.257	0.175	15.720	1.048
3.410	3.130	0.280	900	0.940	1.885	0.149	13.338	0.889
3.410	3.090	0.320	1200	0.930	2.513	0.127	11.432	0.762
3.410	3.050	0.360	1500	0.910	3.142	0.115	10.289	0.686
3.410	3.020	0.390	1800	0.900	3.770	0.103	9.289	0.619

Table-4.89

Benzoyl Chloride treated rice husk composite

Volume fraction= 10% ($\rho=1.082$) Load 5N RPM 200 (V=1.0472 m/sec)

m1 (gm)	m2 (gm)	Δm (gm)	T(Sec)	M	$SD \times 10^3$ (m)	$WX10^{-5}$ (N/m)	$W_v X10^{-11}$ (m³/m)	$W_s X10^{-11}$ (m³/N.m)
3.120	3.080	0.040	300	0.960	0.314	0.127	11.767	2.353
3.120	3.070	0.050	600	0.950	0.628	0.080	7.355	1.471
3.120	3.060	0.060	900	0.940	0.942	0.064	5.884	1.177
3.120	3.050	0.070	1200	0.940	1.257	0.056	5.148	1.030
3.120	3.050	0.070	1500	0.930	1.571	0.045	4.119	0.824
3.120	3.040	0.080	1800	0.920	1.885	0.042	3.922	0.784

Table-4.90

Benzoyl Chloride treated rice husk composite

Volume fraction= 10% ($\rho=1.082$) Load 5N RPM 300 (V=1.5708 m/sec)

m1 (gm)	m2 (gm)	Δm (gm)	T(Sec)	M	$SD \times 10^3$ (m)	$WX10^{-5}$ (N/m)	$W_v \times 10^{-11}$ (m³/m)	$W_s \times 10^{-11}$ (m³/N.m)
2.400	2.330	0.070	300	0.980	0.471	0.149	13.729	2.746
2.400	2.310	0.090	600	0.970	0.942	0.095	8.826	1.765
2.400	2.290	0.110	900	0.950	1.414	0.078	7.191	1.438
2.400	2.270	0.130	1200	0.940	1.885	0.069	6.374	1.275
2.400	2.250	0.150	1500	0.930	2.356	0.064	5.884	1.177
2.400	2.240	0.160	1800	0.930	2.827	0.057	5.230	1.046

Table-4.91

Benzoyl Chloride treated rice husk composite

Volume fraction= 10% ($\rho=1.082$) Load 5N RPM 400 (V=2.0944 m/sec)

m1 (gm)	m2 (gm)	Δm (gm)	T(Sec)	M	$SD \times 10^3$ (m)	$WX10^{-5}$ (N/m)	$W_v \times 10^{-11}$ (m³/m)	$W_s \times 10^{-11}$ (m³/N.m)
3.040	2.930	0.110	300	0.990	0.628	1.716	16.180	3.236
3.040	2.880	0.160	600	0.980	1.257	1.248	11.767	2.353
3.040	2.840	0.200	900	0.960	1.885	1.040	9.806	1.961
3.040	2.810	0.230	1200	0.950	2.513	0.897	8.458	1.692
3.040	2.790	0.250	1500	0.950	3.142	0.780	7.355	1.471
3.040	2.770	0.270	1800	0.950	3.770	0.702	6.619	1.324

Table-4.92

Benzoyl Chloride treated rice husk composite

Volume fraction= 10% ($\rho=1.082$) Load 7.5N RPM 200 (V=1.0472 m/sec)

m1 (gm)	m2 (gm)	Δm (gm)	T(Sec)	M	$SD \times 10^3$ (m)	$WX10^{-5}$ (N/m)	$W_V X10^{-11}$ (m³/m)	$W_S X10^{-11}$ (m³/N.m)
3.210	3.170	0.040	300	0.950	0.314	0.127	11.767	1.569
3.210	3.150	0.060	600	0.950	0.628	0.095	8.826	1.177
3.210	3.140	0.070	900	0.940	0.942	0.074	6.864	0.915
3.210	3.130	0.080	1200	0.940	1.257	0.064	5.884	0.784
3.210	3.120	0.090	1500	0.930	1.571	0.057	5.295	0.706
3.210	3.110	0.100	1800	0.920	1.885	0.053	4.903	0.654

Table-4.93

Benzoyl Chloride treated rice husk composite

Volume fraction= 10% ($\rho=1.082$) Load 7.5N RPM 300 (V=1.5708 m/sec)

m1 (gm)	m2 (gm)	Δm (gm)	T(Sec)	M	$SD \times 10^3$ (m)	$WX10^{-5}$ (N/m)	$W_V X10^{-11}$ (m³/m)	$W_S X10^{-11}$ (m³/N.m)
3.110	3.030	0.080	300	0.960	0.471	0.170	15.690	2.092
3.110	3.000	0.110	600	0.960	0.942	0.117	10.787	1.438
3.110	2.970	0.140	900	0.950	1.414	0.099	9.152	1.220
3.110	2.950	0.160	1200	0.940	1.885	0.085	7.845	1.046
3.110	2.930	0.180	1500	0.910	2.356	0.076	7.060	0.941
3.110	2.920	0.190	1800	0.900	2.827	0.067	6.211	0.828

Table-4.94

Benzoyl Chloride treated rice husk composite

Volume fraction= 10% ($\rho=1.082$) Load 7.5N RPM 400 (V=2.0944 m/sec)

m1 (gm)	m2 (gm)	Δm (gm)	T(Sec)	M	SD x 10³ (m)	WX10⁻⁵ (N/m)	W_vX10⁻¹¹ (m³/m)	W_sX10⁻¹¹ (m³/N.m)
3.510	3.350	0.160	300	0.980	0.628	0.255	23.535	3.138
3.510	3.270	0.240	600	0.980	1.257	0.191	17.651	2.353
3.510	3.210	0.300	900	0.960	1.885	0.159	14.709	1.961
3.510	3.170	0.340	1200	0.950	2.513	0.135	12.503	1.667
3.510	3.140	0.370	1500	0.940	3.142	0.118	10.885	1.451
3.510	3.120	0.390	1800	0.920	3.770	0.103	9.561	1.275

Table-4.95

Benzoyl Chloride treated rice husk composite

Volume fraction= 10% ($\rho=1.082$) Load 10N RPM 200 (V=1.0472 m/sec)

m1 (gm)	m2 (gm)	Δm (gm)	T(Sec)	M	SD x 10³ (m)	WX10⁻⁵ (N/m)	W_vX10⁻¹¹ (m³/m)	W_sX10⁻¹¹ (m³/N.m)
2.420	2.370	0.050	300	0.950	0.314	0.255	14.709	1.471
2.420	2.360	0.060	600	0.940	0.628	0.191	8.826	0.883
2.420	2.350	0.070	900	0.930	0.942	0.159	6.864	0.686
2.420	2.340	0.080	1200	0.930	1.257	0.135	5.884	0.588
2.420	2.330	0.090	1500	0.910	1.571	0.118	5.295	0.530
2.420	2.330	0.090	1800	0.890	1.885	0.103	4.413	0.441

Table-4.96

Benzoyl Chloride treated rice husk composite

Volume fraction= 10% ($\rho=1.082$) Load 10N RPM 300 (V=1.5708 m/sec)

m1 (gm)	m2 (gm)	Δm (gm)	T(Sec)	M	SD x 10^3 (m)	$WX10^{-5}$ (N/m)	W_VX10^{-11} (m^3/m)	W_SX10^{-11} ($m^3/N.m$)
2.710	2.620	0.090	300	0.960	0.471	0.191	17.651	1.765
2.710	2.590	0.120	600	0.960	0.942	0.127	11.767	1.177
2.710	2.560	0.150	900	0.940	1.414	0.106	9.806	0.981
2.710	2.540	0.170	1200	0.930	1.885	0.090	8.335	0.834
2.710	2.520	0.190	1500	0.910	2.356	0.081	7.453	0.745
2.710	2.490	0.220	1800	0.910	2.827	0.078	7.191	0.719

Table-4.97

Benzoyl Chloride treated rice husk composite

Volume fraction= 10% ($\rho=1.082$) Load 10N RPM 400 (V=2.0944 m/sec)

m1 (gm)	m2 (gm)	Δm (gm)	T(Sec)	M	SD x 10^3 (m)	$WX10^{-5}$ (N/m)	W_VX10^{-11} (m^3/m)	W_SX10^{-11} ($m^3/N.m$)
2.330	2.200	0.130	300	0.970	0.628	0.207	19.122	1.912
2.330	2.140	0.190	600	0.950	1.257	0.151	13.974	1.397
2.330	2.090	0.240	900	0.960	1.885	0.127	11.767	1.177
2.330	2.050	0.280	1200	0.940	2.513	0.111	10.297	1.030
2.330	2.020	0.310	1500	0.930	3.142	0.099	9.120	0.912
2.330	2.000	0.330	1800	0.920	3.770	0.088	8.090	0.809

Table-4.98

Benzoyl Chloride treated rice husk composite

Volume fraction= 10% ($\rho=1.082$) Load 15N RPM 200 (V=1.0472 m/sec)

m1 (gm)	m2 (gm)	Δm (gm)	T(Sec)	M	SD x 10^3 (m)	WX10^{-5} (N/m)	W_vX10^{-11} (m³/m)	W_sX10^{-11} (m³/N.m)
2.080	2.020	0.060	300	0.950	0.314	0.191	17.651	1.177
2.080	2.000	0.080	600	0.950	0.628	0.127	11.767	0.784
2.080	1.980	0.100	900	0.940	0.942	0.106	9.806	0.654
2.080	1.960	0.120	1200	0.910	1.257	0.095	8.826	0.588
2.080	1.950	0.130	1500	0.900	1.571	0.083	7.649	0.510
2.080	1.940	0.140	1800	0.880	1.885	0.074	6.864	0.458

Table-4.99

Benzoyl Chloride treated rice husk composite

Volume fraction= 10% ($\rho=1.082$) Load 15N RPM 300 (V=1.5708 m/sec)

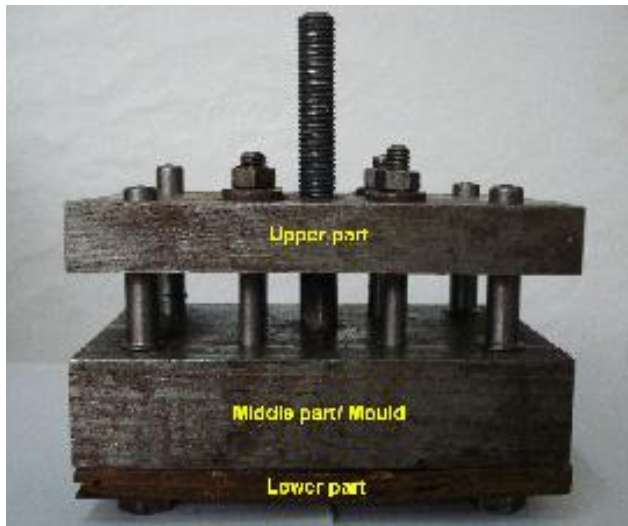
m1 (gm)	m2 (gm)	Δm (gm)	T(Sec)	M	SD x 10^3 (m)	WX10^{-5} (N/m)	W_vX10^{-11} (m³/m)	W_sX10^{-11} (m³/N.m)
3.320	3.180	0.140	300	0.960	0.471	0.297	27.457	1.830
3.320	3.140	0.180	600	0.950	0.942	0.191	17.651	1.177
3.320	3.110	0.210	900	0.940	1.414	0.149	13.729	0.915
3.320	3.080	0.240	1200	0.930	1.885	0.127	11.767	0.784
3.320	3.050	0.270	1500	0.920	2.356	0.115	10.591	0.706
3.320	3.030	0.290	1800	0.910	2.827	0.103	9.479	0.632

Table-4.100

Benzoyl Chloride treated rice husk composite

Volume fraction= 10% ($\rho=1.082$) Load 15N RPM 400 (V=2.0944 m/sec)

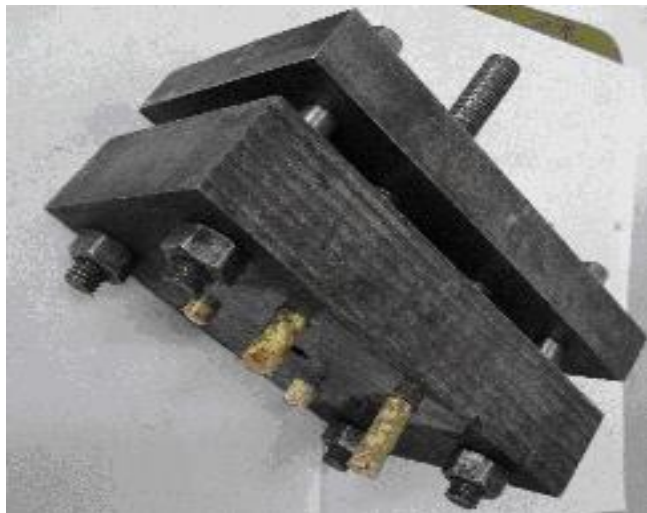
m1 (gm)	m2 (gm)	Δm (gm)	T(Sec)	M	SD x 10^3 (m)	$W \times 10^{-5}$ (N/m)	$W_v \times 10^{-11}$ (m³/m)	$W_s \times 10^{-11}$ (m³/N.m)
2.450	2.320	0.130	300	0.980	0.628	0.207	19.122	1.275
2.450	2.260	0.190	600	0.970	1.257	0.151	13.974	0.932
2.450	2.220	0.230	900	0.950	1.885	0.122	11.277	0.752
2.450	2.180	0.270	1200	0.940	2.513	0.107	9.929	0.662
2.450	2.140	0.310	1500	0.930	3.142	0.099	9.120	0.608
2.450	2.110	0.340	1800	0.910	3.770	0.090	8.335	0.556



(a)



(b)



(c)

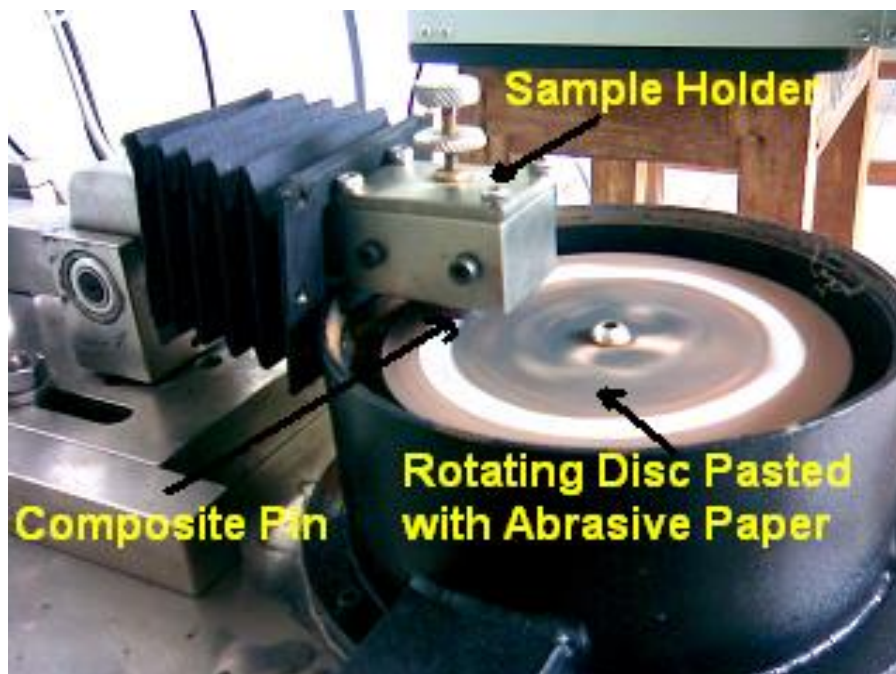


(d)

Figure-4.6. Steel Mould and prepared pin type composite samples; (a) Mould used for preparing samples, (b) Two halves of the mould, (c) Mould with Pin types composite samples, (d) Fabricated Composite Pins



(a)



(b)

Figure-4.7 Experimental set-up; (a) Pin-on-disc type wear testing machine, (b) Composite sample under abrasive wear test

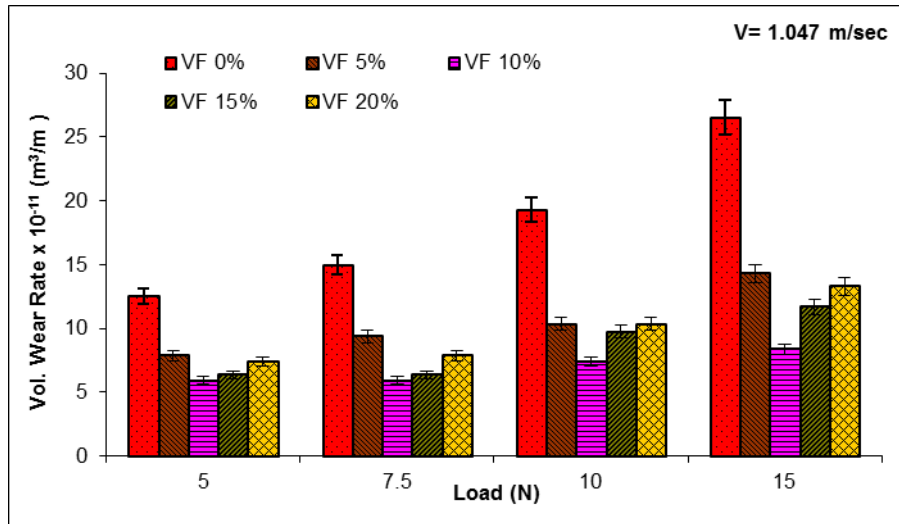


Figure-4.8 Vol. Wear rate (W_v) with Load for Plain RH composite at Sliding Velocity 1.047 m/sec

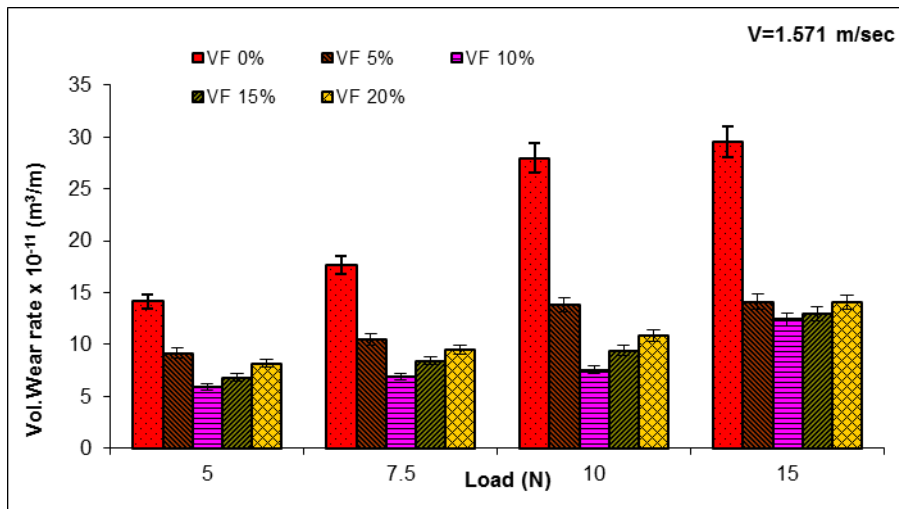


Figure-4.9 Vol. Wear rate (W_v) with Load for Plain RH composite at Sliding Velocity 1.571 m/sec

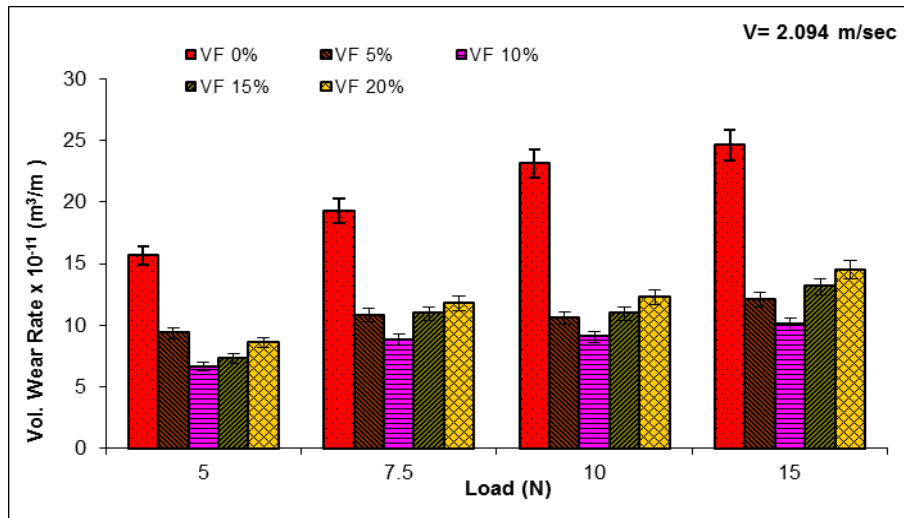


Figure-4.10 Wear rate (W_v) with Load for Plain RH composite at Sliding Velocity 2.094 m/sec

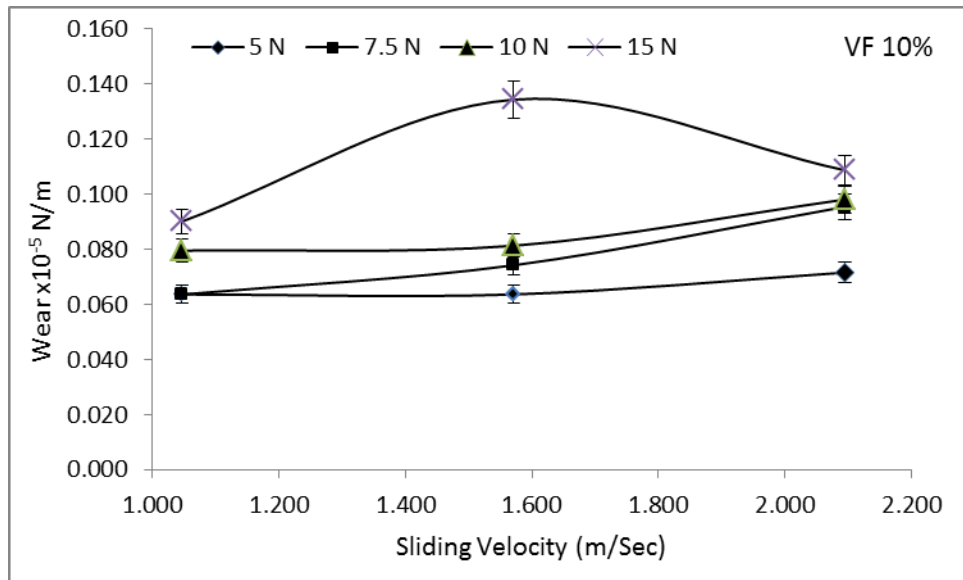


Fig: 4.11 Variation of wear rate as function of sliding velocity for 10 Vol% of rice husk under different loads (5N to 15N)

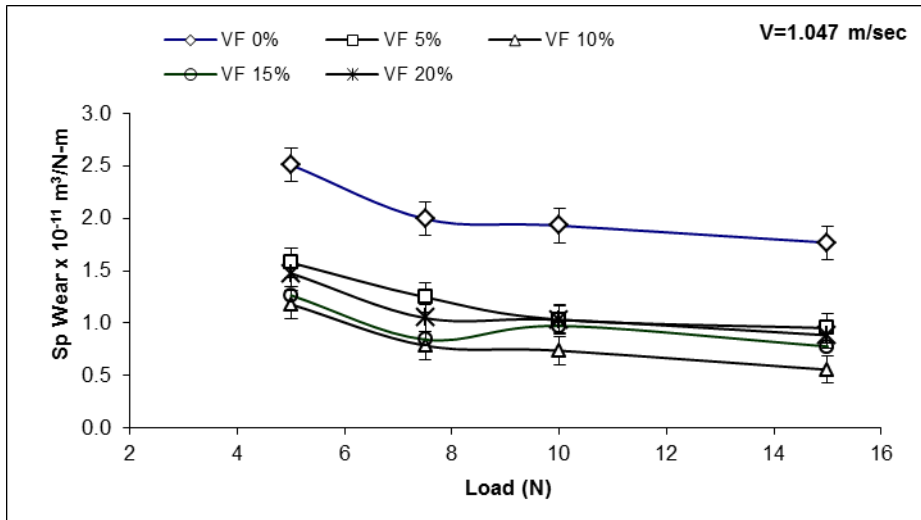


Figure-4.12 Specific Wear rate (W_s) with Load for Plain RH composite at Sliding Velocity 1.571 m/sec

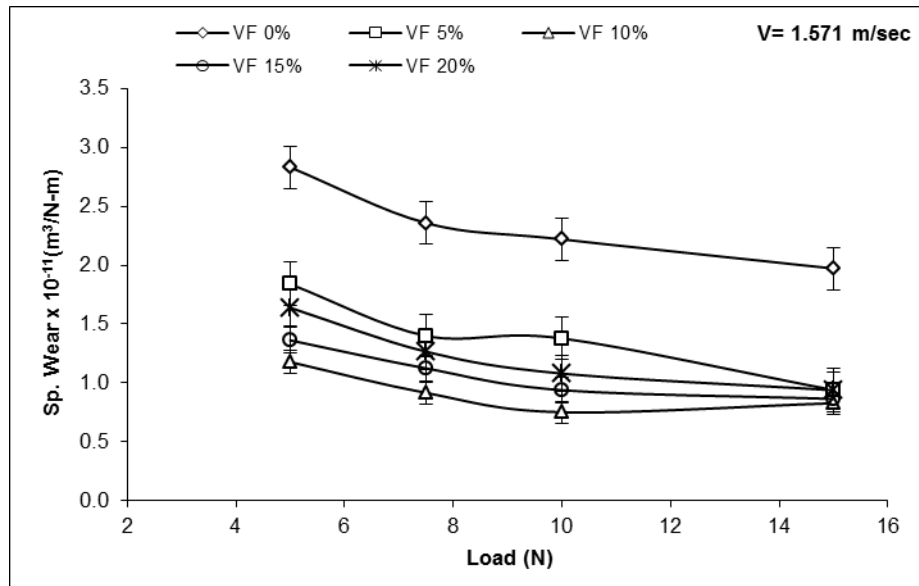


Figure-4.13 Specific Wear rate (W_s) with Load for Plain RH composite at Sliding Velocity 1.571 m/sec

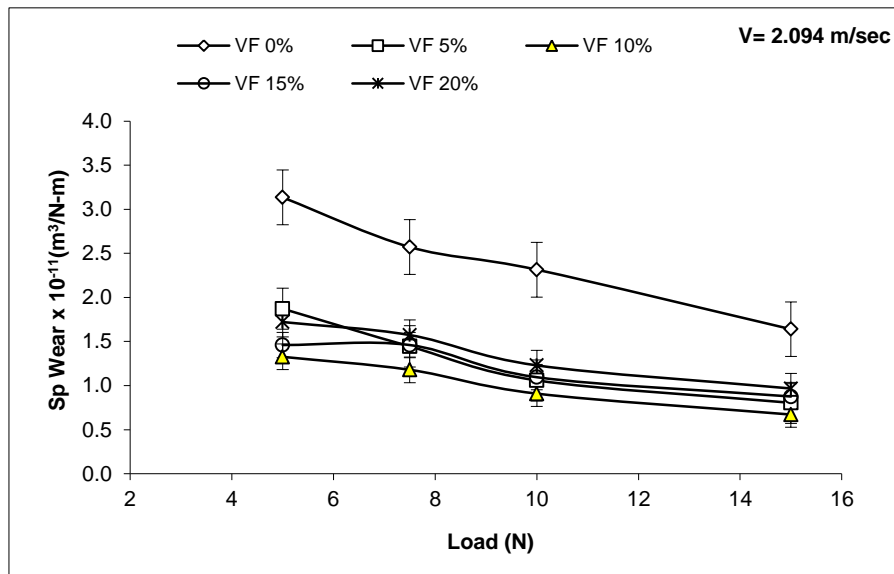


Figure-4.14 Specific Wear rate (W_s) with Load for Plain RH composite at Sliding Velocity 2.094 m/sec

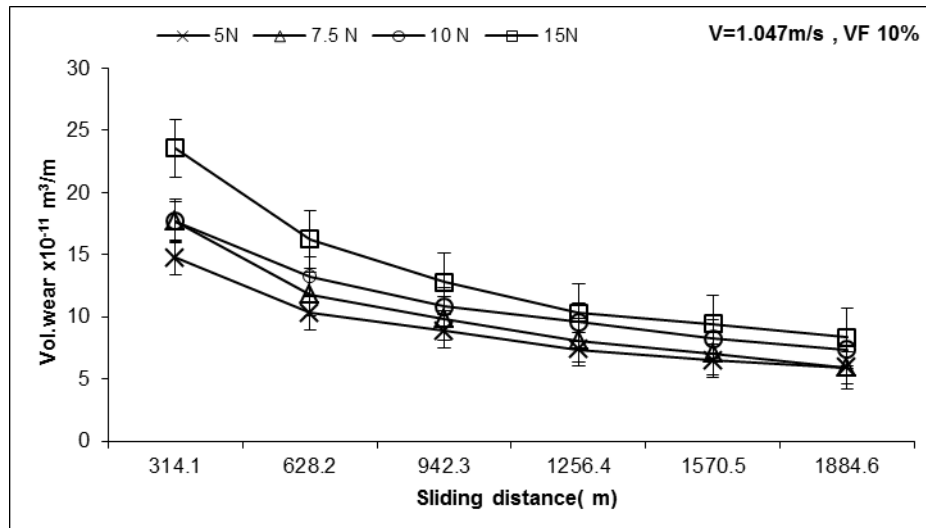


Figure-4.15 Specific Wear rate with Sliding Distance for Plain RH epoxy composite at velocity 1.047 m/sec (200 rpm).

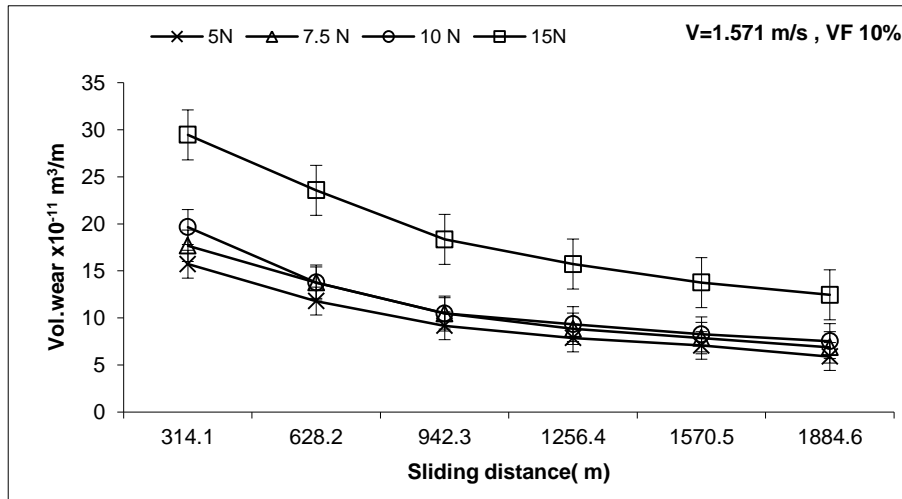


Figure-4.16 Specific Wear rate with Sliding Distance for Plain RH epoxy composite at velocity 1.571 m/sec (300 rpm).

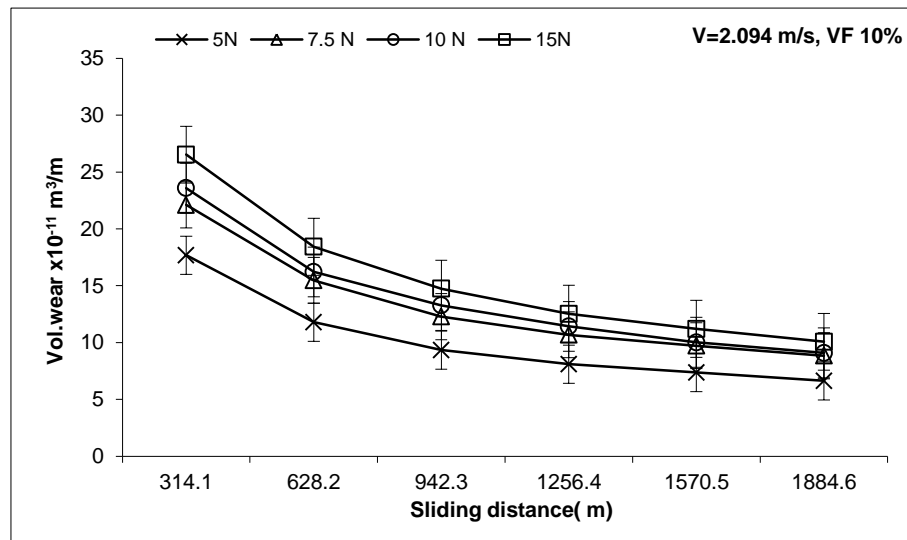


Figure-4.17 Specific Wear rate with Sliding Distance for Plain RH epoxy composite at velocity 2.094 m/sec (400 rpm).

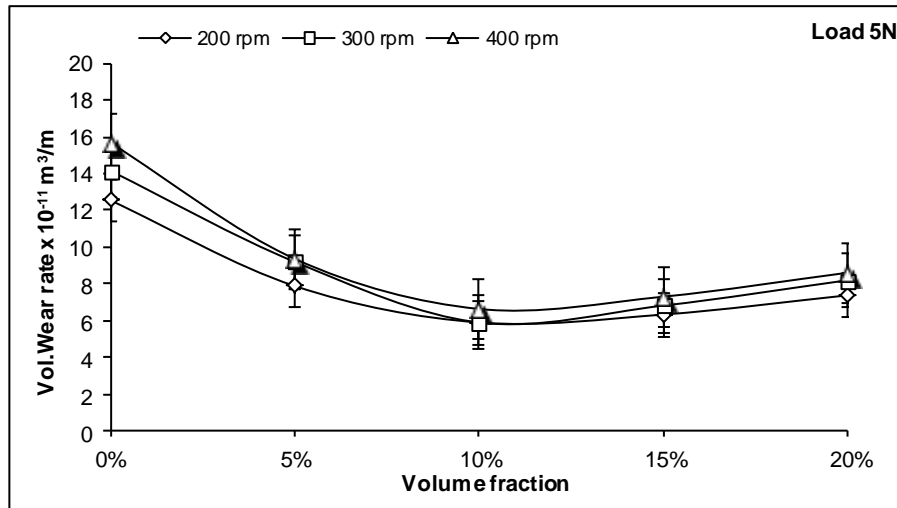


Figure-4.18 Volumetric Wear rate with Volume Fraction for Plain RH composite at 5 N.

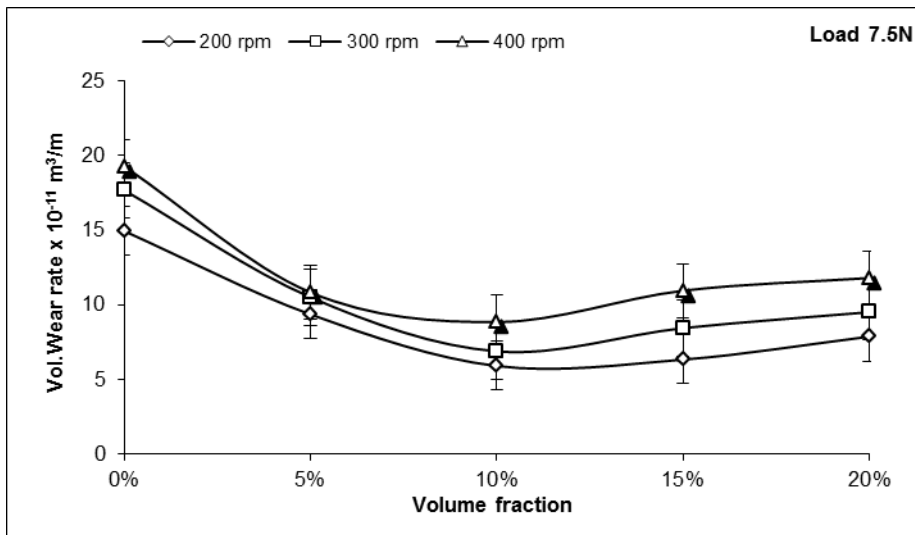


Figure-4.19 Volumetric Wear rate with Volume Fraction for Plain RH composite at 7.5 N.

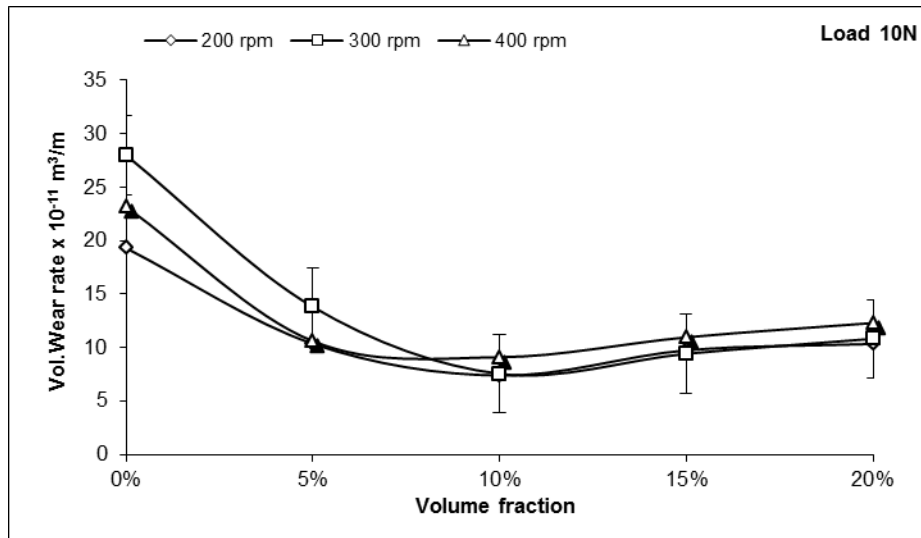


Figure-4.20 Volumetric Wear rate with Volume Fraction for Plain RH composite at 10 N.

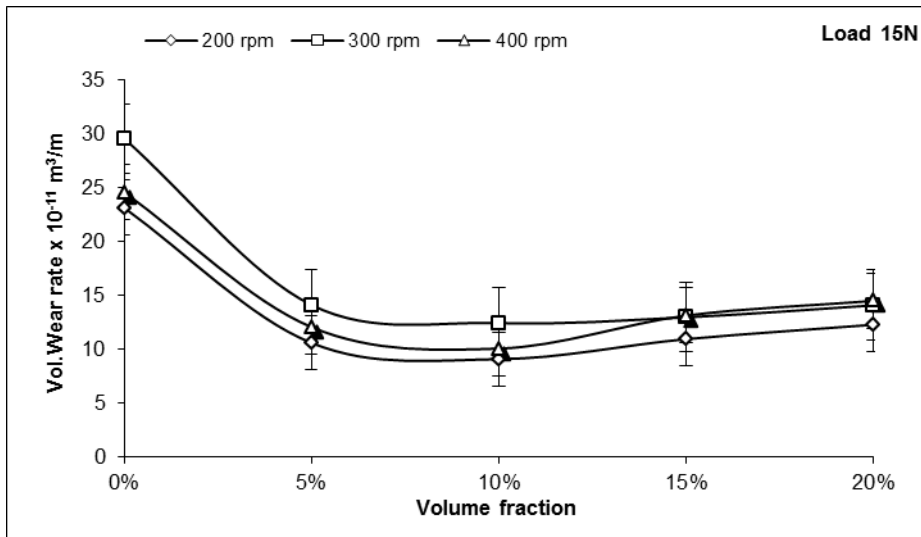


Figure-4.21 Volumetric Wear rate with Volume Fraction for Plain RH composite at 15 N.

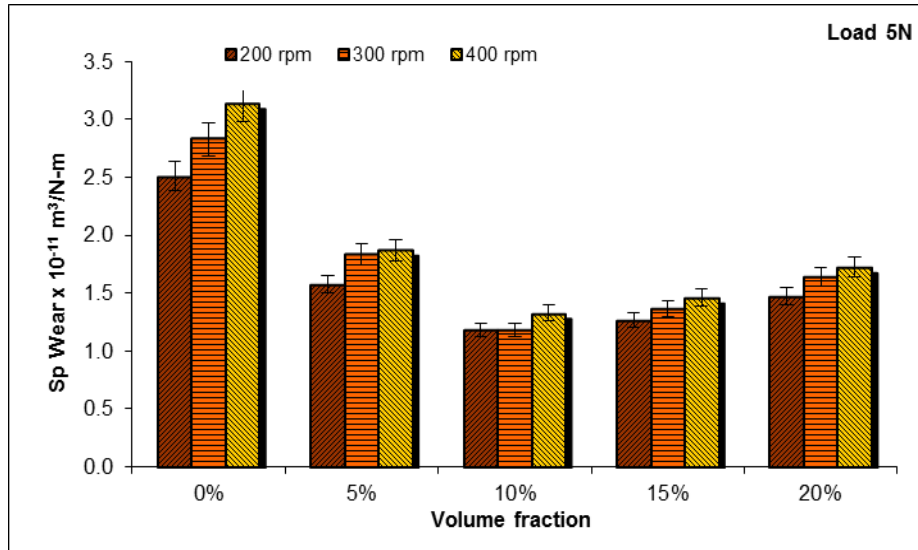


Figure-4.22 Specific Wear rate (W_s) with Volume fraction for Plain RH-epoxy composite at 5 N.

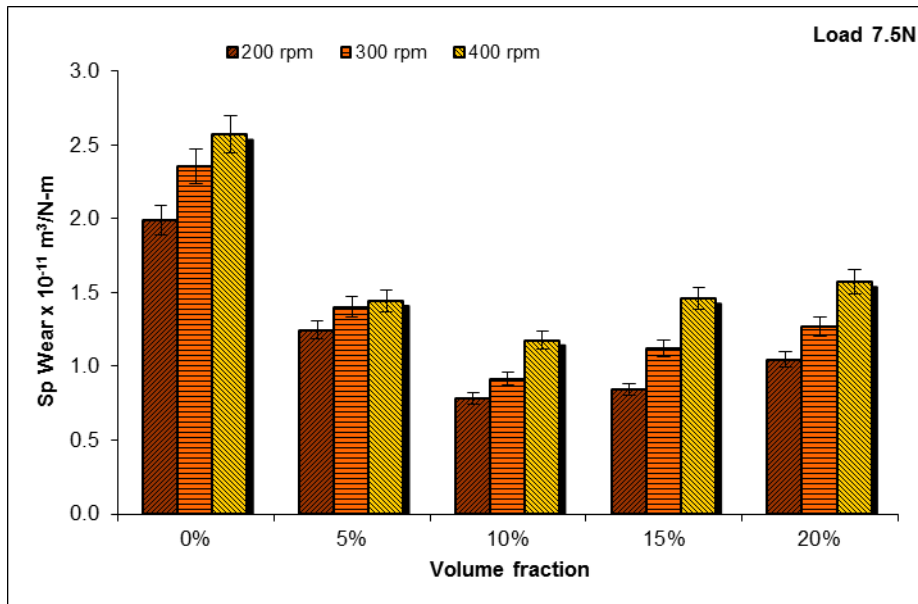


Figure-4.23 Specific Wear rate (W_s) with Volume fraction for Plain RH-epoxy composite at 7.5 N.

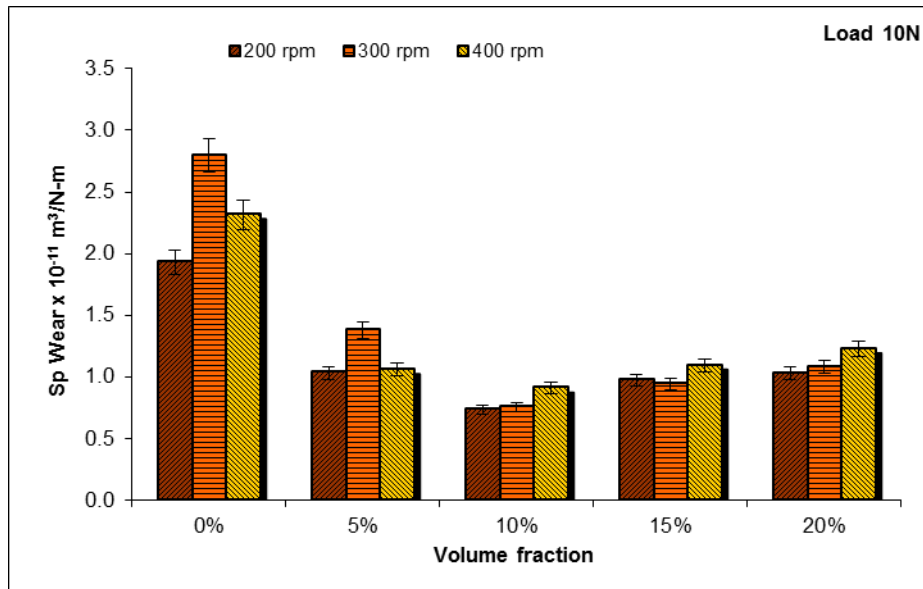


Figure-4.24 Specific Wear rate with Volume Fraction for Plain RH epoxy composite at 10 N.

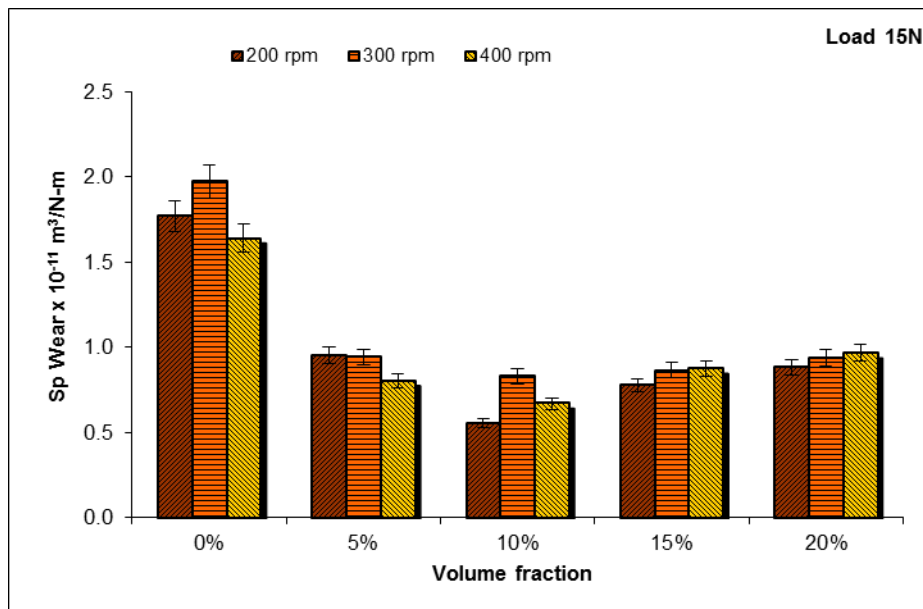


Figure-4.25 Specific Wear rate with Volume Fraction for Plain RH epoxy composite at 15 N.

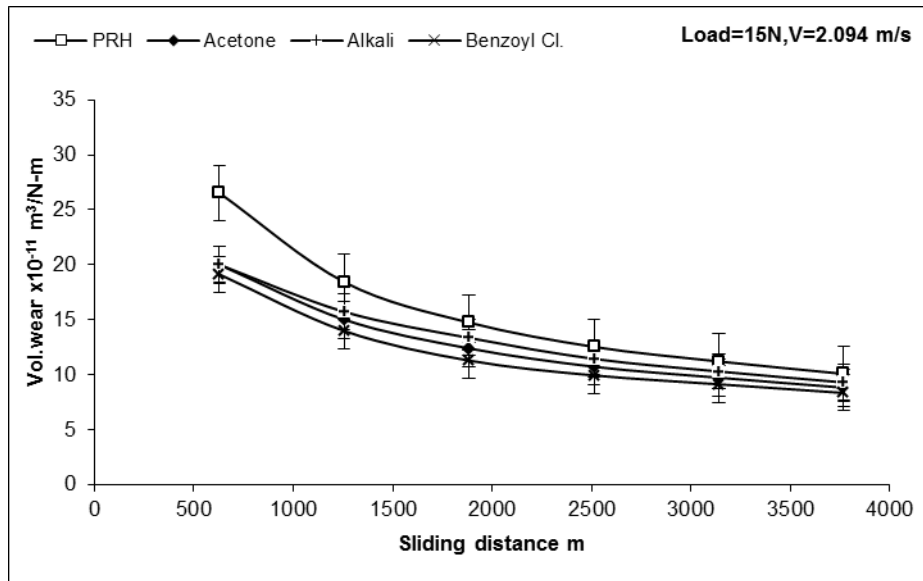


Figure-4.26 Volumetric Wear rate with Sliding Distance for Plain and Chemically treated RH - epoxy composite at velocity 2.094 m/sec (400 rpm).

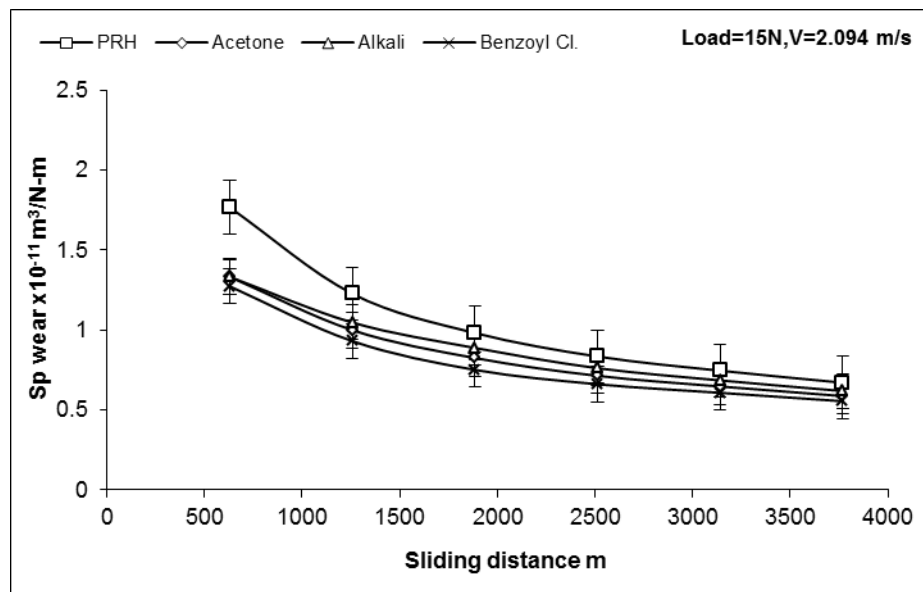


Figure-4.27 Specific Wear rate with Sliding Distance for Chemically treated RH -epoxy composite at velocity 2.094 m/sec (400 rpm).

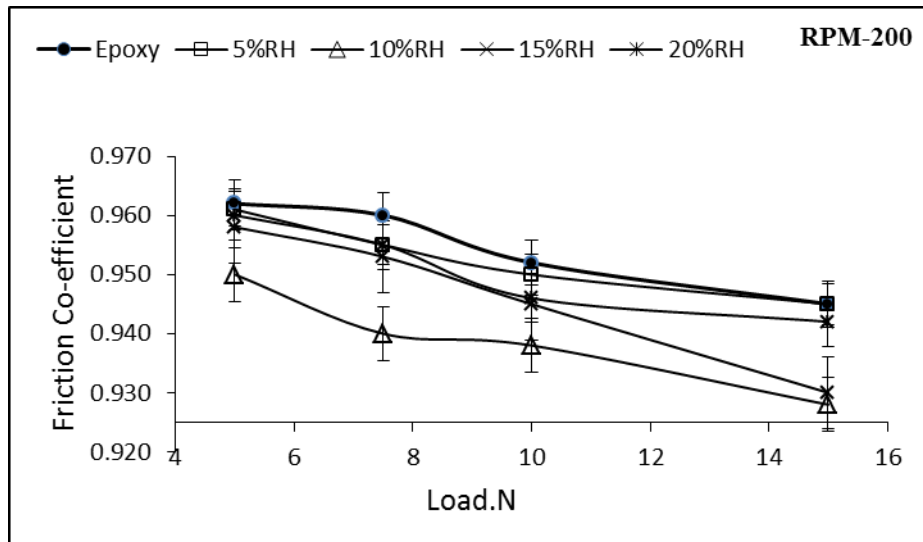


Figure-4.28 Coefficient of friction with Load for RH -epoxy composite of different Volume fraction at sliding velocity 1.047 m/sec (200 rpm).

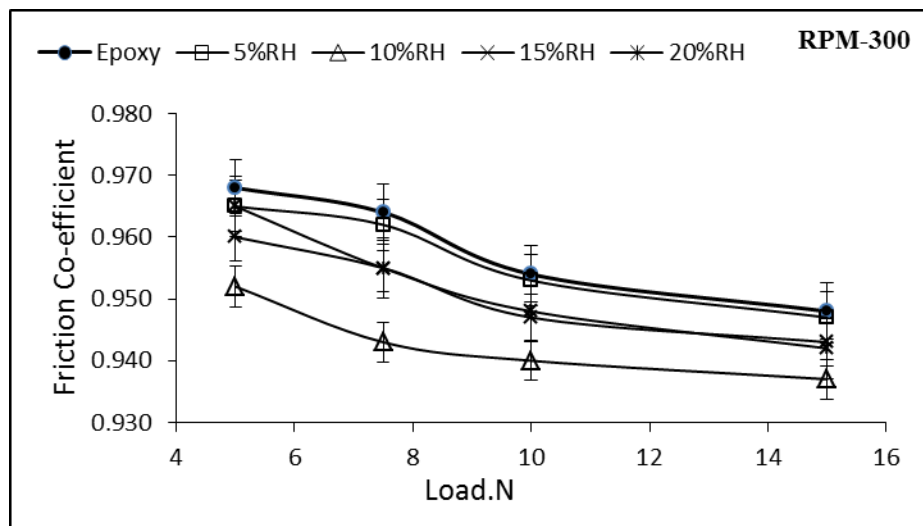


Figure-4.29 Coefficient of friction with Load for RH -epoxy composite of different Volume fraction at sliding velocity 1.571 m/sec (300 rpm).

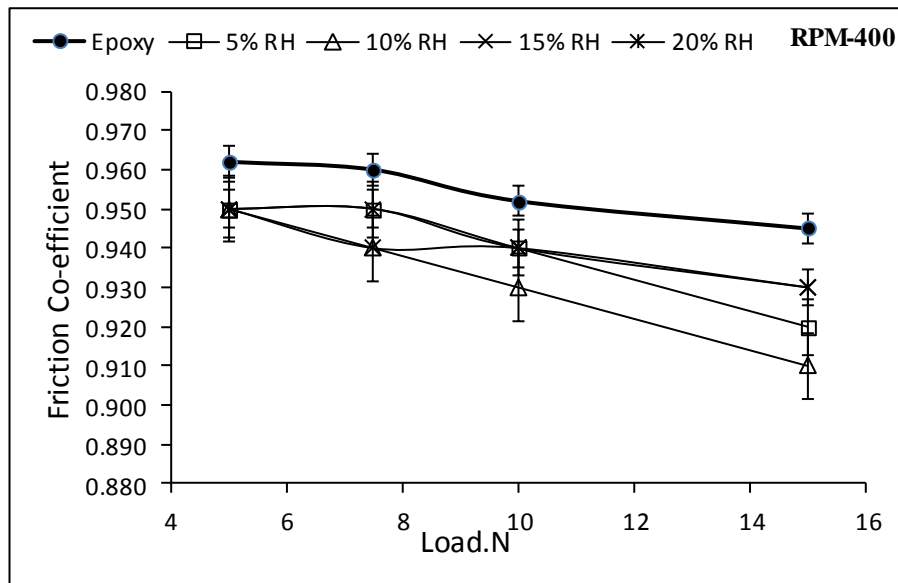
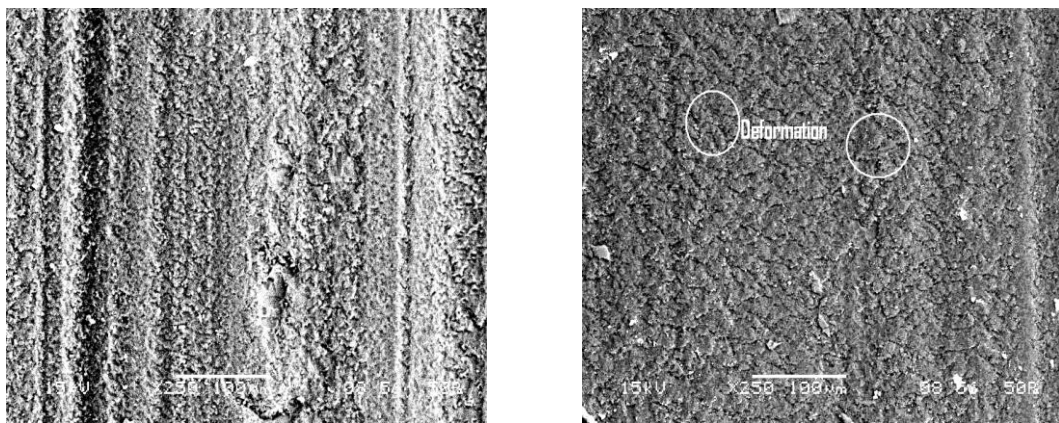


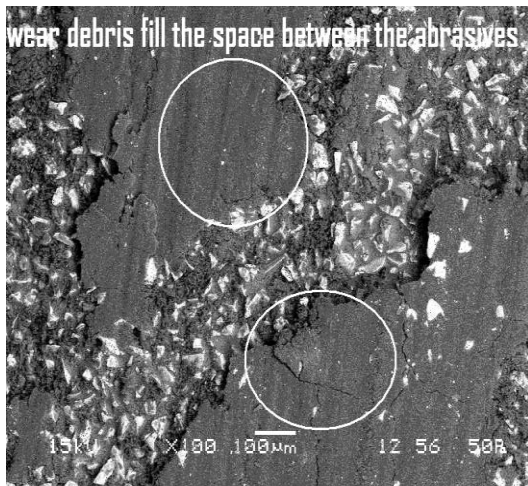
Figure-4.30 Coefficient of friction with Load for RH -epoxy composite of different Volume Fraction at sliding velocity 2.094 m/sec (400 rpm).



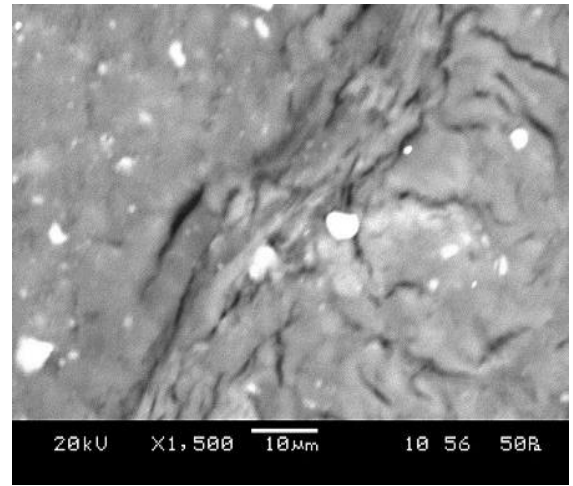
(a)

(b)

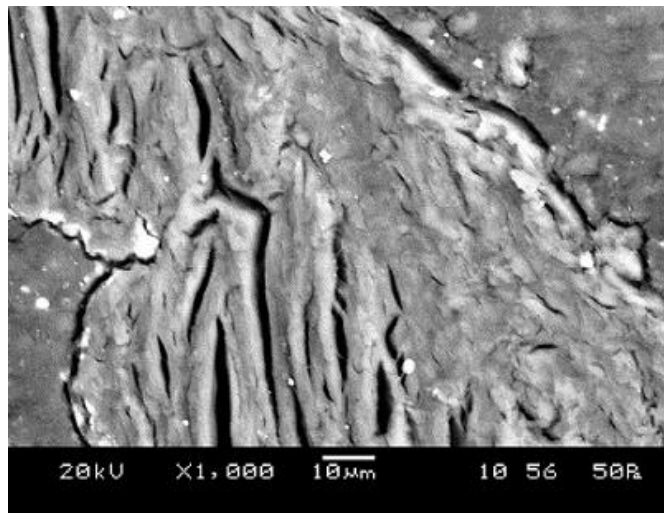
Figure-4.31 (A) Scanning electron micrograph of worn surface of tested composite samples; (a) Neat epoxy under 15N load, (b) Neat epoxy under 25N load,



(c)



(d)



(e)

Figure-4.31(B) (c) abrasive surface after test (d) 10vol% plain Rice husk reinforced composite under 15N load (e) 10vol% Benzoyl chloride treated rice husk reinforced composite under 15Nload.

Chapter 5

STUDY OF WEAR CHARACTERISTICS OF RICE HUSK CHAR EPOXY COMPOSITE

5.1 INTRODUCTION:

Ceramic materials are inorganic, non metallic materials and widely used in various applications. They may be of crystalline or partly crystalline form. They are formed by the action of heat and subsequent cooling. It is solid and inert. Ceramic materials are brittle, hard, and strong in compression, weak in shearing and tension. They withstand chemical corrosion that occurs in an acidic or caustic environment. Ceramics can also withstand very high temperatures such as temperatures that range from 900°C to 1,600°C. Exceptions include inorganic ceramic materials that do not have oxygen such as silicon carbide and Tungsten carbide etc. Traditional ceramic raw materials include clay minerals such as kaolinite, more recent materials include aluminium oxide, more commonly known as alumina. The modern ceramic materials, which are termed as advanced ceramics, include silicon carbide and tungsten carbide. Both are valued for their abrasion resistance, and hence find use in applications such as the wear plates of crushing equipment in mining operations.

These materials do show plastic deformation. However, due to the rigid structure of the crystalline materials, there are very few available slip systems for dislocations to move, and so they deform very slowly. With the non-crystalline (glassy) materials, viscous flow is the dominant source of plastic deformation, and is also very slow. It is therefore neglected in many applications of ceramic materials.

Rice Husk is potential source of Silica. As discussed in chapter 3, the Silica (SiO_2) remains on outside of Rice Husk sheath and protect the paddy from animal attacks. Continuous research is being going on worldwide for effective utilization of this Rice by-product. Rice Husk is valuable due to its high content of amorphous silica in addition to amorphous Carbon as the main constituent. Typically, RH ceramics are composed of roughly 90 wt% amorphous carbon and 10 wt.% amorphous silica.

The silica in the ash undergoes structural transformations depending on the conditions (time, temperature etc.) of combustion. At temperature around 1400°C a phase change of Silica from amorphous to crystalline takes place. It is believed that such phase change contribute to change in mechanical and tribological properties of Rice Husk ceramics. The Rice Husk carbonized at 1500°C temperature has higher porosity, lower bulk density and higher hardness whereas carbonization at 900°C shows lower coefficient of friction, specific wear and higher -

compressive strength. Thus amorphous silica content in Rice Husk Ceramic contributes better tribological properties to the composite [198]. It was suggested that the tribological behaviors of RH ceramics are closely related with the formation of a transferred film, consisted of amorphous silica and carbon particles, on a counterpart surface showing low friction and wear behavior under dry condition. The amorphous silica reacts with water vapor in air to form low shear surface layer of Si-OH, [199]

Rice Husk contains mainly 15-20 wt% silica and organic materials like cellulose, hemicellulose, lignin etc. that will yield carbon when thermally decomposed. Therefore RHA contains two necessary raw materials for the preparation of silicon carbide i.e SiO_2 and C with the very high surface area. It is possible to form SiC at relatively low temperature (much lower than indicated by thermodynamic and kinetic calculations) [200,201]. Both the low density and the space in the raw materials facilitate the production of silicon carbide[202] therefore Rice Husk are the most economical and promising raw material for the producing silicon carbide.

Silicon carbide is extremely hard and has a high thermal conductivity, high thermal-shock resistance, high hot strength, high melting point, a low coefficient of thermal expansion, good oxidization resistance and good corrosion resistance to acid and base. By all the above properties SiC is used as fiber in preparation of composites in the past two decades. The strength and hardness of the ceramics greatly enhanced by the addition of SiC particles into the matrixes, The present chapter discusses the preparation of new hard porous carbon materials called Rice Husk Char. The Carburization process is defined as the extensive thermal degradation of the carbonaceous component in the absence of air, or in the presence of inert gas. During this process, the volatile materials are removed in the form of oxides of carbon and hydrogen there by enriching the carbon content in the solid char. The char obtained by the above method is then utilized to develop composite for tribological applications. In this current study the effect of different concentration of rice husk char, the effect of carbonization temperature, sliding velocity, sliding distance and normal load on abrasive wear behavior of rice husk char reinforced epoxy composite has been evaluated and possible wear mechanism has been discussed with SEM observation.

5.2 PREPARATION OF RH CHAR:

Rice husk obtained from mills directly were cleaned, sheaved from dusts and kept in an oven for one day at the temperature of 110 °C. They were sieved to a size of 100 μ m. They were carbonized in absence of atmospheric gas. The carburization temperature selected was 850°C, 900°C and 950°C. The rice husk were taken in crucibles were placed in the furnace. The heating time was maintained one and half hours to reach the preset temperature followed by one hour soaking time. Then the furnace was cooled to room temperature in next 24h. The carburized rice husks were taken out from the furnace for further use. Figure 5.1 Show the different stages in the preparation of RH-char.



Figure-5.1 Preparation of RH-Char

5.3 PREPARATION OF THE TEST SPECIMENS:

The calculated amount of fibers has been added to the resin to prepared composite samples with 10, 20, 30 and 40% volume fraction of fiber. Pin type composite samples are prepared using a steel mould. The detail of the apparatus is shown in the figure 4.5 and 4.6 in chapter 4. The calculated amount of carburized rice husk char and resin were mixed and poured into the cylindrical cavity of the mould and then the two halves of the mould fixed properly. The

procedure adopted was same as explained in chapter 4 art. 4.6.1. All possible care has been taken in manufacturing to make composite pins of length 35 mm and diameter of 10 mm. The samples were kept in the moulds for curing at room temperature (28 °C) for 24 h. For the purpose of comparison the matrix material was also cast under similar condition. After curing the samples were taken out from the mould, finished ground to required shape, sizes for wear testing. The density has been measured for 10,20,30 and 40% VF of Rice husk char by standard water displacement method and values have been presented in Table 5.1.

5.4 DRY SLIDING WEAR TEST:

Dry sliding wear test has been carried out under multi-pass condition on the pin-on-disc type wear testing machine (As per ASTM G-99 standard) supplied by Magnum Engineers, Bangalore (Figure-4.6). Abrasive paper of 400 grade (grit-23 µm) has been pasted on a rotating disc (EN 32 Steel disc) of 120mm diameter using double-sided adhesive tape. The specimens under tests were fixed to the sample holder. The holder along with the specimen (Pin) was positioned at a particular track diameter. A track radius of 40mm was selected for this experiment and was kept constant for the entire investigation For each test new abrasive paper was used and the sample was abraded for a total sliding distance of 189.9 m. During experiment the specimen remains fixed and disc rotates. Load is applied through a dead weight loading system to press the pin against the disc. The speed of the disc or motor rpm can be varied through the controller and interval of time can be set by the help of timer provided at the control panel. The test conditions under which the experiment has been conducted are presented in Table 5.2. The mass loss in the specimen after each test was estimated by measuring the weight of the specimen before and after each test using an electronic balance with an accuracy of ± 0.001 mg. Care has been taken that the specimen under test are continuously cleaned with woolen cloth to avoid entrapment of wear debris and to achieve uniformity in the experimental procedure. Test pieces are also cleaned with acetone prior and after each test. The machine is fixed with data acquisition system with 'MAGVIEW-2010' software from which the frictional force that arises at the contact can be read out/recorded directly. For a particular type of composite 5 sets of test pieces were tested.

5.5 CALCULATION FOR WEAR:

Experiment were conducted and wear rate ,Specific wear rate etc are calculated as per the procedure given in chapter 4 art 4.6.3 . Experimental results of the wear test of different test pieces at different test conditions are tabulated and presented in table 5.3- 5.50.

5.6 RESULTS AND DISCUSSION:

Based on the tabulated results, various graphs are plotted and presented in figure 5.2-5.13 for different percentages of Rice husk char reinforced epoxy composite for three carbonization temperatures viz. 850⁰C, 900⁰C and 950⁰C at a sliding velocity of 0.628 m/s under different test conditions

Figure 5.2-5.4 shows the variation of wear rate with sliding distance at 10N load for carbonization temperature of 850⁰C,900⁰C and 950⁰C.It is seen from the plot that with addition of RH char particles the wear rate of the composite decreases .It is also seen that the wear rate for all composites first decreases and achieved a steady state at a distance of about 800 m. Since the trend is same for other sliding velocities they have not been shown here.

Figure 5.5-5.7 shows variation of volumetric wear rate with normal load .It is seen from the plot that volumetric wear rate of the composite increases with increase in load for a given volume fraction and carbonization temperature of the Char. However the rate of increase of wear found to be lower for carbonization temperature 950⁰ C. It has also been observed that the abrasive wear rate decreases with addition of RH Char up to 40 Vol % at 900⁰C. However, for 850⁰C and 950⁰C it is seen that there is hardly any difference between 30% and 40% VF. It is also seen that there is sharp increase in wear rate for 40% VF composite at 950⁰ C at 20N normal load. This might have happened due to insufficient wetting of fibers within the matrix. Similar type of behavior was reported by WU at Cheng [197] while they studied the tribological behavior of Kevlar pulp reinforced epoxy composite. Thus it can be conclude that addition of RH Char incomparision to plain rice husk epoxy is not effective in improving its wear resistance in comparison to plain as well as treated rice husk .However the friction coefficient decreases to a greater extent.

Figure 5.8-5.10 shows the tribological data obtained on the composite using different volume fraction of rice husk for three carbonization temperatures viz. 850, 900 and 950 °C at a sliding velocity of 0.633m/sec for a normal load of 15N. In the consideration of all the figures it is observed that as the volume fraction of filler increases the specific wear rate decreases. The minimum specific wear rate is obtained for 40 vf % . At higher VF there may be increase in wear this is due to insufficient wetting of fiber with the matrix material. Further it has been observed from these plots that, in all case the range of specific wear rate is high at initial stage of sliding distance and achieved a steady state at a distance of about 800 m. In other words, there is less removal of material at longer sliding distances and this could be due to the less penetration of abrasive particle in to the composite sample. This could also be attributed to the multipass abrasion condition in which the severity of the abrasives decreases with repeated passes causing minimum wear for maximum test duration. In multipass abrasion (sample is run again and again on the same wear track) is probably due to the transfer of polymer films on the counter surface abrasive [203].

Figure 5.11-5.13 shows the variation of wear rate with different volume fraction of fiber for different normal load and at three carbonization temperatures. It is seen that with increasing the load from 5 to 20 N, wear rate in all cases increases with different magnitudes. The wear rate at lower load (5 N) for all cases is low because very light pressure is applied on the specimen, due to this there is lesser penetration rate and the numbers of abrasive particles in action are less with the rubbing surface. Abrasion wear was greatly increased at higher load because the load applied on the specimen is more, due to this pressure most of the abrasive particles are in action with the surface of the specimen which in turns created more grooves, resulting more material removal due to ploughing action. While comparing the wear rate of the composite with different carbonization temperature under different load (5, 10, 15, 20N) it is observed that for 950 °C carbonization temperature 40 wt% filler shows the minimum wear rate. It means that carbonized RH char is very effective in improving the tribological performance of the composite. As reported by Wei Li et al. [204] the carbonization temperature had great effect on the yields and pore development of the char prepared. With increasing carbonization temperature, more volatiles were released and more micro porous was formed, giving rise to a decrease in yield and increase in the surface area, total volume

and micro porous volume of char. In our case probably at 950 °C carbonization temperature micro porous volume increases, which results in better wear property for the composite under study. As the carbonization temperature increases the volatile matter get vanished and remains elemental carbon in the material this will increase the fixed carbon content. This type of observation is observed by Sanger et al. [205] in their cashew nut shell char carbonization process. The wear rate decreases with the addition of char powder up to 40 % VF in all the carbonized temperature. It means that the char particulates are very effective in improving the tribological performance of the epoxy. The least wear rate is observed for the 950 °C carbonized char filler composites when compared with the other composites. It indicates that due to increase in carbon content the wear resistance increases. It is reported [206, 207] that when ceramic reinforcement was put in to metal matrix composites along with other mechanical properties, hardness also increases. Once the hardness increases for a material, it will certainly increase the wear behaviour of the composite, as hardness is directly related to the wear rate of the composite. In our case also because of inclusion of hard ceramic particles in to the polymer matrix the wear resistance increases.

Figure 5.14-5.16 shows the variation of coefficient of friction with time. It is clear from the figure that the coefficient of friction increases initially to a higher value due to the fresh abrasive paper and as the process continues it almost remains the same for the entire test period. It is also seen that the trend for the coefficient of friction remains the same for all volume fraction of reinforcement.

5.7 WORN SURFACE MORPHOLOGY:

The worn surface morphology of composite at different carbonization temperatures has been examined by scanning electron microscopy (SEM). The influence of carbonization temperature is quite visible from these micrographs. Figure 5.17 (a, b, c) shows the micrographs for 30 wt.% reinforcement rice husk carbonized at 850, 900 and 950⁰C. In Figure 5.17(a), crack lines are clearly visible, but are not so severe that the particle is detached from the matrix. Figure 5.17 (b) shows rough surface with many tearing and branching lines. This tearing seems to be originating from the interface between matrix and filler. Figure

5.17(c) clearly shows some micro voids are caused by detached particles from the composite surface. These micro voids are observed to have originated from the region around the carbonized particles in the matrix but more number of particles is still intact within the matrix. This somehow related to fatigue type of wear mechanism where a particle of material is detached as a result of joining of crack lines [Figure 5.17(b)] grows parallel to the sliding direction [Figure 5.17(c)]. This supplement to the results shown in Figure 5.13 which prompted us to conclude that carbonization temperature increases the micro porous volume as well as the surface area of the rice husk, which results in better wear property for the composite under study.

5.8 CONCLUSIONS:

Based on experimental results of abrasive wear of Rice husk char epoxy composite tested under different carbonization temperature, normal loads, sliding velocity and sliding distances, the following conclusions are drawn:

- The Rice husk char up to 40% volume fraction can successfully be utilized to produce composite by suitably bonding with resin where as maximum 10% Rice Husk in natural form can be utilized to form composite with epoxy.
- By carburizing the Rice husk, amorphous silica and carbon are obtained which provides higher hardness to the composite.
- With increasing sliding distance, wear rate of the composite gradually decreases and attains an almost steady state in multi pass condition.
- The specific wear rate of composite is inverse of the wear rate was found to be considerable less as compared to specific wear rate of neat epoxy.
- It is found that carbonization temperature increases the micro porous volume as well as the surface area of the rice husk, which results in better wear property for the composite under study.

Table-5.1 Density of neat epoxy and RHC reinforced composite samples

Fiber content (%) Volume Fraction	Measured Density (gm/cm³)
10	1.213
20	1.211
30	1.233
40	1.215

Table-5.2 Test parameter for Dry Sliding wear test

Test Parametes	Units	Values
Reinforcement Preparing Temperature	⁰ C	850,900,950
Load (L)	N	5, 10, 15,and 20
Sliding Velocity (v)	m/s	0.6283 (5 observation at an interval 5 min)
Track radius (r)	mm	40
Temperature	⁰ C	25

Table 5.3

Char temp: 850⁰C Load - 5 N VF -10% Density (ρ): 1.213 g/cc

m1 (gm)	m2 (gm)	Δm (gm)	Time (Sec)	SD (m)	WX10⁻⁵ (N/m)	W_vX10⁻¹¹ (m³/m)	W_sX10⁻¹¹ (m³/N.m)
2.23	2.12	0.11	300	188.49	0.57	48.11	9.62
2.23	2.05	0.18	600	376.98	0.47	39.36	7.87
2.23	1.99	0.24	900	565.47	0.42	34.99	7.00
2.23	1.94	0.29	1200	753.96	0.38	31.71	6.34
2.23	1.88	0.35	1500	942.45	0.36	30.62	6.12

Table 5.4

Char temp: 850⁰C Load 5 N VF 20% Density (ρ) : 1.211 g/cc

m1 (gm)	m2 (gm)	Δm (gm)	Time (Sec)	SD (m)	WX10⁻⁵ (N/m)	W_vX10⁻¹¹ (m³/m)	W_sX10⁻¹¹ (m³/N.m)
3.25	3.18	0.07	300	188.49	0.36	30.67	6.13
3.25	3.12	0.13	600	376.98	0.34	28.48	5.70
3.25	3.11	0.14	900	565.47	0.24	20.44	4.09
3.25	3.09	0.16	1200	753.96	0.21	17.52	3.50
3.25	3.07	0.18	1500	942.45	0.19	15.77	3.15

Table 5.5

Char temp: 850⁰C Load - 5 N VF- 30% Density (ρ) : 1.233 g/cc

m1 (gm)	m2 (gm)	Δm (gm)	Time (Sec)	SD (m)	WX10⁻⁵ (N/m)	W_vX10⁻¹¹ (m³/m)	W_sX10⁻¹¹ (m³/N.m)
3.38	3.30	0.08	300	188.49	0.42	34.42	6.88
3.38	3.26	0.12	600	376.98	0.31	25.82	5.16
3.38	3.19	0.19	900	565.47	0.33	27.25	5.45
3.38	3.13	0.25	1200	753.96	0.33	26.89	5.38
3.38	3.09	0.29	1500	942.45	0.30	24.96	4.99

Table 5.6

Char temp: 850⁰C Load 5 N VF 40% Density (ρ) : 1.215 g/cc

m1 (gm)	m2 (gm)	Δm (gm)	Time (Sec)	SD (m)	WX10⁻⁵ (N/m)	W_vX10⁻¹¹ (m³/m)	W_sX10⁻¹¹ (m³/N.m)
3.22	3.15	0.07	300	188.49	0.36	30.57	6.11
3.22	3.11	0.11	600	376.98	0.29	24.02	4.80
3.22	3.07	0.15	900	565.47	0.26	21.83	4.37
3.22	3.04	0.18	1200	753.96	0.23	19.65	3.93
3.22	3.01	0.21	1500	942.45	0.22	18.34	3.67

Table 5.7

Char temp: 850⁰C Load 10 N VF 10% Density (ρ) : 1.213 g/cc

m1 (gm)	m2 (gm)	Δm (gm)	Time (Sec)	SD (m)	$WX10^{-5}$ (N/m)	W_vX10^{-11} (m³/m)	W_sX10^{-11} (m³/N.m)
2.34	2.14	0.20	300	188.49	1.04	87.47	8.75
2.34	1.97	0.37	600	376.98	0.96	80.91	8.09
2.34	1.79	0.55	900	565.47	0.95	80.18	8.02
2.34	1.63	0.71	1200	753.96	0.92	77.63	7.76
2.34	1.47	0.87	1500	942.45	0.91	76.10	7.61

Table 5.8

Char temp: 850⁰C Load 10 N VF 20% Density (ρ) : 1.211 g/cc

m1 (gm)	m2 (gm)	Δm (gm)	Time (Sec)	SD (m)	$WX10^{-5}$ (N/m)	W_vX10^{-11} (m³/m)	W_sX10^{-11} (m³/N.m)
3.42	3.24	0.18	300	188.49	0.94	78.86	7.89
3.42	3.13	0.29	600	376.98	0.75	63.52	6.35
3.42	3.01	0.41	900	565.47	0.71	59.87	5.99
3.42	2.91	0.51	1200	753.96	0.66	55.86	5.59
3.42	2.79	0.63	1500	942.45	0.66	55.20	5.52

Table 5.9

Char temp: 850⁰C Load 10 N VF 30% Density (ρ) : 1.233 g/cc

m1 (gm)	m2 (gm)	Δm (gm)	Time (Sec)	SD (m)	$WX10^{-5}$ (N/m)	W_vX10^{-11} (m³/m)	W_sX10^{-11} (m³/N.m)
2.91	2.77	0.14	300	188.49	0.73	60.24	6.02
2.91	2.66	0.25	600	376.98	0.65	53.78	5.38
2.91	2.61	0.30	900	565.47	0.52	43.03	4.30
2.91	2.55	0.36	1200	753.96	0.47	38.72	3.87
2.91	2.49	0.42	1500	942.45	0.44	36.14	3.61

Table 5.10

Char temp: 850⁰C Load 10 N VF 40% Density (ρ) : 1.215 g/cc

m1 (gm)	m2 (gm)	Δm (gm)	Time (Sec)	SD (m)	$WX10^{-5}$ (N/m)	W_vX10^{-11} (m³/m)	W_sX10^{-11} (m³/N.m)
3.11	2.93	0.18	300	188.49	0.94	78.60	7.86
3.11	2.85	0.26	600	376.98	0.68	56.76	5.68
3.11	2.80	0.31	900	565.47	0.54	45.12	4.51
3.11	2.76	0.35	1200	753.96	0.46	38.21	3.82
3.11	2.72	0.39	1500	942.45	0.41	34.06	3.41

Table 5.11

Char temp: 850⁰C Load 15 N VF 10% Density (ρ) : 1.213 g/cc

m1 (gm)	m2 (gm)	Δm (gm)	Time (Sec)	SD (m)	$WX10^{-5}$ (N/m)	W_VX10^{-11} (m³/m)	W_SX10^{-11} (m³/N.m)
3.09	2.63	0.46	300	188.49	2.39	201.19	13.41
3.09	2.36	0.73	600	376.98	1.90	159.64	10.64
3.09	2.16	0.93	900	565.47	1.61	135.59	9.04
3.09	1.93	1.16	1200	753.96	1.51	126.84	8.46
3.09	1.75	1.34	1500	942.45	1.39	117.22	7.81

Table 5.12

Char temp: 850⁰C Load 15 N VF 20% Density (ρ) : 1.211 g/cc

m1 (gm)	m2 (gm)	Δm (gm)	Time (Sec)	SD (m)	$WX10^{-5}$ (N/m)	W_VX10^{-11} (m³/m)	W_SX10^{-11} (m³/N.m)
3.41	3.13	0.28	300	188.49	1.46	122.67	8.18
3.41	2.98	0.43	600	376.98	1.12	94.19	6.28
3.41	2.82	0.59	900	565.47	1.02	86.16	5.74
3.41	2.67	0.74	1200	753.96	0.96	81.05	5.40
3.41	2.49	0.92	1500	942.45	0.96	80.61	5.37

Table 5.13

Char temp: 850⁰C Load 15 N VF 30% Density (ρ) : 1.233 g/cc

m1 (gm)	m2 (gm)	Δm (gm)	Time (Sec)	SD (m)	$WX10^{-5}$ (N/m)	W_vX10^{-11} (m³/m)	W_sX10^{-11} (m³/N.m)
3.32	3.12	0.20	300	188.49	1.04	86.06	5.74
3.32	2.89	0.43	600	376.98	1.12	92.51	6.17
3.32	2.77	0.55	900	565.47	0.95	78.88	5.26
3.32	2.60	0.72	1200	753.96	0.94	77.45	5.16
3.32	2.46	0.86	1500	942.45	0.90	74.01	4.93

Table 5.14

Char temp: 850⁰C Load 15 N VF 40% Density (ρ) : 1.215 g/cc

m1 (gm)	m2 (gm)	Δm (gm)	Time (Sec)	SD (m)	$WX10^{-5}$ (N/m)	W_vX10^{-11} (m³/m)	W_sX10^{-11} (m³/N.m)
3.55	3.17	0.38	300	188.49	1.98	165.93	11.06
3.55	3.01	0.54	600	376.98	1.41	117.90	7.86
3.55	2.88	0.67	900	565.47	1.16	97.52	6.50
3.55	2.78	0.77	1200	753.96	1.00	84.06	5.60
3.55	2.70	0.85	1500	942.45	0.88	74.23	4.95

Table 5.15

Char temp: 850⁰C Load 20 N VF 10% Density (ρ) : 1.213 g/cc

m1 (gm)	m2 (gm)	Δm (gm)	Time (Sec)	SD (m)	$WX10^{-5}$ (N/m)	W_VX10^{-11} (m³/m)	W_SX10^{-11} (m³/N.m)
3.13	2.68	0.45	300	188.49	2.34	196.82	9.84
3.13	2.20	0.93	600	376.98	2.42	203.38	10.17
3.13	1.83	1.30	900	565.47	2.26	189.53	9.48
3.13	1.70	1.43	1200	753.96	1.86	156.36	7.82
3.13	1.43	1.70	1500	942.45	1.77	148.71	7.44

Table 5.16

Char temp: 850⁰C Load 20 N VF 20% Density (ρ) : 1.211 g/cc

m1 (gm)	m2 (gm)	Δm (gm)	Time (Sec)	SD (m)	$WX10^{-5}$ (N/m)	W_VX10^{-11} (m³/m)	W_SX10^{-11} (m³/N.m)
3.42	3.11	0.31	300	188.49	1.61	135.81	6.79
3.42	2.86	0.56	600	376.98	1.46	122.67	6.13
3.42	2.61	0.81	900	565.47	1.41	118.29	5.91
3.42	2.35	1.07	1200	753.96	1.39	117.19	5.86
3.42	2.10	1.32	1500	942.45	1.37	115.66	5.78

Table 5.17

Char temp: 850⁰C Load 20 N VF 30% Density (ρ) : 1.233 g/cc

m1 (gm)	m2 (gm)	Δm (gm)	Time (Sec)	SD (m)	$WX10^{-5}$ (N/m)	W_VX10^{-11} (m³/m)	W_SX10^{-11} (m³/N.m)
3.52	3.18	0.34	300	188.49	1.77	146.29	7.31
3.52	2.97	0.55	600	376.98	1.43	118.33	5.92
3.52	2.76	0.76	900	565.47	1.32	109.00	5.45
3.52	2.56	0.96	1200	753.96	1.25	103.27	5.16
3.52	2.40	1.12	1500	942.45	1.17	96.38	4.82

Table 5.18

Char temp: 850⁰C Load 20 N VF 40% Density (ρ) : 1.215 g/cc

m1 (gm)	m2 (gm)	Δm (gm)	Time (Sec)	SD (m)	$WX10^{-5}$ (N/m)	W_VX10^{-11} (m³/m)	W_SX10^{-11} (m³/N.m)
5.20	2.90	2.30	300	188.49	11.97	1004.30	50.21
5.20	2.67	2.53	600	376.98	6.58	552.36	27.62
5.20	2.47	2.73	900	565.47	4.74	397.35	19.87
5.20	2.32	2.88	1200	753.96	3.75	314.39	15.72
5.20	2.16	3.04	1500	942.45	3.16	265.48	13.27

Table 5.19

Char temp: 900⁰C Load 5 N VF 10% Density (ρ) : 1.213 g/cc

m1 (gm)	m2 (gm)	Δm (gm)	Time (Sec)	SD (m)	WX10⁻⁵ (N/m)	W_vX10⁻¹¹ (m³/m)	W_sX10⁻¹¹ (m³/N.m)
2.94	2.84	0.10	300	188.49	0.52	43.74	8.75
2.94	2.77	0.17	600	376.98	0.44	37.18	7.44
2.94	2.69	0.25	900	565.47	0.43	36.45	7.29
2.94	2.61	0.33	1200	753.96	0.43	36.08	7.22
2.94	2.52	0.42	1500	942.45	0.44	36.74	7.35

Table 5.20

Char temp: 900⁰C Load 5 N VF 20% Density (ρ) : 1.211 g/cc

m1 (gm)	m2 (gm)	Δm (gm)	Time (Sec)	SD (m)	WX10⁻⁵ (N/m)	W_vX10⁻¹¹ (m³/m)	W_sX10⁻¹¹ (m³/N.m)
3.01	2.94	0.07	300	188.49	0.36	30.67	6.13
3.01	2.91	0.10	600	376.98	0.26	21.90	4.38
3.01	2.86	0.15	900	565.47	0.26	21.90	4.38
3.01	2.82	0.19	1200	753.96	0.25	20.81	4.16
3.01	2.77	0.24	1500	942.45	0.25	21.03	4.21

Table 5.21

Char temp: 900⁰C Load 5 N VF 30% Density (ρ) : 1.233 g/cc

m1 (gm)	m2 (gm)	Δm (gm)	Time (Sec)	SD (m)	WX10⁻⁵ (N/m)	W_vX10⁻¹¹ (m³/m)	W_sX10⁻¹¹ (m³/N.m)
2.84	2.74	0.10	300	188.49	0.52	43.03	8.61
2.84	2.69	0.15	600	376.98	0.39	32.27	6.45
2.84	2.64	0.20	900	565.47	0.35	28.69	5.74
2.84	2.60	0.24	1200	753.96	0.31	25.82	5.16
2.84	2.56	0.28	1500	942.45	0.29	24.10	4.82

Table 5.22

Char temp: 900⁰C Load 5 N VF 40% Density (ρ) : 1.215 g/cc

m1 (gm)	m2 (gm)	Δm (gm)	Time (Sec)	SD (m)	WX10⁻⁵ (N/m)	W_vX10⁻¹¹ (m³/m)	W_sX10⁻¹¹ (m³/N.m)
3.86	3.82	0.04	300	188.49	0.21	17.47	3.49
3.86	3.79	0.07	600	376.98	0.18	15.28	3.06
3.86	3.75	0.11	900	565.47	0.19	16.01	3.20
3.86	3.70	0.16	1200	753.96	0.21	17.47	3.49
3.86	3.67	0.19	1500	942.45	0.20	16.59	3.32

Table 5.23

Char temp: 900⁰C Load 10 N VF 10% Density (ρ) : 1.213 g/cc

m1 (gm)	m2 (gm)	Δm (gm)	Time (Sec)	SD (m)	WX10⁻⁵ (N/m)	W_vX10⁻¹¹ (m³/m)	W_sX10⁻¹¹ (m³/N.m)
3.82	3.67	0.15	300	188.49	0.78	65.61	6.56
3.82	3.55	0.27	600	376.98	0.70	59.05	5.90
3.82	3.42	0.40	900	565.47	0.69	58.32	5.83
3.82	3.28	0.54	1200	753.96	0.70	59.05	5.90
3.82	3.16	0.66	1500	942.45	0.69	57.73	5.77

Table 5.24

Char temp: 900⁰C Load 10 N VF 20% Density (ρ) : 1.211 g/cc

m1 (gm)	m2 (gm)	Δm (gm)	Time (Sec)	SD (m)	WX10⁻⁵ (N/m)	W_vX10⁻¹¹ (m³/m)	W_sX10⁻¹¹ (m³/N.m)
3.68	3.54	0.14	300	188.49	0.73	61.33	6.13
3.68	3.44	0.24	600	376.98	0.62	52.57	5.26
3.68	3.33	0.35	900	565.47	0.61	51.11	5.11
3.68	3.25	0.43	1200	753.96	0.56	47.10	4.71
3.68	3.14	0.54	1500	942.45	0.56	47.31	4.73

Table 5.25

Char temp: 900⁰C Load 10 N VF 30% Density (ρ) : 1.233 g/cc

m1 (gm)	m2 (gm)	Δm (gm)	Time (Sec)	SD (m)	WX10⁻⁵ (N/m)	W_vX10⁻¹¹ (m³/m)	W_sX10⁻¹¹ (m³/N.m)
3.34	3.22	0.12	300	188.49	0.62	51.63	5.16
3.34	3.07	0.27	600	376.98	0.70	58.09	5.81
3.34	2.97	0.37	900	565.47	0.64	53.07	5.31
3.34	2.87	0.47	1200	753.96	0.61	50.56	5.06
3.34	2.76	0.58	1500	942.45	0.60	49.91	4.99

Table 5.26

Char temp: 900⁰C Load 10 N VF 40% Density (ρ) : 1.215 g/cc

m1 (gm)	m2 (gm)	Δm (gm)	Time (Sec)	SD (m)	WX10⁻⁵ (N/m)	W_vX10⁻¹¹ (m³/m)	W_sX10⁻¹¹ (m³/N.m)
3.72	3.62	0.10	300	188.49	0.52	43.67	4.37
3.72	3.57	0.15	600	376.98	0.39	32.75	3.27
3.72	3.50	0.22	900	565.47	0.38	32.02	3.20
3.72	3.44	0.28	1200	753.96	0.36	30.57	3.06
3.72	3.40	0.32	1500	942.45	0.33	27.95	2.79

Table 5.27

Char temp: 900⁰C Load 15 N VF 10% Density (ρ) : 1.213 g/cc

m1 (gm)	m2 (gm)	Δm (gm)	Time (Sec)	SD (m)	WX10⁻⁵ (N/m)	W_vX10⁻¹¹ (m³/m)	W_sX10⁻¹¹ (m³/N.m)
3.43	3.05	0.38	300	188.49	1.98	166.20	11.08
3.43	2.71	0.72	600	376.98	1.87	157.45	10.50
3.43	2.34	1.09	900	565.47	1.89	158.91	10.59
3.43	2.02	1.41	1200	753.96	1.83	154.17	10.28
3.43	1.76	1.67	1500	942.45	1.74	146.08	9.74

Table 5.28

Char temp: 900⁰C Load 15 N VF 20% Density (ρ) : 1.211 g/cc

m1 (gm)	m2 (gm)	Δm (gm)	Time (Sec)	SD (m)	WX10⁻⁵ (N/m)	W_vX10⁻¹¹ (m³/m)	W_sX10⁻¹¹ (m³/N.m)
3.47	3.20	0.27	300	188.49	1.41	118.29	7.89
3.47	2.98	0.49	600	376.98	1.28	107.33	7.16
3.47	2.81	0.66	900	565.47	1.14	96.38	6.43
3.47	2.58	0.89	1200	753.96	1.16	97.48	6.50
3.47	2.46	1.01	1500	942.45	1.05	88.50	5.90

Table 5.29

Char temp: 900⁰C Load 15 N VF 30% Density (ρ) : 1.233 g/cc

m1 (gm)	m2 (gm)	Δm (gm)	Time (Sec)	SD (m)	WX10⁻⁵ (N/m)	W_vX10⁻¹¹ (m³/m)	W_sX10⁻¹¹ (m³/N.m)
3.54	3.34	0.20	300	188.49	1.04	86.06	5.74
3.54	3.11	0.43	600	376.98	1.12	92.51	6.17
3.54	2.92	0.62	900	565.47	1.08	88.92	5.93
3.54	2.75	0.79	1200	753.96	1.03	84.98	5.67
3.54	2.58	0.96	1500	942.45	1.00	82.61	5.51

Table 5.30

Char temp: 900⁰C Load 15 N VF 40% Density (ρ) : 1.215 g/cc

m1 (gm)	m2 (gm)	Δm (gm)	Time (Sec)	SD (m)	WX10⁻⁵ (N/m)	W_vX10⁻¹¹ (m³/m)	W_sX10⁻¹¹ (m³/N.m)
3.25	3.10	0.15	300	188.49	0.78	65.50	4.37
3.25	2.96	0.29	600	376.98	0.75	63.31	4.22
3.25	2.84	0.41	900	565.47	0.71	59.68	3.98
3.25	2.72	0.53	1200	753.96	0.69	57.86	3.86
3.25	2.61	0.64	1500	942.45	0.67	55.89	3.73

Table 5.31

Char temp: 900⁰C Load 20 N VF 10% Density (ρ) : 1.213 g/cc

m1 (gm)	m2 (gm)	Δm (gm)	Time (Sec)	SD (m)	WX10⁻⁵ (N/m)	W_vX10⁻¹¹ (m³/m)	W_sX10⁻¹¹ (m³/N.m)
3.46	2.93	0.53	300	188.49	2.76	231.81	11.59
3.46	2.49	0.97	600	376.98	2.52	212.13	10.61
3.46	2.07	1.39	900	565.47	2.41	202.65	10.13
3.46	1.71	1.75	1200	753.96	2.28	191.35	9.57
3.46	1.28	2.18	1500	942.45	2.27	190.69	9.53

Table 5.32

Char temp: 900⁰C Load 20 N VF 20% Density (ρ) : 1.211 g/cc

m1 (gm)	m2 (gm)	Δm (gm)	Time (Sec)	SD (m)	WX10⁻⁵ (N/m)	W_vX10⁻¹¹ (m³/m)	W_sX10⁻¹¹ (m³/N.m)
3.65	3.32	0.33	300	188.49	1.72	144.57	7.23
3.65	3.06	0.59	600	376.98	1.54	129.24	6.46
3.65	2.82	0.83	900	565.47	1.44	121.21	6.06
3.65	2.63	1.02	1200	753.96	1.33	111.71	5.59
3.65	2.39	1.26	1500	942.45	1.31	110.40	5.52

Table 5.33

Char temp: 900⁰C Load 20 N VF 30% Density (ρ) : 1.233 g/cc

m1 (gm)	m2 (gm)	Δm (gm)	Time (Sec)	SD (m)	WX10⁻⁵ (N/m)	W_vX10⁻¹¹ (m³/m)	W_sX10⁻¹¹ (m³/N.m)
3.62	3.30	0.32	300	188.49	1.67	137.69	6.88
3.62	3.00	0.62	600	376.98	1.61	133.39	6.67
3.62	2.74	0.88	900	565.47	1.53	126.21	6.31
3.62	2.52	1.10	1200	753.96	1.43	118.33	5.92
3.62	2.28	1.34	1500	942.45	1.39	115.31	5.77

Table 5.34

Char temp: 900⁰C Load 20 N VF 40% Density (ρ) : 1.215 g/cc

m1 (gm)	m2 (gm)	Δm (gm)	Time (Sec)	SD (m)	WX10⁻⁵ (N/m)	W_vX10⁻¹¹ (m³/m)	W_sX10⁻¹¹ (m³/N.m)
2.93	2.63	0.30	300	188.49	1.56	131.00	6.55
2.93	2.41	0.52	600	376.98	1.35	113.53	5.68
2.93	2.21	0.72	900	565.47	1.25	104.80	5.24
2.93	2.00	0.93	1200	753.96	1.21	101.52	5.08
2.93	1.79	1.14	1500	942.45	1.19	99.56	4.98

Table 5.35

Char temp: 950⁰C Load 5 N VF 10% Density (ρ) : 1.213 g/cc

m1 (gm)	m2 (gm)	Δm (gm)	Time (Sec)	SD (m)	WX10⁻⁵ (N/m)	W_vX10⁻¹¹ (m³/m)	W_sX10⁻¹¹ (m³/N.m)
2.63	2.56	0.07	300	188.49	0.36	30.62	6.12
2.63	2.52	0.11	600	376.98	0.29	24.06	4.81
2.63	2.48	0.15	900	565.47	0.26	21.87	4.37
2.63	2.46	0.17	1200	753.96	0.22	18.59	3.72
2.63	2.42	0.21	1500	942.45	0.22	18.37	3.67

Table 5.36

Char temp: 950⁰C Load 5 N VF 20% Density (ρ) : 1.211 g/cc

m1 (gm)	m2 (gm)	Δm (gm)	Time (Sec)	SD (m)	WX10⁻⁵ (N/m)	W_vX10⁻¹¹ (m³/m)	W_sX10⁻¹¹ (m³/N.m)
2.62	2.57	0.05	300	188.49	0.26	21.90	4.38
2.62	2.52	0.10	600	376.98	0.26	21.90	4.38
2.62	2.48	0.14	900	565.47	0.24	20.44	4.09
2.62	2.43	0.19	1200	753.96	0.25	20.81	4.16
2.62	2.39	0.23	1500	942.45	0.24	20.15	4.03

Table 5.37

Char temp: 950⁰C Load 5 N VF 30% Density (ρ) : 1.233 g/cc

m1 (gm)	m2 (gm)	Δm (gm)	Time (Sec)	SD (m)	WX10⁻⁵ (N/m)	W_vX10⁻¹¹ (m³/m)	W_sX10⁻¹¹ (m³/N.m)
2.72	2.66	0.06	300	188.49	0.31	25.82	5.16
2.72	2.63	0.09	600	376.98	0.23	19.36	3.87
2.72	2.59	0.13	900	565.47	0.23	18.65	3.73
2.72	2.56	0.16	1200	753.96	0.21	17.21	3.44
2.72	2.52	0.20	1500	942.45	0.21	17.21	3.44

Table 5.38

Char temp: 950⁰C Load 5 N VF 40% Density (ρ) : 1.215 g/cc

m1 (gm)	m2 (gm)	Δm (gm)	Time (Sec)	SD (m)	WX10⁻⁵ (N/m)	W_vX10⁻¹¹ (m³/m)	W_sX10⁻¹¹ (m³/N.m)
3.24	3.19	0.05	300	188.49	0.26	21.83	4.37
3.24	3.15	0.09	600	376.98	0.23	19.65	3.93
3.24	3.11	0.13	900	565.47	0.23	18.92	3.78
3.24	3.08	0.16	1200	753.96	0.21	17.47	3.49
3.24	3.05	0.19	1500	942.45	0.20	16.59	3.32

Table 5.39

Char temp: 950⁰C Load 10 N VF 10% Density (ρ) : 1.213 g/cc

m1 (gm)	m2 (gm)	Δm (gm)	Time (Sec)	SD (m)	WX10⁻⁵ (N/m)	W_vX10⁻¹¹ (m³/m)	W_sX10⁻¹¹ (m³/N.m)
2.82	2.72	0.10	300	188.49	0.52	43.74	4.37
2.82	2.64	0.18	600	376.98	0.47	39.36	3.94
2.82	2.57	0.25	900	565.47	0.43	36.45	3.64
2.82	2.50	0.32	1200	753.96	0.42	34.99	3.50
2.82	2.42	0.40	1500	942.45	0.42	34.99	3.50

Table 5.40

Char temp: 950⁰C Load 10 N VF 20% Density (ρ) : 1.211 g/cc

m1 (gm)	m2 (gm)	Δm (gm)	Time (Sec)	SD (m)	WX10⁻⁵ (N/m)	W_vX10⁻¹¹ (m³/m)	W_sX10⁻¹¹ (m³/N.m)
2.57	2.44	0.13	300	188.49	0.68	56.95	5.70
2.57	2.33	0.24	600	376.98	0.62	52.57	5.26
2.57	2.24	0.33	900	565.47	0.57	48.19	4.82
2.57	2.15	0.42	1200	753.96	0.55	46.00	4.60
2.57	2.04	0.53	1500	942.45	0.55	46.44	4.64

Table 5.41

Char temp: 950⁰C Load 10 N VF 30% Density (ρ) : 1.233 g/cc

m1 (gm)	m2 (gm)	Δm (gm)	Time (Sec)	SD (m)	WX10⁻⁵ (N/m)	W_vX10⁻¹¹ (m³/m)	W_sX10⁻¹¹ (m³/N.m)
3.18	3.05	0.13	300	188.49	0.68	55.94	5.59
3.18	2.99	0.19	600	376.98	0.49	40.88	4.09
3.18	2.96	0.22	900	565.47	0.38	31.55	3.16
3.18	2.91	0.27	1200	753.96	0.35	29.04	2.90
3.18	2.86	0.32	1500	942.45	0.33	27.54	2.75

Table 5.42

Char temp: 950⁰C Load 10 N VF 40% Density (ρ) : 1.215 g/cc

m1 (gm)	m2 (gm)	Δm (gm)	Time (Sec)	SD (m)	WX10⁻⁵ (N/m)	W_vX10⁻¹¹ (m³/m)	W_sX10⁻¹¹ (m³/N.m)
3.38	3.30	0.08	300	188.49	0.42	34.93	3.49
3.38	3.25	0.13	600	376.98	0.34	28.38	2.84
3.38	3.20	0.18	900	565.47	0.31	26.20	2.62
3.38	3.16	0.22	1200	753.96	0.29	24.02	2.40
3.38	3.12	0.26	1500	942.45	0.27	22.71	2.27

Table 5.43

Char temp: 950⁰C Load 15 N VF 10% Density (ρ) : 1.215 g/cc

m1 (gm)	m2 (gm)	Δm (gm)	Time (Sec)	SD (m)	WX10⁻⁵ (N/m)	W_vX10⁻¹¹ (m³/m)	W_sX10⁻¹¹ (m³/N.m)
2.99	2.90	0.09	300	188.49	0.47	39.36	2.62
2.99	2.83	0.16	600	376.98	0.42	34.99	2.33
2.99	2.76	0.23	900	565.47	0.40	33.53	2.24
2.99	2.71	0.28	1200	753.96	0.36	30.62	2.04
2.99	2.65	0.34	1500	942.45	0.35	29.74	1.98

Table 5.44

Char temp: 950⁰C Load 15 N VF 20% Density (ρ) : 1.211 g/cc

m1 (gm)	m2 (gm)	Δm (gm)	Time (Sec)	SD (m)	WX10⁻⁵ (N/m)	W_vX10⁻¹¹ (m³/m)	W_sX10⁻¹¹ (m³/N.m)
2.71	2.55	0.16	300	188.49	0.83	70.10	4.67
2.71	2.41	0.30	600	376.98	0.78	65.71	4.38
2.71	2.27	0.44	900	565.47	0.76	64.25	4.28
2.71	2.13	0.58	1200	753.96	0.75	63.52	4.23
2.71	1.99	0.72	1500	942.45	0.75	63.09	4.21

Table 5.45

Char temp: 950⁰C Load 15 N VF 30% Density (ρ) : 1.233 g/cc

m1 (gm)	m2 (gm)	Δm (gm)	Time (Sec)	SD (m)	$W \times 10^{-5}$ (N/m)	$W_v \times 10^{-11}$ (m³/m)	$W_s \times 10^{-11}$ (m³/N.m)
2.80	2.64	0.16	300	188.49	0.83	68.84	4.59
2.80	2.52	0.28	600	376.98	0.73	60.24	4.02
2.80	2.43	0.37	900	565.47	0.64	53.07	3.54
2.80	2.34	0.46	1200	753.96	0.60	49.48	3.30
2.80	2.26	0.54	1500	942.45	0.56	46.47	3.10

Table 5.46

Char temp: 950⁰C Load 15 N VF 40% Density (ρ) : 1.215 g/cc

m1 (gm)	m2 (gm)	Δm (gm)	Time (Sec)	SD (m)	$W \times 10^{-5}$ (N/m)	$W_v \times 10^{-11}$ (m³/m)	$W_s \times 10^{-11}$ (m³/N.m)
3.45	3.33	0.12	300	188.49	0.62	52.40	3.49
3.45	3.23	0.22	600	376.98	0.57	48.03	3.20
3.45	3.17	0.28	900	565.47	0.49	40.75	2.72
3.45	3.12	0.33	1200	753.96	0.43	36.02	2.40
3.45	3.07	0.38	1500	942.45	0.40	33.19	2.21

Table 5.47

Char temp: 950⁰C Load 20 N VF 10% Density (ρ) : 1.213 g/cc

m1 (gm)	m2 (gm)	Δm (gm)	Time (Sec)	SD (m)	WX10⁻⁵ (N/m)	W_vX10⁻¹¹ (m³/m)	W_sX10⁻¹¹ (m³/N.m)
3.07	2.95	0.12	300	188.49	0.62	52.40	2.62
3.07	2.88	0.19	600	376.98	0.49	41.48	2.07
3.07	2.83	0.24	900	565.47	0.42	34.93	1.75
3.07	2.79	0.28	1200	753.96	0.36	30.57	1.53
3.07	2.76	0.31	1500	942.45	0.32	27.07	1.35

Table 5.48

Char temp: 950⁰C Load 20 N VF 20% Density (ρ) : 1.211 g/cc

m1 (gm)	m2 (gm)	Δm (gm)	Time (Sec)	SD (m)	WX10⁻⁵ (N/m)	W_vX10⁻¹¹ (m³/m)	W_sX10⁻¹¹ (m³/N.m)
3.38	2.88	0.50	300	188.49	2.60	219.05	10.95
3.38	2.68	0.70	600	376.98	1.82	153.33	7.67
3.38	2.52	0.86	900	565.47	1.49	125.59	6.28
3.38	2.44	0.94	1200	753.96	1.22	102.95	5.15
3.38	2.40	0.98	1500	942.45	1.02	85.87	4.29

Table 5.49

Char temp: 950⁰C Load 20 N VF 30% Density (ρ) : 1.233 g/cc

m1 (gm)	m2 (gm)	Δm (gm)	Time (Sec)	SD (m)	WX10⁻⁵ (N/m)	W_vX10⁻¹¹ (m³/m)	W_sX10⁻¹¹ (m³/N.m)
3.02	2.78	0.24	300	188.49	1.25	103.27	5.16
3.02	2.58	0.44	600	376.98	1.14	94.66	4.73
3.02	2.44	0.58	900	565.47	1.01	83.19	4.16
3.02	2.32	0.70	1200	753.96	0.91	75.30	3.76
3.02	2.19	0.83	1500	942.45	0.86	71.43	3.57

Table 5.50

Char temp: 950⁰C Load 20 N VF 40% Density (ρ) : 1.215 g/cc

m1 (gm)	m2 (gm)	Δm (gm)	Time (Sec)	SD (m)	WX10⁻⁵ (N/m)	W_vX10⁻¹¹ (m³/m)	W_sX10⁻¹¹ (m³/N.m)
3.44	2.92	0.52	300	188.49	2.71	227.06	11.35
3.44	2.48	0.96	600	376.98	2.50	209.59	10.48
3.44	2.10	1.34	900	565.47	2.32	195.04	9.75
3.44	1.78	1.66	1200	753.96	2.16	181.21	9.06
3.44	1.44	2.00	1500	942.45	2.08	174.66	8.73

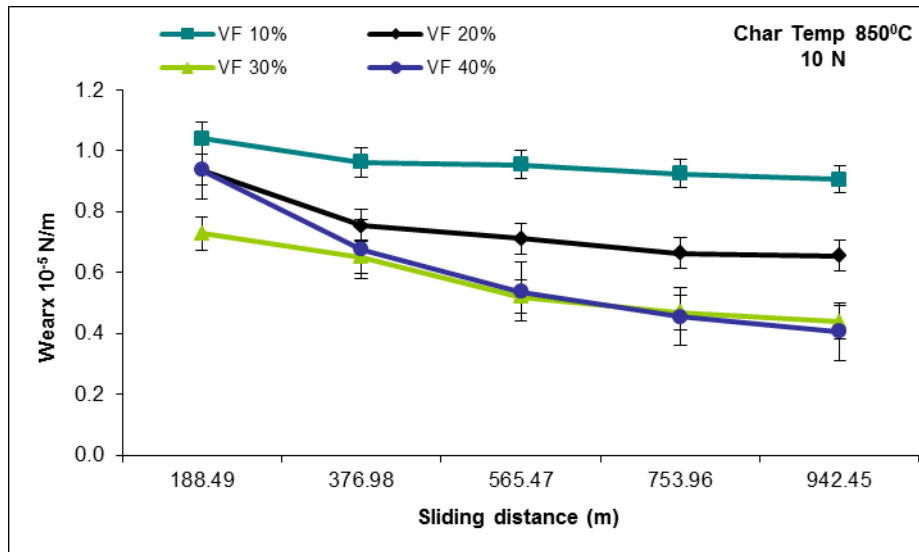


Figure-5.2 Variation of wear rate with sliding distance at load of 10N and carbonization temperature 850°C.

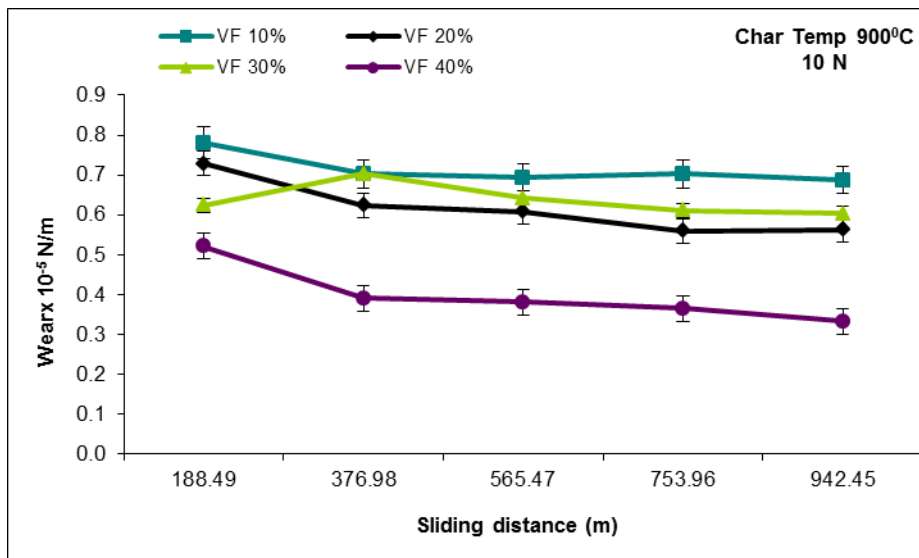


Figure-5.3 Variation of wear rate with sliding distance at load of 10N and carbonization temperature 900°C.

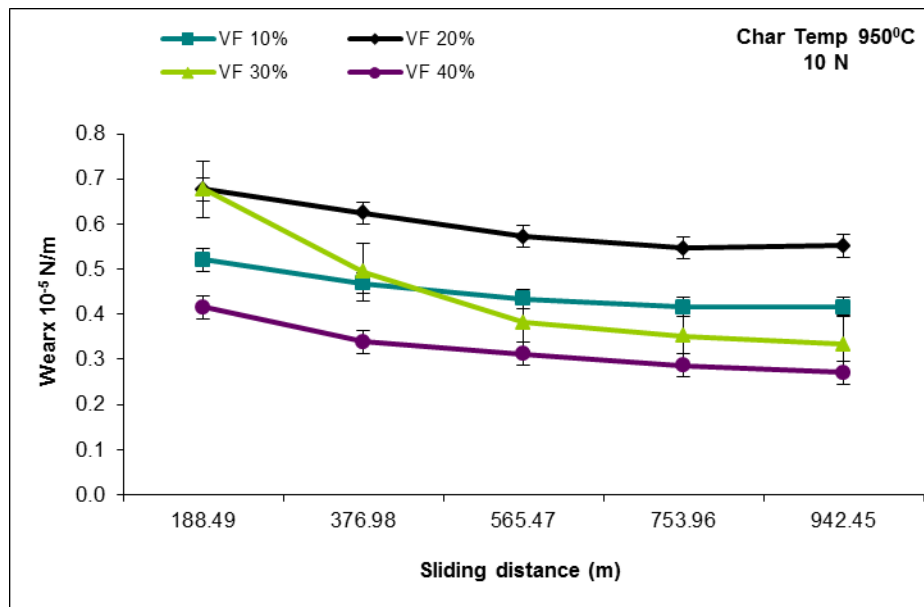


Figure-5.4 Variation of wear rate with sliding distance at load of 10N and carbonization temperature 950°C.

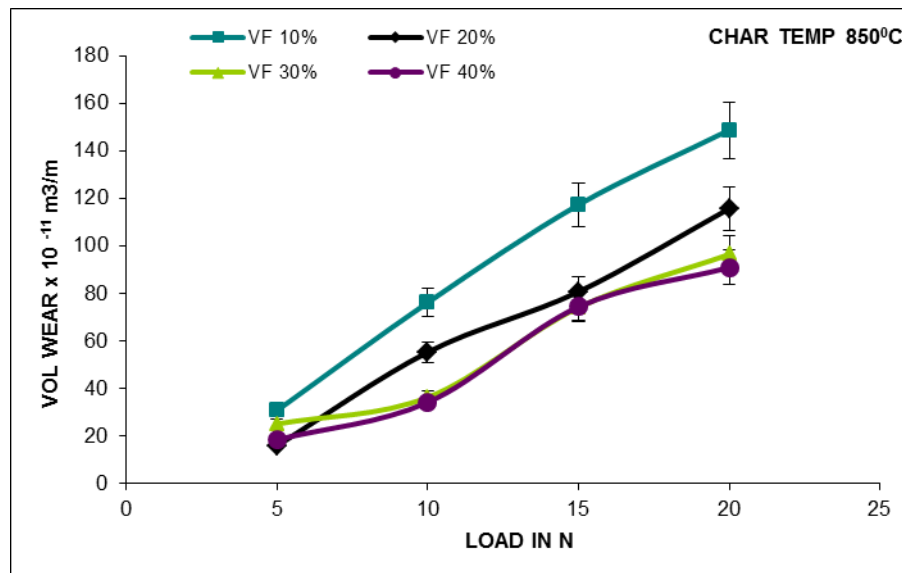


Figure-5.5 Variation of volumetric wear rate with normal load at sliding velocity of $v=0.633$ m/s and at different volume fraction.

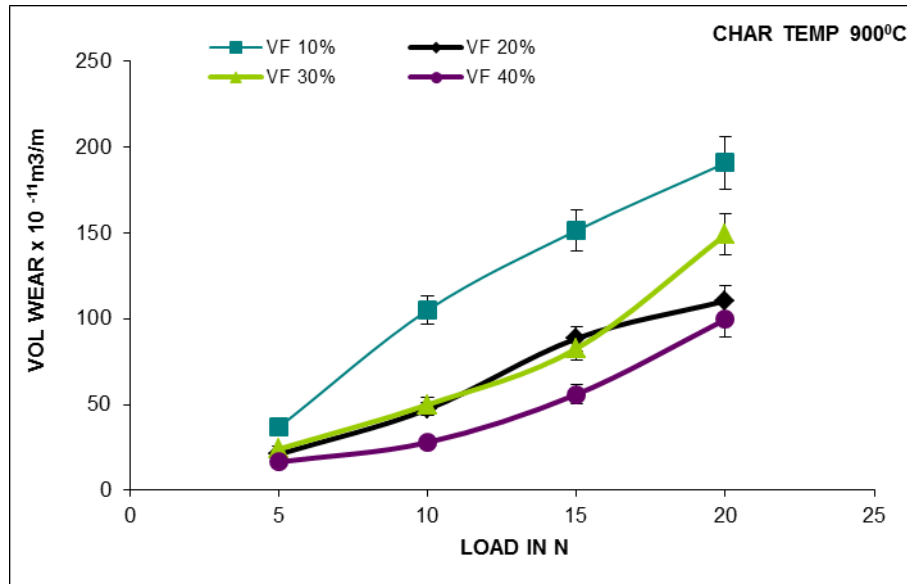


Figure-5.6 Variation of volumetric wear rate with normal load at sliding velocity of $v=0.633$ m/s and at different volume fraction.

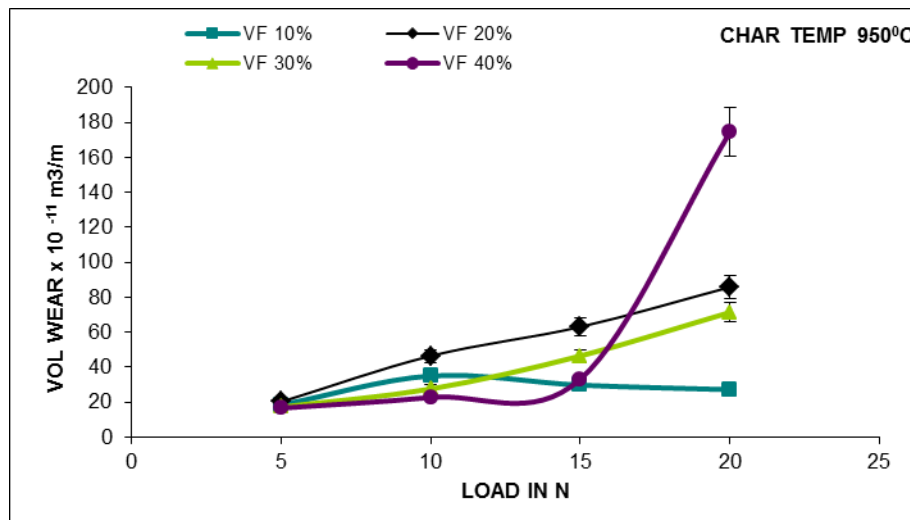


Figure-5.7 Variation of volumetric wear rate with normal load at sliding velocity of $v=0.633$ m/s and at different volume fraction.

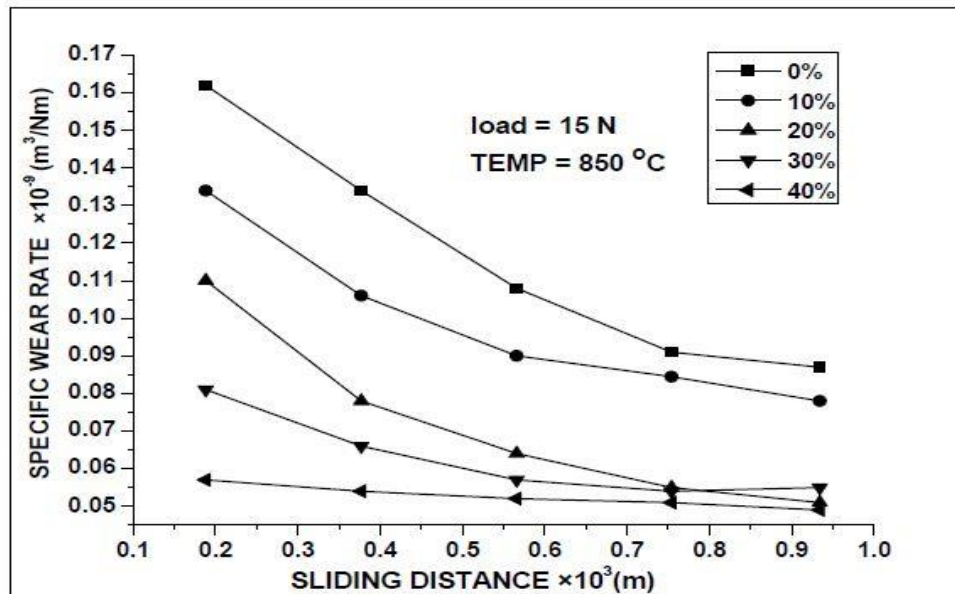


Figure 5.8 Variation of specific wear rate with sliding distance at sliding velocity of $v=0.633$ m/s and at different volume fraction at 15N normal load.

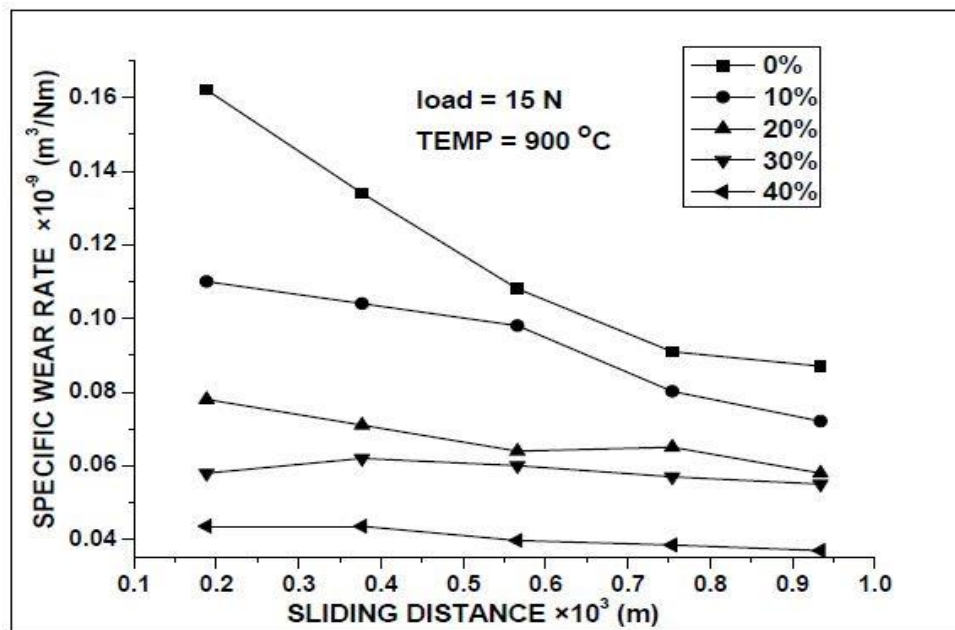


Figure 5.9 Variation of specific wear rate with sliding distance at sliding velocity of $v=0.633$ m/s and at different volume fraction at 15N normal load.

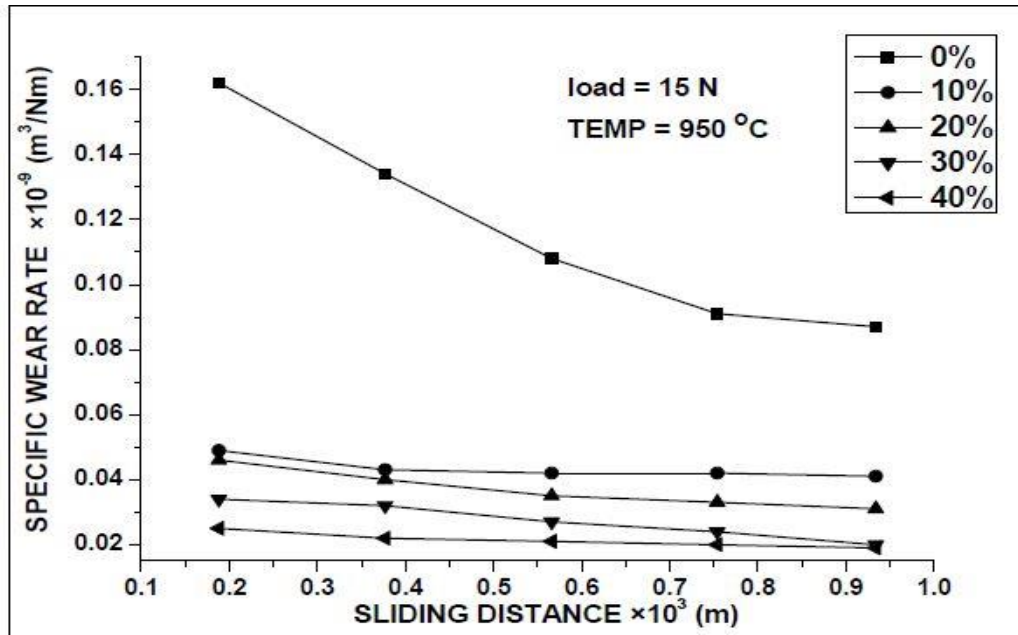


Figure 5.10 Variation of specific wear rate with sliding distance at sliding velocity of $v=0.633$ m/s and at different volume fraction at 15N normal load.

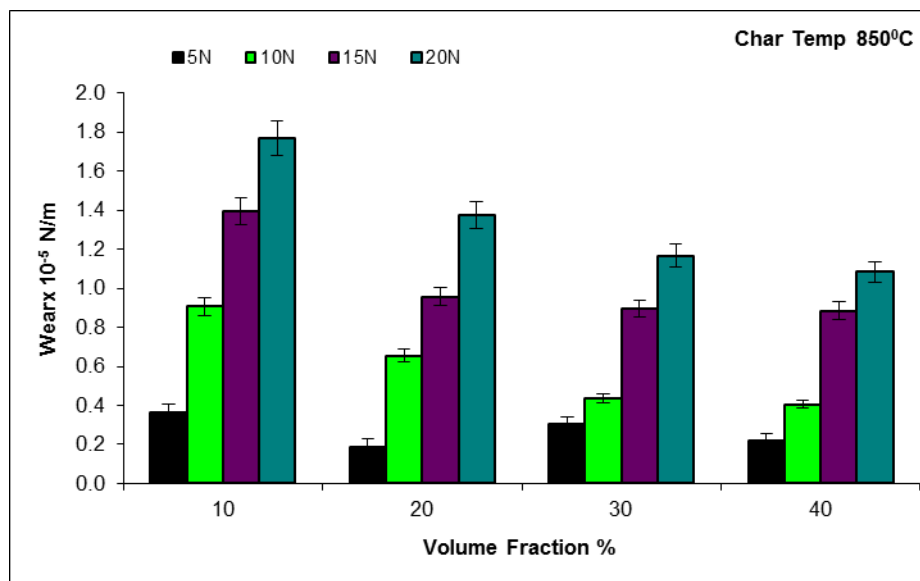


Figure-5.11 Variation of wear rate with volume fraction at different normal load with carbonization temperature 850°C.

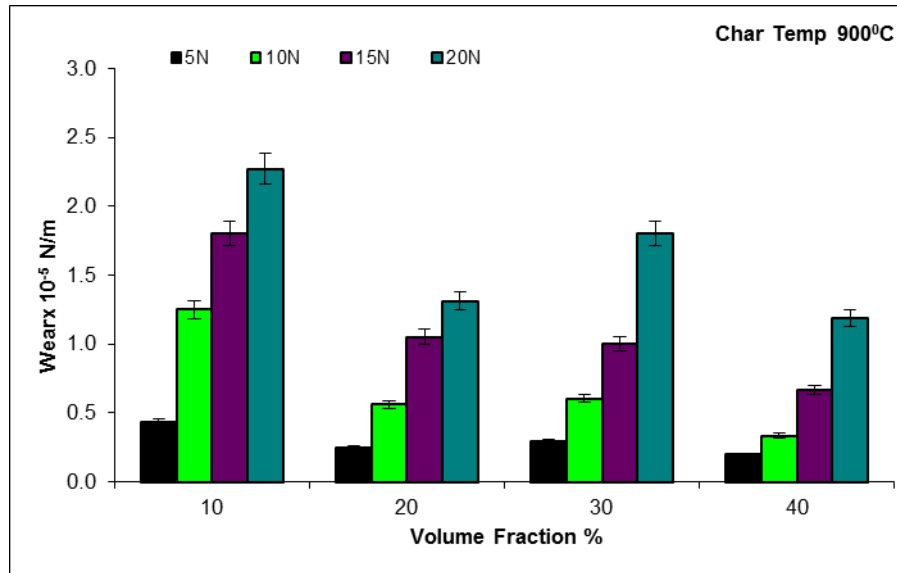


Figure-5.12 Variation of wear rate with volume fraction at different normal load with carbonization temperature 900°C.

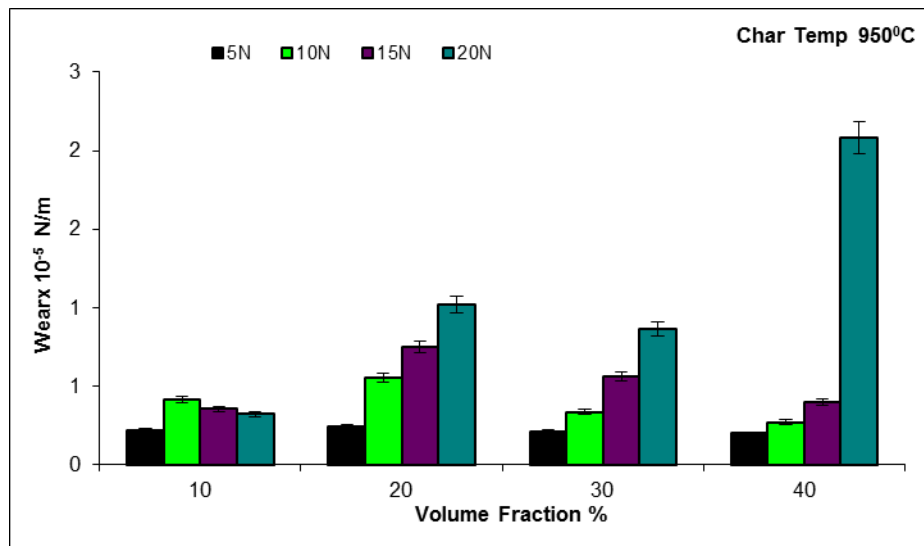


Figure-5.13 Variation of wear rate with volume fraction at different normal load with carbonization temperature 950°C.

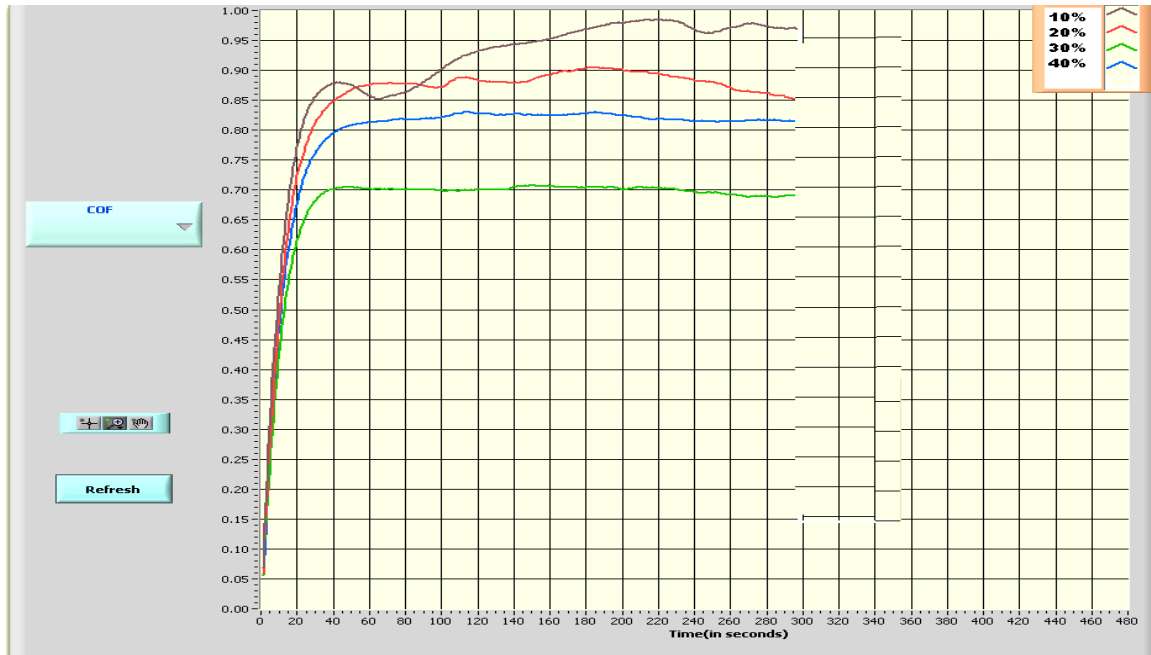


Figure-5.14 Plots between the friction coefficients and time for composites of different volume fraction at 20N applied normal load, 0.62832m/s sliding velocity and fiber made at 850° c .

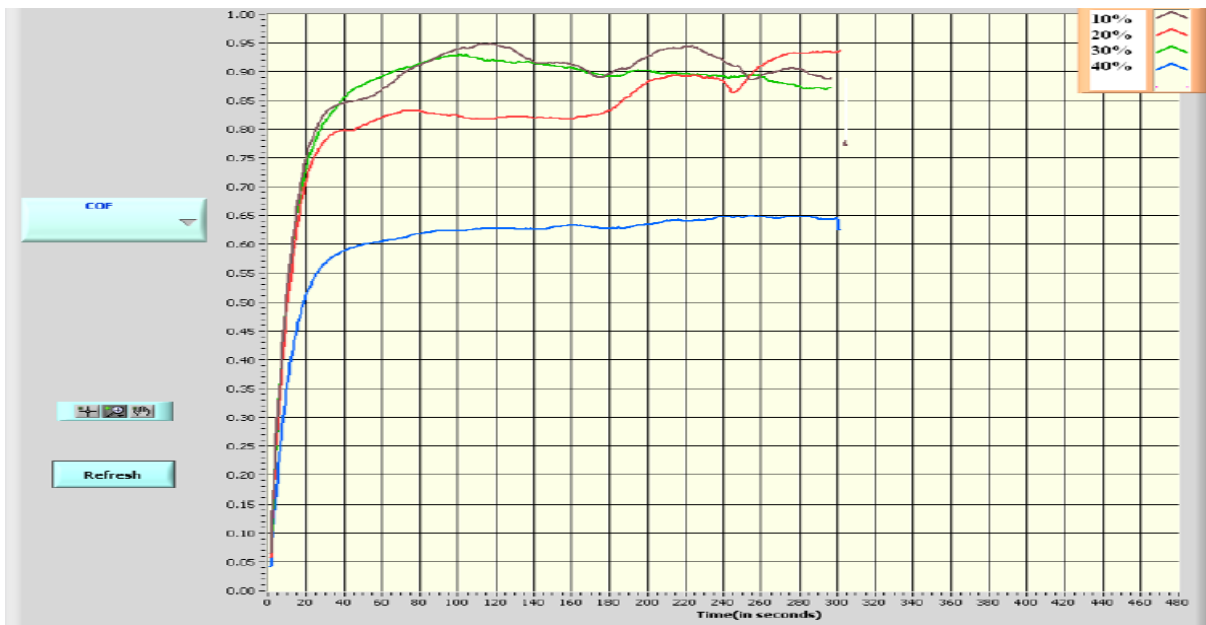


Figure-5.15 Plots between the friction coefficients and time for composites of different volume fraction at 20N applied normal load, 0.62832m/s sliding velocity and fiber made at 900° c .

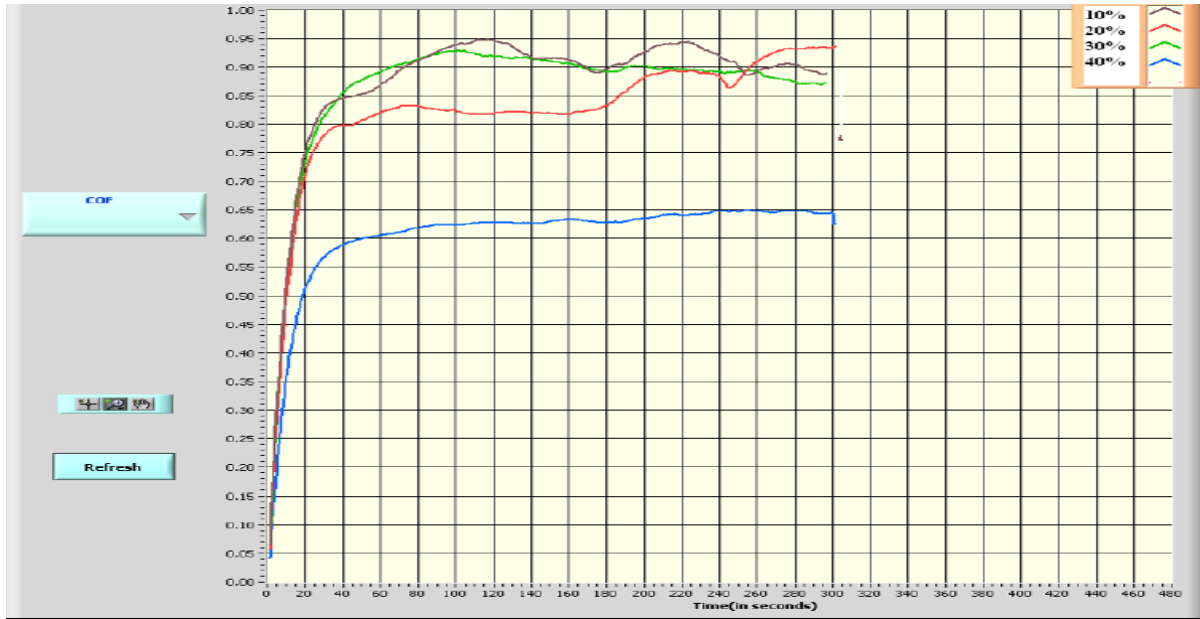


Figure-5.16 Plots between the friction coefficients and time for composites of different volume fraction at 20N applied normal load, 0.62832m/s sliding velocity and fiber made at 950°c .

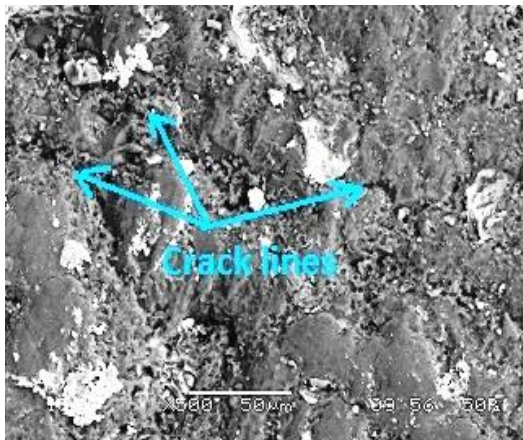


Figure-5.17 (a)

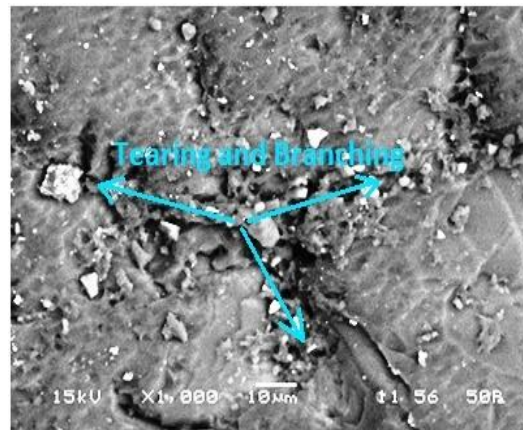


Figure-5.17 (b)

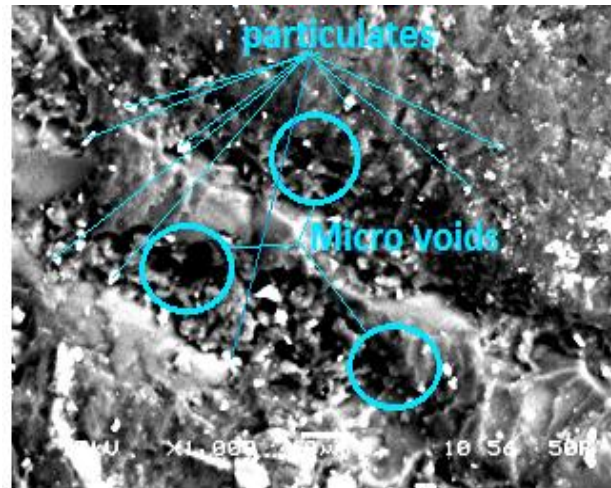


Figure-5.17(c)

Figure 5.17 Worn surface morphology of composite at different carbonization temperature of (a) 850°C (b) 900°C (c) 950 °C.

Chapter 6

SOLID PARTICLE EROSION STUDIES OF RICE HUSK EPOXY COMPOSITE

6.1 INTRODUCTION

Solid particle erosion occurs whenever hard particles along with gas or liquid medium impinged on a surface at any significant velocity which results in progressive loss of material from a solid surface due to mechanical interaction between that surface and the erodent particles. The structural components like gas turbine blade, helicopter rotor blades and wings of an aircraft are exposed to rainy and dusty environment at high speed encounter the problem of erosion. The process of erosion causes thinning of components, surface roughening, surface degradation, macroscopic scooping appearance and reduction in functional life of the structure. Hence, solid particle erosion has been considered as a serious problem as it is responsible for many failures in engineering applications. The studies of basic mechanisms of erosion were made in the last half of the 20th century and have been continued to the present. In the year of 1995 an article on the past and the future of erosion was presented by Finnie [208]. In this article, the influencing parameters and dominating mechanisms during solid particle erosion were reviewed, on the erosion response of metals and ceramic materials. In the same year another article was published by Meng et al. [209] to provide information about the existing wear models and prediction equations.

6.2 DEFINITION

According to Bitter [210], erosion is a material damage caused by the attack of particles entrained in a fluid system impacting the surface at high speed. Hutchings [211] defines it as an abrasive wear process in which the repeated impact of small particles entrained in a moving fluid against a surface result in the removal of material from the surface. Erosion due to the impact of solid particles can either be constructive (material removal desirable) or destructive (material removal undesirable), and therefore, it can be desirable to either minimize or maximize erosion, depending on the application. The constructive applications include sand blasting, high-speed water-jet cutting, blast stripping of paint from aircraft and automobiles, blasting to remove the adhesive flash from bonded parts, erosive drilling of hard materials. Whereas the solid particle erosion is destructive in industrial applications such as erosion of machine parts, surface degradation of steam turbine blades, erosion of pipelines carrying slurries and particle erosion in fluidized bed combustion systems. In most erosion processes, target material removal typically occurs as the result of a

large number of impacts of irregular angular particles, usually carried in pressurized fluid streams.

6.3 SOLID PARTICLE EROSION OF POLYMER COMPOSITES

Polymers are finding an ever increasing application as structural materials in various components and engineering systems. The high specific strength and stiffness of polymers are primarily responsible for their popularity. These composites after being widely accepted in household, automobiles and in aerospace applications are heading their way towards tribological application. Depending upon the application area such as surfing boats, gas and steam turbine blades, conveyor belts, gears of locomotives, pump impellers in mineral slurry processing units, their components generally encounter lots of abrasion from dust, sand, slurry of solid particles and finally fails. This type of failure is generally termed as erosive wear [212-214]

Many researchers have evaluated the resistance of various types of polymers like nylon, epoxy, polypropylene, bismileimide, etc and their composites to solid particle erosion. Harsha et al. [215] has summarized the work done by some of the investigators on solid particle erosion of polymer composites. Roy et al. while working on erosive wear of polymer composite revealed that the composite materials present a rather poor erosion resistance as compared to metallic materials [216].

The most important factors influencing the erosion rate of the composite materials can be summarized under four categories; (i) The properties of the target materials (matrix material properties and morphology, reinforcement type, amount and orientation, interface properties between the matrices and reinforcements, etc.), (ii) Environment and testing conditions (temperature, chemical interaction of erodent with the target), (iii) Operating parameters (angle of impingement, impinging velocity, particle flux–mass per unit time, etc.) and (iv) The properties of the erodent (size, shape, type, hardness, etc.) [214, 217-219]. This given us an idea that the erosion resistance of any material can be evaluated, if we investigate the combine effect of all or some of these parameters. In general, erosive behavior of materials can be grouped into ductile and brittle when erosion rate is evaluated as a function of impact angle. The ductile behaviour is characterized by maximum erosion at low impact angle in the range of 15°–30°. On the other hand, if maximum erosion occurs at 90°, then the behaviour can be termed as brittle. Reinforced composites have also been some time found to

exhibit an intermediate behaviour known as semi-ductile with maximum erosion occurring at an angle in the range of 45°–60° [220]. However, the above classification is not absolute as the erosion behaviour of a material has a strong dependence on erosion conditions such as impact angle, impact velocity and erodent properties such as shape, hardness, size etc. In the literature, the erosion behaviour of polymers and its composites has also been characterized by the value of the velocity exponent, ' n ' ($E \propto v^n$) [212].

In the pursuit of visualizing the influence of the natural fiber reinforced polymer composite for tribological applications, extensive research work has already been published on various type of polymers and fibers[218,221-223]. Mishra and Acharya [224] Deo and Acharya [225] and Gupta et.al. [226] Have utilized sugarcane; lantana camara and bamboo fiber reinforcement in thermoset polymer to enhance the erosive wear resistance of pure polymer. Recently Mohanty et.al. [227] and Ojha et.al. [228] studied the erosive wear behavior of Date Palm leaf fiber reinforced polyvinyl alcohol composite and wood apple shell particle fiber reinforced epoxy composite and have reported the enhancement in wear resistance due to incorporation of these fibers in matrix. Basing on the above works, in this present investigation an attempt has been made to study the erosive wear behaviors of Rice Husk (RH) reinforced epoxy composite. In the present work the influence of impinging velocity, impingement angle and fiber loading on erosive wear has been carried out and results of these investigations are presented in the subsequent sections.

6.4 EXPERIMENT

6.4.1 Preparation for the test specimens

The preparation of the test specimens were carried out as per the procedure discussed in chapter-3, Art-3.4.3. Specimens of dimension 30 x 30 x 3.0 mm were cut from the composite slabs. Adequate care has been taken to keep the thickness constant (3mm) for all the samples.

6.4.2 Test apparatus & Experiment

The schematic figure of the erosion test apparatus used for the present investigation designed as per ASTM-G76 standard is shown in figure 6.1. The rig consists of an air compressor, a particle feeder, and an air particle mixing and accelerating chamber. The compressed dry air is mixed with the erodent particles, which are fed at a constant rate from a conveyor belt-type feeder in to the mixing chamber and then accelerated by passing the mixture through a tungsten carbide converging nozzle of 4 mm diameter. These accelerated particles impact the specimen, and the specimen could be held at various angles with respect to the impacting particles using an adjustable sample holder. The test apparatus has also been fitted with a rotating double disc to measure the velocity of the erodent particle. The impact velocities of the erodent particles has been evaluated experimentally using this rotating double disc method developed as explained by Ives and Ruff [229]. The velocities obtained from this method for various pressures are given in Table-6.1.

The conditions under which the erosion test has been carried out are given in Table 6.2. A standard test procedure is employed for each erosion test. The samples are cleaned in acetone, dried and weighed to an accuracy of 1×10^{-3} gm using an electronic balance, prior and after each test. The test samples after loading in the test rig were eroded for 3 min. at a given impingement angle and then weighed again to determine weight loss (Δw). The erosion rate (E_r) is then calculated by using the following equation:

$$E_r = \frac{\Delta w}{w_e} \quad (6.1)$$

Where Δw is the mass loss of test sample in gm and w_e is the mass of eroding particles (i.e., testing time \times particle feed rate). This procedure has been repeated until the erosion rate attains a constant steady-state value. In the present study the same procedure is repeated for 5 times (i.e. expose time was 5min).

The erosion efficiency (η) for the process was obtained by using the equation:

$$\eta = \frac{2E_r H}{\rho \times v^2} \quad (6.2)$$

Where ' E_r ' is erosion rate (kg/kg), ' H ' is hardness of eroding material (Pa) and ' v ' is velocity of impact (m/s), proposed by Sundararajan et al. [230]. Erosive experiments were conducted with specimen reinforced with plain rice husk with different doses of rice husk (5, 10, 15 and 20 vol. %) .To increase the performance of the fiber in the composite the fiber surface were modified with acetone, alkali and Benzolyzation treatment. Experiment on the treated fiber composite with same volume fraction of fiber as conducted for plain rice husk were also carried out. Erosion test for plain rice husk and modified rice husk epoxy composite for different volume fraction of fiber with different impingement angle and velocities are tabulated and presented in table 6.3 to 6.18

6.5 RESULT AND DISCUSSION

Based on the tabulated results various graphs were plotted and presented in Figure-6.2 to 6.25 for different percentage of reinforcement under different test conditions.

Figure-6.2 to 6.17 illustrate the erosion wear rates of both treated and plain RH reinforced epoxy composite as a function of impingement angle under different impact velocities (48m/s to 109m/s) . It is observed that Rice Husk epoxy composite shows peak erosion rate ($E_{r \max}$) at 45° impact angle at low velocity (48, 70 m/sec) and the peak erosion shift towards 60° as the velocity of impingement increases (i.e. at 82 and 109 m/s).Minimum erosion rate ($E_{r \min}$) is observed at an impact angle of 30° for all composite under all velocity of impact. It is known that impact angle is one of the most important parameter for classifying the erosion behavior of the materials. In the literature materials are classified as ductile or brittle based on the dependence of their erosion rate. It has been recognized that peak erosion exists at low impact angles (15°–30°) for ductile materials and at a high impact angle (90°) for brittle materials [231]. However the maximum erosion occurring in the angular range between 45°–60° indicates the semi-ductile behavior of the material [232]. From the experiment result it is seen that maximum erosion occur at 45°, for RH composites respond to solid particle impact neither behaves in a purely ductile nor in a purely brittle

manner. This behaviour can be termed as semi-ductile in nature. The same type of behavior was also reported by Biswas et al. [233] while studying the erosive behaviour of red mud filled Bamboo-epoxy composite. N.Sari et.al [234] while studying the Erosive wear behaviour of carbon fibre/polyetherimide composites under low particle speed have reported increase in particle speed results in more brittle response of the material, the angle which causes highest wear rate shift to higher angle. However the interesting point here is that at higher velocity the maximum erosion from 45° shifted towards 60° impact angle for treated fiber composite. This gives an indication that the ductile behavior of the composite shifted towards the brittle behavior.

It is further noticed that irrespective of impact velocity and impact angle, the erosion rate decreases with increase in volume fraction. The RH composite with 20 vol% volume fraction has lowest erosion at all angle and all velocity. Further treated fiber composite shows lower erosion rate with respect to plain rice husk composite. Among all types of treated condition Benzoyl chloride treated fiber composite gives the best result i.e. the erosion rate is minimum for these fibers.

The variation of steady-state erosion rate of all composite samples with impact velocity at different impact angles are shown in the form of a histogram in Figure-6.18 to 6.21. It can be observed from these histograms that erosion rate of all composite samples increases with increase in the impact velocity. Irrespective of impingement angle and impact velocity, there is a steady decrease in erosion rate with increase in fiber content has also observed. However, the observation is contrary to the report by Miyazaki et al. [235], while worked with glass and carbon fiber reinforced polyether ketone composites. This may be possible due to the fact that in a continuous fiber composite, the perpendicular impact of erodent on the fiber causes micro-bending of fiber, leading to breakages, de-bonding and finally higher erosion [219]. It is also found from these plots that Benzoyl chloride treated fiber composite gives the minimum erosion rate with all impact velocities.

In the solid particle impact experiments the impact velocity of the erosive particles has a very strong effect on erosion rate. For any material, once steady state conditions have reached, the erosion rate ' E_r ' can be expressed as a simple power function of impact velocity (v) [212]:

$$E_r = kv^n \quad (6.3)$$

Where k is the constant of proportionality includes the effect of all the other variables. The value of ' n ' and ' k ' are found by least-square fitting of the data points in plots which represent the erosion rate dependence on impact velocity by using the power law. The value of ' n ', the velocity exponent, is typically between 2 and 3, although much higher exponent is seen under some circumstances [216]. According to Pool et. al. [212], for polymeric materials behaving in ductile manner, the velocity exponent ' n ' varies in the range 2-3 while for polymer composites behaving in brittle fashion the value of ' n ' should be in the range of 3-5. Figure 6.22 to 6.25 illustrates the erosion rate with impact velocity at 60° impingement angle for plain and treated fiber composite. From these figure it is clear that steady state erosion rate of all composite (i.e. for different chemically modified fibers) increases with increase in impact velocity. The least-square fits to data point were obtained by using power law and the values of ' n ' and ' k ' are summarized in Table-6.19 to 6.22. The velocity exponents found for PRH, Acetone trated, Alkali treated and Benzoyl Chloride Treated RH composites are in the range of 2.53-3.14, 2.5-3.19, 2.4-3.15 and 2.38- 3.19 respectively. This velocity exponent at various impingement angles are in conformity with Harsha et al. [221].

It has been reported by Sundararajan et al. [216, 226] that the erosion efficiency (η), can be used to characterize the nature and mechanism of erosion. They also showed that the ductile material possesses very low erosion efficiency i.e. is very $\eta \lll 100\%$, where as the brittle material exhibits an erosion efficiency even greater than 100%. The values of erosion efficiencies of composites under this study are calculated using equation-6.2 and are listed in Table-6.23 to 6.26 along with their hardness values and operating conditions. According to the categorization made by Roy et al. [216], it has been observed that the erosion efficiencies of Rice Husk epoxy composite varies from 1.532% to 5.44% for different impact velocities, indicating a semi-ductile erosion response. Similar observations are also reported by Srivastava et al. [236] for glass fiber epoxy composite. Thus it can be conclude that the erosion efficiency is not exclusively a material property; but also depends on other operational variables such as impact velocity and impingement angle. The data shown in Table-6.23 to 6.26 also indicates that the erosion efficiency of Rice Husk epoxy composite

varies with increase in fiber content and sometime with impact velocity . This lower erosion efficiency of rice husk composite indicates a better erosion resistance .

6.6 SURFACE MORPHOLOGY

The morphology of the untreated and treated fiber surfaces has been studied using scanning electron microscope (SEM) JEOL JSM-6480LV. The sample surfaces were platinum coated to make them conductive prior to SEM observation. The eroded surfaces of RH-epoxy composites subjected to 45° impingement angle are shown in figure 6.26 .Figure 6.26(a) shows the surface of 20 vol% of plain rice husk epoxy composite. It can be seen from the surface of the samples that due to impingement of the erodent a crater has been formed indicating easy removal of material from the surface of the composite. Material removal is mainly due to micro-cutting and micro-drilling. Figure 6.26(b-d) shows the micrograph of surfaces of 20 vol% of Rice Husk epoxy composite for Acetone ,Alkali and Benzoyl Chloride treated fiber composite. It can be said that in all the treated fiber composite due to good compatibility of fiber with the matrix there is less removal of material. Matrix cracking is seen in alkali treated (c) fiber composite but fibers are still found to be intact .For Benzoyl chloride treated fiber (d) composite pulverization type surface damage is found on the surface. This means the pulverized wear debris adhered to the matrix and helps in reducing further wear of the composite. This also confirms experimental results that Benzoyl chloride treated fiber composite gives the minimum erosion rate.

6.7 CONCLUSIONS

The solid particle erosion study of Rice Husk reinforced epoxy composites for various impingement angles and impact velocities led to the following conclusions:

- The influence of impingement angle on erosive wear of composites under consideration exhibits pseudo semi-ductile erosive wear behaviour with maximum wear rate at 45° impingement angle at lower velocities. The maximum wear rate occurs at 60° at higher velocities.

- The erosion rate of composites decreases with increase in fiber content and velocity of impact.
- In RH epoxy composites the erosion rate (E_r) displays power law behaviour with particle velocity (v), $E_r \propto v^n$, where 'n' varies from 2.38 to 3.19. The erosion rate increases with increase in velocity.
- The erosion efficiency (η) values obtained experimentally also indicate that the Rice Husk reinforced epoxy composites exhibit semi-ductile erosion response (1.532% to 5.44%).
- The chemical treatment of Rice Husk reduces the erosion rate. The chemical treatment of Rice Husk with Benzoyl Chloride offers maximum erosion resistance.
- The morphologies of eroded surface of the samples observed by SEM indicate that, material removal is mainly due to micro-cutting and micro-ploughing.

Table-6.1 Particle velocity under different air pressure

Sl. No.	Air Pressure (Bar)	Particle velocity (m/s)
1	1	48
2	2	70
3	3	82
4	4	109

Table-6.2 Experimental condition for the erosion test

Test parameters

Erodent:	Silica sand
Erodent size (μm):	200 \pm 50
Erodent shape:	Angular
Hardness of silica particles (HV):	1420 \pm 50
Impingement angle (α^0):	30, 45, 60 and 90
Impact velocity (m/s):	48, 70, 82 and 109.
Erodent feed rate (gm/min):	11 \pm 0.02
Test temperature:	(27 ^0C)
Nozzle to sample distance (mm):	10

Table-6.3 weight loss and erosion rate of 5% plain rice husk epoxy composites with respect to impingement angle due to erosion for a period of 300 seconds.

Velocity (m/s)	Impact Angle (^o)	PRH 5%	
		Weight loss (Δw) (g)	Erosion Rate x 10 ⁻⁴ (g/g)
48	30	0.010	1.853
	45	0.012	2.240
	60	0.009	1.700
	90	0.007	1.309
70	30	0.020	3.636
	45	0.045	8.255
	60	0.037	6.764
	90	0.024	4.450
82	30	0.044	8.000
	45	0.063	11.436
	60	0.071	12.891
	90	0.051	9.200
109	30	0.083	15.000
	45	0.100	18.182
	60	0.108	19.564
	90	0.082	14.891

Table-6.4 weight loss and erosion rate of 10% plain rice husk epoxy composites with respect to impingement angle due to erosion for a period of 300 seconds.

Velocity (m/s)	Impact Angle (^o)	PRH 10%	
		Weight loss (Δw) (g)	Erosion Rate x 10 ⁻⁴ (g/g)
48	30	0.008	1.469
	45	0.012	2.151
	60	0.009	1.600
	90	0.007	1.335
70	30	0.025	4.491
	45	0.039	7.109
	60	0.035	6.309
	90	0.021	3.782
82	30	0.043	7.727
	45	0.060	10.836
	60	0.066	11.945
	90	0.048	8.727
109	30	0.080	14.455
	45	0.095	17.291
	60	0.103	18.764
	90	0.076	13.873

Table-6.5 weight loss and erosion rate of 15% plain rice husk epoxy composites with respect to impingement angle due to erosion for a period of 300 seconds.

Velocity (m/s)	Impact Angle ($^{\circ}$)	PRH 15%	
		Weight loss (Δw) (g)	Erosion Rate x 10^{-4} (g/g)
48	30	0.009	1.633
	45	0.011	2.007
	60	0.008	1.480
	90	0.006	1.164
70	30	0.017	3.145
	45	0.036	6.618
	60	0.031	5.636
	90	0.021	3.782
82	30	0.035	6.327
	45	0.052	9.400
	60	0.058	10.545
	90	0.042	7.600
109	30	0.075	13.636
	45	0.086	15.673
	60	0.097	17.618
	90	0.073	13.182

Table-6.6 weight loss and erosion rate of 20% plain rice husk epoxy composites with respect to impingement angle due to erosion for a period of 300 seconds.

Velocity (m/s)	Impact Angle (^o)	PRH 20%	
		Weight loss (Δw) (g)	Erosion Rate x 10 ⁻⁴ (g/g)
48	30	0.006	1.169
	45	0.009	1.562
	60	0.007	1.336
	90	0.007	1.229
70	30	0.018	3.273
	45	0.033	5.927
	60	0.028	5.091
	90	0.019	3.364
82	30	0.031	5.600
	45	0.045	8.127
	60	0.052	9.527
	90	0.040	7.255
109	30	0.069	12.545
	45	0.078	14.127
	60	0.089	16.218
	90	0.068	12.418

Table-6.7 weight loss and erosion rate of 5% Acetone treated RH Epoxy composites with respect to impingement angle due to erosion for a period of 300 seconds.

Velocity (m/s)	Impact Angle (⁰)	Acetone 5%	
		Weight loss (Δw) (g)	Erosion Rate x 10 ⁻⁴ (g/g)
48	30	0.010	1.753
	45	0.012	2.164
	60	0.010	1.805
	90	0.006	1.175
70	30	0.024	4.436
	45	0.045	8.164
	60	0.036	6.545
	90	0.023	4.182
82	30	0.041	7.382
	45	0.056	10.255
	60	0.068	12.364
	90	0.045	8.145
109	30	0.077	14.055
	45	0.094	17.055
	60	0.101	18.364
	90	0.079	14.400

Table-6.8 weight loss and erosion rate of 10% Acetone treated RH epoxy composites with respect to impingement angle due to erosion for a period of 300 seconds.

Velocity (m/s)	Impact Angle (^o)	Acetone 10%	
		Weight loss (Δw) (g)	Erosion Rate x 10 ⁻⁴ (g/g)
48	30	0.009	1.725
	45	0.011	2.087
	60	0.009	1.549
	90	0.008	1.442
70	30	0.023	4.182
	45	0.037	6.691
	60	0.033	6.000
	90	0.020	3.636
82	30	0.039	7.091
	45	0.056	10.182
	60	0.063	11.527
	90	0.053	9.691
109	30	0.075	13.636
	45	0.090	16.400
	60	0.097	17.709
	90	0.085	15.527

Table-6.9 weight loss and erosion rate of 15% Acetone treated RH epoxy composites with respect to impingement angle due to erosion for a period of 300 seconds.

Velocity (m/s)	Impact Angle ($^{\circ}$)	Acetone 15%	
		Weight loss (Δw) (g)	Erosion Rate x 10^{-4} (g/g)
48	30	0.009	1.573
	45	0.011	1.913
	60	0.008	1.373
	90	0.006	1.091
70	30	0.023	4.091
	45	0.034	6.091
	60	0.028	5.091
	90	0.023	4.182
82	30	0.033	6.000
	45	0.048	8.800
	60	0.054	9.891
	90	0.046	8.309
109	30	0.071	12.855
	45	0.080	14.545
	60	0.093	16.891
	90	0.077	14.055

Table-6.10 weight loss and erosion rate of 20% Acetone treated RH epoxy composites with respect to impingement angle due to erosion for a period of 300 seconds.

Velocity (m/s)	Impact Angle ($^{\circ}$)	Acetone 20%	
		Weight loss (Δw) (g)	Erosion Rate x 10^{-4} (g/g)
48	30	0.006	1.053
	45	0.008	1.475
	60	0.007	1.218
	90	0.007	1.209
70	30	0.015	2.727
	45	0.028	5.145
	60	0.023	4.145
	90	0.016	2.896
82	30	0.028	5.000
	45	0.041	7.527
	60	0.049	8.836
	90	0.037	6.782
109	30	0.062	11.345
	45	0.067	12.255
	60	0.086	15.564
	90	0.073	13.327

Table-6.11 weight loss and erosion rate of 5% Alkali treated RH epoxy composites with respect to impingement angle due to erosion for a period of 300 seconds.

Velocity (m/s)	Impact Angle (^o)	Alkali 5%	
		Weight loss (Δw) (g)	Erosion Rate x 10 ⁻⁴ (g/g)
48	30	0.008	1.515
	45	0.011	2.078
	60	0.008	1.527
	90	0.008	1.382
70	30	0.027	4.873
	45	0.040	7.273
	60	0.031	5.618
	90	0.023	4.182
82	30	0.040	7.273
	45	0.050	9.091
	60	0.063	11.527
	90	0.049	8.836
109	30	0.070	12.727
	45	0.088	16.000
	60	0.094	17.055
	90	0.074	13.527

Table-6.12 weight loss and erosion rate of 10% Alkali treated RH epoxy composites with respect to impingement angle due to erosion for a period of 300 seconds.

Velocity (m/s)	Impact Angle (^o)	Alkali 10%	
		Weight loss (Δw) (g)	Erosion Rate x 10 ⁻⁴ (g/g)
48	30	0.008	1.424
	45	0.011	1.971
	60	0.008	1.442
	90	0.007	1.256
70	30	0.016	2.998
	45	0.033	6.036
	60	0.029	5.182
	90	0.018	3.200
82	30	0.035	6.273
	45	0.047	8.509
	60	0.060	10.818
	90	0.044	7.909
109	30	0.063	11.473
	45	0.080	14.545
	60	0.090	16.291
	90	0.064	11.636

Table-6.13 weight loss and erosion rate of 15% Alkali treated RH epoxy composites with respect to impingement angle due to erosion for a period of 300 seconds.

Velocity (m/s)	Impact Angle (⁰)	Alkali 15%	
		Weight loss (Δw) (g)	Erosion Rate x 10 ⁻⁴ (g/g)
48	30	0.008	1.402
	45	0.010	1.796
	60	0.007	1.253
	90	0.005	0.987
70	30	0.016	2.836
	45	0.028	5.091
	60	0.023	4.200
	90	0.019	3.418
82	30	0.025	4.600
	45	0.042	7.636
	60	0.050	9.164
	90	0.036	6.545
109	30	0.059	10.655
	45	0.069	12.600
	60	0.084	15.182
	90	0.066	12.018

Table-6.14 weight loss and erosion rate of 20% Alkali treated RH epoxy composites with respect to impingement angle due to erosion for a period of 300 seconds.

Velocity (m/s)	Impact Angle (⁰)	Alkali 20%	
		Weight loss (Δw) (g)	Erosion Rate x 10 ⁻⁴ (g/g)
48	30	0.005	0.905
	45	0.007	1.335
	60	0.006	1.164
	90	0.006	1.104
70	30	0.013	2.331
	45	0.023	4.255
	60	0.019	3.473
	90	0.015	2.718
82	30	0.023	4.164
	45	0.035	6.436
	60	0.044	8.036
	90	0.033	6.000
109	30	0.051	9.273
	45	0.060	10.964
	60	0.078	14.236
	90	0.061	11.073

Table-6.15 weight loss and erosion rate of 5% Benzoyl Chloride treated RH epoxy composites with respect to impingement angle due to erosion for a period of 300 seconds.

Velocity (m/s)	Impact Angle (⁰)	Benzoyl 5%	
		Weight loss (Δw) (g)	Erosion Rate x 10 ⁻⁴ (g/g)
48	30	0.009	1.600
	45	0.011	2.000
	60	0.008	1.464
	90	0.007	1.236
70	30	0.018	3.236
	45	0.036	6.618
	60	0.029	5.236
	90	0.020	3.636
82	30	0.037	6.636
	45	0.046	8.364
	60	0.058	10.618
	90	0.045	8.255
109	30	0.065	11.891
	45	0.082	14.891
	60	0.089	16.091
	90	0.071	12.964

Table-6.16 weight loss and erosion rate of 10% Benzoyl Chloride treated RH epoxy composites with respect to impingement angle due to erosion for a period of 300 seconds.

Velocity (m/s)	Impact Angle ($^{\circ}$)	Alkali 10%	
		Weight loss (Δw) (g)	Erosion Rate x 10^{-4} (g/g)
48	30	0.008	1.424
	45	0.011	1.971
	60	0.008	1.442
	90	0.007	1.256
70	30	0.016	2.998
	45	0.033	6.036
	60	0.029	5.182
	90	0.018	3.200
82	30	0.035	6.273
	45	0.047	8.509
	60	0.060	10.818
	90	0.044	7.909
109	30	0.063	11.473
	45	0.080	14.545
	60	0.090	16.291
	90	0.064	11.636

Table-6.17 weight loss and erosion rate of 15% Benzoyl Chloride treated RH epoxy composites with respect to impingement angle due to erosion for a period of 300 seconds.

Velocity (m/s)	Impact Angle (⁰)	Benzoyl 15%	
		Weight loss (Δw) (g)	Erosion Rate x 10 ⁻⁴ (g/g)
48	30	0.007	1.249
	45	0.009	1.615
	60	0.006	1.133
	90	0.006	1.038
70	30	0.011	1.927
	45	0.025	4.545
	60	0.020	3.636
	90	0.017	3.000
82	30	0.030	5.364
	45	0.037	6.636
	60	0.047	8.473
	90	0.039	7.055
109	30	0.053	9.673
	45	0.061	11.145
	60	0.078	14.200
	90	0.059	10.764

Table-6.18 weight loss and erosion rate of 20% Benzoyl Chloride treated RH epoxy composites with respect to impingement angle due to erosion for a period of 300 seconds.

Velocity (m/s)	Impact Angle (^o)	Benzoyl 20%	
		Weight loss (Δw) (g)	Erosion Rate x 10 ⁻⁴ (g/g)
48	30	0.005	0.867
	45	0.007	1.247
	60	0.006	1.071
	90	0.006	1.007
70	30	0.011	1.945
	45	0.019	3.473
	60	0.016	2.964
	90	0.013	2.395
82	30	0.019	3.509
	45	0.031	5.709
	60	0.040	7.236
	90	0.031	5.618
109	30	0.058	10.545
	45	0.053	9.636
	60	0.071	12.927
	90	0.054	9.891

Table-6.19 Parameters characterizing the velocity dependence of erosion rate of plain rice husk composites.

Fiber Type	Angle (Degree)	$k \times 10^{-6}$	n
PRH (5%)	30	66	2.62
	45	121	2.58
	60	13	3.06
	90	10	3.05
PRH (10%)	30	27	2.83
	45	127	2.53
	60	12	3.08
	90	14	2.96
PRH (15%)	30	55	2.63
	45	111	2.58
	60	10	3.09
	90	9	3.03
PRH (20%)	30	14	2.91
	45	52	2.70
	60	8	3.11
	90	16	2.91
	60	5	3.14
	90	14	2.88

Table-6.20 Parameters characterizing the velocity dependence of erosion rate of Acetone treated RH composites.

Fiber Type	Angle (Degree)	k x 10-6	n
Acetone (5%)	30	85	2.57
	45	147	2.52
	60	25	2.91
	90	7	3.12
Acetone (10%)	30	88	2.55
	45	120	2.55
	60	12	3.05
	90	11	3.03
Acetone (15%)	30	79	2.55
	45	134	2.50
	60	8	3.13
	90	5	3.19
Acetone (20%)	30	12	2.92
	45	67	2.61
	60	5	3.19
	90	10	3.01

Table-6.21 Parameters characterizing the velocity dependence of erosion rate of Alkali treated RH composites.

Fiber Type	Angle (Degree)	k x 10-6	n
Alkali (5%)	30	65	2.62
	45	158	2.48
	60	13	3.04
	90	21	2.88
Alkali (10%)	30	54	2.61
	45	162	2.45
	60	11	3.06
	90	21	2.84
Alkali (15%)	30	90	2.47
	45	175	2.40
	60	7	3.14
	90	6	3.11
Alkali (20%)	30	13	2.86
	45	63	2.60
	60	6	3.15
	90	14	2.89

Table-6.22 Parameters characterizing the velocity dependence of erosion rate of Benzoyl Chloride treated RH composites.

Fiber Type	Angle (Degree)	k x 10-6	n
Benzoyl (5%)	30	90	2.51
	45	176	2.44
	60	13	3.02
	90	13	2.97
Benzoyl (10%)	30	40	2.65
	45	144	2.46
	60	8	3.10
	90	10	3.00
Benzoyl (15%)	30	43	2.61
	45	174	2.38
	60	5	3.19
	90	11	2.97
Benzoyl (20%)	30	6	3.03
	45	72	2.53
	60	5	3.14
	90	14	2.88

Table-6.23 Erosion efficiency of PRH-epoxy composites.

Impact Velocity (m/s)	Impact Angle (Degree)	PRH 5%	PRH 10%	PRH 15%	PRH 20%
		H=149.1 (MPa)	H=159.9 (MPa)	H=167.7 (MPa)	H=181.4 (MPa)
		$\rho=1106$ (Kg/m ³)	$\rho=1044$ (Kg/m ³)	$\rho=1132$ (Kg/m ³)	$\rho=1026$ (Kg/m ³)
48	30	2.168	1.953	2.100	1.794
	45	2.621	2.860	2.581	2.397
	60	1.989	2.127	1.903	2.051
	90	1.532	1.774	1.496	1.886
70	30	2.001	2.807	1.902	2.362
	45	4.542	4.444	4.002	4.277
	60	3.722	3.944	3.408	3.674
	90	2.449	2.364	2.287	2.427
82	30	3.208	3.520	2.788	2.945
	45	4.586	4.937	4.142	4.274
	60	5.169	5.442	4.647	5.010
	90	3.689	3.976	3.349	3.815
109	30	3.404	3.727	3.401	3.734
	45	4.126	4.458	3.908	4.205
	60	4.440	4.838	4.394	4.827
	90	3.379	3.577	3.287	3.696

Table-6.24 Erosion efficiency of Acetone treated RH-epoxy composites.

Impact Velocity (m/s)	Impact Angle (Degree)	Acetone 5%	Acetone 10%	Acetone 15%	Acetone 20%
		H=136.3 (MPa)	H=144.2 (MPa)	H=153 (MPa)	H=162.8 (MPa)
		$\rho=1148$ (Kg/m ³)	$\rho=1161$ (Kg/m ³)	$\rho=1133$ (Kg/m ³)	$\rho=1129$ (Kg/m ³)
48	30	1.806	1.860	1.844	1.318
	45	2.230	2.250	2.242	1.846
	60	1.861	1.670	1.609	1.525
	90	1.211	1.555	1.279	1.513
70	30	2.150	2.120	2.255	1.605
	45	3.956	3.392	3.357	3.028
	60	3.172	3.042	2.806	2.440
	90	2.027	1.843	2.305	1.705
82	30	2.607	2.620	2.410	2.145
	45	3.621	3.761	3.535	3.228
	60	4.366	4.259	3.973	3.790
	90	2.877	3.580	3.337	2.909
109	30	2.809	2.851	2.922	2.754
	45	3.409	3.429	3.306	2.975
	60	3.670	3.703	3.840	3.778
	90	2.878	3.246	3.195	3.235

Table-6.25 Erosion efficiency of Alkali treated RH-epoxy composites.

Impact Velocity (m/s)	Impact Angle (Degree)	Alkali 5%	Alkali 10%	Alkali 15%	Alkali 20%
		H=168.7 (MPa)	H=177.5 (MPa)	H=203 (MPa)	H=194.2 (MPa)
		$\rho=1125$ (Kg/m ³)	$\rho=1131$ (Kg/m ³)	$\rho=1131$ (Kg/m ³)	$\rho=1133$ (Kg/m ³)
48	30	1.971	1.939	2.184	1.347
	45	2.705	2.685	2.799	1.986
	60	1.988	1.964	1.952	1.731
	90	1.799	1.712	1.538	1.642
70	30	2.982	1.920	2.078	1.631
	45	4.451	3.867	3.730	2.977
	60	3.439	3.319	3.077	2.430
	90	2.560	2.050	2.504	1.902
82	30	3.244	2.928	2.456	2.123
	45	4.055	3.972	4.077	3.281
	60	5.142	5.050	4.892	4.097
	90	3.941	3.692	3.494	3.059
109	30	3.213	3.031	3.219	2.675
	45	4.039	3.843	3.807	3.163
	60	4.305	4.304	4.587	4.108
	90	3.415	3.074	3.631	3.195

Table-6.26 Erosion efficiency of Benzoyl Chloride treated RH-epoxy composites.

Impact Velocity (m/s)	Impact Angle (Degree)	Benzoyl 5%	Benzoyl 10%	Benzoyl 15%	Benzoyl 20%
		H=152 (MPa)	H=157.9 (MPa)	H=128.5 (MPa)	H=142.2 (MPa)
		$\rho=1152$ (Kg/m ³)	$\rho=1141$ (Kg/m ³)	$\rho=1145$ (Kg/m ³)	$\rho=1136$ (Kg/m ³)
48	30	1.833	1.485	1.217	0.942
	45	2.291	2.143	1.573	1.355
	60	1.676	1.551	1.103	1.164
	90	1.416	1.409	1.011	1.095
70	30	1.743	1.438	0.883	0.994
	45	3.564	3.184	2.082	1.774
	60	2.820	2.588	1.666	1.514
	90	1.958	1.858	1.374	1.223
82	30	2.604	2.118	1.790	1.307
	45	3.282	3.039	2.215	2.126
	60	4.167	3.914	2.828	2.694
	90	3.240	3.203	2.355	2.092
109	30	2.641	2.423	1.827	2.222
	45	3.307	3.130	2.106	2.031
	60	3.574	3.558	2.683	2.724
	90	2.879	2.923	2.033	2.084



Figure-6.1 Details of erosion test rig. (1) Sand hopper, (2) Conveyor belt system for sand flow, (3) Pressure transducer, (4) Particle-air mixing chamber, (5) Nozzle, (6) X-Y and h axes assembly, (7) Sample holder.

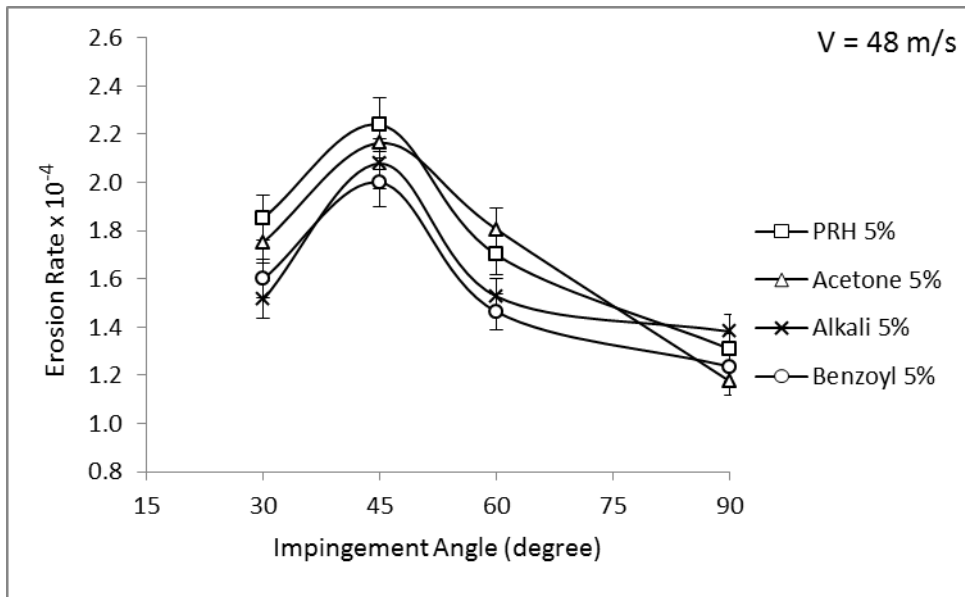


Figure-6.2 Erosion rate with angle of impingement Velocity 48 m/Sec, VF 5%

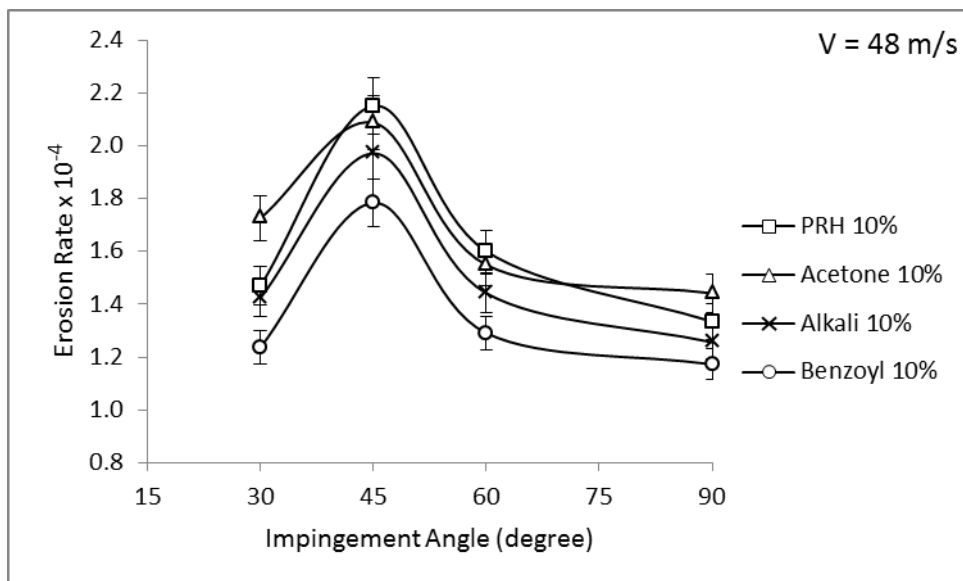


Figure-6.3 Erosion rate with angle of impingement Velocity 48 m/Sec, VF 10%

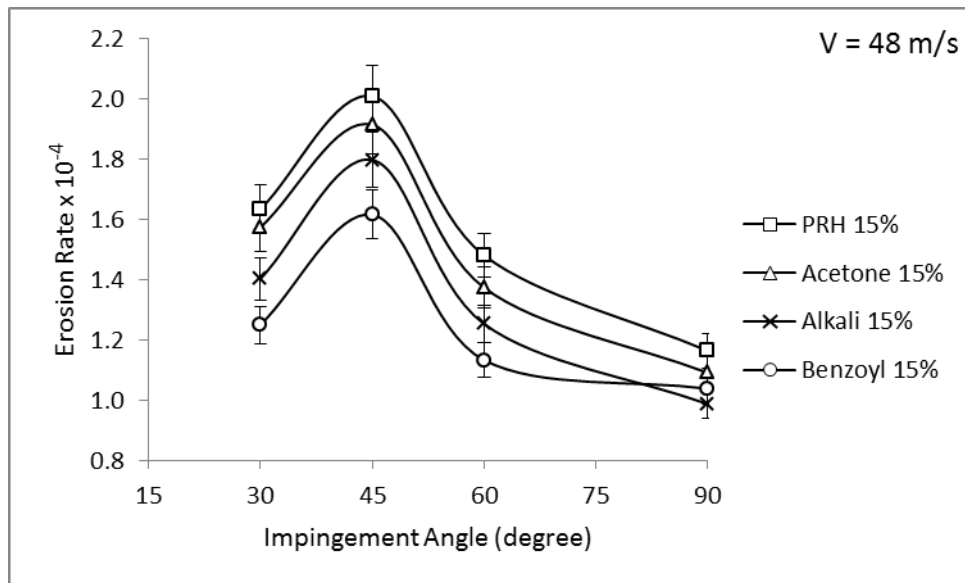


Figure-6.4 Erosion rate with angle of impingement Velocity 48 m/Sec, VF 15%

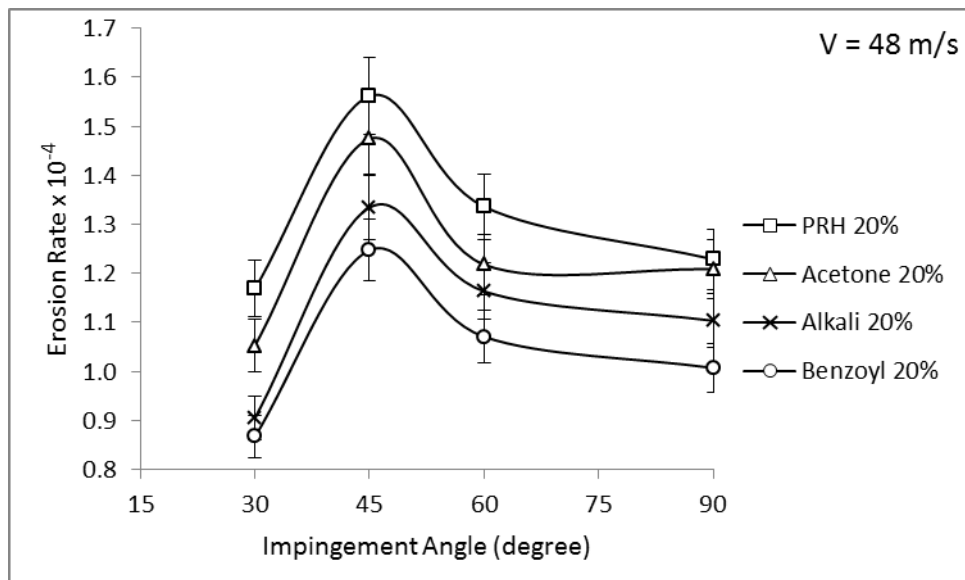


Figure-6.5 Erosion rate with angle of impingement Velocity 48 m/Sec, VF 20%

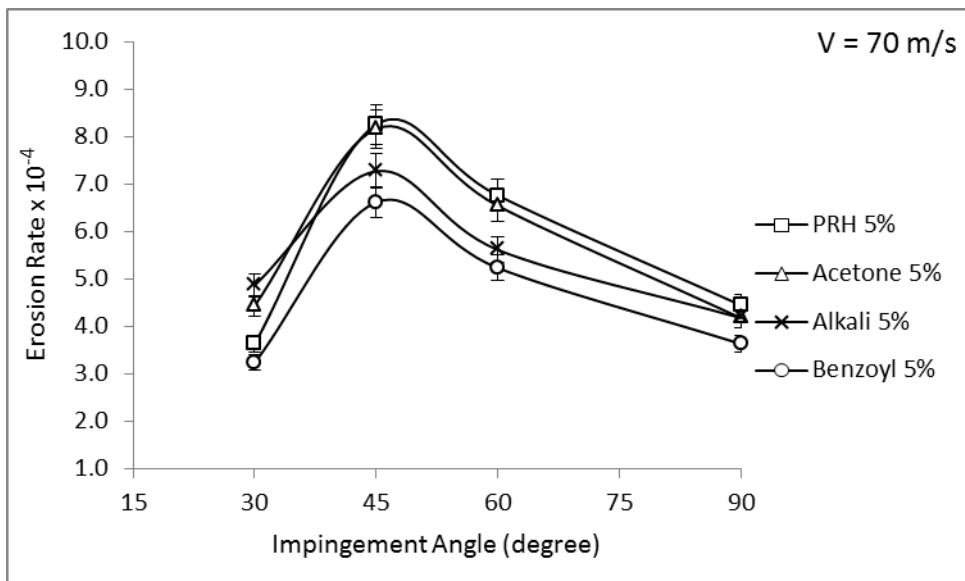


Figure-6.6 Erosion rate with angle of impingement Velocity 70 m/Sec, VF 5%

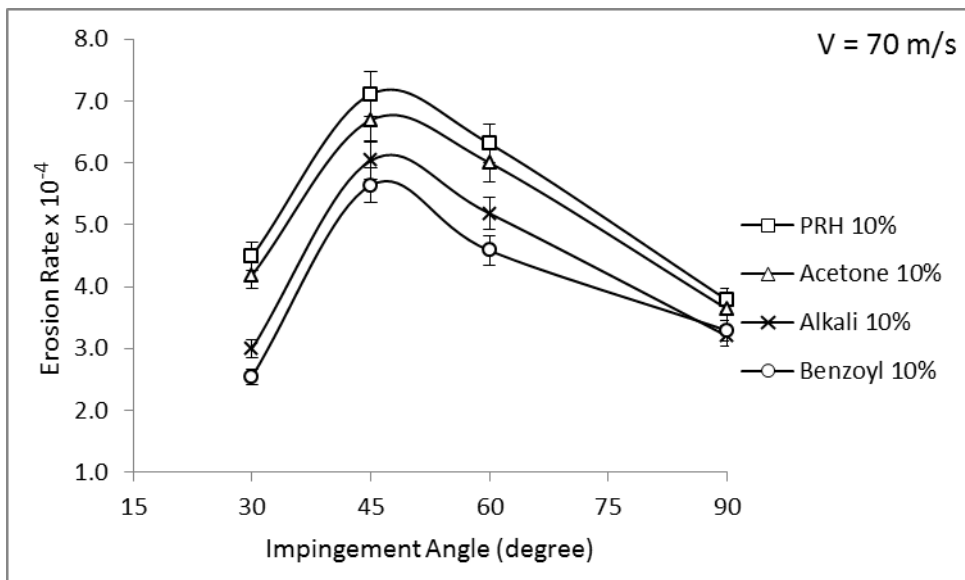


Figure-6.7 Erosion rate with angle of impingement Velocity 70 m/Sec, VF 10%

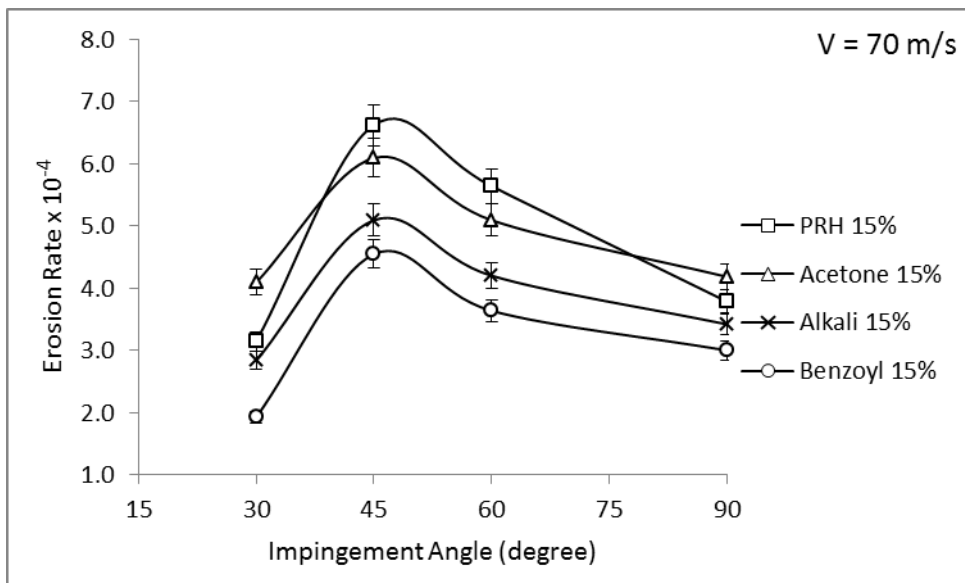


Figure-6.8 Erosion rate with angle of impingement Velocity 70 m/Sec, VF 15%

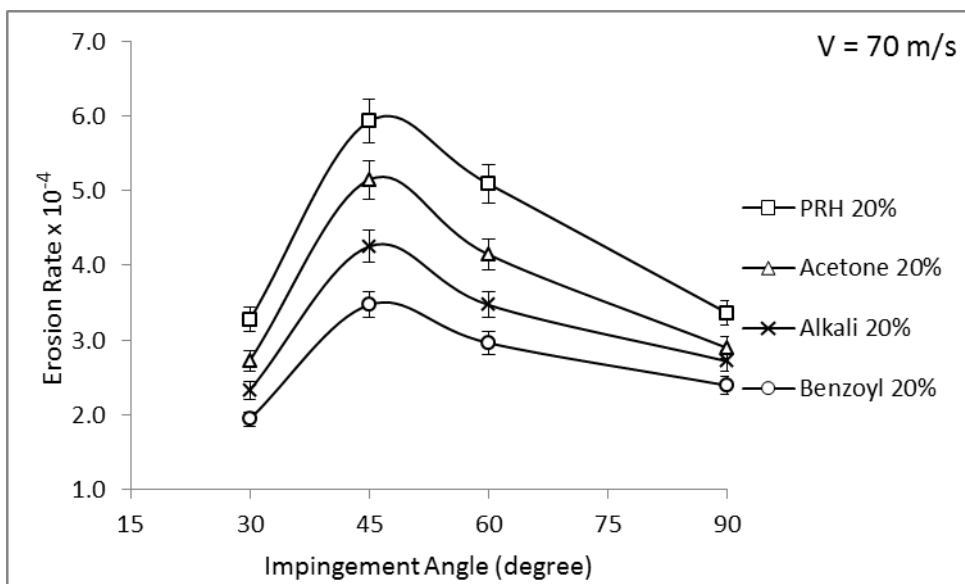


Figure-6.9 Erosion rate with angle of impingement Velocity 70 m/Sec, VF 20%

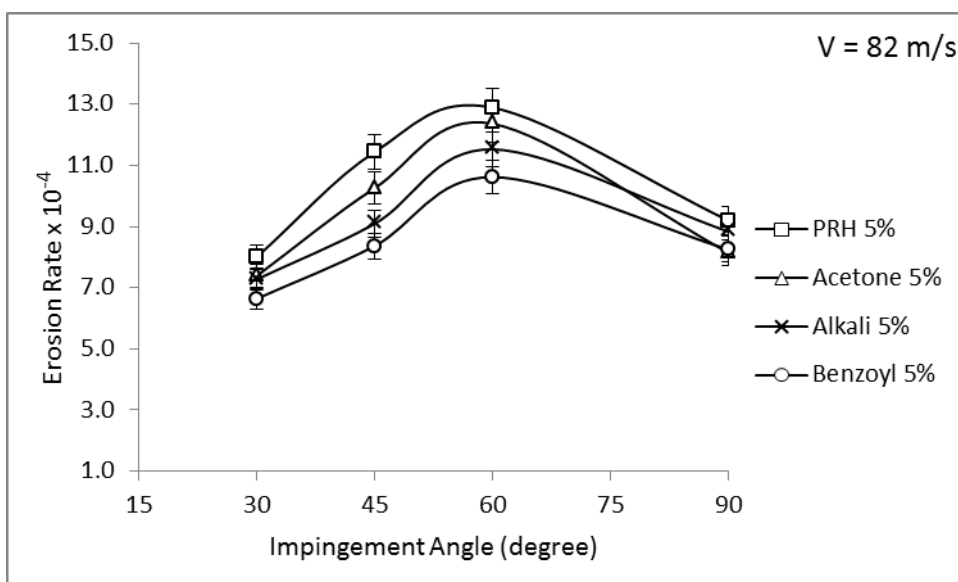


Figure-6.10 Erosion rate with angle of impingement Velocity 82 m/Sec, VF 5%

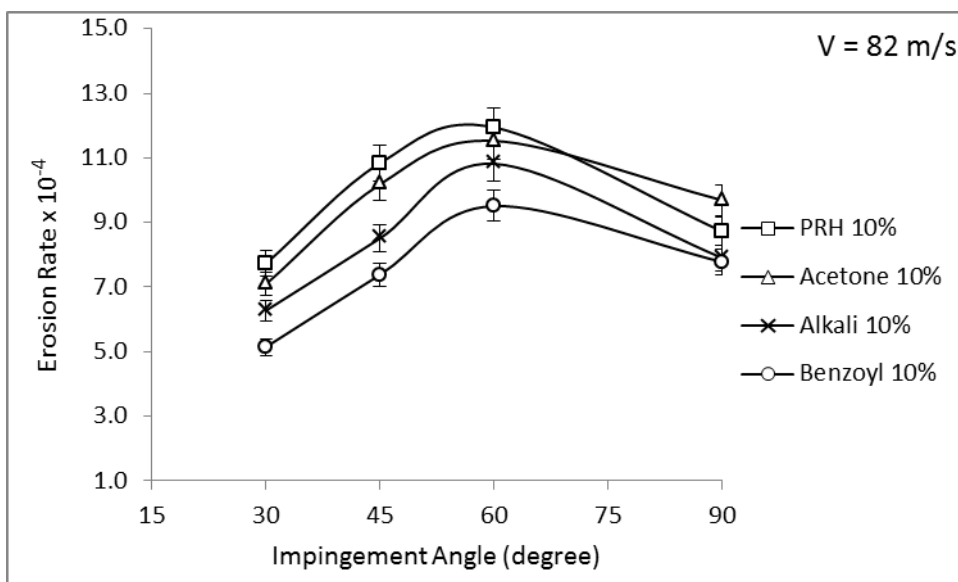


Figure-6.11 Erosion rate with angle of impingement Velocity 82 m/Sec, VF 10%

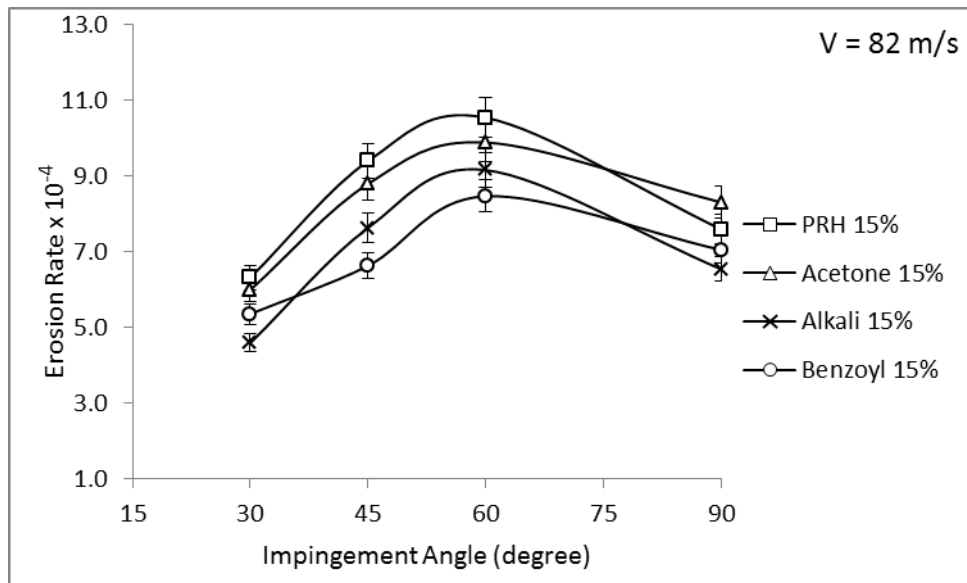


Figure-6.12 Erosion rate with angle of impingement Velocity 82 m/Sec, VF 15%

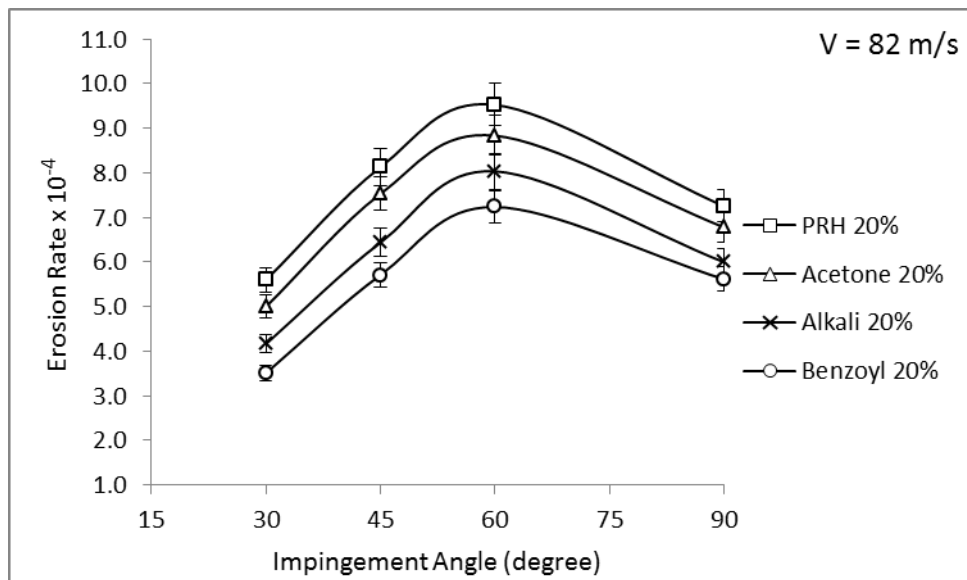


Figure-6.13 Erosion rate with angle of impingement Velocity 82 m/Sec, VF 20%

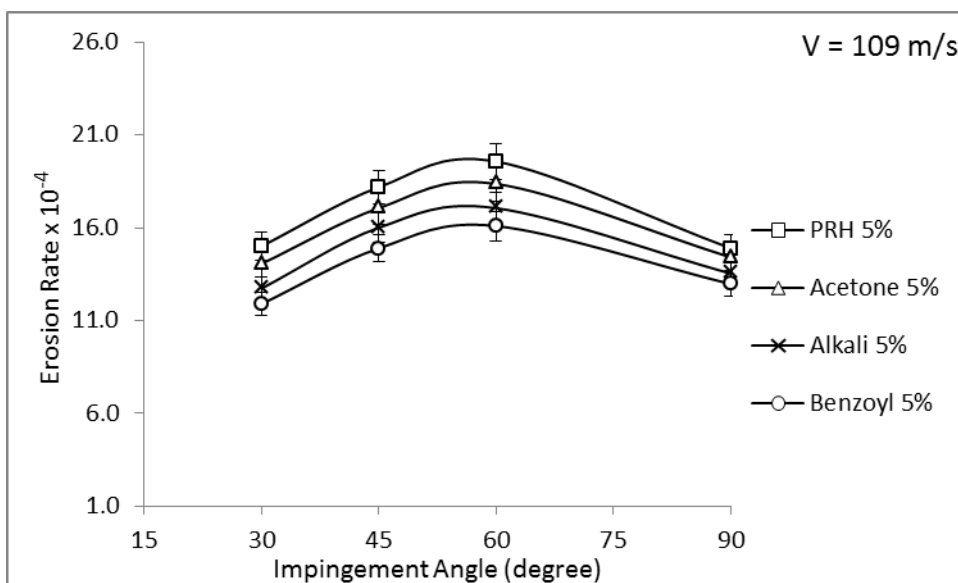


Figure-6.14 Erosion rate with angle of impingement Velocity 109 m/Sec, VF 5%

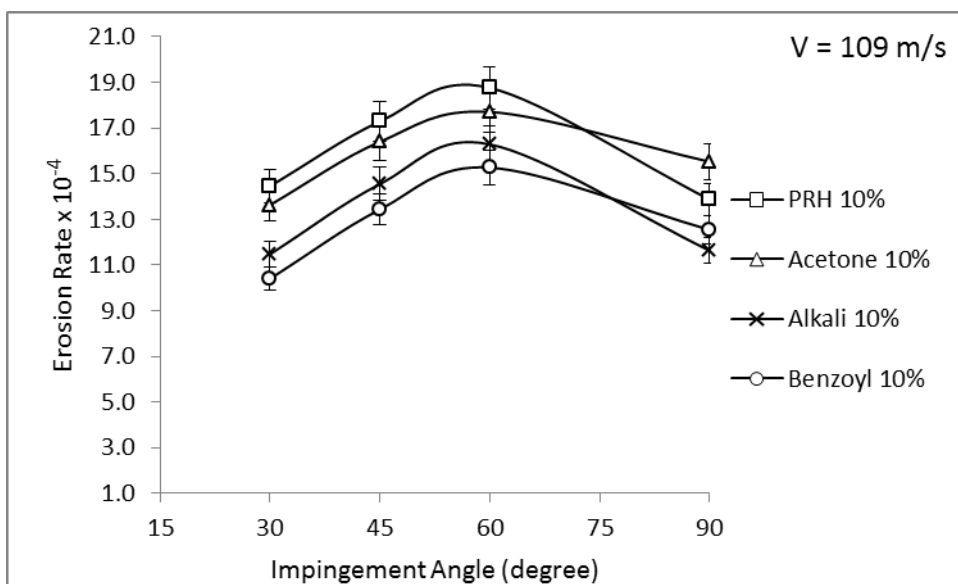


Figure-6.15 Erosion rate with angle of impingement Velocity 109 m/Sec, VF 10%

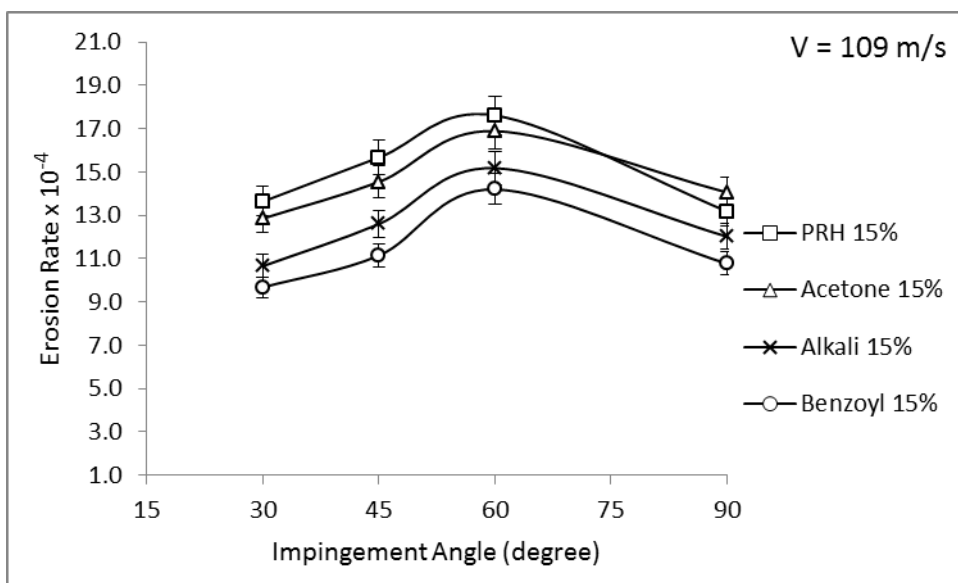


Figure-6.16 Erosion rate with angle of impingement Velocity 109 m/Sec, VF 15%

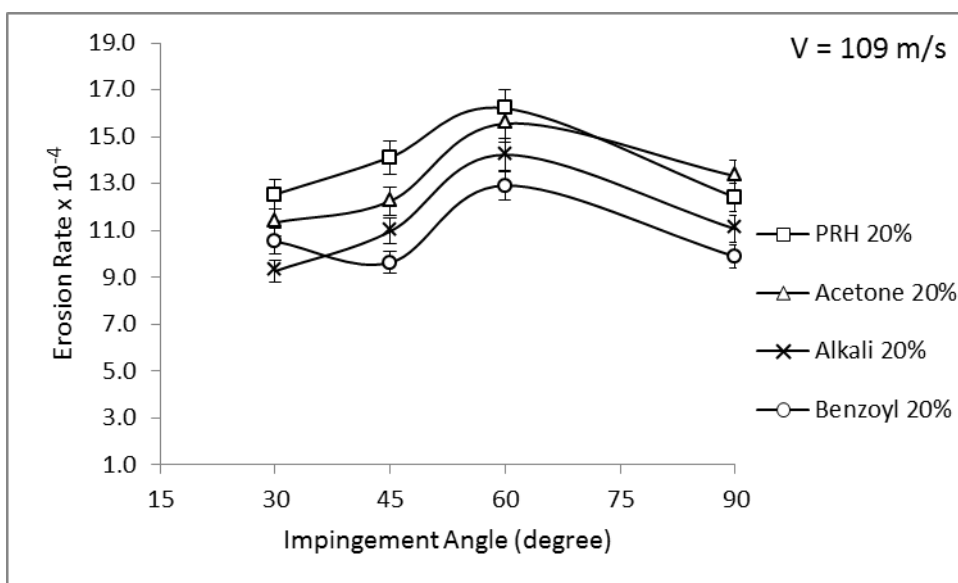


Figure-6.17 Erosion rate with angle of impingement Velocity 109 m/Sec, VF 20%

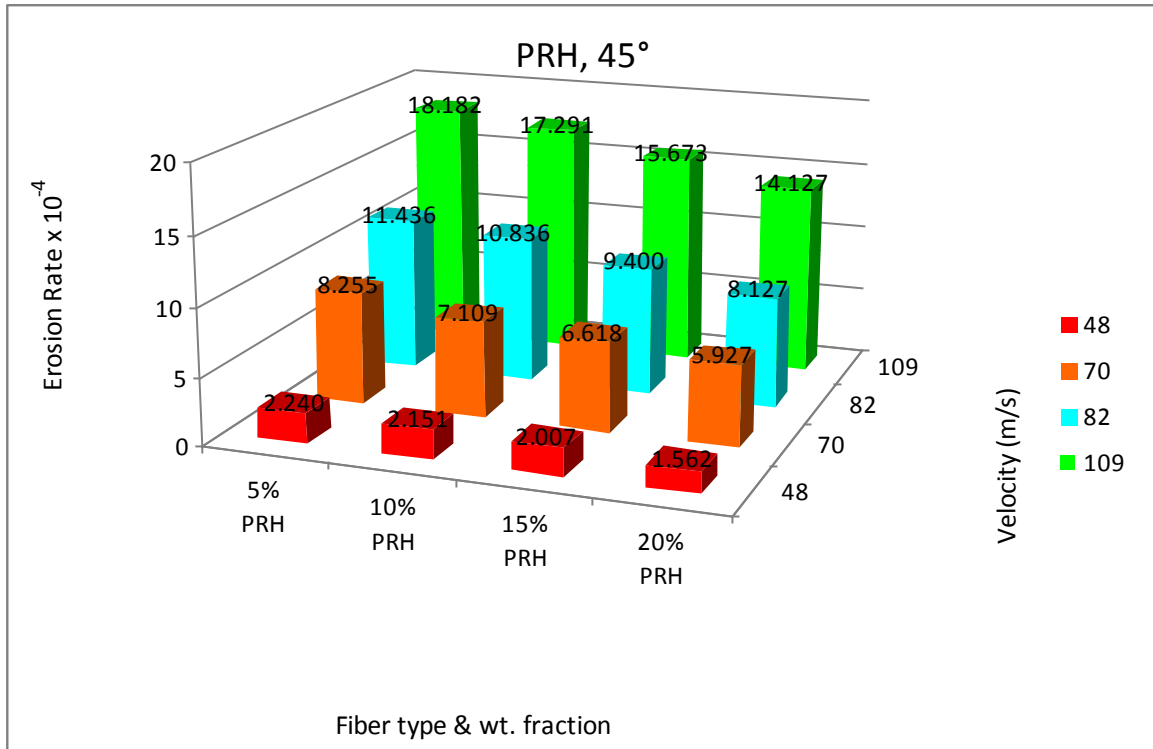


Figure-6.18 Histogram showing the erosive wear rates of PRH composite at four impact velocities (i.e. at 48, 70, 82 and 109 m/s) for 45° impact angle

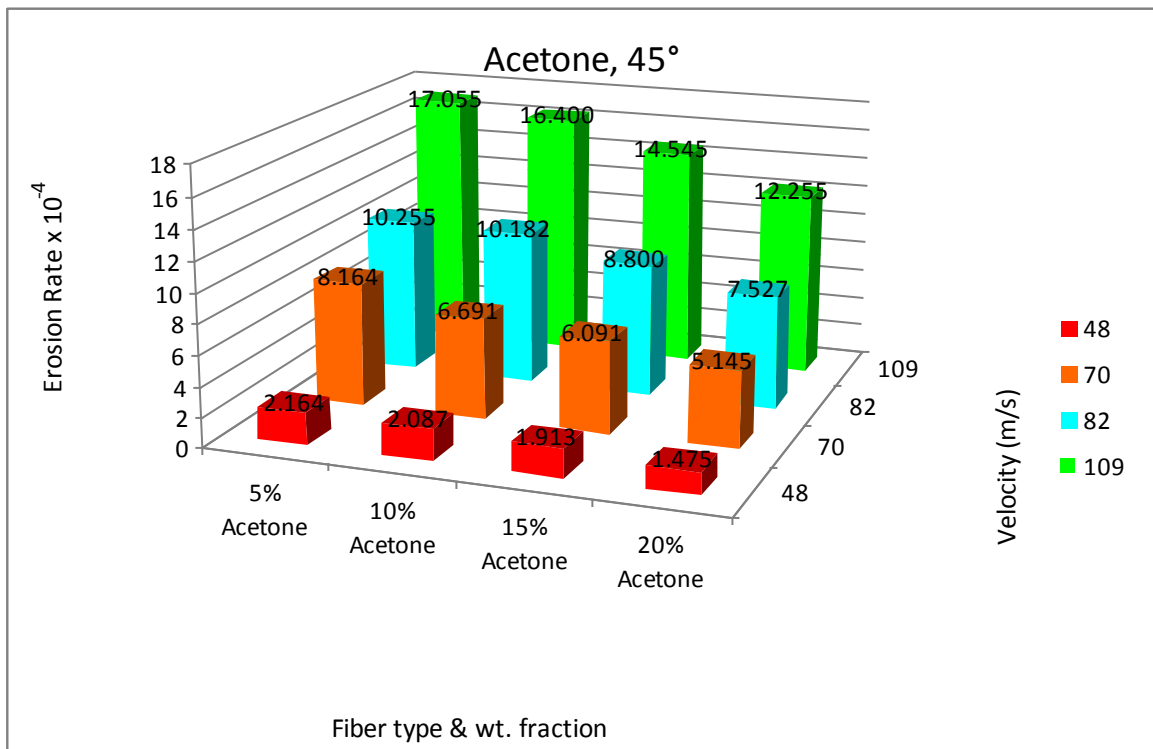


Figure-6.19 Histogram showing the erosive wear rates of Acetone treated composites at four impact velocities (i.e. at 48, 70, 82 and 109 m/s) for 45° impact angle

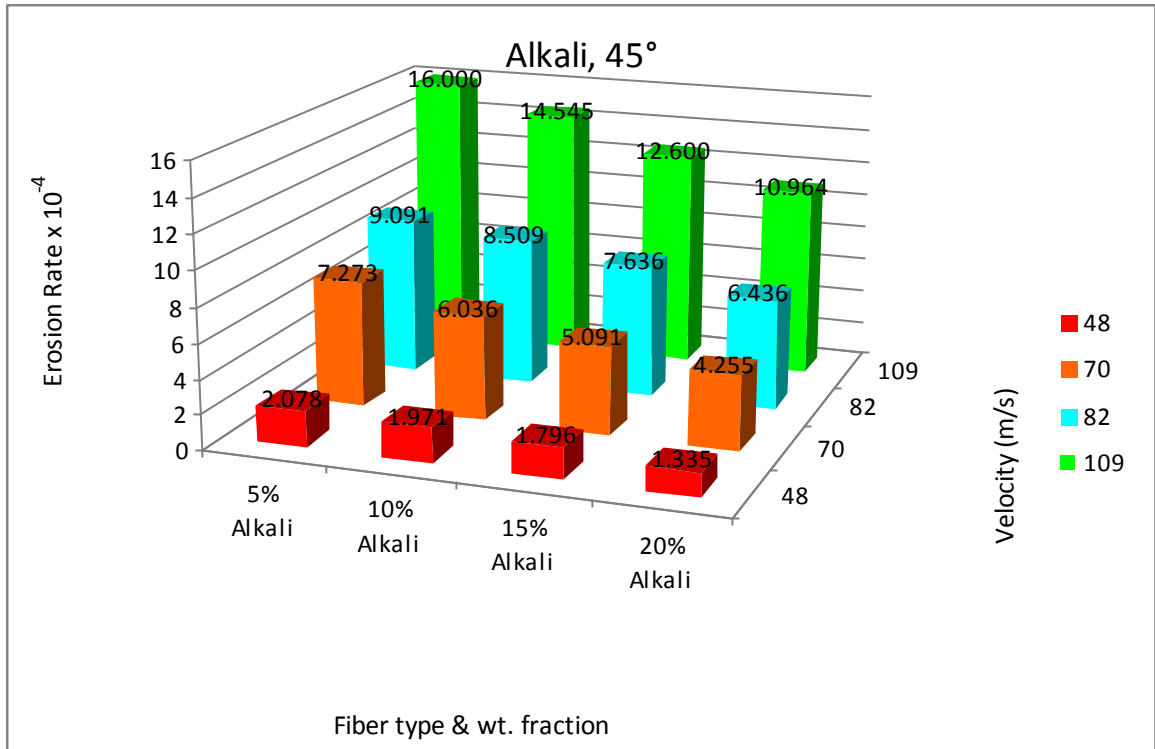


Figure-6.20 Histogram showing the erosive wear rates of Alkali RH composites at four impact velocities for 45° impact angle

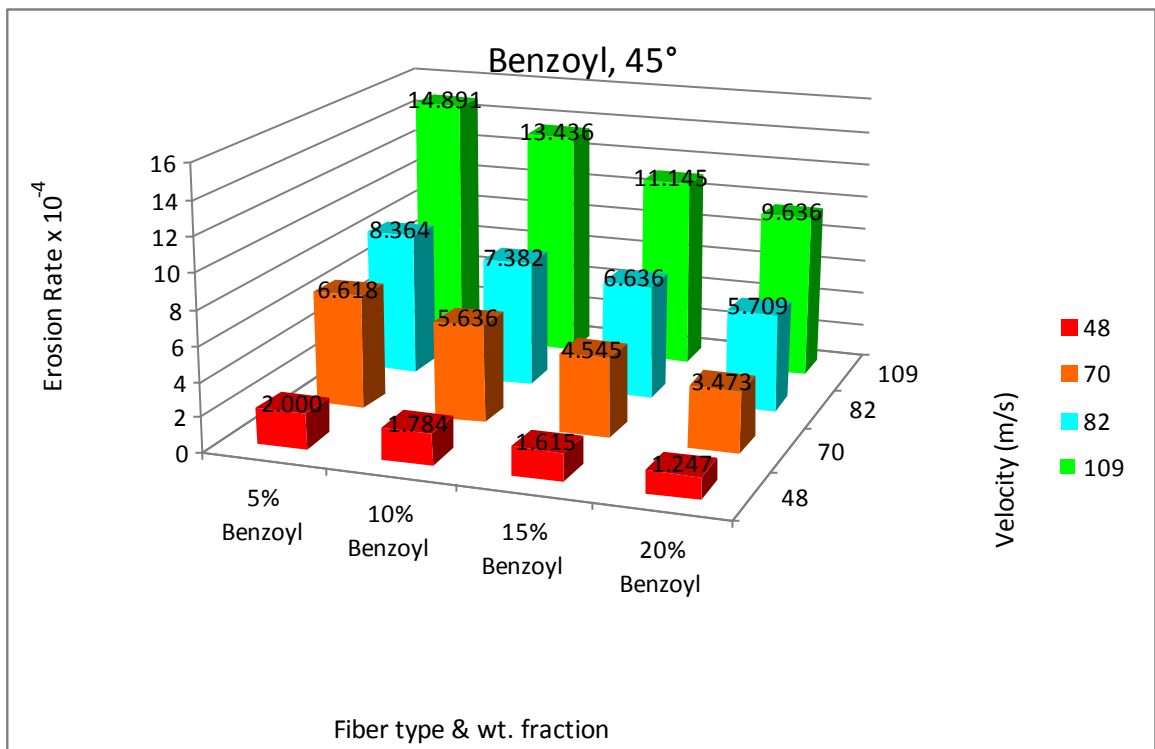


Figure-6.21 Histogram showing the erosive wear rates of Benzoyl Chloride RH composites at four impact velocities for 45° impact angle

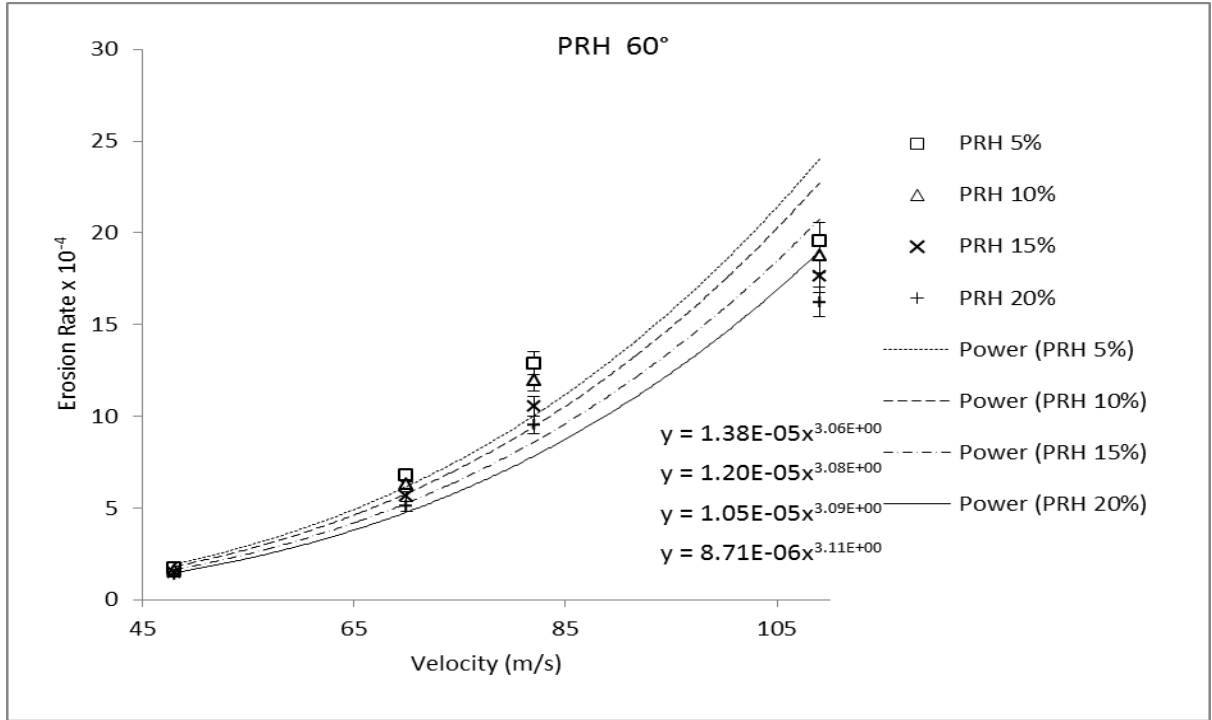


Figure-6.22 Erosion parameter for Plain Rice Husk epoxy composite at impingement angle 60°.

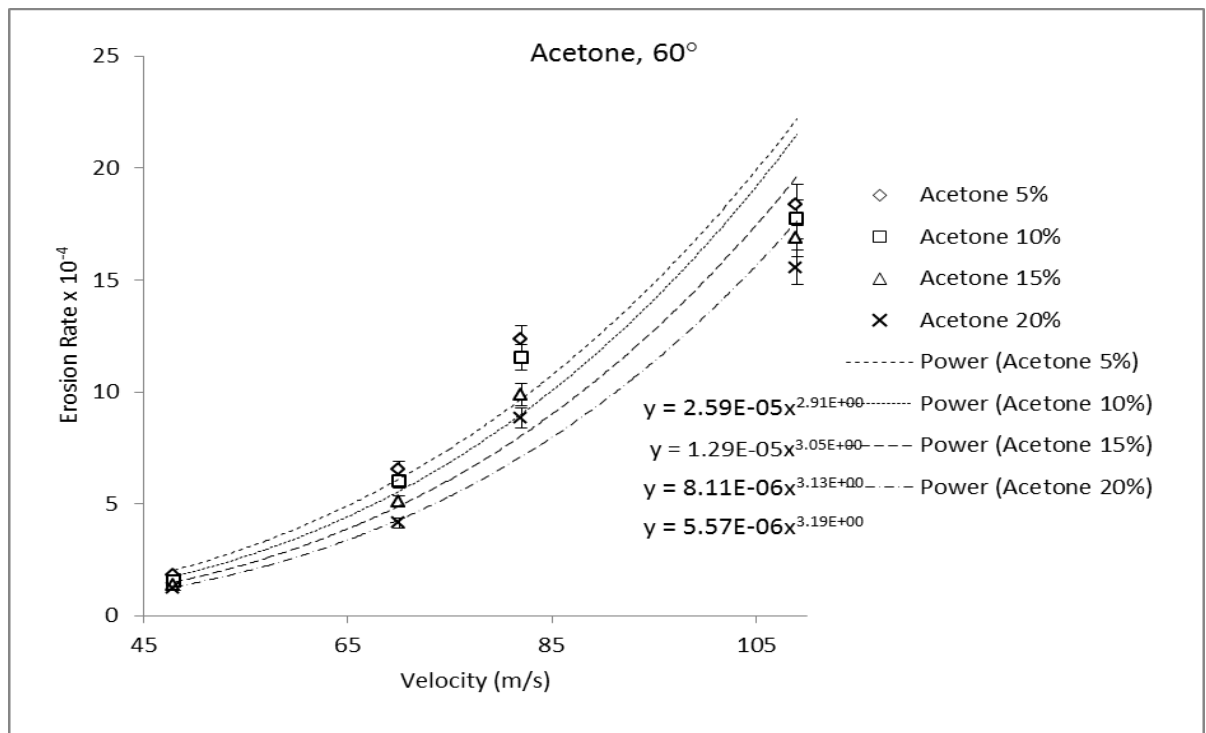


Figure-6.23 Erosion parameter for Acetone treated Rice Husk epoxy composite at impingement angle 60°.

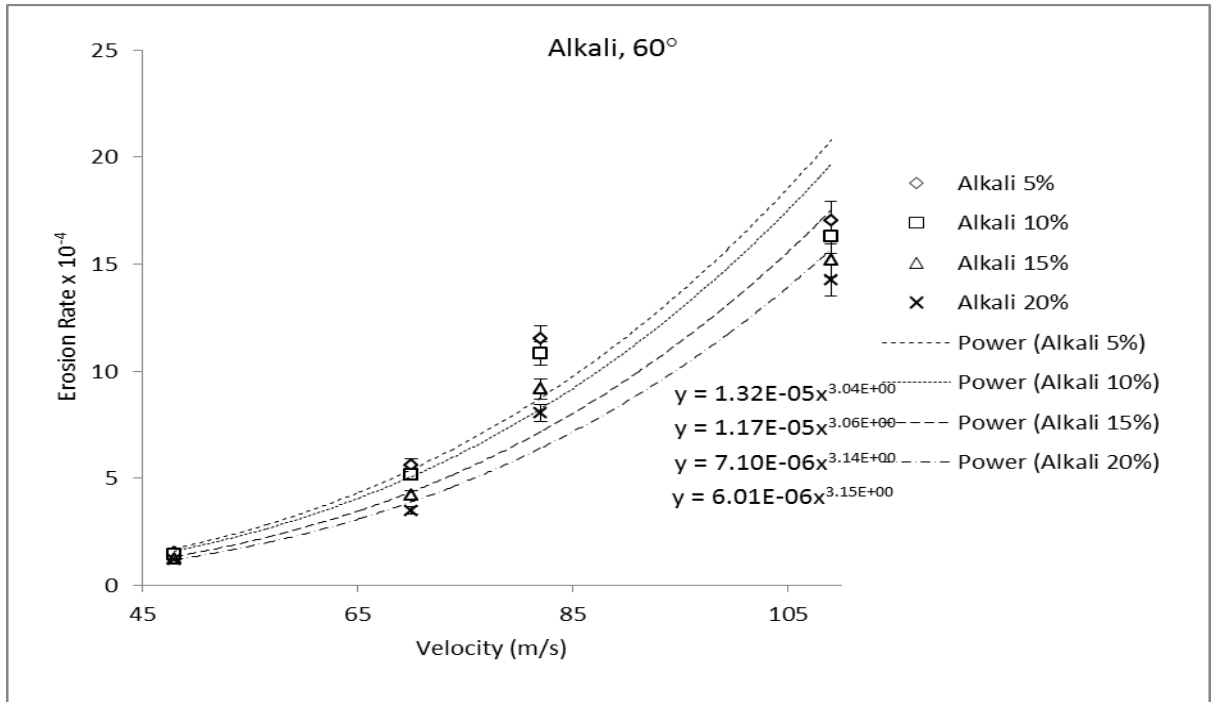


Figure-6.24 Erosion parameter for Benzoyl Chloride treated Rice Husk epoxy composite at impingement angle 60°.

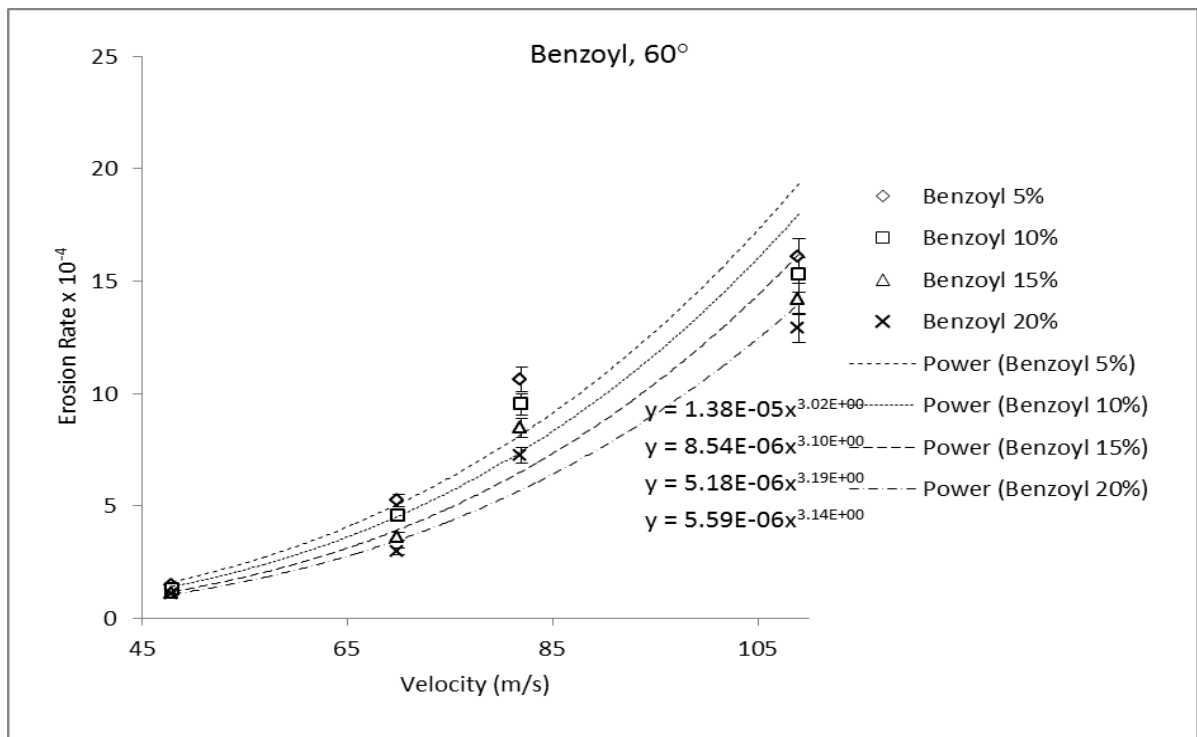


Figure-6.25 Erosion parameter for Benzoyl Chloride treated Rice Husk epoxy composite at impingement angle 60°.

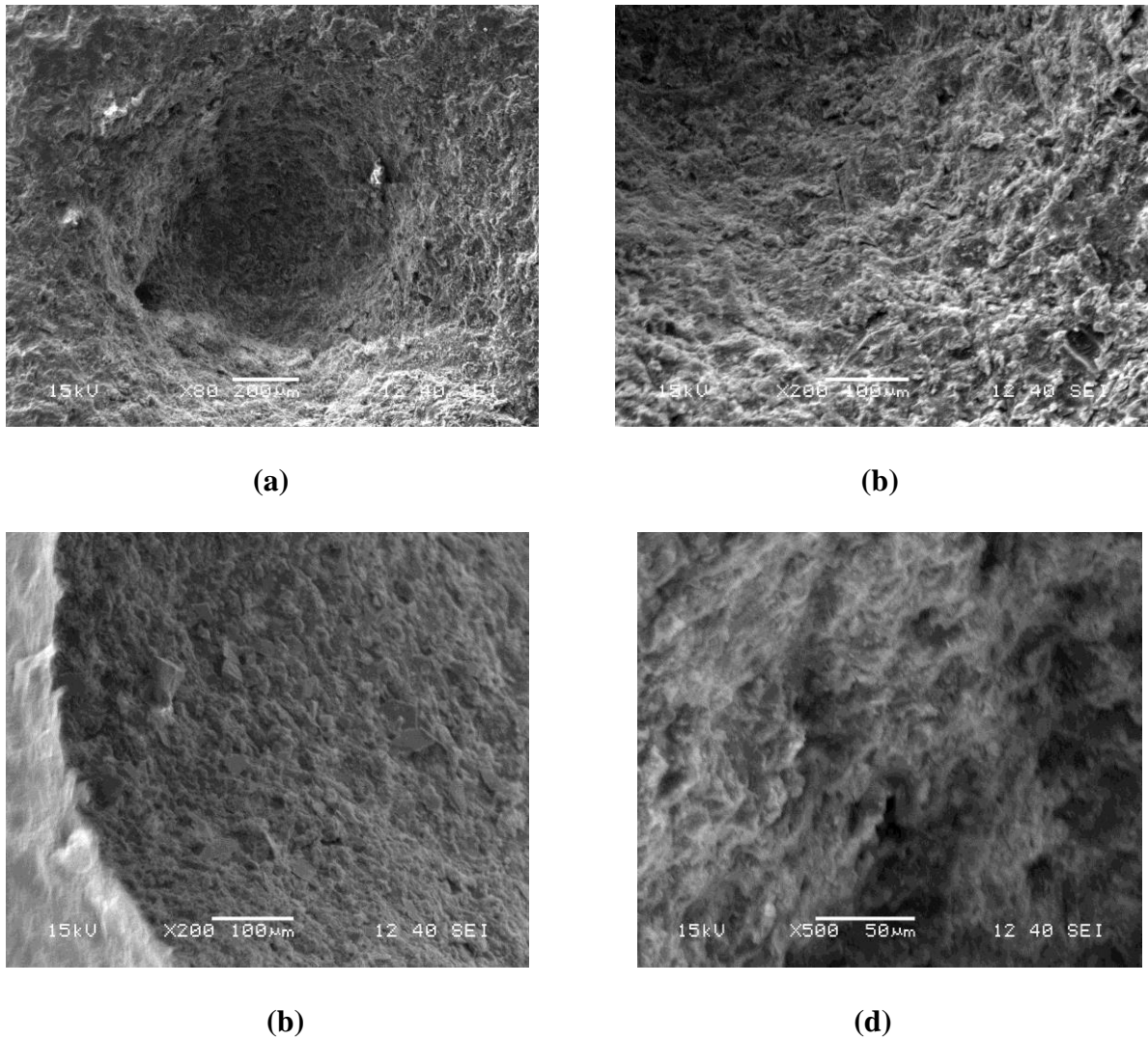


Figure 6.26 : SEM micrographs of eroded surface of a) Plain, b) Acetone, c) Alkali and d) Benzoylchloride treated composite at 45degree impingement angle

Chapter 7

CONCLUSIONS

7.1 CONCLUSIONS

The conclusions drawn from the present investigations are as follows:

1. The Rice Husk can successfully be used as reinforcing agent to fabricate composite by suitably bonding with resin for the development of value added products.
2. There is a good dispersibility of rice husk in the matrix, which improves the hardness, strength, modulus and work fracture of the composite. Fifteen volume percent of plain rice husk reinforcement gives the best combination among the tested composites.
3. The surface modification of rice husk significantly improves the fiber matrix adhesion which in turn enhances the mechanical properties of the composite. The benzoyl-chloride treatment provides the highest improvement in strength and modulus in-comparison to alkali and acetone treatment.
4. Fickian's diffusion can be used to describe the moisture absorption behaviour of both treated and untreated rice husk reinforced epoxy composite.
5. The abrasive wear resistance of neat epoxy is appreciably enhanced by incorporation of rice husk . The specific wear rate of the composite also decreases with addition of fiber. In this present study the optimum fiber volume fraction which gives maximum wear resistance to the composite is found to be 10 vol%.
6. The abrasive wear rate of the rice husk epoxy composite is influenced by several parameters e.g. sliding velocity, sliding distance and normal load. The wear rate of the composite is found to be more sensitive to normal load in comparison to sliding velocity. The coefficient friction of the composites decreases with addition of rice husk which confirms that the addition of this fiber is beneficial in reducing the wear of neat epoxy.

7. Different chemical modification of fiber surface improves the wear and specific wear resistance properties of rice husk epoxy composites. Out of all the processes carried out for the present investigation Benzoyl chloride treated fibers gives the best result.
8. By carburizing the Rice husk, amorphous silica and carbon are obtained which provides higher hardness to the composite. The rice husk char up to 30% volume fraction can successfully be utilized to produce composite by suitably bonding with resin where as maximum 10% rice husk in natural form can be utilized to form composite with epoxy.
9. It is found that carbonization temperature increases the micro porous volume as well as the surface area of the rice husk, which results in better wear property for the composite under study.
10. Rice husk epoxy composite shows a semi-ductile behavior to solid particle erosion. From the experimental result the erosion efficiency (η) is found in the range of 1.532% to 5.44%).
11. The interesting point in the present investigation for treated fiber composite is that at higher velocity the maximum erosion for untreated fiber which occurs at 45° shifted towards 60° impact angle. This gives an indication that the ductile behavior of the composite shifted towards brittle behavior due to modification of fiber surface. In addition the chemical treatment of rice husk reduces the erosion rate. The chemical treatment of rice Husk with Benzoyl Chloride offers maximum erosion resistance.

7.2 RECOMMENDATION FOR FURTHER RESEARCH

1. In the present investigation hand-lay-up technique is used to fabricate the composite. However there exists other manufacturing process for polymer matrix composite. They could be tried and analyzed, so that a final conclusion can be drawn there from. However the results provided in this thesis can act as a base for the utilization of this fiber.
2. From this work it is found that chemical modification of the fiber with alkali, acetone and benzoyl-chloride significantly improves the mechanical performance of the composite. Other chemical modification methods such as silane treatment, acetylation treatment, acrylation treatment isocyanates treatment, Permanganate treatment, Maleated coupling agents could be tried and a final conclusion can be drawn thereafter.
3. In the erosion test sand particle of 200 ± 50 microns only have been used. This work can be further extended to other particle size and types of particle like glass bead etc, to study the effect of particle size and type of particles on wear behavior of the composite.

REFERENCES

- [1] Mohite PM , “Composite Material AE 681” AE 11, Aerospace Engineering , IIT Kanpur, India
- [2] Wetter, R., (1970), “Kunststoffe in der Luft-und Raumfahrt,” Kunststoffe, 60, Heft-10.
- [3] Schmidt, K. A. F., (1967), Verstärkungsfasern in Glasfaserverstärkte Kunststoffe, Ed. P. H. Selden, Springer-Verlag, Berlin, pp.159-221.
- [4] Berghezan, A.,(1966), “Non-ferrous Materials,” Nucleus, 8: pp. 5–11.
- [5] Van Suchtelen., (1972), "Product properties: a new application of composite materials," Philips Res. Reports, Vol. 27, pp. 28.
- [6] Agarwal, B.D. and Broutman, L.J., (1980), “Analysis and performance of fiber composites,” John Wiley & Sons, New York, pp.3-12.
- [7] Outwater J.O., “The Mechanics of Plastics Reinforcement Tension,” Mod. Plast: March- 1956.
- [8] Mohanty, A.K., Misra, M., and Drzal, L.T. (2002) “Sustainable bio composites from renewable resources: opportunities and challenges in the green materials world.” J Polymers and the Environment, 10: 19-26.
- [9] Wambua, P., Ivens, J. and Veroest, I. (2003) “ Natural fibers: can they replace glass in fiber reinforced plastics.” Composites Science and Technology, 63(9):1259-1264.
- [10] Gamstedt, E. K. and Almgren, K. M. (2007) ” Natural fiber composites - with special emphasis on effects of the interface between cellulosic fibers and polymers.” Proceedings of the 28th Ris* International Symposium on Materials Science.
- [11] Hinrichsen, G., Khan, M.A. and Mohanty, A.K., (2000), “Composites”: Part A, Elsevier Science Ltd, 31:pp.143–150.
- [12] Joseph, P.V., Kuruvilla J, Thomas S., (1999), “Composites Science And Technology”; 59(11): pp.1625-1640.
- [13] Mukherjee, P. S. & Satyanarayana, K. G., (1986), “Structure and properties of some vegetable fibers-II. Pineapple leaf fiber,” J. Material Science 21 (January), pp. 51–56.
- [14] Jain, S., Kumar, R., Jindal, U. C., (1992), “Mechanical Behavior of Bamboo and Bamboo Composites,” J. Mater. Sci., **27**, pp. 4598-4604.

- [15] Hirao, K., Inagaki, H., Nakamae, K., Kotera, M. and Nishino, T. K., (2003), “Kenaf Reinforced Biodegradable Composite,” *Composites Science and Technology*, 63: pp.1281-1286.
- [16] Vazquez, A., Dominguez V. A., Kenny J. M., (1999), “Bagasse Fiber-Polypropylene Based. Composites.” *Journal of Thermoplastic Composite Materials.*” Volume 12, (6): pp. 477-497.
- [17] Ei-Tayeb N.S.M., (2008), “A study on the potential of sugarcane fibers/polyester composite for tribological applications,” *Wear*, Vol. 265, pp. 223-235.
- [18] Vinay Kumar¹, Shishir Sinha, Manohar Singh, Saini, Bikram Kishore Kanungo and Prakash Biswas “Rice husk as reinforcing filler in polypropylene composites “ *Rev Chem Eng* 26 (2010): 41–53 _ 2010 by Walter de Gruyter • Berlin • New York. DOI 10.1515/REVCE.2010.001
- [19] Bronzeoak Ltd UK “Rice Husk ash market study “ (2003).
- [20] Navin Chanda, Prabhat Sharma, M. Fahim “Tribology of maleic anhydride modified rice-husk filled polyvinylchloride.” *Wear* 269 (2010) 847–853
- [21] Luyi Sun, Kecheng Gong “Silicon-Based Materials from Rice Husks and Their Applications ” *Ind. Eng. Chem. Res.* (2001), 40, 5861-5877
- [22] B.S. Ndazi , S. Karlsson, J.V. Tesha , C.W. Nyahumwa, (2007) “Chemical and physical modifications of rice husks for use as composite panels .” *Science Direct Composites: Part A* 38 925–935
- [23] S. Kumagai, J. Sasaki, (2009) “Carbon/silica composite fabricated from rice husk by means of binderless hot-pressing, *Bioresource Technology* .” 100 (13):pp. 3308–3315.
- [24] A.I. Khalf, A.A. Ward, (2009) “Use of rice husks as potential filler in styrene butadiene rubber/linear low density polyethylene blends in the presence of maleic anhydride,” *Materials & Design* 31 (5):pp. 2414–2421.
- [25] J. Umeda, K. Kondoh, H. Imai, (2009) “Friction and wear behavior of sintered magnesium composite reinforced with CNT-Mg₂Si/MgO,” *Materials Science and Engineering A* 504 (1–2) :pp.157–162.
- [26] W.-L. Dai, (2003) “Blendability and processing methodology of an environmental material rice-hush/PVA composite,” *Materials Letters* 57 (20):pp. 3128–3136.
- [27] Ibrahim Mutlu,(2009), “Investigation of Tribological Properties of Brake Pad by using Rice straw and Rice husk dust.” *Journal of applied sciences* 9(2) : 377-381, ISSN 1812-5654

- [28] Franck, R.R., (2005), "Bast and Other Plant Fibers," Cambridge: Woodhead Publishing Limited.
- [29] Robson D. and Hague J.A., (1995), "Comparison of wood and plant fibre properties," in Third International Conference on Wood-fiber-plastic composites, Madison, Wisconsin, USA: Forest Products Society.
- [30] Rong, M.Z., Zhang, M.Q., Liu, Y., Yang, G.C. and Zeng, H.M., (2001), "The effect of fiber treatment on the mechanical properties of unidirectional sisal-reinforced epoxy composites," *Compos. Sci. Technol.*, 61: pp. 1437–1447.
- [31] Haigler, C. H., (1985), "The Functions and Biogenesis of Native Cellulose," *Cellulose Chemistry and Its Applications*. T. P. Nevell and S. H. Zeronian. West Sussex, Ellis Horwood Limited: pp.30-83.
- [32] Thygesen, A. et al.,(2006), "Comparison of composites made from fungal defibrated hemp with composites of traditional hemp yarn, " *Industrial Crops and Products*.
- [33] Rowell, R.M., Young, R.A., and Rowell, J.K., (1997), "Chemical Composition of Fibers: Paper and Composites from Agro-based Resources," Lewis Publishers, CRC Press: pp.85-91.
- [34] Bjerre, A.B. and Schmidt, A.S., (1997), "Development of chemical and biological processes for production of bioethanol: Optimization of the wet oxidation process and characterization of products," Riso-R-967(EN), Riso National Laboratory: pp. 5-9.
- [35] Morvan, C., Jauneau, A., Flaman, A., Millet, J. and Demarty, M., (1990), "Degradation of flax polysaccharides with purified endo-polygalacturonase", *Carbohydrate Polymers*, 13(2): pp.149-163.
- [36] Madsen, B., (2004), "Properties of plant fibre yarn polymer composites – An experimental study," (2004), PhD Thesis, Department of civil Engineering, Technical University of Denmark.
- [37] Sakakibara, A. and Shiraishi, N., (1991), "Wood and Cellulose Chemistry," New York: Marcel Dekker.
- [38] Rowell, R.M., (1995), "A new generation of composite materials from agro-based fibre," in *The Third International Conference on Frontiers of Polymers and Advanced Materials*, Kuala Lumpur, Malaysia.
- [39] Leaversuch, R.D., (2000), "Modern Plastics," 77(12): pp. 56-60.

- [40] Holbery, J., Houston, D., (2006), "Natural-Fiber-Reinforced Polymer Composites in Automotive Applications", *JOM*, 58(11): pp.80-6.
- [41] Burgueno, R., Quagliata, M.J., Mehta, G.M., Mohanty, A.K., Misra, M. and Drzal, L.T. (2005), "Sustainable Cellular Biocomposites from Natural Fibers and Unsaturated Polyester Resin for Housing Panel Applications", *Journal of Polymers and the Environment*, 13(2): pp.139-149.
- [42] Rials, T.G., Wolcott, M.P. and Nassar, J.M., (2001), "Interfacial Contributions in Lignocellulosic Fiber-Reinforced Polyurethane Composites", *Journal of Applied Polymer Science*, 80(4): pp.546-555.
- [43] Mueller, D.H. and Krobjilowski, A., (2003), "New Discovery in the Properties of Composites Reinforced with Natural Fibers", *Journal of Industrial Textiles*, 33(2): pp.111-129.
- [44] Bledzki, A.K. and Gassan, J., (1999), "Composites Reinforced with Cellulose Based Fibres", *Progress in Polymer Science*, 24(2): pp.221-274.
- [45] Eichhorn, S.J., Baillie, C.A., Zafeiropoulos, N., Mwaikambo, L.Y., Ansell, M.P., Dufresne, A., Entwistle, K.M., Herrera-Franco, P.J., Escamilla, G.C., Groom, L.H., Hughes, M., Hill, C., Rials, T.G. and Wild, P.M., (2001), "Review: Current international research into cellulosic fibres and composites", *Journal of Materials Science*, 36(9): pp.2107-2131.
- [46] Brouwer, W.D., (2000), "Natural Fibre Composites in Structural Components: Alternative Applications for Sisal," *FAO, Common Fund for Commodities—Alternative Applications for Sisal and Henequen – Technical Paper No. 14.*
- [47] Oksman, K., M. Skrifvars, and J.F.Selin, (2003), "Natural fibres as reinforcement in polylactic acid (PLA) composites," *Composites Science and Technology*, 2003. 63: pp. 1317-1324.
- [48] Bodros, E., Pillin, I., Montrelay, N., Baley, C., (2007), "Could biopolymers reinforced by randomly scattered flax fiber be used in structural applications", *Composites Science and Technology*, 67(3-4): pp.462-470.
- [49] Pal, P.K., (1984), "Plastics Rubber Process Appl," 4: pp. 215-219.
- [50] Bledzki, A.K. and Gassan, J., (1999), "Composites reinforced with cellulose based fibre," *Prog. Polym. Sci.* 24: pp. 221–274.
- [51] Mohanty, A.K., Misra, M. and Drzal, L.T., (2002), "Sustainable bio-composites from renewable resources: opportunities and challenges in the green materials world," *J. Polym. Environ.* 10: pp. 19–26.

- [52] Joseph, S., Sreekalab, M.S., Oommen, Z., Koshyc, P. and Thomas, S., (2002), “A comparison of the mechanical properties of phenol formaldehyde composites reinforced with banana fibres and glass fibres”, *Compos. Sci. Technol.* 62: pp.1857–1868.
- [53] Roe, P.J. and Ansel, M.P., (1985), “Jute reinforced polyester composites”, *J. Mater. Sci.* 20: pp.4015.
- [54] Qiu Zhang, X. M., Zhi Rong, M., Shia, G. and Cheng Yang, G., (2003), “Self reinforced melt processable composites of sisal”, *Compos. Sci. Technol.* 63 : pp.177–186.
- [55] Baiardo, M., Zini, E. and Scandola, M., (2004), ‘Flax fibre–polyester composites’, *J.Compos.: Part A* 35 : pp.703–710.
- [56] George, J., Sreekala, M.S., and Thomas, S., (2002), “A review on interface modification and characterization of natural fibre reinforced plastic composites”, *Ploym. Eng. Sci.* 41 (9): pp.1471–1485.
- [57] Valadez-Gonzales, A., Cetvantes-Uc, J.M., Olayo, R. and Herrera Franco, P.J., (1999), “Effect of fibre surface treatment on the fibre-matrix bond strength of natural fibre reinforced composites”, *Composites, Part B* 30 (3): pp.309–320.
- [58] Rana, A.K., Mitra, B.C. and Banerjee, A.N., (1999), “Short jute fibre-reinforced polypropylene composites: dynamic mechanical study”, *J. Appl. Polym. Sci.* 71: pp.531–539.
- [59] Manikandan Nair, K.C., Diwan, S.M. and Thomas, S., (1996), “Tensile properties of short sisal fiber reinforced polystyrene composites”, *J. Appl Polym. Sci.* 60: pp.1483–1497.
- [60] Bax, B. and Mussig, J., (2008), “Impact and tensile properties of PLA/Cordenka and PLA/flax composites”, *Composites Science and Technology*, 68: pp. 1601-1607.
- [61] El-Tayeb, N.S.M., (2009), “Development and characterisation of low-cost polymeric composite materials”, *Materials and Design* 30: pp.1151–1160.
- [62] Jacoba, M. Thomas, S. and Varugheseb, K.T., (2004), “Mechanical properties of sisal/oil palm hybrid fiber reinforced natural rubber composites”, *Compos. Sci. Technol.* 64: pp. 955–965.
- [63] Pothana, L.A., Oommen, Z. and Thomas, S., (2003), “Dynamic mechanical analysis of banana fiber reinforced polyester composites”, *Compos. Sci. Technol.* 63 (2): pp.283–293.

- [64] Yousif, B.F. and El-Tayeb, N.S.M., 2006, "Mechanical and tribological characteristics of OPRP and CGRP composites", in: The Proceedings ICOMAST, GKH Press, Melaka, Malaysia, pp. 384–387,
- [65] Tong, J., Arnell, R.D. and Ren, L.-Q., (1998), "Dry sliding wear behaviour of bamboo", *Wear* 221: pp.37–46.
- [66] Tong, J., Ma, Y., Chen, D., Sun, J. and Ren, L., (2005), "Effects of vascular fiber content on abrasive wear of bamboo", *Wear* 259: pp.37–46.
- [67] Hornsby, P.R., Hinrichsen, E. and Tarverdi, K., (1997), "Preparation and properties of polypropylene composites reinforced with wheat and flax straw fibres", Part II. Analysis of composite microstructure and mechanical properties, *J. Mater. Sci.* 32: pp. 1009–1015.
- [68] Pothan, L.A., Thomas, S. and Neelakantan, N.R., (1997), "Short banana fibre reinforced polyester composites: mechanical, failure and aging characteristics", *J. Reinf. Plast. Comp.* 16: pp.744.
- [69] Roger M. Rowell , (1998), "Property Enhanced Natural Fiber Composite materials based on chemical modification Science and Technology of Polymer and Advanced Materials."
- [70] Gassan J., (2002), "A study of fiber and interface parameters affecting the fatigue behaviour of natural fiber composites", *Composite Part A* 33: pp.369–374.
- [71] Hepworth, D.G., Hobson, R.N., Bruce, D.M. and Farrent, J.W., (2003), "The use of unretted hemp in composite manufacture", *Composites A* 31: pp.1279–1283.
- [72] Joseph, P.V., Kuruvilla, J. and Sabu T., (2002), "Short sisal fibre reinforced polypropylene composites: the role of interface modification on ultimate properties", *Compos. Interf.* 9 (2): pp.171–205.
- [73] El-Sayed, A.A., El-Sherbiny, M.G., Abo-El-Ezz, A.S. and Aggag, G.A., (1995), "Friction and wear properties of polymeric composite materials for bearing applications", *Wear* 184: pp.45–53.
- [74] Chin CW, Yousif BF., (2009) "Potential of kenaf fibres as reinforcement for tribological applications." *Wear* 267:1550–7.
- [75] Yousif B, El-Tayeb N. (2008) "Adhesive wear performance of T-OPRP and UT-OPRP composites. *Tribol Lett* 32:199–208.
- [76] Chand N, Dwivedi UK. (2008) "Sliding wear and friction characteristics of sisal fibre reinforced polyester composites: effect of silane coupling agent and applied load." *Polym Compos* 29:280–4.

- [77] Hashmi SAR, Dwivedi UK, Chand N. (2007) “Graphite modified cotton fibre reinforced polyester composites under sliding wear conditions.” *Wear* 262:1426–32.
- [78] Chand N, Dwivedi UK. (2006) “Effect of coupling agent on abrasive wear behaviour of chopped jute fibre-reinforced polypropylene composites.” *Wear* 261:1057–63.
- [79] Yousif BF, Lau STW, McWilliam S. (2010) “Polyester composite based on betelnut fibre for tribological applications.” *Tribol Int* 43:503–11.
- [80] W. Wang, M. Sain , P.A. Cooper, (2005) “Study of moisture absorption in natural fiber plastic composites” *Composites Science and Technology* 66 (2006) :379–386
- [81] Chi-Hung Shen and George S. Springer ,(1976) “Moisture Absorption and Desorption of Composite Materials.” *Journal of Composite Materials*.
- [82] J. L. ABOT A. YASMIN AND I. M. DANIEL, (2005) “Hygroscopic Behavior of Woven Fabric Carbon–Epoxy Composites”. *Journal of REINFORCED PLASTICS AND COMPOSITES*, Vol. 24, No. 2/2005
- [83] Hyo Jin Kim , Do Won Seo, (2006) “Effect of water absorption fatigue on mechanical properties of sisal textile-reinforced composites” *International Journal of Fatigue* 28 (2006): 1307–1314
- [84] Xue Li,Lope G.Tabil,S.Panigrahi, (2007) “Chemical treatments of Natural fiber for use in natural fiber reinforced composite:A review”,*J Polym Environ*:15,25-33.
- [85] Kabir,M.M,Wang,H ,Aravinthan,T,Cardona,F and Lau.K.T, (2011) “Effect of natural fiber surface on composite properties:A review”*Journal of Energy,Environment and Sustainability*:pp.94-99.
- [86] Maya Jacob John, Anandjiwala Rajesh D., (2008), “Recent Developments in Chemical Modification and Characterization of Natural Fiber-Reinforced Composites”, *Polymer composites*: pp.187-207.
- [87] Joseph, K., Thomas, S. and Pavithran, C., (1996), “Effect of chemical treatment on the tensile properties of short sisal fibre-reinforced polyethylene composites”, *Polymer* 37: pp. 5139–49.
- [88] Joseph, P.V., Joseph, K. and Thomas, S., (1999), “Effect of processing variables on the mechanical properties of sisal-fiber-reinforced polypropylene composites”, *Compos Sci Techol.*, 59: pp.1625–40.
- [89] George, J., Bhagawan, S.S. and Thomas, S., 1998, “Effects of environment on the properties of low-density polyethylene composites reinforced with pineapple-leaf fiber”, *Compos. Sci. Techno.*, 58: pp.1471–85.

- [90] K. Hardinnawirda and I. SitiRabiatull Aisha, (2012), “Effect of rice husks as filler in polymer matrix composites”, *Journal of Mechanical Engineering and Sciences (JMES)* e-ISSN: 2231-8380; Volume 2: pp. 181-186
- [91] Joseph, P.V., Rabello, M.S., Mattoso, L.H.C., Joseph, K., and Thomas, S., (2002), “Environmental effects on the degradation behaviour of sisal fibre reinforced polypropylene composites”, *Composites Science and Technology*, **62**(10-11): pp.1357-1372.
- [92] Stark, N., (2001), “Influence of moisture absorption on mechanical properties of wood flour-polypropylene composites”, *J. Thermoplast. Compos. Mater.*,14: pp.421–32.
- [93] Yuan, X., Jayaraman, K. and Bhattacharya, D., (2002), “Plasma treatment of sisal fibers and its effects on tensile strength and interfacial bonding”, In *Proceedings the Third International Symposium on Polymer Surface Modification: Relevance to Adhesion*, *Journal of Adhesion Science and Technology Special Publication* (0):1-25. Newark, NJ: MST Conferences, LLC.
- [94] Stamboulis, A., Baillie, C.A., Garkhail, S.K., Van Melick, H.G.H. and Peijs T., (2000), “Environmental durability of flax fibers and their composites based on polypropylene matrix”, *Applied Composite Materials*, 7: pp.273-294.
- [95] Thomas, Selvin P., Sreekumar, P.A., Saiter, J.M., Joseph K., Unnikrishnan, G. and Thomas, S., (2009), “Effect of fiber surface modification on the mechanical and water absorption characteristics of sisal/polyester composites fabricated by resin transfer molding”, *Compos Part A* 40: pp.1777–1784.
- [96] A. Athijayamania, M. Thiruchitrambalamb, U Natarajana, B. Pazhanivel , (2009), “Effect of moisture absorption on the mechanical properties of randomly oriented natural fibers/polyester hybrid composite,” *Materials Science and Engineering A* 517 (2009) 344–353.
- [97] Z. Leman, S.M. Sapuan, A.M. Saifol, M.A. Maleque, M.M.H.M. Ahmad, (2008), “Moisture absorption behavior of sugar palm fiber reinforced epoxy composites”. *Materials and Design* 29 (2008) 1666–1670.
- [98] Chitaranjan Deo and S.K.Acharya, (2010), “Effect of moisture absorption on mechanical properties of chopped natural fiber reinforced epoxy composite.” *Journal of Reinforced Plastic and Composite*, Vol.29: pp.2513-2521

- [99] P.Mishra & S.K.Acharya, (2009), “ The influence of fiber treatment on the performance of bagasse fiber reinforced composite.” *International Journal of Reinforced Plastic Composites*, Stanford University, USA, Vol.28 No.24: pp.3029-3036
- [100] Singleton, A.C.N., Baillie, C.A., Beaumont, P.W.R. and Peijs, T., (2003), *Compos B: Eng* 34:519
- [101] Rana AK, Mandal A, Bandyopadhyay B. (2003), “Short jute fiber reinforced composites: effect of compatibilizer, impact modifier and fiber loading.” *Compos Sci Technol*; 63: pp.801–806.
- [102] Mukherjee, R.N., Pal S.K., Sanyal S.K., Phani K.K., (1984), “Role of interface in fiber reinforced polymer composites with special reference to natural fibers.” *Journal of Polymer Material*, (1): pp. 69-81.
- [103] Gassan J, Bledzki AK, (1999), “Alkali treatment of jute fibers: relationship between structure and mechanical properties.” *Journal of Applied Polymer Science*, (71): pp. 623-629.
- [104] Zadorecki P., Flodin P., (1985), “Surface modification of cellulose fibers. I. Spectroscopic characterization of surface-modified cellulose fibers and their copolymerization with styrene.” *J Appl Polym Sci*, (30): pp. 2419–2429.
- [105] Zadorecki, P. and Flodin, P., (1985), “Surface modification of cellulose fibres. II. The effect of cellulose fibre treatment on the performance of cellulose– polyester composites.” *J Appl Polym Sci*, (3): pp. 3971–3983.
- [106] Xue, Li., Lope G. and Panigrahi, S., (2007) “Chemical treatments of natural fiber for use in natural fiber reinforced composites: A review”. *Springer Science*, Volume 15: pp. 25-33.
- [107] Mohanty, A.K., Misra, M. and Drzal, L.T., (2001), *Compos Interfaces* 8: pp.313.
- [108] Agrawal, R., Saxena, N.S., Sharma, K.B., Thomas, S. and Sreekala, M.S., (2000), *Material Science Engg. A* 277: pp.77.
- [109] Jahn, A., Schroder, M.W., Futing, M. and Schezel, K, Diepenbrock, (2002), *Wear , Spectrochim,Acta A: Mol Biomol Spectrosc* 58: pp.2271.
- [110] Paul, S., Puja, N. and Rajive, G., (2003). *Molecules* 8: pp.374
- [111] Joseph, K., L.H.C. Mattoso, R.D. Toledo, S. Thomas, de-Carvalho, L.H., Pothan, L., Kala, S. and James, B., (2000), “Natural fiber reinforced thermoplastic composites, In *Natural Polymers and Agrofibers Composites*, ed. E. Frollini, A.L.

- Leão and L.H.C. Mattoso, 159-201. São Carlos, Brazil: Embrapa, USP-IQSC, UNESP
- [112] Wang, B., (2004), MSc. Thesis. University of Saskatchewan.
- [113] Sreekala, M. S.; Kumaran, M. G.; Sabu, M. G., (1998), “Oil Palm Fibers: Morphology, Chemical Composition, Surface Modification, and Mechanical Properties”, *J Appl Polym Sci*, 66(5): pp.821-835
- [114] Ray, D. and Sarkar, B. K., (2001), “Characterization of alkali-treated jute fibers for physical and mechanical properties.” *J Appl Polym Sci* , 80: pp. 1013–1020.
- [115] Aziz, S. H., and Ansell, M. P., (2004), “The effect of alkalization and fibre alignment on the mechanical and thermal properties of kenaf and hemp bast fibre composites: Part 1 – polyester resin matrix.” *Compos Sci Technol*, 64: pp.1219.
- [116] Samal, R. K., Acharya, S., Mohanty, M. and Ray, M. C., (2001), “FTIR spectra and physico-chemical behavior of vinyl ester participated transesterification and curing of jute.” *J Appl Polym Sci.*, 79: pp. 575.
- [117] Higgins, G. H., V. Goldsmith, and A. N. Mukherjee, (1958), *J. Polym. Sci.*, 32: pp.57.
- [118] Roncero, M.B., Torres, A.L., Colom, J.F., and Vidal, T., (2005), “The effect of xylanase on lignocellulosic components during the bleaching of wood pulps”, *Bioresource Technology*, 96(1): pp. 21-30.
- [119] Kelly C.C Karvalho, Daniella R. Mulinary, Herman J.C Voorwald and Maria O.H Cioffi, (2010), Chemical Modification effect on the Mechanical properties of HIPS/Coconut fiber composites.” *Bio-Resources* 5(2):pp.1143-1155
- [120] Noor Ida Amalina Ahamad Nordin , Hidayah Ariffin, Yoshito Andou, Mohd Ali Hassan, Yoshihito Shirai, Haruo Nishida, Wan Md Zin Wan Yunus, Subbian Karuppuchamy and Nor Azowa Ibrahim, (2013), Modification of Oil Palm Mesocarp Fiber Characteristics Using Superheated Steam Treatment’ *Molecules* 2013, 18, 9132-9146
- [121] A.K. Mohanty, Mubarak A. Khan , G. Hinrichsen, (2000), Surface modification of jute and its influence on performance of biodegradable jute-fabric/Biopol composites.” *Composites Science and Technology* 60: pp.1115-1124
- [122] Susan Wong, Robert Shanks, Alma Hodzic, (2004), “Interfacial improvements in poly(3-hydroxybutyrate)-flax fibre composites with hydrogen bonding additives.” *Composites Science and Technology* 64 :pp. 1321–1330

- [123] Vijay K. Kaushik, Anil Kumar¹, Susheel Kalia, (2012), "Effect of Mercerization and Benzoyl Peroxide Treatment on Morphology, Thermal Stability and Crystallinity of Sisal Fibers." *International Journal of Textile Science* , 1(6):pp. 101-105
- [124] M Panda, S Paridab, A Parijac, SC Das , (2010), "Synthesis and characterization of agro based biocomposite with amino resin." *Research Journal of Pharmaceutical, Biological and Chemical Sciences* ISSN 0975-8585
- [125] Raj, R.G., Kokta, B.V., Grouleau, G., and Daneault, C., (1990), "The influence of coupling agents on mechanical properties of composites containing cellulosic fillers", *Polymer.-Plast.Technol.Eng*, 29(4): pp. 339-353.
- [126] Newson, W.R. and Maine, F.W., (2002), "Second generation woodfibre-polymer composites." In *Progress in Woodfibre-Plastic Composites*. Toronto, Canada.
- [127] Abdul Khalil, H.P.S., Chow, W.C., Rozman, H.D., Ismail, H., Ahmad, M.N., and Kumar, R.N., (2001), "The effect of anhydride modification of sago starch on the tensile and water absorption properties of sago-filled linear low-density polyethylene (LLDPE)." *Polym.-Plast.Technol.Eng*, 40(3): pp. 249-263.
- [128] Karmakar, A., Chauhan, S.S., Modak, J.M. and Chanda, M., (2007), "Mechanical properties of wood-fiber reinforced polypropylene composites." *Comp A*, 38: pp.227–33.
- [129] Thwe M.M. and Liao, K., (2003), "Environment degradation of bamboo/glass fibre hybrid polypropylene composites." *J Mater Sci Lett*, 38:pp.363–81.
- [130] Sreenivasan, S., Iyer, P.B, and Krishna Iyer K.R., (1996), "Influence of delignification and alkali treatment on the fine structure of coir fibers (*Cocos Nucifera*)." *J Mater Sci*, 31: pp.721–726.
- [131] Britton, P., Hodzic, A., Curro, R., Shu, L., Berndt, C.C. and Shanks, R.A., (2006), "Mechanical properties of PHB-Bagasse Composites", *Proc ACUN-5, Developments in composites: Advanced, Infrastructural, natural, and Nano-composites*, UNSW, Sydney, Australia , July 11-14.
- [132] Shinichi Shibata, Yong Cao, Isao Fukumoto, (2005), "Press forming of short natural fiber-reinforced biodegradable resin:Effects of fiber volume and length on flexural properties." *Polymer Testing* 24 :pp. 1005–1011

- [133] Cao, S. Shibata, I. Fukumoto, (2006), “Mechanical properties of biodegradable composites reinforced with bagasse fibre before and after alkali treatments.” *Composites: Part A* 37 :pp. 423–429
- [134] J. Giridhar, Kishore and R.M.V.G.K. Rao, (1985), “Moisture Absorption Characteristics of Natural Fibre Composites.” *Journal of reinforced plastics and composites*, Vol. 5-April/ 1986
- [135] H.N. Dhakal , Z.Y. Zhang, M.O.W. Richardson, (2006), “Effect of water absorption on the mechanical properties of hemp fibre reinforced unsaturated polyester composites.” *Composites Science and Technology* 67 (2007) :pp.1674–1683
- [136] Ana Espert, Francisco Vilaplana, Sigbritt Karlsson, (2004), “Comparison of water absorption in natural cellulosic fibres from wood and one-year crops in polypropylene composites and its influence on their mechanical properties. ” *Composites: Part A* 35 :pp. 1267–1276
- [137] Csari, P., Davies, P., and Mazeas, F., (2001), “Sea Water Aging of Glass Reinforced Composites: Shear Behavior and Damage Modeling.” *Journal of Composite Materials*, 35: pp.1343–1371.
- [138] Chiou, J.S. and Paul, D.R., (1986), “Sorption equilibria and kinetics of ethanol in miscible poly(vinylidene fluoride)/poly(methyl methacrylate) blends.” *Journal of Polymer Engineering Science*, 26: pp.1218-1227.
- [139] Nawadon Petchwattana & Sirijutaratana Covavisaruch & Dhisana Pitidhamabhorn, (2013), “Influences of water absorption on the properties of foamed poly(vinyl chloride)/rice hull composites.” *J Polym Res* (2013) 20:pp.172
- [140] Marcovich, N.E., Reboredo, M.M. and Aranguren, M.I., (1999), “Moisture diffusion in polyesterwood flour composites.” *Polymer* 40(26): pp.7313-7320.
- [141] Wang, W., Sain, M. and Cooper, P.A., (2006), “Study of moisture absorption in natural fibre plastic composites.” *Composites Science and Technology*, 66(3-4): pp.379-86
- [142] P.V. Joseph, Marcelo S. Rabello, L.H.C. Mattoso, Kuruvilla Joseph, Sabu Thomas, (2002), “Environmental effects on the degradation behaviour of sisal fibre reinforced polypropylene composites.” *Composites Science and Technology* 62 :pp. 1357–1372
- [143] Shen, C.H. and Springer, G.S., (1976), “Moisture Absorption and Desorption of Composite Materials.” *Journal of Composite Materials*, 10: pp.1-20.

- [144] Shi, S.Q. and Gardner, D.J., (2006), "Effect of density and polymer content on the hygroscopic thickness swelling rate of compression molded wood fiber/polymer composites." *Wood Fiber Sci.* 38: pp.520–526.
- [145] Amontons, G., (1699), *Mem. Acad. T. , Ser. A:* pp. 257-282.
- [146] Petrov, N.P., (1893), "Friction in machines and the effect of the lubricant", *Inzh. Ah*, 1893, pp 71-140, Vol. 2: pp. 227-279.
- [147] Tower, B., (1983), "First report on friction experiments", *Proc., Inst. Mech. Eng.*, London, Nov: pp. 632-659.
- [148] Renolds, O., (1886), "On the theory of lubrication and its application to Mr. Beauchamp Tower's experiments." *Philos. Trans. T. Soc. London*, Vol. 177: pp. 157-234.
- [149] Holm, R., (1983), "The frictional force over the real area of Contact", *Wiss. Vereoff. Siemens Werken*, Vol. 17 (4):pp. 38-42.
- [150] Peterson, M. B., (1990), "Advanced in tribo-materials-I Achievements in Tribology." *Amer, Soc, Mech. Eng.*, Vol.1, New York: pp.91-109.
- [151] Rigney, D.A., (1981), In: D.A. Rigney (Ed.), "Fundamentals of Friction and Wear of Materials." *American Society for Metals, Metals Park, Ohio:* pp.1–12.
- [152] Ashby, M.F. and Lim, S.C., (1990), "Wear-mechanism maps", *Scripta Metallurgical et Materialia*, Vol.24: pp. 805-810.
- [153] Wang, Y., Lei, T.C. and Gao, C.Q., (1990), "Influence of isothermal hardening on the sliding wear behaviour of 52100 bearing steel." *Tribology International*, Vol. 23(1): pp. 47-53.
- [154] Lim, S. C., (1998), "Recent developments in wear mechanism Maps." *Tribology International* Vol. 31, Nos 1–3: pp. 87–97.
- [155] Eyre, L.S., (1976), "Wear Characteristics of metals." *Tribology International*, October-1976: pp. 203-212.
- [156] Dowson, (1985), "Wear oh where." *International Conference on wear of Materials*, Vancouver Canada, April 14-18,
- [157] Blau, J., (1997), "Fifty years of research on the wear of metals." *Tribology International*, Vol. 30(5): pp. 321-331.
- [158] Barwell, F. T. and Strang, C. D., (1952), "Metallic Wear", *Proc. Roy. Soc. London*, A, 212 (III): pp. 470-477.
- [159] Archard, J.F., (1953), "Contact Rubbing of flat Surfaces." *J. Appl, Phys* 24: pp. 981-988.

- [160] Archard, J.F. and Hirst, W, 1957, "The Wear of Metal Under Unlubricated Conditions." Proc. Roy. Soc. London, A, Vol. 238: pp 515-528.
- [161] Kragelski, I. V., (1983), "Grundlagen der Berechnung von Reibung und VerschleiR." Carl Hanser Verlag. Miinchenu. Wien.
- [162] Fleischer, G., (1973), "Energetische Methode der Bestimmung des VerschleiRes." Schtnierungsrechnik 4(9): pp. 269-274.
- [163] Gahr, K.H.Z., (1987), "Microstructure and wear of materials."Tribology series 10, Elsevier Science Publishers.
- [164] Stachowiak, G.W. and Batchelor, A.W., (1993), Engineering tribology. Amsterdam: Elsevier.
- [165] Friedrich, K., (1986), "Friction and wear of polymer composites." In: Friedrich K, editor. Composite materials series-1, Amsterdam: Elsevier; Chapter-8.
- [166] Thorp, J.M., (1982), "Abrasive wear of some commercial polymers." Tribol. Int., 15: pp.89–135.
- [167] Budinski, K.G., (1997), "Abrasion resistance of plastics." Wear, (203) (204): pp.302–309.
- [168] Evans, D.C., and Lancaster, J.K., (1979). "The Wear of Polymers." In: Scott, D. (Ed.), Treatise on Materials Science and Technology, New York, USA; Academic Press, Vol. 13: pp. 85—139.
- [169] Unal, H., Sen, U. and Mimaroglu, A., 2005, "Abrasive behaviour of polymeric materials", Mater. Des. 26: pp.705–710.
- [170] Unal, H., Sen, U. and Mimaroglu, A., (2004), "Dry Sliding Wear Characteristics of Some Industrial Polymers Against Steel Counter Face." Journal of Tribo, 37: pp.727–732.
- [171] Shipway, P.H. and Ngao, N.K., (2003), "Microscale abrasive wear of polymeric materials", Wear, 255: pp.742–750.
- [172] Harsha, A.P. and Tewari, U.S., (2003), "Two-body and three-body abrasive wear behaviour of polyaryletherketone composites", Polymer Testing,22: pp. 403–418.
- [173] Cirino, M., Pipes, R.B. and Friedrich, K., (1987), "The Abrasive Wear Behavior of Continuous Fiber Polymer Composites", J. Mater. Sci., 22: pp.2481–2492.
- [174] Cirino, M., Friedrich, K. and Pipes, R.B., (1988), "Evaluation of Polymer Composites for Sliding and Abrasive Wear Application", Composites, 19: pp.383–392.

- [175] Chand, N., Nayak, A. and Neogi, S., (2000), "Three-Body Abrasive Wear of Short Glass Fiber Polyester Composite." *Wear*, 242: pp.32–46.
- [176] Bijwe, J., Logani, C.M. and Tewari, U.S., (1989), "Influence of fillers and fibre reinforcement on abrasive wear resistance of some polymeric composites." In: *Proceeding of the International Conference on Wear of Materials*, Denver, CO, USA, April 8–14: pp. 75–92.
- [177] Liu, C., Ren, L., Arnell, R.D. and Tong, J., (1999), "Abrasive wear behavior of particle reinforced ultrahigh molecular weight polyethylene composites", *Wear*; 225–229: pp.199–204.
- [178] Chand, N. and Dwivedi, U.K., (2006), "Effect of coupling agent on abrasive wear behaviour of chopped jute fibre-reinforced polypropylene composites." *Wear*, 261 (10): pp.1057–1063.
- [179] Zhang, H., Zhang, Z., Guo, F., Jiang, W. and Liu W.M., (2009), "Study on the tribological behavior of hybrid PTFE/ cotton fabric composites filled with Sb_2O_3 and melaminecyanurate," *Tribol. Int.*, 42(7): pp.1061–1066.
- [180] Hashmi, S.A.R., Dwivedi, U.K. and Chand, N., (2007), "Graphite modified cotton fiber reinforced polyester composites under sliding wear conditions, *Wear*, 262 (11–12): pp.1426–1432.
- [181] Yousif, B.F. and El-Tayeb, N.S., (2007), "The effect of oil palm fibers as reinforcement on tribological performance of polyester composite." *Surface Review and Letters (SRL)*, 14 (6): pp.1095–1102.
- [182] Yousif, B.F., (2009), "Frictional and wear performance of polyester composites based on coir fibers." *Proc IME J. J. Eng Tribol.*, 223(1): pp.51–9.
- [183] Chin, C.W. and Yousif, B.F., (2009), "Potential of kenaf fibers as reinforcement for tribological applications", *Wear*, 267: pp.1550–1557
- [184] Yousif, B.F., Lau, Saijod, T.W. and Mc-William, S., (2010), "Polyester composite based on betelnut fibre for tribological applications." *Tribology International*, 43: pp.503–511.
- [185] Lai, W.L. and Mariatti, M., (2008), "The properties of woven betel palm (areca catechu) reinforced polyester composites." *J. Reinf. Plast. Compos.*; 27: pp.925-935
- [186] Dwivedi, U.K. and Chand, N., (2008), "Influence of Wood Flour Loading on Tribological Behavior of Epoxy Composites." *Polymer Composites*; 29: pp.1189-1192

- [187] Mishra Punyapriya and Acharya S.K , (2010), “ Effect of fiber loading on the abrasive wear behaviour of baggasse fiber composite.”*Journal of Tribology Research* Vol.1 No.2.
- [188] Chitaranjan Deo and S.K.Acharya, (2009), “Effect of Load and Sliding Velocity on Abrasive Wear of Lantana-Camara Fiber reinforced epoxy composite.” *I.Mech Engg(UK) Part J ,Journal of Engineering tribology*.On line first published on November 25, 2009, DOI:0.1243/13506501JET699
- [189] Kamal Kumar Basumatary & Niharika Mohanta & S. K. Acharya, (2014), “Effect of fiber loading on abrasive wear behaviour of Ipomoea carnea reinforced epoxy composite.” *Int J Plast Technol* DOI 10.1007/s12588-014-9065-0
- [190] Dwivedi, U. K., Ghosh, A., and Chand, N., (2007), “Abrasive wear behaviour of bamboo powder filled polyester composites.” *BioResources*; 2(4): pp.693-698.
- [191] Soda, N., (1975), “Wear of some F.F.C metals during unlubricated sliding part-1. Effects of load, velocity and atmospheric pressure on wear.” *Wear*, 33: pp.1-16.
- [192] Burwell, J.T. and Strang, C.D., (1953), “Metallic wear”, *Proc.Soc (London)*, 212 A May: pp.470-477.
- [193] Burwell, J.T., (1957), “Survey of possible wear mechanisms.” *Wear-1*; 58: pp.119-141.
- [194] Zumgahr, K.H., (1987), “Microstructure and wear of materials.” Elsevier, Amsterdam.
- [195] Ko, P.L., (1987), “Metallic wear-a review with special references to vibration-induced wear in power plant components.” *Tribology International*, April,Vol.20, No.1: pp.66-78.
- [196] Verma, A. P. and Sharma, P. C., (1992), “Abrasive Wear Behaviour of GRP Composite.”*The Journal of the Institute of Engineers (India) , Pt MC2,Vol.72*: pp. 124.
- [197] Wu, J. and Cheng, X.H., (2006), “The tribological properties of Kevlar pulp reinforced epoxy composites under dry sliding and water lubricated condition.” *Wear*, 261: pp.1293–1297

- [198] Tuvshin, Dugarjav, Takashi Yamaguchi, Shohei Katakura and Kazuo Hokkirigawa, (2009), “ The effect of Carbonizing Temperature on Friction and Wear Properties of Hard Porous Carbon Materials made from Rice Husk.” *Tribology Online*, 4,1 (2009) 11-16
- [199] Tuvshin Dugarjav, Takeshi Yamaguchi, Kei Shibata and Kazuo Hokkirigawa, (2010), “Friction and wear properties of rice husk ceramics under dry condition.” *Journal of Mechanical Science and Technology* 24 (2010) 85~88
- [200] Krishnarao, R. V.: Godkhindi, M. M., (1992), “Distibution of silica in rice husks and its effect on the formation of silicon carbide.” *Ceram. Int.*1992, 18, 243.
- [201] Kumar, B. Godkhindi, (1996), “ M. M. Studies on the formation of SiC, Si₃N₄ and Si₂N₂O during pyrolysis of rice husk .” *J.Mater. Sci.Lett.*1996, 15,403.
- [202] Wang, Q.B.: Guo, M. X.: Xu, H., (1997), “ Study on synthesizing SiC whiskers from the rice hulls and to be reinforcement for Si₃N₄ ceramic matrix composite materials. Adv.” *Ceram.*1997, 18(4), 13.
- [203] Chand N and Dwivedi UK, (2006), “ Effect of coupling agent on abrasive wear behaviour of chopped jute fibre-reinforced polypropylene composites”. *Wear* 261: 1057-1063.
- [204] Wei Li, Kunbin Yang, Jinhui Peng, Libo Zhang, Shenghui Guo, Hongying Xia, (2008), “Effects of carbonization temperature on characteristics of porosity in coconut shell chars and activated carbons derived from carbonized coconut shell chars.” *Ind Crop Prod* ; 28: 190-198.
- [205] Sanger SH, Mohod AG, Khandetode YP, Shrirame HY and Deshmukh AS, (2011), “Study of Carbonization for Cashew Nut Shell.” *Res J Chem Sci* ;1: pp.43-55.
- [206] Vencel A, Bobic I, Arostegui S, Bobic B, Marinkovic A and Babic M, (2010), “Structural, mechanical and tribological properties of A356 aluminium alloy reinforced with Al₂O₃, SiC and SiC + graphite particles”. *J Alloys Compd* ; 506:pp. 631–639.
- [207] Sajjadi SA, Torabi Parizi M, Ezatpour HR and Sedghi A, (2012), “Fabrication of A356 composite reinforced with micro and nano Al₂O₃ particles by a developed compo casting method and study of its properties.” *J Alloys Compd*; 511: pp.226–231.
- [208] Finnie, I., (1995), “Some reflections on the past and future of erosion: Part-I.” *Wear*, 186/187: pp.1-101.209]

- [209] Meng, H. C. and Ludema, K. C., (1995), "Solid Particle Erosion Resistance of Ductile Wrought Super Alloys and Their Weld Overlay Coatings." *ibid*, 181–183: pp.443.
- [210] Bitter, J.G.A., (1963), "A study of erosion phenomena." Part I. *Wear*; 6: pp.5–21.
- [211] Hutchings, I.M., Winter, R.E. and Field, J.E, (1976), "Solid particle erosion of metals: the removal of surface material by spherical projectiles." *Proc Roy Soc Lond, Ser A*; 348: pp.379-392.
- [212] Pool, K.V., Dharan, C.K.H. and Finnie, I., (1986), "Erosive wear of composite materials." *Wear*;107: pp.1-12.
- [213] Kulkarni, S.M., Kishore, K., (2001), "Influence of matrix modification on the solid particle erosion of glass/epoxy composites." *Polymer and Polymer Composites*,9: pp.25-30.
- [214] Rajesh, J.J, Bijwe, J., Tewari, U.S. and Venkataraman, B., (2001), "Erosive wear behavior of various polyamides", *Wear*, 249: pp.702 – 714.
- [215] Harsha, A.P., Tewari, U.S., Venkataraman, B., (2003), "Solid particle erosion behaviour of various polyaryletherketone composites." *Wear*,254: pp. 693–712.
- [216] Roy, M., Vishwanathan, B. and Sundararajan, G., (1994), "The solid particle erosion of polymer matrix composites." *Wear*, 171: pp.149–161.
- [217] Hager A, Friedrich K, Dzenis YA, Paipetis SA. (1995), " Study of erosion wear of advanced polymer composites." In: Street K, editor. *ICCM-10 Conference Proceedings*, Whistler, BC, Canada. Cambridge (UK):,Woodhead Publishing: pp. 155–62.
- [218] Barkoula, N.M. and Karger-Kocsis, J., (2002), "Review-processes and influencing parameters of the solid particle erosion of polymers and their composites." *J. Mater. Sci.* 37: pp. 3807–3820.
- [219] Tewari, U.S., Harsha, A.P., Hager, A.M. and Friedrich, K., (2003), "Solid particle erosion of carbon fibre– and glass fibre–epoxy composites." *Compos Sci Technol.* 63: pp.549–57.
- [220] Bhushan, B., (1999), " Principles and applications of tribology,"New York: Wiley.
- [221] Harsha, A.P. and Thakre, A.A., (2007), "Investigation on solid particle erosion behaviour of polyetherimide and its composites," *Wear*; 262: pp.807–818.
- [222] Bijwe, J., Indumathi, J., John, R.J. and Fahim, M., (2001), "Friction and wear behavior of polyetherimide composites in various wear modes", *Wear*, 249: pp.715–726.

- [223] Bijwe, J., Indumathi, J. and Ghose, A.K., (2002), "On the abrasive wear behavior of fabric-reinforced polyetherimide composites." *Wear*, 253: pp.768–777.
- [224] Mishra Punyapriya & Acharya S.K ,(2010), " Solid particle erosion of baggasse fiber reinforced epoxy composite." *International Journal of Physical Science*, Volume 5, No.2:pp. 109-115
- [225] Chitaranjan Deo and S.K.Acharya, (2009), "Solid particle erosion of Lantana-Camara Fiber reinforced Polymer Matrix Composite ." *Polymer-Plastic technology and Engineering*, 48:pp. 1084-1087
- [226] Anu Gupta, Ajit Kumar Amar Patnaik and Sandhya Rani Biswas, (2011), " Effect of Different Parameter on Mechanical and Erosion Behaviour of Bamboo Fiber Reinforced Epoxy Composite." *International Journal of Polymer Science*, Article ID 59290644
- [227] Jyoti R.Mohanty, Sankar N. Das, Haris C.Das, Tapan K. Mahanta and Sata,(2014), " Solid Particle Erosion of Date Palm Leaf Fiber Reinforced Polyvinyl Alcohol Composite" *Advances in Tribology*, Volume 2014
- [228] Sakuntala Ojha, Gujjala Raghavendra, S.K.Acharya,(2012), " An investigation into the erosive wear performance of reinforced carburised coconut shell powder in polymer composite using taguchi approach." *International Journal of System Algorithms & Applications(IJSAA)*, Volume 2: pp. 77-80
- [229] Ruff, A.W. and Ives, L.K., (1975), "Measurement of solid particle velocity in erosive wear", *Wear*, 35: pp.195–199.
- [230] Sundararajan, G. and Roy, B.V., (1990), "Erosion efficiency– a new parameter to characterize the dominant erosion mechanism", *Wear*,140: pp.369–381.
- [231] Suresh, A. and Harsha, A.P., (2006), "Study of erosion efficiency of polymers and polymer composites." *Polymer testing*, 25: pp.188-196.
- [232] Barkoula, N.M. and Karger-Kocsis, J., (2002), "Effects of fibre content and relative fibre-orientation on the solid particle erosion of GF/PP composites." *Wear*, 252: pp.80–87.
- [233] Biswas, S. and Satapathy, A., (2010), "A Comparative Study on Erosion Characteristics of Red Mud Filled Bamboo-Epoxy and Glass-Epoxy Composites", *Journal of Materials and Design*, 4: pp. 1752-1767.
- [234] Nejat Sarı, Tamer Sınmazcelik, (2007), " Erosive wear behaviour of carbon fibre/polyetherimide composites under low particle speed." *Materials and Design* 28 :pp. 351–355

- [235] Miyazaki, N. and Hamao, T., (1994), "Solid Particle Erosion of Thermoplastic Resins Reinforced by Short Fibers." *Journal of Composite Materials*, 28: pp.871-883.
- [236] Srivastava, V.K. and Pawar, A.G., (2006), "Solid particle erosion of glass fiber reinforced fly-ash filled epoxy resin composites." *Composites Science and Technology*, 66: pp.3021–3028.

PUBLICATIONS

International/National Conferences:

1. S.P.Samantarai,, S.K.Acharya, “ Friction and wear behaviour of rice husk (RH) ceramic reinforced epoxy composite, 7th International Conference on Industrial Tribology (ICIT 2010), December 2-4, 2010 Ispat Bhawan, RDCIS, SAIL, Ranchi.
2. S.P.Samantarai, S.K.Acharya. “Friction And Wear Behaviour of Rice Husk (Rh) Char Reinforced Epoxy Composite”. Futuristic Trends In Materials & Energy Systems (FTME-2011) 2011, Dec 29-30th, VR Siddhartha, Vijayawada, pp 159-163.
3. S.P.Samantarai, S.K.Acharya. “Dry Sliding Wear Behaviour Of Rice Husk (Rh) Char Reinforced Epoxy Composite”. National Tribology Conference (NTC-2011), IIT Roorkee, Dec 8-10th 2011.
4. S.P.Samantarai, S.K.Acharya , “Tribology Of Modified Rice Husk Filled Epoxy Composite (TSI 812604)”. 8th International conference on Industrial Tribology (ICIT 2012) Tribology Society of India, Pune, 7th-9th December 2012
5. SP.Samantrai, S.K.Acharya “Effect of Surface modification on the mechanical properties of rice husk reinforced epoxy composite”. presented at the International Conference on Metallurgical and Material process, products and application Jan-8-10, 2014 Raigard, C.G.

International Journals

1. S.P.Samantrai,S.K.Acharya ‘Investigation in to Tribo potential of Biomass based carbon black filler in epoxy composite’ Journal of Scientific and Engineering Research,Vol-3,Issue 6 ,2012. pp 1-4.
2. S.P.Samantrai, S.K.Acharya “Tribological Behaviour of modified Rice Husk Filled Epoxy Composite” International Journal of Scientific and Engineering Research,Vol-3,Issue 6 ,2012.
3. S.P.Samantarai, Gujjala Raghavendra S.K.Acharya “Effect of carbonization temperature and fiber content on the abrasive wear of rice husk char reinforced epoxy composite” Institution of Mech Engg (UK) Part J, Journal of Engg Tribology DOI: 10.1177/1350650113516435,January 2014.

4. S.P.Samantarai, S.K.Acharya. "Dry Sliding Wear Behaviour Of Rice Husk (Rh) Char Reinforced Epoxy Composite". The Institute of Engineers(India) , The Odisha State Center, 10th Feb 2013. pp 309-314.
5. S.P.Samantrai, S.K.Acharya"Water absorption behavior of rice husk epoxy composite" communicated to Journal of Bioresources.
6. S.P.Samantrai, S.K.Acharya "Investigation in to erosive wear behavior of rice husk epoxy composite" Journal of polymer plastic and engineering,(Under review)

BIBLIOGRAPHY



Mr. Sakti Prasad Samantarai is currently working as Deputy General Manager (MM) in Raw Materials Division of Steel Authority of India Limited. He did MSc (Engg), Production from NIT Rourkela. This dissertation is being submitted for the fulfillment the Ph.D. degree. The contact address is:

Address:-

Qr. No. B/17, Sector-20

Rourkela-5

Dist. Sunderagarh, Odisha

PIN: 769005

E mail:sp_samantarai@yahoo.com

Phone:08986881104(M)

0661-2645974 (Res)